DOCTOR OF PHILOSOPHY

Variations of alkalinity in the Northeast Atlantic

Muller, Kerstin

Award date:
2000

Awarding institution:
Bangor University

VARIATIONS OF ALKALINITY

IN THE NORTHEAST ATLANTIC

A thesis submitted to
the University of Wales
by

Kerstin Müller

in candidature for the
Degree of Philosophiae Doctor

University of Wales, Bangor
School of Ocean Sciences
Menai Bridge, U.K.

July 2000

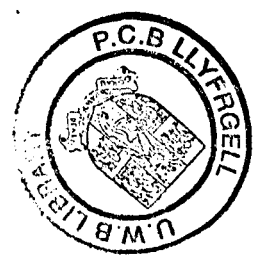

ABSTRACT

Total alkalinity (TA) is an important parameter in determining the uptake capacity of anthropogenic CO_2 by the ocean. So far, oceanic carbon cycle models do not accurately represent TA and its variations. A spectrophotometric method was developed to measure variations of TA during two JGOFS cruises to the Northeast Atlantic in the early summer of 1990 and 1991 and in *Emiliania huxleyi* batch cultures. Short-term precision averaged around $\pm 0.1\%$. A discrepancy of $< 0.5\%$ with coulometric results was observed in Na_2CO_3 standards. In natural seawater photometric TA was lower than potentiometric and calculated (pCO_2, TCO_2) TA by about 1 and 2%, respectively. Discrepancies varied with hydrographic and/or biological regime. Possible reasons for methodological shortcomings were considered, but without certified TA standards for different sample types, it was not possible to make an absolute statement about the accuracy of the methods involved. Combining the cruise results, photometric TA ranged by 90 and 20 $\mu eq\ kgSW^{-1}$ in the surface mixed layer (SML) and at sub-thermocline depths, respectively. Some horizontal variation in the SML was related to salinity, but most of it could be linked to coccolithophorid growth during a bloom in 1991. Associated small-scale changes in TA of up to 40 $\mu eq\ kgSW^{-1}$ occurred over 40 km. Independent estimates of seasonal net production of PIC and its relation to that of particulate organic carbon (POC) were established. Based on preceding investigations, a seasonal and latitudinal sequence of changes in surface TA was proposed which was corroborated by the photometric results from this study. The culture experiments revealed reductions in photometric TA which were half of those expected from parallel changes in measured PIC and nitrate concentrations. Proposed explanations for this included methodological shortcomings of all three methods and increases in final TA due to algal sulphate uptake and/or organic acid release. As the main conclusion, further targeted intercomparisons of TA methods are needed to identify the causes for errors in various TA methods in samples covering realistic hydrographic and biological ranges.

PREFACE

This project was carried out as part of the European Community Research and Development (DGXII) programme in the field of Climatology. The original objective of this study was to investigate the effect of CO_2 concentrations on the growth and metabolism of oceanic phytoplankton as a possible feedback mechanism to the increasing atmospheric CO_2 concentrations due to growing human impact. Later on during the study, the aim of the research was changed to focus on the effect of phytoplankton growth on total alkalinity (TA). The practical investigations were carried out within the framework of the U.K. contribution to the Joint Global Ocean Flux Studies (JGOFS) programme. The introductory chapter of this thesis forms part of a review which was carried out as a contribution to the Global Change and the Biosphere programme of the Natural History Museum, London, focussing on the link between climate and calcifying oceanic algae.

ACKNOWLEDGEMENT

First of all I would like to express my gratitude to the Commission of the European Union for having provided the financial basis for this study.

I further owe my thanks to my former supervisor Prof. Peter J. leB. Williams for having paved the way for this study and all the help he has given me. For further support I am also grateful to my current supervisor Dr. Hilary Kennedy.

My special gratitude for scientific and other support is directed at the late Dr. Peter Spencer, Prof. David Turner, and Dr. Jeremy Young.

Throughout periods of this study I have received plenty of help from the staff at the School of Ocean Sciences in Menai Bridge. In particular I owe my thanks to Dr. John Wrench, Mr. Malcolm Budd, Mrs. Vivien Ellis, and Dr. Carol Robinson. A further source of much help were various scientists from the Plymouth Marine Laboratories, the Natural History Museum in London, and other research institutions within and outside the U.K..

For the provision of additional cruise data I would like to thank Prof. David Turner, Mr. Roger Ling, Dr. Miles Finch, Dr. Kay Pegler, Ms. Helen Edmunds, Dr. James Aiken, Mr. Ian Waddington, Prof. Patrick Holligan, Dr. Emilio Fernandez, Dr. William Balch, Dr. Philip Boyd, Ms. Polly Machin and many others who have made the cruises on the RRS 'Discovery' and RRS 'Charles Darwin' work.

I express my apology to all those who should have been acknowledged but who have been mistakenly omitted from this list.

Most of all I thank my friends and family for their friendship, love, and other support.

1. GENERAL INTRODUCTION

Climate change results from the alteration of the energy balance of the Earth, which in turn may be brought about by

(i) natural internal fluctuations of components within the climate system, including the atmosphere, oceans, hydrosphere, cryosphere, continents and biosphere; e.g. El Niño/Southern Oscillation (ENSO) and variations in thermohaline circulation;

(ii) natural external forcings, such as changes in the output of solar radiation, the Earth's rotation, Sun-Earth geometry and orbit, the distribution of continents and oceans and their landscapes, the mass and composition of the atmosphere and oceans, biospheric change due to organismal evolution;

(iii) changes in anthropogenic activity, e.g. the burning of fossil fuel or biomass, land use, cement production, agriculture, industrial processes.

The current concern over climate change has arisen chiefly from the increase in the atmospheric concentrations of greenhouse gases since 1750, i.e. since the eve of the industrial revolution. This increase is widely anticipated to cause global warming, sea level rise and other hydrological changes, as well as shifts in regional climates.

Studies into climate change generally serve the attempt to discriminate the effect of human activity on climate change from the naturally occurring variations in the planetary climate system. The ultimate aim is to assist policy makers in their decisions regarding greenhouse gas and aerosol emissions, land use, etc. by providing them with projections of future climate changes for a range of anthropogenic emission scenarios. Recent estimates and projections have been detailed and summarized in the scientific contribution of the Working Group I of the Intergovernmental Panel on Climate Change (IPCC) to the Second Assessment Report of the IPCC (IPCC, 1996). This reference and references therein have been widely used as a basis for the ongoing scientific and political discussions and actions, and they form the main source for sections 1.1 - 1.3 below.

1.1. CLIMATE CHANGE

1.1.1. EVIDENCE

1.1.1.1. Indirect evidence: greenhouse gases

Indirect evidence of current global climate change has been derived from ice core measurements. The data shows that atmospheric greenhouse gases such as carbon dioxide (CO_2), methane (CH_4), and nitrous oxide (N_2O) were present at relatively stable concentrations in the several centuries preceding 1750, but have increased since then by about 30%, 145%, and 15%, respectively. Shortwave radiation from the Sun is either reflected, absorbed or transmitted by the Earth's atmosphere. The transmitted radiation which reaches the Earth's atmosphere, including clouds, or the ground will be either absorbed or reflected as longwave radiation back to the atmosphere or into space. Greenhouse gases generally trap this infra-red radiation emitted by the Earth's surface or clouds by absorbing and emitting part of this thermal energy back down, thus warming the troposphere. The natural greenhouse effect is vital for maintaining the global energy balance of the Earth. The concern therefore focusses on the potential enhanced greenhouse effect, which is caused by the additional effect of atmospheric greenhouse gases originating from anthropogenic activity (Schimel et al., 1996).

1.1.1.2. Direct evidence

1.1.1.2.1. Atmospheric temperature

Direct evidence of climate change is largely based on instrumental observations, most of which only started less than 150 years ago. Global mean surface air temperature has risen by between 0.3° and 0.6 °C over the last 100 years, possibly tending towards the higher end of this range during the last 40 years. While the warming has been greatest over the continents between 40° and 70°N in winter and spring, regional variations have in fact led to localized year-round cooling, e.g. over the northwest North Atlantic and the mid-latitude North Pacific. The warming has been accompanied by generally, but not globally, fewer extremely low minimum temperatures as well as a reduction in the diurnal temperature range over land, at least in recent decades. The lower stratosphere, at an altitude of 17 to 22 km, has cooled since 1979 when data started being more reliable. The impact of transient events like the eruption of Mount Pinatubo in 1991 is reflected in the subsequent reversal of

the vertical temperature trend, i.e. the surface and troposphere cooled for two years while the lower stratosphere warmed. Thereafter, temperatures returned to their previous values (Nicholls et al., 1996).

1.1.1.2.2. Atmospheric circulations and their interactions with the ocean

Atmospheric circulation acts as the main control behind regional changes in wind, temperature, precipitation, etc.. Prominent examples for this are the ENSO, the Northern Hemisphere Circulation which gives rise to the North Atlantic Oscillation (NAO), and the Southern Hemisphere Circulation (Nicholls et al., 1996).

The NAO fluctuates on a time-scale of 9-12 years but also on a lower frequency mode, which appears to vary regionally from 50 to 88 years. It represents a large-scale alternation of the atmospheric pressure gradient at sea level between the North Atlantic regions of subtropic high pressure centred near the Azores and subpolar low pressure extending south and east of Greenland. The state of the NAO determines the strength and orientation of mid-latitude westerlies across the ocean, which, in turn, affect the tracks of the European-sector low-pressure storm system (Lamb & Peppler, 1991). During a positive phase of the NAO the relatively high pressure gradient leads to stronger westerlies. These are associated with warmer winters in northern Europe and anomalously increased precipitation from Iceland eastward to Scandinavia (Hurrell, 1995). Such a positive phase has persisted in the North Atlantic since 1989 (until at least 1995). There is also some evidence of increases in extreme tropical cyclones over the North Atlantic since 1988. Anomalous atmospheric circulation regimes have also been observed over the North Pacific from 1976 to 1988 (Nicholls et al., 1996). Nicholls et al. regard it as likely that there is a dynamic coupling between atmosphere and ocean which would involve, for example, the ocean thermohaline circulation (see also section 1.1.1.2.5).

1.1.1.2.3. Precipitation, snow and cloud cover

Information about precipitation over the oceans is limited. Intense rainfall around the periphery of the North Atlantic since early this century appears to be the result of an increase in the number of heavy rainfall events (Frich, 1994). The decrease of the snow cover extent in recent years has been found to be closely coupled to the temperature increase in the Northern Hemisphere, and has led to earlier snow-melt related floods in

some parts. Evaporation is difficult to measure, especially over the oceans, but calculations indicate an increase over much of the Atlantic due to an increased vertical humidity gradient and maybe also increased wind speed. The amount of clouds has generally increased over the oceans in recent decades (Nicholls et al., 1996).

1.1.1.2.4. Ocean temperature

Signs of climate change are also beginning to be detected in the interior of the oceans. Large-scale and coherent changes in subsurface temperatures are apparently linked to the changes at the surface of the formation regions of the relevant water masses. In contrast to sea surface temperature (SST), subsurface ocean temperatures bear the advantage of levelling out the noise of temperature variability observed in surface waters. Accordingly, subsurface Labrador Sea Water, which originates from the subpolar northwest North Atlantic, has cooled by 0.9 °C between 1970 and 1995, and is currently colder, fresher, and larger than ever before (Read & Gould, 1992; Lazier, 1995; Rhines & Lazier (1995) referred to by Nicholls et al. (1996)). On the other hand, subsurface waters from 1100 m depth across the Atlantic Ocean have increased by an average of 0.3 °C between 1957 and 1992. Temperature increases of subsurface waters have also been observed in the Indian and Pacific Oceans (Nicholls et al., 1996).

1.1.1.2.5. Ocean circulations and sea level

Changes and variability in ocean circulation can also be important factors influencing climate. There is still insufficient data available to detect any changes potentially taking place at present. However, modelling results suggest possible variations in the thermohaline circulation over about 50 years (Delworth et al., 1993). It is likely that these changes involve dynamic coupling between atmosphere and ocean parameters exerted beyond the domain of the Atlantic Ocean (see also section 1.1.1.2.2). For example, changes in precipitation, run off, and evaporation alter the salinity and thus density at the point of deep water formation in the North Atlantic. This has a large impact on the thermohaline circulation. It has been suggested that fluctuations in this global conveyor belt circulation may be associated with the abrupt climate changes observed in recent Greenland ice core records relating to the last ice age (Nicholls et al., 1996), which are described in section 1.1.2. below.

Observed increases in sea level of 10 to 25 cm within the last 100 years are likely consequences of the thermal expansion of the oceans and melting of glaciers, ice caps, and ice sheets, which have been induced by global warming (IPCC, 1996).

1.1.2. PALAEOCLIMATE CHANGES AND VARIABILITY

Knowledge of the extent of climate changes and variability during the more distant past gives an indication of whether recent climatic trends are significant. Further, an understanding of palaeoclimatic changes allows detection of possible analogues between past and present or future climate scenarios. Palaeoclimatic data is also used in the verification of climate computer models, in particular, when dealing with climate regimes differing from the present.

Information about climate prior to the instrumental era comes mostly from palaeontological proxy records of climate-sensitive phenomena. Examples of these include sediment core records of algal and faunal abundances, stable isotope analyses from sediment-, coral-, and ice cores, and saturation of algal long-chain alkenones. The use of proxy data in relating past climates to radiative forcing and its use in validating models remains limited at present. This is because of dating uncertainties, regional differences or lack of data, and considerable inconsistencies between records from different parameters (Crowley, 1994). However, while calibrations may cause problems in deducing absolute temperature values from proxy records, there is considerably more confidence in the detection of changes in temperature.

1.1.2.1. Pleistocene to Holocene

The Pleistocene (0.01 - 2 million years before present (mbp)) was mostly cooler than today but 100-thousand-year glacial/interglacial cycles gave rise to global temperature fluctuations of 5° to 7° C. In mid- and high latitudes they reached up to 10° to 15° C. Proposed causes for this cyclicity are the Milankovitch orbital effect (Berger, 1980) and variations in atmospheric CO_2 and CH_4 concentrations (Barnola et al., 1987; Chappellaz et al., 1990; Hansen et al., 1984; Broccoli & Manabe, 1987). Accordingly, during part of the last interglacial period, 125 to 130 thousand years before present (ka), the doubled eccentricity of the Earth's orbit is thought to have led to temperatures 1° to 2° C higher than today's even

though the atmospheric CO_2 concentration was only about 300 ppm. On the other hand, the Dansgaard-Oeschger cyclicity and periodicity of Heinrich events, which characterize the last glacial period (20 to 100 ka), cannot be directly associated with orbital forcing or changes in atmospheric composition. Dansgaard-Oeschger events occurred every 1 to 10 thousand years (kyr). They represent cold phases at least in the North Atlantic and adjacent continents which were terminated by large and rapid warming of 5° to 7° C within a few decades. There were about 20 of these warm interstadials, which lasted about 500 to 2000 years, and which were followed by slow cooling and a generally rapid return to glacial conditions (Johnson et al., 1992; Dansgaard et al., 1993). Variations in Atlantic deep water circulation and surface temperatures were found to be closely related to the Dansgaard-Oeschger cycles (Keigwin et al., 1994; McManus et al., 1994). Heinrich events occurred during the most intense cold phase of a package of Dansgaard-Oeschger cycles at a periodicity decreasing from about 13 to 7 kyr. These events may be associated with rapid iceberg discharge presumably from Northern Hemisphere ice sheets (Bond et al., 1993; Mayewski et al., 1994; Bond & Lotti, 1995). It has been suggested that the melting of these icebergs in higher latitudes first led to a reduction or cessation of the thermohaline circulation, and hence a reduction in the heat transport from the tropics. Subsequently, a decrease in meltwater would give rise to a rapid restart of the thermohaline circulation which could explain the associated abrupt warming of the sea surface after the Heinrich events.

Duplessy et al. (1992) found that parallel changes in SST and salinity have led to reduced oceanic convection in the North Atlantic and to a weakened global conveyor belt ocean circulation during the last 20 thousand years. Damped signals of corresponding climatic events have been observed in the Southern Hemisphere (Jouzel et al., 1995). An increase and reduction in North Atlantic Deep Water (NADW) formation have also been linked to a rapid and relatively short-lived warming and cooling event at the end of the transition to the present interglacial phase, the Holocene. At about 11.5 ka Central Greenland ice cores indicate a temperature increase of about 7° C within a few decades and even more rapid changes in precipitation and a reorganisation in atmospheric circulation. Concomitant SST changes of approximately 5° C in less than 40 years were observed in the Norwegian Sea (Lehman & Keigwin, 1992). The Younger Dryas cold event, which represents the last Dansgaard-Oeschger event, started about 10.5 ka and lasted for only about 500 years. It abruptly reversed the general warming trend within about 100 years and also ended very

suddenly. Its signals were strongest in the North Atlantic and have been observed in other but possibly not all parts of the globe. While the Milankovitch effect and changes in CO_2 and CH_4 concentrations are not considered as possible direct causes, there is no general consensus regarding a possible explanation for this event (IPCC, 1990). Some proposals involve the final melting of the Laurentide Ice sheet, freshwater influx to the North Atlantic Ocean (Broecker et al., 1985a) and its temporary impact on the deep water formation, thermohaline circulation and temperatures (Street-Perrot & Perrot, 1990).

Compared to the Pleistocene, the Holocene (10 ka to present) is characterized by much smaller temperature fluctuations, which have not exceeded 2° C and may not have been truly global (IPCC, 1990). However, abrupt regional events have occurred (e.g. Berger & Labeyrie, 1987). During the last of several short-lived warm epochs of the Early and Middle Holocene, high northern latitudes had higher summer temperatures than at present (Varushenko et al., 1980). Combined climate reconstructions indicate that the temperature elevation reached up to 4° C north of 70°N , 1-2° C in mid-latitudes, while temperatures further south were often lower than today. Annual precipitation was increased in subtropical and high latitudes. These reconstructions are still somewhat uncertain but are expected to become more accurate with more regional data (IPCC, 1990).

1.1.2.2. Last 1 kyr: interpretation of current climatic developments

The analysis of whether the global climate change of this century is unusual in the context of the last 1000 years is complicated by considerable regional climate differences. Northern Hemisphere summer data from 16 proxy records, for example, demonstrates that recent decades have been the warmest since 1400 AD, while this does not necessarily apply regionally (Bradley & Jones, 1993; 1995). Further, due to geographical complexity it is not yet possible to state on a hemispheric scale whether temperatures declined from the Medieval Warm Period (11th to 12th century) to the Little Ice Age (16th to 17th century). It is, however, clear that the instrumental record started during a cooler period of the last thousand years. On a global scale, ice core records from several, widespread sites reveal that the 20th century is at least as warm as any century since 1400 AD (e. g. Briffa et al., 1995; Thompson et al., 1995). Further, independent of somewhat differing interpretations, the temperature record of the last 1000 years demonstrates two important points. The mid/late 20th century temperatures have been warmer than in any similar period since 1400

AD, and in at least some regions the 20th century temperatures have been warmer than in any other century for some thousands of years. Nicholls et al. (1996) conclude that it is possible that rapid changes in climate can occur naturally, and they draw attention to the unlikelihood that global mean temperatures have varied by more than 1°C during the last 10 kyr (e.g. Wigley & Kelly, 1990).

1.1.2.3. Potential use as analogues for current/ future climate developments

Three palaeontological warm epochs have been considered by Budyko and Israel (1987) as possible analogues to our current greenhouse scenario, i.e. the Pliocene, Eemian, and Middle Holocene. Three to 4 million years (Ma), during the Pliocene, temperatures and precipitation were higher in the Northern Hemisphere. However, comparisons to the present situation are hampered by a controversy over the extent of increased CO_2 concentrations, dating uncertainties, and differences in boundary conditions such as surface geography including topography and ecology, which may affect the proxy records. Dating problems and lack of regional data have also given rise to uncertainties in using the Eemian (130 - 115 ka) as a parallel scenario. It has been argued that a changed seasonal distribution of the incoming solar radiation due to the eccentricity of the Earth's orbit may not necessarily have produced the same climate as would result from the globally averaged increase in greenhouse gases. The warm Middle Holocene appears to be a more valid analogue to the expected early 21st century climate, since the boundary conditions such as the positioning of the continents and ice sheets, sea level and vegetation are more comparable to the present. It is anticipated that disputes over regional temperature deviations shall be removed as more data from both hemispheres becomes available (IPCC, 1990). As in the case of the Eemian, climate may have been predominantly affected by the Earth's eccentricity.

The Younger Dryas (11 - 10 ka) has been used by Broecker (1987) as an analogue for possible abrupt climate shifts caused by changes in thermohaline circulation, which in turn may be caused by the greenhouse effect. He suggests that the current general warming and precipitation increase over the extra-tropical Atlantic may lead to qualitatively similar although probably much smaller changes in thermohaline circulation.

1.1.3. FUTURE CLIMATE PROJECTIONS AND ATTRIBUTION TO HUMAN ACTIVITY

Coupled climate models are increasingly used for projections of future climate and attribution to natural and human influences. These models consist of atmosphere, ocean, sea-ice and land-surface component models, all of which are based on well-established physical principles. Before any projections can be conducted, it is necessary to evaluate a model, i.e. to establish the degree of correspondence between a model and the real world. This is most reliably done by conducting several different tests each of which involves either a selected aspect, a single component, or a link between two components of the coupled model. Due to insufficient palaeoclimate data, the use of palaeontological simulations is limited to only general climate regimes, which is insufficient for current resolution requirements.

While the land surface component still suffers from widespread discrepancies, and considerably more work needs to be done on sea-ice models, the atmospheric component provides encouraging results given the correct input of SST. Ocean general circulation models (OGCMs) manage to provide realistic portrayals of large-scale structures of ocean gyres and general structures of the thermohaline circulation. However, they still require considerable improvements on smaller horizontal, vertical, and temporal scales as well as the inclusion of biogeochemical feedback processes as described in section 1.3.2. below. This is currently prevented by computational constraints, lack of data, or inadequate understanding of the processes involved. The shortcomings seem to be reflected in the remaining reliance on non-physical manipulations of the models in form of so-called spin-ups, flux adjustments, and relaxations. Nevertheless, the accuracy currently achieved with coupled climate models is encouraging on a hemispheric and continental scale. Since it is not feasible to run general circulation models (GCMs) for large numbers of future climate simulations due to their large requirements for computer resources, simple upwelling diffusion-energy balance models have been calibrated against GCMs and run instead.

According to the modelled climate projections, global mean temperatures are expected to increase by 1° to 3.5° C by the year 2100. The projected range arises chiefly from the range of projected radiative forcing scenarios used and from uncertainties in the climate sensitivity to these scenarios. Concomitant sea level rise is anticipated to range from 15 to

95 cm with the melting of the major ice sheets as a chief source of uncertainty. Additional continental-scale projections include

(i) minimum warming around the northern North Atlantic and Antarctica, due to deep oceanic mixing in those areas;

(ii) maximum surface warming in high northern latitudes in winter, due to the reduction in sea-ice and snow cover;

(iii) little surface warming over the Arctic in the summer;

(iv) enlarged global mean hydrological cycle with increased precipitation and soil moisture in high latitudes in winter;

(v) greater surface warming of land than of sea in winter.

Most models also indicate a weakening of the thermohaline circulation and a widespread reduction in the diurnal temperature range. The latter is linked to increased cloud cover and possibly aerosol concentrations. Confidence in these projections is higher for temperature than for hydrological developments, and for hemispheric and continental than regional scales. Regional sea level changes are expected as a consequence of regional changes in heating, ocean circulation and land movement.

The results from these projections demonstrate several important points:

(i) climate changes are expected to involve considerable temporal and regional natural variability;

(ii) the average rate of warming is anticipated to be greater than any seen in the last 10 thousand years;

(iii) due to the thermal inertia of the oceans only 50 to 90% of the eventual temperature change will be reached by the year 2100, therefore temperatures will continue to rise beyond that point, even if concentrations of greenhouse gases are stabilized by then;

(iv) due to the inertia of the ice masses as well as the oceans, sea level will continue to rise even beyond the date of temperature stabilization.

Statistical tests to detect whether the Earth's climate is indeed changing significantly beyond what can be expected from its natural variability have been carried out using multi-century models. The estimation of natural climatic 'noise' is complicated by large uncertainties remaining in the current estimates of magnitude and patterns of climate variability,

especially on decadal to century time-scales. However, it is spatial patterns of temperature change which provide the most convincing evidence in the attribution of the current climate change to human activities. The use of changes in global mean, annually averaged temperature over the last 10 to 100 years is restricted by uncertainties in the natural internal variability and in the histories and magnitudes of natural and anthropogenic climate forcing. Pattern-based studies compare observations with patterns of temperature change predicted by models in response to human forcing from greenhouse gases and anthropogenic aerosols. This method makes use of the fact that different forcing mechanisms have different patterns of response or characteristic 'fingerprints', especially if the response is considered in three or four dimensions, i.e. as a function of longitude, latitude, altitude, and time. The results of these studies, which have dealt with the largest spatial scales such as hemisphere, land versus ocean, and troposphere versus stratosphere have all shown significant correspondences between observations and model predictions. As expected from a human signal which increases with time, the pattern correspondence has also increased with time for the last 20 to 50 years. The statistical probability is low for correspondences to be due to chance as a result of natural internal variability. Further, vertical atmospheric patterns are inconsistent with the response pattern expected for solar and volcanic forcing. The human factor finds further support in qualitative commonalities such as the reduction in diurnal temperature range, sea level rise, and high latitude precipitation increases.

The IPCC (1996) summarize and conclude that the observed trend in global mean temperature is unlikely to be entirely of natural origin, and that there is an emerging pattern of climate response to forcings by greenhouse gases and sulphate aerosols in the observed climate record. The body of statistical evidence, examined in the context of the present physical understanding of the climate system, points towards human influence on global climate, the extent of which remains uncertain. Nevertheless, Santer et al. (1996) acknowledge that this attribution issue remains subjective. Thus, for some scientists the large uncertainties in the natural noise and the human signal are thought to preclude any answers. While few scientists regard the available statistical evidence as sufficient to accept the attribution as 'completely unambiguous', it has at least been accepted with 'confidence' by others.

1.2. GREENHOUSE GASES AND THE RELEVANCE OF CO_2

Greenhouse gases may conveniently be divided into three groups, i.e.

(i) naturally occurring gases whose atmospheric concentrations are not directly altered by human activity; e.g. water vapour and ozone (O_3);

(ii) naturally occurring gases whose atmospheric concentrations are directly affected by anthropogenic activity; e.g. CO_2, CH_4, N_2O, various halocarbons, and carbon monoxide (CO);

(iii) exclusively synthetic gases; e.g. hydrofluorocarbons (HFCs), perfluorocarbons (PFCs) and sulphur hexafluoride (SF_6).

The concentrations and spatial distributions of all these gases are determined by their atmospheric lifetimes and the size and location of their sources and sinks. Their lifetimes are in turn influenced by physical and biogeochemical factors. Gases with short lifetimes such as water vapour, O_3, and CO generally exhibit more heterogeneous horizontal and vertical distributions, which have so far imposed practical constraints on the accurate estimation of potential changes in their radiative impact on the atmosphere.

Human activity has an increasing effect on concentrations and distributions of various greenhouse gases. Radiative forcing estimates are used to approximate the impact which these anthropogenic additions of individual greenhouse gases and other external forcings are having on our climate. They are globally and annually averaged measures of the perturbation of the planetary radiation budget which triggers a climate response, and which also takes account of the radiative properties of the gases. For example, the depletion of stratospheric O_3 is represented as a negative forcing value. However, confidence in the radiative forcing values remains low or even very low for all but the major well-mixed greenhouse gases (IPCC, 1996). The radiative forcing values for changes in the concentrations of CO_2, CH_4, N_2O, and various halocarbons from pre-industrial times up to 1992 reached a total of 2.45 W m^{-2} with an uncertainty of 15%. The individual gases accounted for 1.56, 0.47, 0.14, and 0.28 W m^{-2}, respectively. An obvious drawback of using global averages is that they do not reflect the substantial geographical differences of the forcing by the individual gases. Thus climate may change regionally, or even globally, although the forcing value equals zero. Major uncertainties regarding radiative forcing involve changes in the tropospheric chemistry and constituents due to the increased exposure to UV radiation, and the effects of different types of aerosols, whose forcings

predominantly oppose those of greenhouse gases. Further uncertainties are associated with possible tropospheric and stratospheric changes of the most abundant natural greenhouse gas, i.e. water vapour.

In order to facilitate the comparison of projected radiative effects from individual greenhouse gases on a molecular basis, the global warming potential (GWP) index has been introduced (IPCC, 1994). It has a typical uncertainty of 35% relative to CO_2, which is used as the reference gas. Values of GWP for CH_4 and N_2O exceed that of CO_2 by roughly 10 to 10^2 times. Most striking, though, is the large effect anticipated for most HFCs, PFCs, and SF_6, unless their emissions are halted or at least significantly reduced. Values of GWP for these compounds are typically 10^2 to 10^4 times greater than those for CO_2. Moreover, due to very long atmospheric lifetimes, PFCs and SF_6 will accumulate in the atmosphere and will therefore continue to influence climate for thousands of years to come.

1.2.1. CARBON DIOXIDE

Ice core measurements from Greenland and Antarctica indicate that the atmospheric CO_2 concentration was depressed to the range of 180 - 220 parts per million by volume (ppmv; sometimes also shortened to ppm although not strictly accurate) for 50 kyr during the last glacial period before it increased most notably by about 80 ppmv parallel to the last interglacial warming. Temperature signals in the Southern Hemisphere generally preceded those in the north, and there is no evidence that the CO_2 signal ever significantly preceded the temperature changes in the south. It is possible that changes in atmospheric CO_2 may have led to temperature changes in the Northern Hemisphere, and there is evidence that CO_2 concentrations started to change ahead of any significant melting of continental ice. Therefore, it may be the case that changes in climate triggered CO_2 changes, which in turn amplified palaeoclimatic changes. Pre-industrial concentrations of atmospheric CO_2 stayed at around 280 ppmv, only varying by up to 10 ppmv over several centuries until about 1800. Since then annually averaged concentrations have increased significantly (Schimel et al. 1995; IPCC, 1996). Direct measurements of the gas indicate that the atmospheric CO_2 concentration reached an annually averaged value of 358 ppmv at Mauna Loa, Hawaii, in 1994 (IPCC, 1996). Data from this site tends to be close, but not the same, as the global average value.

Precise and direct measurements from the South Pole and Mauna Loa, Hawaii, have shown that the growth rate of atmospheric CO_2 concentration has generally increased since the late 1950s, when it was about 0.6 ppmv yr^{-1}. During the 1980s this rate averaged 1.53 ppmv yr^{-1}. Annually averaged growth rates have varied considerably over time, e.g. in 1987-88 it reached 2.5 ppmv yr^{-1}, which is the highest rate recorded until recently. Between 1992 and 1994 it changed from about 0.6 to 1.65 ppmv yr^{-1} (Feely et al., 1999). These recent fluctuations are thought to represent relatively large but transitory perturbations of the global carbon cycle. There is no direct evidence in the ice core record that past changes have been as rapid as those in the 20th century. The CO_2 record *per se* and ^{14}C measurements suggest that this is largely attributable to human activity. Keeling et al. (1989a; 1995) removed seasonal and short-term interannual variations and found that the rise in atmospheric CO_2 approximated 50% of anthropogenic emissions (e.g. see table 1.1 below). In addition, interhemispheric differences have been growing in parallel to the increase in emissions (Keeling et al., 1989b; Siegenthaler & Sarmiento, 1993). Further evidence for anthropogenic pCO_2 increase between 1800 and 1950 stems from the decreasing concentration of ^{14}C, i.e. as measured in tree rings and corals over that period. This is an example of the so-called Suess effect, which implies a negative correlation between anthropogenic CO_2 and ^{14}C in biological material (Suess, 1955).

The turnover time of CO_2 in the atmosphere is about 4 years due to the relatively fast exchange with the surface ocean. By contrast, the equilibration time of about 100 years is determined by the removal rate from the surface to the deep ocean. An even longer equilibration time of about 10^4 years relates to compensatory shifts of the calcium carbonate compensation depth (Broecker, 1973). The latter has generally not been regarded as relevant to the mission of the IPCC. However, the slow flux between surface and deep ocean forms an important component of the global carbon cycle, and consequently, any additional CO_2 emissions will cause long-lasting perturbations to this cycle. Further, in 1992 the radiative forcing of CO_2 was estimated to represent 64% of the total radiative forcing from the well-mixed greenhouse gases. In conclusion, elevated atmospheric CO_2 concentrations are expected to remain a major contributing factor to human-induced climate change, at least in the near future. Accurate projections of atmospheric CO_2 concentrations therefore remain a significant element in the projections of future climate change.

1.3. GLOBAL CARBON CYCLE AND THE RELEVANCE OF THE OCEANS

1.3.1. GLOBAL CARBON FLUX AND SINKS FOR ANTHROPOGENIC CO_2

Two main types of projections examining the relationship between atmospheric CO_2 concentrations and fossil fuel carbon emissions have been presented by the IPCC (1996). Atmospheric CO_2 concentrations were calculated for a range of fossil fuel carbon emission scenarios. A range rather than a specific value is used to account for the uncertainty in the estimates of future emissions due to changes in the human population and its behaviour. These so-called IS92 emission scenarios were used in the climate projections. The second and inverse type of projection involved calculating fossil fuel carbon emission scenarios required for atmospheric CO_2 concentrations to stabilise at a range of concentrations by a given future date. The purpose of these so-called S350 - S1000 concentration stabilisation profiles is to provide policy-makers with a scientific basis for their decisions regarding future fossil fuel emission strategies. These projections show that concentrations of atmospheric CO_2 are estimated to surpass 700 ppmv before the year 2100, if the existing policies remain unaltered, i.e. if anthropogenic carbon emissions are not substantially reduced. Further, anthropogenic emissions must fall to about half of today's value within a century and further thereafter, if atmospheric concentrations are to be stabilised at about 500 ppmv.

While the main uncertainty about future growth of atmospheric CO_2 originates from political and socio-economic factors (Siegenthaler & Sarmiento, 1993), the atmospheric CO_2 projections also depend on the accuracy of models to estimate the fate of anthropogenic CO_2 within the global carbon cycle. A simplified schematic overview of the global carbon cycle which is limited to the reservoirs and fluxes generally regarded to be relevant to human perturbation is presented in figure 1.1.

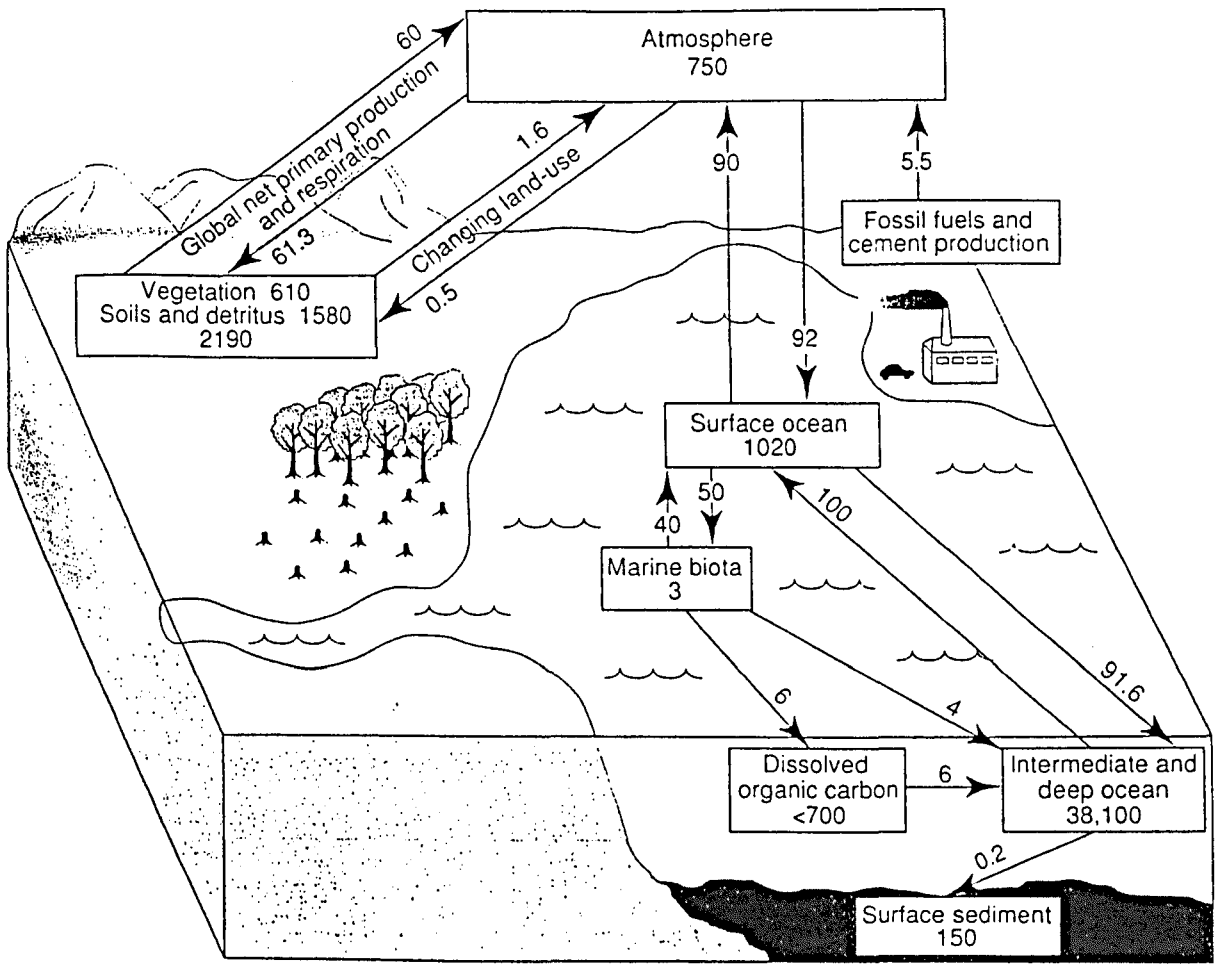

Figure 1.1: A grossly simplified scheme of the global carbon cycle showing reservoirs in gigatonnes of carbon (Gt C) and fluxes (Gt C yr^{-1}) relevant to the human perturbations as annual averages over the period 1980 to 1989. The values are subject to considerable uncertainties. Riverine fluxes are not included. (Figure and values from IPCC (1996))

For the IPCC (1996) projections three different carbon cycle models were used, i.e. the Bern model (Siegenthaler & Joos, 1992; Joos et al., 1996) and those described by Wigley (1993) and Jain et al. (1995). They had been chosen as representatives from a set of 18 models employed in the preceding projections which had revealed a time-dependent discrepancy between models of up to ± 15% about the median value (IPCC, 1994). For calibration purposes, reference values for annually averaged fluxes and reservoir changes of the anthropogenic CO_2 perturbations were taken from the period 1980 to 1989. These values are given in table 1.1.

Emissions from fossil fuel combustion and cement production were 5.5 ± 0.5 Gt C yr^{-1} during the period of 1980 to 1989 and reached 6.6 ± 0.6 Gt C yr^{-1} in 1990. The annual average rate of change in atmospheric carbon amounts to 3.3 ± 0.2 GtC yr^{-1}, which corresponds to the globally averaged concentration increase of 1.53 ppmv yr^{-1} during the 1980s. The total atmospheric concentration of other carbon-containing compounds like CH_4, CO, and larger hydrocarbons is ignored here, as they only make up about 1% of total atmospheric carbon.

Table 1.1: Average annual budget of CO_2 perturbations for 1980 to 1989. Fluxes and reservoir changes of carbon are expressed in Gt C yr^{-1}, error limits correspond to an estimated 90% confidence interval (from IPCC, 1996).

	IPCC 1992†	IPCC 1994*	IPCC 1995
	Estimates for 1980s budget		
CO_2 sources			
(1) Emissions from fossil fuel combustion and cement production	5.5 ± 0.5Δ	5.5 ± 0.5	5.5 ± 0.5§
(2) Net emissions from changes in tropical land-use	1.6 ± 1.0Δ	1.6 ± 1.0	1.6 ± 1.0§
(3) Total anthropogenic emissions = (1)+(2)	7.1 ± 1.1	7.1 ± 1.1	7.1 ± 1.1
Partitioning amongst reservoirs			
(4) Storage in the atmosphere	3.4 ±0.2Δ	3.2 ± 0.2	3.3 ± 0.2§
(5) Ocean uptake	2.0 ± 0.8Δ	2.0 ± 0.8	2.0 ± 0.8§
(6) Uptake by Northern Hemisphere forest regrowth	not accounted for	0.5 ± 0.5	0.5 ± 0.5§
(7) Other terrestrial sinks = (3)–((4)+(5)+(6))			
(CO_2 fertilisation, nitrogen fertilisation, climatic effects)	1.7 ± 1.4	1.4 ± 1.5	1.3 ± 1.5

† Values given in IPCC (1990, 1992).

* Values given in IPCC (1994).

Δ Values used in the carbon cycle models for the calculations presented in IPCC (1994).

§ Values used in the carbon cycle models for the calculations presented here.

Some uncertainties in the global carbon cycle estimates arise from models which do not incorporate short-term interannual variations or other short-term variations in exchange fluxes between the different reservoirs. It has been suggested that these variations, possibly also caused by physical and biogeochemical feedback processes in response to climate fluctuations, could have led to the observed shift in the rate of atmospheric CO_2 increase between 1991/92 and 1994. Relative and absolute magnitudes of processes in the oceans and on land show substantial year-to-year variability (Ciais et al., 1995a,b). There is also strong evidence for variability of exchange fluxes with the atmosphere (Bacastow, 1976; Francey et al., 1995). However, the exact timing and magnitude of these fluxes remain controversial (Keeling et al., 1989a, 1995; Feely et al., 1995; Francey et al., 1995). The global carbon cycle models used for the IPCC (1994) exercise have addressed only longer-term direct perturbations of the global carbon cycle, i.e. on a 10-year time-scale, and only as a function of anthropogenic CO_2 increase. More inclusive models are in the process of being developed to include interannual variations (Kaduk & Heimann, 1994; Winguth et al., 1994; Sarmiento et al., 1995). However, improved understanding of the rapid fluctuations of the global carbon cycle is needed before these models can be further developed and validated, and before potential feedback mechanisms can be quantified.

Due to the difficulties in estimating changes in terrestrial carbon storage, estimates of the global carbon budget and projections of atmospheric CO_2 increase in the future rely on the improvement in the estimates of CO_2 uptake by the oceans.

1.3.1.1. Oceanic carbon sink

The oceans cover 72% of the surface area on Earth. They have the highest thermal inertia of all the components of the climate system, make a major contribution to total planetary heat transport, and form a major source of water vapour to the atmosphere. As shown in figure 1.1 and table 1.1, they also hold considerably more carbon than any other climate component and act as a major sink for anthropogenic carbon.

Several box model studies have demonstrated that changes in the oceanic carbon cycle are capable of causing quite large perturbations in atmospheric CO_2 (e.g. Sarmiento & Toggweiler, 1984; Siegenthaler & Wenk, 1984; Sarmiento et al., 1988; Joos et al., 1991). The ocean is thought to have acted as the main trigger for the increase in the concentration of

atmospheric pCO_2 from the glacial to the present interglacial period. Terrestrial factors have been disregarded as a trigger for this change, because during glaciation the carbon stored in land biota, soil and detritus was significantly reduced by ice cover and colder drier climate (Broecker, 1982). Due to human emissions, the fluxes and reservoir sizes have changed. The cycle observed today represents a superposition of the natural situation and man-made perturbations (Siegenthaler & Sarmiento, 1993).

The estimate of excess atmospheric CO_2 uptake by the oceans for the 1980- 89 period used by the IPCC (1996) as a reference has been derived by a combination of modelling and measurements of carbon isotopes and atmospheric oxygen/nitrogen ratios. The modelling effects comprise a range of model types of varying complexity. The uncertainty term of ±0.8 Gt C yr^{-1} was obtained by simply doubling the difference between the mean and the most distant model result (U. Siegenthaler, pers. comm. in Orr (1993)). Orr argues that this approach does not account for the individual model uncertainties, but uncertainties are in fact reduced to ± 0.5 Gt C yr^{-1} in his reassessment due to the use of updated and improved models. Nevertheless, this lower uncertainty term has not been adopted by the IPCC (1996), because the accuracy of this value has been put into question by an assessment of bomb ^{14}C data in the entire global system (Broecker & Peng, 1994; Hessheimer et al., 1994).

It has been suggested that data from the Geochemical Ocean Section Study (GEOSECS) programme has overestimated the oceanic ^{14}C inventory by approximately 25%, which is slightly more than the generally accepted uncertainty. This would lead to overestimation of the ocean uptake value by 0.5 GtC yr^{-1}, which is considerable but within the stated error range. However, a re-assessment of the oceanic observations does not support the explanation involving a reduced ocean sink (Broecker et al., 1995). On the above grounds alone, the relative importance of the oceans in the global carbon cycle remains uncertain. Further, ocean carbon storage may be influenced by yet unaccounted for physical, chemical, and biological ocean processes and their changes in response to anthropogenic forcing. Various oceanic processes and remaining uncertainties in the models are outlined below.

1.3.2. RELEVANCE OF DIFFERENT OCEANIC PROCESSES IN REMOVING ANTHROPOGENIC CO_2

The uptake of atmospheric CO_2 into the oceans depends predominantly on the disequilibrium of the partial pressure of CO_2 (pCO_2) across the atmosphere-ocean interface, near-surface wind speed, and the skin effect. The pCO_2 of the surface seawater is determined by its temperature, salinity, and CO_2 concentration. Apart from the atmospheric exchange, the sea surface CO_2 concentration is influenced by physical exchange of dissolved and particulate carbon between the surface and deep ocean, the settling of particulate carbon and ultimately its sequestration in the sediments. The transfer of carbon into and through the oceans occurs via physico-chemical and biogeochemical exchange processes. These are largely interconnected and, in turn, determined by physical processes, i.e. seawater motions.

1.3.2.1. Physical processes

The wide range of space- and time-scales covered by physical processes of seawater are shown in figure 1.2.

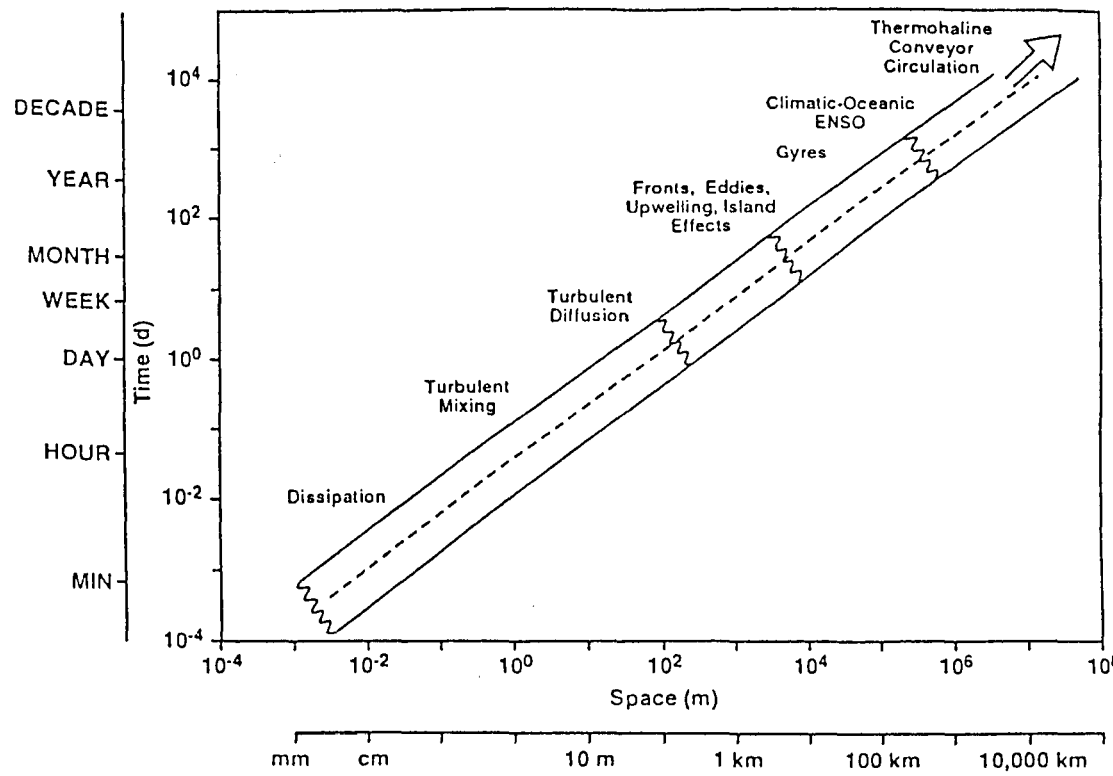

Figure 1.2.: Schematic diagram of physical motions and their space- and time-scales in the ocean. (from IPCC, 1996)

The thermohaline circulation is important for global heat and water transport. It determines the vertical structure of the world oceans (Manabe & Stouffer, 1988) and thereby also influences the distribution of chemical tracers such as dissolved carbon species. This global circulation is predominantly driven by deep water formation in the Greenland, Norwegian, Iceland, and Labrador Seas as the density of saline surface water originating from the equatorial regions is increased by heat loss to the atmosphere. In a simplified form, this convectively formed deep water moves southwards, through the South Atlantic, and is joined by bottom water from the Weddell and Ross Seas as it passes round Antarctica as part of the Circumpolar Current. From there it enters the Indian and Pacific Oceans. Throughout this global journey fractions of this deep water emerge to the surface, where much of it eventually returns to the North Atlantic. One such cycle takes in the order of 500 years. The saline forcing arises chiefly from the fact that the Atlantic Ocean loses more fresh water through evaporation than it receives via precipitation and river run-off. The general climatic impact of the thermohaline circulation has been modelled by Manabe and Stouffer (1988). Their coupled model showed that without this circulation the northern North Atlantic would be ice-covered to south of Iceland with temperatures much lower than at present.

While there is little evidence for recent dramatic changes in the ocean circulation, palaeontological evidence from sea floor sediments demonstrates that the intensity and penetration depth of the thermohaline circulation has varied on a time-scale ranging between 20 thousand years and decades (e.g. GRIP Members, 1993; Dansgaard et al., 1993). The mechanism by which the thermohaline circulation can be weakened include a reduction in

(i) the cooling of the surface water;
(ii) salinity via increased river run-off, precipitation, and ice melt in the regions of deep water formation;
(iii) wind strength.

Such weakening effects due to global warming have been supported by most climate models. Manabe and Stouffer (1994) investigated the effect of radiative forcing on the stability of the conveyor circulation by increasing the atmospheric CO_2 concentration in a coupled atmosphere-ocean model. As anticipated, the circulation weakened, but they also found that the circulation would return to its original mode after a certain length of time

which depended on the extent, rapidity, and duration of the elevation of the atmospheric CO_2 concentration. The overall impact of increases in high latitude fresh water influx has been investigated in ocean-only models. The results suggest that imbalances between the increased input of high latitude fresh water to and its removal by the conveyor could lead to multiple equilibrium solutions (Stommel, 1961; Bryan, 1986; Marotzke, 1988) and variability on a large range of time-scales (Weaver & Sarachik, 1991; Winton & Sarachik, 1993; Winton, 1993). The relative strength of high latitude thermal to fresh water forcing and its effect on the stability and variability of the thermohaline circulation has been investigated using a coarse resolution OGCM (Weaver et al., 1991; 1993). It should be noted that the results obtained with the above mentioned models are useful in pointing out potential circulation changes caused by radiative and/or fresh water forcing as well as potential feedback on climate, but that they fall short of quantification due to significant modelling imperfections.

The overall portrayal of large-scale processes such as the thermohaline circulation and the gyres in coupled models is regarded as reasonably realistic in spite of various remaining shortcomings. Different coarse-resolution ocean-only models have demonstrated the ability of reproducing the major features of global ocean circulation. This includes models such as various box-diffusion models, some of which have been used in ocean carbon uptake studies (Orr, 1993; Siegenthaler & Sarmiento, 1993). While intercomparisons of modelling results for low and mid-latitude regions are encouraging, discrepancies between observed and modelled results in regions of deep convection have revealed significant uncertainties. Data assimilation experiments indicate that these may be caused by weaknesses in model formulation and/or errors in the data (Marotzke & Wunsch, 1993). Gates et al. (1992) outlined the deficiencies in coarse resolution models to that date, i.e.

(i) the representation of geometry and bathymetry;
(ii) parametrization of small-scale processes such as convection, mixing, and meso-scale eddies;
(iii) error of surface-forcing for ocean-alone simulations;
(iv) a thermocline that is often too deep and too diffuse;
(v) weak poleward heat transport;
(vi) distortion of upper ocean and deep boundary currents;
(vii) temperature and salinity errors in deep water.

With coarse resolution models generally split into 1 - 4 vertical and 6 - 30 horizontal levels (30 levels $\propto$ > 1000 km), some of the above points have been addressed by eddy-resolving models. These latter models are split into up to 60 vertical levels with a horizontal breakdown of about 1/6° ($\approx$ 20 km). Nevertheless, some discrepancies between observed and modelled results imply that a resolution of 1/12° ($\approx$ 10 km) may ultimately be needed. Recent modelling efforts for the North Atlantic involved an OGCM with a resolution of 10 - 15 km (Bryan & Holland, 1989; Boning et al., 1991) and a high-resolution model with an alternative formulation based on isopycnal coordinates (Campos & Bleck, 1992). The importance of incorporating smaller bathymetric features has been shown by Döscher et al. (1994). Their simulation of water and heat flow was improved by incorporating details of sills which control the North Atlantic deep water flow. Convection, which is caused by unstable density stratification and which leads to mixing and overturning (Killworth, 1983), usually occurs on a scale of a few kilometers. This makes it difficult to observe and to be picked up by coarse-resolution models. Further deficiencies in ocean models arise from lack of data to evaluate models and to conduct climate projections. This applies to certain geographical regions and the interior of the ocean in general. There is also insufficient account taken of geological influences such as flux from fissures in the ocean floor (Riser (1995) referred to by Dickinson et al. (1996)). On a smaller scale, the representation of the seasonal-interannual variability of upper ocean stratification is adequate in ocean-only but not in coupled models. Further uncertainty in the simulation of global circulation include the accurate simulation of ENSO events and of processes involving sea ice.

Smaller-scale physical processes in the ocean can have a significant effect on local climate, and their representation in models tends to improve the simulation of larger-scale processes in models. The employment of fine-resolution component models in coupled climate simulations is therefore a prerequisite for more reliable projections of global and local climate alike. Similarly, it forms the basis for more reliable carbon cycle models.

1.3.2.2. Physico-chemical and biogeochemical processes

1.3.2.2.1. Seawater carbonate system and the solubility pump

The CO_2 in the atmosphere ($CO_{2(g)}$) tends to equilibrate with the CO_2 dissolved in seawater ($CO_{2(aq)}$) according to the equation:

$$CO_{2(g)} \overset{K_o}{\Leftrightarrow} CO_{2(aq)}, \quad (1.1)$$

where K_o is the solubility coefficient for CO_2 in seawater. The partial pressure of CO_2 (pCO_2) relates to the concentration of CO_2 in seawater by:

$$pCO_2 = [CO_{2(aq)}] / K_o, \quad (1.2)$$

where the quantity in square brackets represents the concentration in the solution. The solubility of CO_2 rises with decreasing temperature and salinity (Weiss, 1974), so that a cooling or freshening of surface seawater leads to a reduction of the pCO_2 in the seawater and, consequently, also in the atmosphere. The transfer across the gas-liquid boundary layer is by molecular diffusion, i.e. a physical process.

The dissolved CO_2 becomes hydrated:

$$CO_{2(aq)} + H_2O \overset{K_H}{\Leftrightarrow} H_2CO_3 \quad (1.3)$$

where K_H is the association constant of CO_2 ($\approx 10^{-3}$)

$$K_H = [H_2CO_3] / [CO_{2(aq)}], \quad (1.3a)$$

so that most CO_2 is in the $CO_{2(aq)}$ form ($H_2CO_3 \approx 0.2\%$ of $CO_{2(aq)}$). In determinations of dissociation constants one does not differentiate between $CO_{2(aq)}$ and H_2CO_3 and the sum of their concentrations is used, usually denoted by CO_2 or H_2CO_3*.

Since the rate coefficient of reaction (1.3) is so slow, another pathway is much more important for the reaction of CO_2 with H_2O:

$$CO_2 + H_2O \overset{K_1}{\Leftrightarrow} H^+ + HCO_3^-, \quad (1.4)$$

where K_1 is the first dissociation constant of carbonic acid. Setting the activity of water equal to one

$$K_1 = (H^+) [HCO_3^-] / [CO_2], \quad (1.5)$$

where (H^+) represents the activity, or chemical potential, of the hydrogen ions. Upon further dissociation:

$$HCO_3^- \overset{K_2}{\Leftrightarrow} H^+ + CO_3^{2-}, \quad (1.6)$$

where K_2 is the second dissociation constant of carbonic acid:

$$K_2 = (H^+)\,[CO_3^{2-}] \,/\, [HCO_3^-]\,. \qquad (1.7)$$

All quantities in square brackets are stoichiometric (i.e. total) concentrations, i.e. any speciation or interaction with other ionic constituents are disregarded. For this reason it is necessary to specify the constants not only as a function of temperature and pressure, but also of salinity and the pH scale used in the determination of the dissociation constants. The values of the activity of hydrogen (H^+) also depend on the pH scale used.

There are three different pH-scales commonly in use. These include the N.B.S. scale ($pH_{(NBS)}$), the $pH_{(SWS)}$ or 'total' hydrogen ion concentration scale, and the 'free' hydrogen ion concentration scale (pH_{free}). A thorough account of these pH scales and the interconversion between them is given by Dickson (1984). In contrast to $pH_{(NBS)}$, the calibrations for the $pH_{(SWS)}$ and pH_{free} are carried out in synthetic seawater. For $pH_{(SWS)}$ the seawater contains sulphate (Hansson, 1973). Dickson and Riley (1979) defined a $pH_{(SWS)}$ which included HF as well as HSO_4^-. Owing to the formation of HSO_4^- and HF, the total hydrogen ion concentration differs from the concentration of free unassociated H^+ ions. $pH_{(SWS)}$ is derived from pH_{free} by correcting for HSO_4^- (and HF if necessary). Dickson (1993) suggests that the inclusion of HF is often not necessary.

Seawater is characterized by an excess cation charge from Na^+, K^+, Mg^{2+}, and Ca^{2+} over the anion charge from strong acids such as Cl^-, SO_4^{2-}, and Br^-. This excess cation charge is balanced chiefly by the dissociation of H_2CO_3 into HCO_3^- and CO_3^{2-} and to a lesser extent by the dissociation of other weak acids present in seawater. It is for this reason that the pH of seawater is on the alkaline side of neutrality, being around 8.1. This balancing of the excess cation charge with bases from dissociated weak acids is one way of describing the total alkalinity (TA) of seawater, usually preferred by geologists. More specific descriptions will be provided in section 1.4 below.

At a normal seawater pH, CO_2, HCO_3^-, and CO_3^{2-} will make up about 0.75%, 90%, and 10% of the total dissolved inorganic carbon (TCO_2), respectively, with

$$[TCO_2] = [CO_2] + [HCO_3^-] + [CO_3^{2-}]. \qquad (1.8)$$

The general relationship between pH and the relative amount of dissolved inorganic carbon species becomes clear by looking at the following sequence:

$$CO_2 + H_2O \Leftrightarrow H^+ + HCO_3^- \Leftrightarrow 2\,H^+ + CO_3^{2-}. \qquad (1.9)$$

The more CO_2 is added to the system, the more this sequence of reactions is shifted to the right leading to an increase in H^+ concentration, i.e. a fall in pH. For every excess CO_2 molecule entering the seawater and which remains undissociated, about 20 additional excess CO_2 molecules will dissociate into the ionic forms of carbonic acid. This dissociation also leads to the release of hydrogen ions, which partially counteract the shift from the non-ionic to ionic dissolved inorganic carbon forms by preferentially binding with the carbonate rather than with the bicarbonate ions. The pH of seawater is therefore largely buffered while there are sufficient carbonate ions to be converted to bicarbonate. This bicarbonate buffering effect is often summarized as

$$CO_2 + CO_3^{2-} + H_2O \Leftrightarrow 2\,HCO_3^- . \qquad (1.10)$$

As the pCO_2 of the seawater increases and the pH decreases, fewer carbonate ions or dissociated forms of other weak acids will be available to buffer this system, and the uptake capacity of the seawater for inorganic carbon decreases. This non-linear relationship between pCO_2 and total dissolved inorganic carbon (TCO_2) can be expressed in terms of

$$\Delta pCO_2 / pCO_2 = \zeta\, \Delta TCO_2 / TCO_2 , \qquad (1.11)$$

where Δ represents the change in the following parameter and ζ is the buffer, or Revelle, factor. The magnitude of the buffer factor reflects the pH change in response to changes in the CO_2 concentration. It assumes that temperature, salinity and alkalinity of the seawater remain constant, and that ΔTCO_2 is much less than TCO_2 (Broecker et al., 1979). It varies in the range of about 7 to 18 between low and high latitude waters, implying that for a 7 to 18% increase in pCO_2 the TCO_2 will increase by only 1% (Shaffer, 1993). This latitudinal range stems from the temperature effect on pCO_2 and biologically induced differences in TCO_2. On a time-scale of usually more than a thousand years the buffering of seawater also involves the interaction between seawater and carbonate sediments:

$$CO_2 + CaCO_3 + H_2O \Leftrightarrow Ca^{2+} + 2\,HCO_3^-. \qquad (1.12)$$

Although the average annual increase in atmospheric CO_2 is about 1.5 ppmv yr^{-1}, the global mean gradient of pCO_2 across the atmosphere-surface ocean interface is currently about 8

μatm. The exchange rate for CO_2 between the atmosphere and surface ocean is determined predominantly by the rate of molecular diffusion across the gas-liquid interface which depends on the thickness of the stagnant boundary layer and the gradient of pCO_2. The boundary layer is about 1 mm thick, but varies with wind speed, possibly also duration of the wind stress and turbulence in the liquid phase. Equilibration is speeded up, if this turbulence gives rise to bubble entrainment. Chemical enhancement of CO_2 uptake results from the dissociation of CO_2, the impact of which depends upon the pH, and the presence of catalysts such as carbonic anhydrase. Since the solubility of CO_2 is greater in colder water, it is also important to take account of the 'surface skin effect', i.e. the fact that the boundary layer is generally cooler than the bulk surface water by about 0.3 °C (Robertson & Watson, 1992).

As far as surface waters are concerned, even at its most rapid, the gas-liquid phase transfer is slow compared with the dissociation steps of CO_2 in seawater and is hence rate determining. This explains why the exact equilibration between the atmospheric and seawater CO_2 concentrations is rarely found. The same is true for the reverse process, i.e. evasion of CO_2 from solution into the gas phase. However, with regard to long-term removal of anthropogenic CO_2 from the atmosphere, gas exchange rates are generally presumed to be fast enough to ensure that the atmospheric and surface ocean pCO_2 are near equilibrium except in regions where vertical water exchange is vigorous. Jain et al. (1995) therefore regard vertical mixing across a stably stratified thermocline as almost certainly the main bottleneck to oceanic uptake of fossil fuel carbon. The typical equilibration time for pCO_2 between the atmosphere and the surface ocean is in the order of a year, and the penetration of excess CO_2 into the thermocline takes several decades. Equilibration with the entire ocean occurs over several centuries, i.e. matching the time-scale of the global conveyor circulation. Modelling the progressive decay of a hypothetical CO_2 pulse indicates that the average CO_2 penetration depth is about 600 meters (Siegenthaler & Sarmiento, 1993). More direct measurements, described in section 1.4.4.2 below, give results in the same range.

All the factors described above which influence carbon flux across the atmosphere-ocean interface lead to considerable regional variations of this flux. Polar regions where deep convection removes the cooled CO_2-enriched seawater from the surface tend to act as global carbon sinks. The reverse tends to apply to equatorial regions with cold seawater rising to the surface and releasing CO_2 to the atmosphere while warming up. Carbon dioxide

drawdown is particularly pronounced in the northern North Atlantic where the conveyor circulation sustains a continuous and long-term removal of CO_2 from the atmosphere. In contrast to earlier believes (Bolin, 1983), Poisson and Chen (1987) have provided evidence that deep and bottom water forming areas of the Antarctic Ocean are less effective as carbon sinks, since the CO_2 exchange between atmosphere and ocean is largely reduced by ice cover (Weiss et al., 1979).

The above physico-chemical mechanisms of atmospheric CO_2 drawdown are sometimes referred to as the 'solubility pump' (Volk & Hoffert, 1985). Its general relevance as a pump has been demonstrated by Sarmiento and Orr (1991), who reviewed the findings from various box-models. Ignoring the anthropogenic CO_2 perturbations, the results suggest that without any atmosphere-ocean carbon flux, the atmospheric CO_2 level would reach about 720 ppmv, while the solubility pump reduces CO_2 to about 450 or 530 ppmv. Consequently, the observed glacial-interglacial change in atmospheric CO_2 concentration cannot be accounted for by this pump alone.

Broecker (1982) estimated that the temperature and salinity effects on pCO_2 would be too small and would largely cancel each other out, e.g. a temperature rise of 1.5 °C would cause a pCO_2 increase of about 20 µatm while the salinity decrease of 3.5 % due to meltwater would decrease the pCO_2 by about 14 µatm. In their polar alkalinity hypothesis, Broecker and Peng (1989) proposed that a restart of the ocean conveyor circulation at the end of the glacial period would reintroduce the low-alkalinity NADW into the circumpolar region. They calculated that this would decrease the TA of Antarctic surface water by 75 µeq kg^{-1}, which could explain the relatively abrupt glacial-interglacial increase in atmospheric pCO_2 of 80 µatm.

Using a more complex OGCM, Heinze et al. (1991) studied the sensitivity of atmospheric CO_2 concentration to changes in the ocean circulation. A general weakening in the ocean circulation during the glacial period finds support in evidence by Shackleton et al. (1988) and Broecker et al. (1988, 1990). The modelled halving of the deep ocean current velocity and its ventilation results in a fall of the CO_2 concentration by 26 ppm. There is evidence that the advective pattern of the thermohaline circulation was altered to a second stable mode, which increases the gradient between well-ventilated surface and intermediate water and less ventilated bottom water (Duplessy et al., 1988; Boyle, 1988; Boyle & Keigwin, 1987).

Heinze et al. (1991) also studied the effects of this change. Simulation of this second mode was achieved by changing the initial geographic distribution of the salinity, i.e. removing 1 ‰ from all areas north of 30°N and adding exactly the same amount of salt to the area south of 30 °S. The resulting reduction in NADW formation was found to lower the CO_2 by 9 ppm. The authors concluded that results involving this change in ocean circulation obviously did not match the observed glacial-interglacial change in CO_2 concentration, but that it at least showed good agreement with observed palaeoceanographic parameters, so that it may well have taken place in combination with biogeochemical changes described below.

With respect to the anticipated CO_2 emissions in the next decades and centuries, Sarmiento et al. (1995) showed that the efficiency of the solubility pump would be significantly reduced at the higher pCO_2 levels which are being considered by the IPCC. This is due to the reduced buffering capacity of the seawater as the pCO_2 of the seawater increases. Nevertheless, Schimel et al. (1995) concluded that, on the time-scale of interest to the IPCC, the exchange of surface seawater with the rest of the ocean would be the main factor limiting the capacity of the oceans to serve as a sink for anthropogenic CO_2.

1.3.2.2.2. Organic carbon pump

In addition to the solubility pump, the pCO_2 in the ocean and atmosphere may be significantly reduced by phytoplankton growth in the euphotic layer of the oceans. The main and obvious mechanism is the utilization of CO_2. To a lesser extent the CO_2 concentration is also decreased indirectly by nitrate utilization, which increases the pH and TA of the seawater. Most of the organic carbon usually gets remineralized in the surface mixed layer (SML), but a fraction of varying size is exported out of this surface layer. This may occur via sinking particles (Martin et al., 1987), mixing and advection of small particles and dissolved organic carbon (DOC) (Shaffer, 1993) and vertical migration of zooplankton (Longhurst & Harrison, 1988). It has been estimated that about 30% of the particulate organic carbon (POC) end up as export production, and it is likely that up to 50% of the exported organic carbon is in form of DOC (Shaffer, 1993). The exported production is remineralized at greater depth, mainly by bacteria. The dissolved inorganic carbon is sooner or later recycled back to the SML via mixing and advection, thus completing this organic carbon cycle within the ocean.

The export production described above has been referred to as the 'organic carbon pump', which forms part of the biological pump. Its strength is determined chiefly by the availability of limiting nutrients such as nitrogen and phosphorus or micronutrients such as iron, the availability of light, and zooplankton grazing. The organic carbon pump creates a deficit of about 10% in TCO_2 between surface and deep waters. Estimates of this flux due to this pump range from 3 to 22 Gt C yr^{-1} depending largely on the methodology employed (Shaffer, 1993). Model simulations suggest a narrower range of 5 - 10 Gt C yr^{-1} (Shaffer, 1993; Bacastow & Maier-Reimer, 1991; Najjar et al., 1992).

Most remineralization tends to take place in subsurface waters and decreases exponentially with depth, but vertical patterns may vary. For example, regeneration of nitrogen and phosphorus occurs higher in the oceans than the release of CO_2 (Shaffer, 1993). Variability in primary production can also lead to considerable horizontal gradients in surface water pCO_2, e.g. Watson et al. (1991) observed parallel changes of several 10 µatm within less than 100 km in the North East Atlantic. On a regional scale, the role of the biological pump in coastal seas remains poorly understood. Up to 30% of total ocean productivity occurs in coastal seas which comprise only 8% of the oceanic surface area. Nevertheless, it is still unclear how large a fraction simply gets reoxidised and how much is permanently removed from the surface by export to deep oceans or by sequestration in sediments of shallow seas and shelves (Schimel et al., 1995). Globally, about 48% of new production takes place in high latitudes, i.e. in the polar North Atlantic and the Southern Ocean (Shaffer, 1993).

While there are considerable daily, seasonal, and interannual variations in export production, there is insufficient evidence to conclude that the strength of the biological pump has been significantly affected by any changes in our current climate (Sarmiento & Siegenthaler, 1992). Furthermore, the absence of variability in atmospheric pCO_2 from the 10th to 18th century and during interglacials has led to the common assumption that the biological pump has operated in a steady-state (Orr, 1993). On the other hand, glacial-interglacial changes in the organic carbon pump may well have played a considerable part in the atmospheric pCO_2 reduction of about 80 ppmv during the last glacial period. Sarmiento and Toggweiler (1984), who used a relatively simple 3-ocean box model, found that a change of 70 ppm could be achieved within a thousand years by a 4 to 5-fold increase in high latitude primary production if combined with a halving of the thermohaline

circulation strength. Similarly, Heinze et al. (1991) tested the 'polar nutrient hypothesis' and discovered that doubling POC production at high latitudes would lead to a reduction in pCO_2 of about 30 ppm. Although they consider possible changes in circulation, they did not make it clear whether or how the concomitant changes in the solubility pump are accounted for in this model test.

One of the mechanisms which could operate on a decade-to-century time-scale involves changes in the so-called Redfield ratio, which quantifies the molecular ratio of particulate C:N:P:-O ratio in living organic matter as 106 : 16 : 1 : -138 according to Redfield et al. (1963). This ratio also applies to the concentration of respective inorganic nutrients dissolved in ocean waters other than the SML. Revisions of this originally proposed ratio include attempts by e.g. Takahashi et al. (1985), Boulahdid and Minster (1989) and Anderson and Sarmiento (1994), with the exact values of this Redfield ratio remaining a matter of dispute. For example, Anderson and Sarmiento suggested a ratio of 117 : 16 : 1: - 170 on the basis of nutrient concentration determinations from several different ocean basins between 400 to 4000 m depths. Measurements from the upper 400 m were excluded to avoid interference from anthropogenic CO_2 which is assumed to have penetrated the upper layers of the oceans by now. Unfortunately, most of the regeneration of POM takes place there (Martin et al., 1987), thus leading to local deviations from the mean nutrient ratio, which ideally ought to be taken into account in the proposed mean ratio. Nevertheless, Brewer et al. (1997) recommend the use of the ratio according to Anderson and Sarmiento (1994).

The effect of changes in the Redfield ratio and other mechanisms have been examined by Heinze et al. (1991). Their results suggest that a 30% increase in the ratio of particulate carbon to phosphorus provided the greatest qualitative consistency with palaeoceanographic data and also triggered the largest reduction in atmospheric CO_2 concentration, i.e. 72 ppm. This mechanism had been suggested by P. Weyl as cited by Broecker (1982). A lowering of 61 ppm was achieved by a 30% increase in the nutrient input to the oceans. The phosphate increase was in actual fact intended to simulate a nitrate increase as an inverse test for the denitrification hypothesis proposed by Berger and Keir (1984). It implies that nitrogen could have been expelled to the atmosphere from shallow anoxic shelf regimes through denitrification, leading to a strong reduction of nitrate and a weakening of the organic carbon pump at the end of the ice age. The results from either test indicate that neither mechanism can singularly account for the observed glacial-interglacial

change in pCO_2. The overall potential of the organic carbon pump to affect atmospheric pCO_2 was estimated by Shaffer (1993), who employed a more complex 4-ocean-box model. Doubling of the Redfield ratio and of high latitude new production was found to reduce the pCO_2 by about 120 and 50 ppm, respectively.

There is a different angle to the potential significance of oceanic denitrification which is not yet included in most biogeochemical ocean models. Dinitrogen may be fixed in well-oxygenated surface layers of the ocean although molecular O_2 is a potent inhibitor of N_2 fixation in many marine microorganisms. Paerl and Carlton (1988) demonstrated that growth of nitrifying organisms such as eubacteria and cyanobacteria could nevertheless be maintained in O_2-depleted microzones which were associated with colonizable inorganic and organic surfaces. Karl et al. (1997) have provided supportive evidence for the potential importance of N_2 fixation to export production in the subtropical North Pacific Ocean, at least on a short term (< 100 years) time-scale. The fixation of N_2 depends on nitrogenase, an enzyme-complex which relies on iron and molybdenum for synthesis and functioning. Denitrification, the reverse process to N_2 fixation in the surface layers of the oceans, reduces nitrate to gaseous nitrogen species, usually N_2 and N_2O. This represents the dominant mechanism for removal of fixed nitrogen from the biosphere. It is mediated by bacteria in sub-oxic environments, i.e. where oxygen saturation is less than 1-2%. Half of the global marine denitrification occurs in the water column, the other half in shelf sediments (Devol, 1991). The main regions contributing to global denitrification in the water column are the eastern tropical North Pacific and the Arabian Sea (Codispoti, 1995; Altabet et al., 1995). Isotopic evidence from sediments indicates that variations in denitrification were occurring in parallel to the Milankovitch cycles with greatly reduced denitrification occurring during the last glacial maximum (LGM) (Altabet et al.; Ganeshram et al., 1995).

The implications of the above findings are discussed and summarized by Codispoti (1995). Unless changes in denitrification are balanced by N_2-fixation, these shifts in the oceanic nitrogen budget could have a significant effect on atmospheric CO_2, i.e. reduced denitrification would have made more NO_3 available for primary production thus strengthening the biological pump. This finds further support by Falkowski (1997) who argues that the ratio of the two opposing processes appear to have been determined by the oxidation state of the ocean and supply of trace elements, especially iron. With respect to the near future, Falkowski considers it difficult to predict the extent or even the direction of

any changes in the ratio of N_2 fixation/ denitrification in the oceans and he stresses the importance of including these processes in biogeochemical ocean models.

The primary production in high-nutrient-low-chlorophyll regions such as the Southern Ocean or subarctic North Pacific may presently be limited by iron (Martin & Fitzwater, 1988). Hence increased aeolian supply of iron from exposed shelf regions may have enhanced global POC production during the glacial period. On the basis of the above 'iron hypothesis', Sarmiento and Orr (1991) used a 3-dimensional OGCM to test the effectiveness of possible iron-fertilization treatment in reducing atmospheric pCO_2 levels. Assuming the business-as-usual-emission scenario and 100% nutrient removal over a period of 100 years, iron fertilization was found to have the greatest impact in the Southern Ocean, reducing the CO_2 by about 70 ppm compared to no fertilization treatment. The reduction in other regions of interest only amounted to about 10 ppm, or less, because of the shallow depth of the SML in the North Pacific and the prevalance of other limiting factors in the North Atlantic. Total global reduction of atmospheric pCO_2 by this treatment would therefore represent less than 10% of the atmospheric pCO_2 level anticipated by the year 2100. Assuming a constant-emission scenario, this fraction would still only amount to about 20%.

Sarmiento and Toggweiler (1984) estimated that the introduction of a fully efficient organic carbon pump, which uses all the available surface nutrients, to an abiotic ocean with only a solubility pump in operation would lower the atmospheric pCO_2 from about 450 or 530 to 160 ppm. A partially operational organic carbon pump as found in the pre-industrial ocean reduces the pCO_2 to 250 ppm (Shaffer, 1993). This value takes account of the nitrate utilization effect on TA and thus on pCO_2 but excludes calcification effects. Nevertheless, the above assumed changes in the Redfield ratio by 50% or 30% are unlikely to occur (Shaffer, 1993).

In summary, with respect to the anticipated atmospheric pCO_2 levels neither of the mechanisms causing a change in the organic carbon pump are likely to have a significant impact on reducing the anthropogenic CO_2 burden, at least not on the time-scale of concern to the IPCC. In view of this and other findings, additional mechanisms of oceanic carbon uptake have been considered, which are not constrained by carbon-nutrient coupling, at least not directly.

1.3.2.2.3. $CaCO_3$ pump

Various groups of organisms produce particulate calcium carbonate, or particulate inorganic carbon (PIC), in the oceans. Up to half of the oceanic $CaCO_3$ removal from the dissolved phase may occur in shelf regions in the form of aragonite and calcite production by coral reef complexes (Opdyke & Walker, 1992). The remaining marine calcification is attributed to calcite producing coccolithophorids, motile and encysted dinoflagellates , foraminifera, and aragonite forming pteropods (e.g. Riding, 1991; J. Young, pers. comm.). Coccolithophorids are estimated to make up approximately 70% on average of the calcite in open ocean sediments (J. Young, pers. comm.). Aragonite is less stable than calcite, and it dissolves at relatively shallow depths. It is therefore only of biogeochemical significance in shallow coastal waters and on continental shelves.

Independent of the particulate $CaCO_3$ form, calcification may proceed from bicarbonate, with net reaction following equation 1.12, or carbonate:

$$Ca^{2+} + CO_3^{2-} \overset{K_{sp}}{\Leftrightarrow} CaCO_3 , \qquad (1.13)$$

where K_{sp} is the solubility product of aragonite or calcite. Surface coatings of a composition different from those of the bulk phases were shown to retard precipitation by Chave and Suess (1970). Carter (1978) demonstrated that biogenic and non-biogenic carbonate surfaces selectively adsorb aspartic-acid-rich organic matter.

Even though the TCO_2 is reduced by calcification, the concomitant reduction in pH increases the relative proportion of the non-ionic dissolved inorganic carbon to such an extent that the concentration of CO_2 and the pCO_2, in fact, increase. For example, high rates of $CaCO_3$ production by coccolithophorid-dominated populations were found to increase the pCO_2 by 15 µatm during a cruise in the Northeast Atlantic in 1991 (Robertson et al., 1994). Similar trends were observed during early growth of an *Emiliania huxleyi* bloom in a mesocosm study by Purdie and Finch (1994).

The ratio of released CO_2 to precipitated carbonate has been calculated by Frankignoulle and Canon (1994) to be about 0.65 for our present ocean. This ratio increases with increasing pCO_2 due to the non-linearity of the bicarbonate buffer system and shows a negative relationship with temperature and salinity. In this context, it is important to bear in mind that this ratio only refers to $CaCO_3$ production *per se* and not to the growth of

calcifying algae altogether. Coccolithophorids require CO_2 for POC production like most photosynthesing algae and are thought to derive it either from the external medium or from inside the cell when it is liberated during calcification (e.g. Paasche, 1962). Disregarding the net effect of nutrient uptake on TA and thus on pCO_2, it follows that coccolithophorid growth raises pCO_2 levels only if the diel POC:PIC net production ratio by these organisms is smaller than about 0.65. In the case of nitrate utilization this value is in fact slightly smaller still, and the reverse is true for ammonia utilization. Paasche (1962) reported POC:PIC production ratios of near 1 for *Emiliania huxleyi*, however, subsequent work has suggested that this ratio is likely to vary greatly between coccolithophorid species, and with the growth stage of the organism (Purdie & Finch, 1994). Due to diurnal variations in net photosynthesis and net calcification, Crawford and Purdie (1997) also draw attention to the importance of considering the time-scale of the experiments when estimating POC:PIC production ratios in field and culture.

Until recently it has generally been assumed that in the open ocean all or most of the particulate $CaCO_3$ is exported out of the SML, either via sinking or transport in the guts of zooplankton. Depth-dependent pressure increase, temperature decrease and pCO_2 increase promote the dissolution of particulate $CaCO_3$, thus reversing the chemical processes of the surface layer. However, about 20% of the particulate $CaCO_3$ produced is estimated to settle on the ocean floor and to be sequestered in the sediments. This loss is assumed to be in balance with input from rivers. As with the organic carbon cycle, the dissolved $CaCO_3$ will be returned to the SML by advection or mixing, thus completing the shorter of the the $CaCO_3$ cycles operating in the ocean. The time-scale of this cycle is longer than for organic carbon since the mean depth of $CaCO_3$ regeneration is greater.

A range of conclusions have been drawn with respect to the vertical profile of dissolution, which may all be valid under different circumstances (Boyle, 1988). While some authors have assumed that dissolution occurs only on the ocean floor (Dymond & Lyle, 1985; Sarmiento et al., 1988), there is multiple evidence indicating that some dissolution occurs even above the saturation horizons for aragonite and calcite in the deep water column and even in the SML (e.g. Milliman et al., 1999; Young, 1994; Bleijswijk et al., 1994). This phenomenon may be explained by respiratory CO_2 release creating microenvironments sufficiently acidic to cause localized dissolution of PIC. In the SML, however, the kinetics of calcification and concomitant pCO_2 increase depend on the dominant phytoplankton

species and their growth and calcification rates. These rates may vary with season and environmental conditions, e.g. coccolithophorids are clearly outcompeted by certain diatom species during spring phytoplankton bloom conditions in mid- and high latitudes (Winter & Siesser, 1994).

The global and regional distribution of particulate $CaCO_3$ production has been mainly related to conditions which offer a competitive advantage over non-calcifying phytoplankton, in particular, diatoms. This condition is given under limiting silicate availability (Maier-Reimer (1993) and references therein), and possibly also under low concentrations of dissolved CO_2 as may be implied by the findings of Riebesell et al. (1993). Superimposed is a temperature effect, i.e. calcification is decreased at lower temperatures of approximately less than 4°C (Lisitzin, 1971; Dymond & Lyle, 1985; Tsunogai & Noriki, 1991). Shaffer (1993) estimated that total biogenic $CaCO_3$ production amounts to about 0.9 Gt C yr^{-1}, of which approximately 40% takes place at high latitudes. He has calculated that, for an ocean which is already influenced by the solubility and a partially operative organic carbon pump, the inclusion of this so-called '$CaCO_3$ pump' would raise the atmospheric pCO_2 from 250 to the pre-industrial level of 280 ppm.

With respect to the near future, Frankignoulle and Canon (1994) have demonstrated that a fixed amount of calcification will have a greater impact under the anticipated elevated pCO_2 levels in the atmosphere due to the decreased buffering of the seawater bicarbonate system. At the same time, the temperature increase will have a slight reverse effect. At 15° C, for instance, a doubling of the pre-industrial level to 580 ppmv will raise the ratio of released CO_2 toprecipitated carbonate from 0.64 to 0.76, while a temperature increase of 5° C will lower it by about 0.02 - 0.03. Assuming a current estimate of annual carbonate production of about 1 Gt C yr^{-1}, the purely thermodynamically driven increase in CO_2 release by calcification would amount to about 0.13 Gt C yr^{-1}. Shaffer (1993), who noted the non-linearity of the seawater carbonate system, estimated that a doubling of $CaCO_3$ production without long-term compensatory interactions with the sediments would lead to a pCO_2 increase of about 20 ppm in low and mid-latitudes. In high latitudes, on the other hand, it had little effect. Presumably, this meridional difference arises from the greater buffer capacity and the much shorter exposure time of surface water with the atmosphere due to deep convection in these latitudes. Shaffer further found that the doubling of the $CaCO_3$

dissolution depth had only a very small increasing effect on pCO_2, even if sedimentary $CaCO_3$ compensation was accounted for.

Implicit in the assumed steady-state of the biological pump throughout the recent centuries is the relative stability of the $CaCO_3$ pump. On the other hand, changes in the relative or absolute strength or operational sites of the $CaCO_3$ pump have been considered as likely causes for glacial-interglacial shifts in atmospheric pCO_2. However, in all suggested scenarios this involves the so-called CO_3 compensating mechanism. Due to the pressure effect on the solubility of calcite in seawater, the ocean is typically supersaturated at shallow and intermediate depths and undersaturated in the deepest waters. The fraction of calcite that is sequestered in the sediments therefore is determined by the depth of calcite saturation (Archer & Maier-Reimer, 1994) or aragonite compensation or lysocline (Broecker, 1982), depending upon whether a chemical or a palaeoceanographic view point is taken. The saturation horizon defines the depth below which $CaCO_3$ is no longer supersaturated, and the lysocline distinguishes the depth below which the effect of $CaCO_3$ solution is observed in ocean sediments. These depths remain relatively constant provided the predominantly riverine input of dissolved $CaCO_3$ from terrestrial weathering and alterations is balanced by loss of $CaCO_3$ through deep and shallow sea deposition. In case of an imbalance such as caused by increased POC production at the end of the glacial period, the carbonate concentration and thus TA would be raised with the inverse effect on TCO_2 and pCO_2. This imbalance would be compensated for by an increase in the fraction of $CaCO_3$ being lost to the sediments, which would be reflected in the deepening of the $CaCO_3$ saturation and compensation depths. This would lower the pH and raise the pCO_2, thus counterbalancing much of the original pCO_2 reduction at the end of the glacial period. However, TCO_2 and TA would be lowered by roughly equimolar amounts, since the loss of TCO_2 to POC production would be counterbalanced more or less by the same amount of TCO_2 loss to $CaCO_3$ sediments.

Assuming a mean replacement time of carbon in the oceans of 200 kyr and the concentration of carbonate comprising 1/30th of that of TCO_2, Broecker (1982) derives a time-scale of 7 kyr for this CO_3 compensating mechanism. Shaffer (1993) states a time-scale of 10 kyr, while Boyle (1988) assumes a response lag of 2.5 - 6 kyr. In any case, these periods would be too long to explain the observed glacial-interglacial change in atmospheric pCO_2, which occurred within about 1000 years. Further, this time-scale is of no concern to the IPCC.

However, temporary imbalances in the pCO_2 may have been triggered by changes in ocean circulation and biology which could match at least the glacial-interglacial constraint of time.

It is now generally accepted that glacial-interglacial shifts were related to a substantial reorganization of TCO_2 and TA in the oceans (Boyle, 1988; Broecker & Peng, 1989). Various mechanisms have been put forward, some of which may also affect atmospheric pCO_2 levels on a century-time-scale.

One such mechanism was proposed by Berger (1982) as the 'coral reef hypothesis', and further refined by Berger and Keir (1984) and Opdyke and Walker (1992). Berger summarizes the atmospheric CO_2 changes over 100 kyr cycles with a two-step equilibration between the atmosphere and ocean. His hypothesis calls for shelf carbonate build up by corals and other shelf inhabiting organisms during glacial transgression, which releases some CO_2 to the upper ocean and the atmosphere. The remaining CO_2 is subsequently mixed into the deep ocean and neutralized on the deep sea floor by the dissolution of carbonate. In essence, his hypothesis uses the concept of basin-to-shelf transfer of carbonate during transgression. Heinze et al. (1991) tested this hypothesis by assuming an addition of about 2500 Gt C in form of $CaCO_3$ (assuming 30%increase of PO_4, equimolar POC increase, and a 1:2 ratio for POC:PIC addition). They found that the reduction in atmospheric CO_2 was only 17 ppm. In addition, Archer and Maier-Reimer (1994) pointed out that this hypothesis would require the deep sea burial to be 2 to 3 times greater than is presently the case. Under such circumstances, high calcite sediments would dominate the sea floor, which is not confirmed by the sedimentary record of the LGM. Although this mechanism does not account for the entire glacial-interglacial pCO_2 signal, it may have played a partial role. Since the anticipated change in sea level over the next centuries by no means matches the glacial-interglacial rise, this specific mechanism is not regarded as relevant to the IPCC.

Boyle (1988) proposed that the reduction of atmospheric pCO_2 during the last glacial period had been caused by a shift of metabolic CO_2 and other nutrients from intermediate to deeper waters. This would have occurred at the end of the last interglacial period. As possible triggers for this vertical nutrient shift, Boyle considered changes in ocean circulation such as a shift from NADW to NAIW (North Atlantic Intermediate Water) formation (Boyle & Keigwin, 1987), an increase in Mediterranean outflow (Oppo & Fairbanks, 1987), or an increase in upwelling at low latitudes. The latter would increase

surface POC production giving rise to a proportional increase in export production reaching the deep ocean (Boyle, 1986). Further, increased aeolian supply of iron to the subpolar higher nutrient waters which form Pacific intermediate waters could have also increased POC production (Martin & Fitzwater, 1988), and could account for a nutrient shift from intermediate to deep waters in the Pacific. Boyle's fifth suggestion is based on the finding that high-productivity events lead to larger proportions of export production reaching greater depths, so that this mechanism relies on an increase in the frequency of these events during the glacial period.

Boyle (1988) points out that in any of these scenarios the atmospheric pCO_2 would only be affected indirectly via the CO_3 compensating mechanism. However, all five suggestions by Boyle would inadvertently imply concomitant changes in the organic carbon pump to varying extents, which would directly influence atmospheric pCO_2. This was, for example, demonstrated by the iron sensitivity study conducted by Sarmiento and Orr (1991) as described above. It therefore appears questionable whether Boyle's assumption is justified. Apart from the coral reef hypothesis, which depends on shelf exposure, it may be altogether inappropriate to assume that the $CaCO_3$ cycle changes without affecting the organic carbon cycle and vice versa.

1.3.2.2.4. Interaction between and relative importance of carbon pumps

On a time scale of millions of years, $CaCO_3$ burial will remove carbon more effectively from the ocean/atmosphere system than will $CaSiO_3$ burial, since the metamorphosis of $CaCO_3$ to $CaSiO_3$ leads to the release of one CO_2 molecule:

$$CaCO_3 + SiO_2 \longrightarrow CaSiO_3 + CO_2 \qquad (1.14)$$

Accordingly, phytoplankton species may be more appropriately grouped into carbonate producers, silicate producers (diatoms), and those which produce only organic carbon. However, the net removal of one CO_2 molecule by $CaCO_3$ burial is balanced out during silicate rock weathering in the soil (Berner & Lasaga, 1989):

$$2\,CO_2 + H_2O + CaSiO_3 \longrightarrow Ca^{++} + 2HCO_3^- + SiO_2 \qquad (1.15)$$

This process involves a time-scale far beyond the concerns of the IPCC.

The aspect of the relative importance of the two biological carbon pumps is incorporated in the 'rain ratio hypothesis'. Berger and Keir (1984) and Dymond and Lyle (1985) proposed that the export production of biogenic $CaCO_3$ was reduced relative to that of POC during glacial periods. This would have lowered the effect of the $CaCO_3$ pump on pCO_2 in the SML, and the surface ocean would have absorbed more CO_2 from the atmosphere.

The reported range of the ratio for exported POC:PIC, which is usually derived from alkalinity data, is 2.6 to 8.6 (Broecker, 1982; Garcon & Minster, 1988). A commonly used mean ratio is 4, but Boyle (1988) for example used a ratio of 5. He argues that the discrepancy between this and the former value accounts for a fraction of riverine $CaCO_3$ which forms part of the PIC rain without involvement in biological new production. Shaffer (1993) observed a ratio of 5.5 from modelling derived annual export production of POC and PIC, which amounted to 5.0 and 0.9 Gt C yr^{-1}, respectively.

Geographical variations in this ratio largely match the criteria established by Lisitzin (1971), which link low productivity regimes and higher temperatures to a competitive advantage of coccolithophorids over diatoms. Modelling results by Shaffer (1993) confirmed the reviewed notion that the ratios may be highest in high latitude waters where calcifying organisms are less common. Maier-Reimer (1993), who included a numerical formulation of the dependence of silicate availability and temperature, substantiates Lisitzin's observations and in parts also Shaffer's results, i.e. ratios are highest at the equator due to strong upwelling of silicate, lowest in subtropical waters, and they increase again towards higher latitudes with declining temperatures. Accordingly, increased upwelling and decreased temperatures during the glacial period may also have caused a decline in coccolithophorid growth and an increase in the POC:PIC ratio. In Broecker's (1982) investigation of potential causes for the glacial-interglacial change, he made the assumption that the ratio had not changed. He calculates that the observed range in ratio of 2.6 to 8.2 leads to a difference in atmospheric pCO_2 of only about 60 ppm which led him to conclude that changes in this ratio would not have been important. Likewise, Heinze et al. (1991) found that doubling of the ratio to 8 only reduced the atmospheric pCO_2 by 28 ppm, and their model results did not always match the observed sedimentary record.

In a more inclusive model, Archer and Maier-Reimer (1994) demonstrated that the above results had significantly underestimated the impact of changes in the POC:PIC ratio due to

the omission of modelled POC and PIC interactions in sediment pore water. In their 'respiratory calcite dissolution hypothesis' they took account of the CO_2 release during oxic POC degradation in sediments and its promotion of PIC dissolution (Emerson & Bender, 1991; Archer, 1991). They argued that a change in relative rates at which POC and PIC are deposited would create a CO_3 imbalance at the ocean-sediment interface which would set off the CO_3 compensation mechanism and ultimately a change in atmospheric pCO_2. By combining the ocean-circulation-carbon cycle model used by Heinze et al. (1991) and Maier-Reimer (1993) with the sediment calcite dissolution model by Archer (1991) they found that a 40% increase in organic carbon degradation in pore waters would be sufficient to achieve the glacial reduction of atmospheric pCO_2. Their results are corroborated by the equatorward move of the front between calcifying and silicifying algae (Howard & Prell, 1992). This implies a general increase in POC production and potentially a shift from calcifying to silicifying organisms during the glacial period. Although Archer and Maier-Reimer (1994) did not dismiss the coral reef hypothesis entirely, they pointed out that this hypothesis would imply a uniformly high calcite content in the glacial sediments. This has not been observed in these sediments, which show a better match with the constraints imposed by the respiratory calcite hypothesis.

Using a box model of the atmosphere and ocean, Hausman and McElroy (1996) evaluated mechanism involving changes in nutrients, productivity, ocean circulation and the alkalinity budget to reconstruct the glacial-interglacial shift in pCO_2 in accordance with palaeoceanographic data. They found that neither of these mechanisms on their own reproduced the observed magnitude or apparent rapidity of the transitions in atmospheric pCO_2. Consequently, Hausman and McElroy presented a composite mechanism instead.

While changes in the POC:PIC ratio may have played a significant role in palaeontological times, they are not considered relevant to the present climate change concerns as the mechanisms as described above rely on sedimentary CO_3 compensation.

The relative importance of the different carbon pumps in regulating the pCO_2 in a modern pre-industrial ocean was estimated by Shaffer (1993) as 1 : 0.56 : -0.16 for the organic pump: solubility pump: $CaCO_3$ pump. He stresses, though, that the physical pump is an integral part of the biological pump. This had already been demonstrated by Sarmiento and Toggweiler (1984) who modelled the potential impact of the biological pump on a pre-

industrial atmospheric pCO_2 under varying strength of the thermohaline circulation. They estimated that without any such circulation a fully functional biological pump would lower the CO_2 concentration from the pre-industrial level to 160 ppm, while its absence would raise the CO_2 to 425 ppm. Applying the present strength of circulation, the biological impact is lessened and this range is narrowed to 190 and 300 ppm, respectively. According to these calculations, the biological pump is assigned a much smaller role than stipulated by Shaffer. Similarly, Broecker (1991) estimated the biological role as only 10%, unfortunately, without specifying the origin of this value. A possible reason for this discrepancy may be Broecker's earlier assumption that atmospheric CO_2 is greater than 1000 ppm if no carbon pumps are in operation and the ocean is completely mixed and isochemically heated (Broecker, 1982).

The above examples of estimates of the impact of the different carbon pumps on the CO_2 concentration demonstrate the degree of uncertainty amongst different marine scientists with respect to the exact operation of the oceanic carbon cycle. This uncertainty becomes even more apparent in the various attempts to predict changes in the relative strengths of the pumps under the conditions of the anticipated changed climate. For example, Broecker (1991) reckons that the strength of the biological pump would only change if associated with changes in transport of carbon into the interior of the ocean. Considering the predicted reduction in the thermohaline circulation as a result of global warming (e.g. Manabe & Stouffer, 1993), Broecker (1991) expects this transport to be reduced, thus causing a pCO_2 increase. He considers it likely that this effect will be greater than the pCO_2 reduction due to extended residence time of water in the SML, which would allow more effective stripping of nutrients by phytoplankton. The net effect is expected to be minimal. On this basis, and the apparent stability of the biological pump in the recent past, Broecker (1991) does not assign a significant role to the biological pump in influencing the anticipated changes in atmospheric pCO_2.

Other scientists have used a somewhat different argument. As a consequence of the reduced thermohaline circulation and vertical mixing, nutrient transport to the surface would be reduced, which would weaken the biological pump. At the same time, reduced water mass transport of CO_2-rich water to the surface would have the opposite effect on the atmospheric CO_2. Models which use a constant Redfield ratio indicate that the latter effect is slightly larger, leading to a small increase in oceanic carbon storage in the order of 10s

rather than 100s ppm (Bacastow & Maier-Reimer, 1991; Keir, 1994). For example, Heinze et al. (1991) estimate a CO_2 reduction of 26 ppm in response to halving the deep ocean current velocity and its consequences on nutrient recycling and primary production. So, although there is little evidence so far that the biological pump will play an important part one way or the other with respect to increasing atmospheric CO_2 levels, marine scientists are still unable to agree on the relative importance of the different pumps and mechanisms (see also Siegenthaler & Sarmiento, 1993; Schimel et al., 1995).

On the basis of the findings by Heinze et al. (1991), the IPCC (1996) concludes that dramatic changes in marine biology would have to occur before a change in atmospheric CO_2 of more than 10 ppm would take place. However, the IPCC stresses that those and other modelling results are still preliminary, and the panel points out that climate change may trigger biogeochemical imbalances which are not yet adequately understood and quantified and therefore not yet considered in carbon cycle models. Fiadeiro (1980), for instance, demonstrates that potential changes in the ecosystem structure would influence the form in which the carbon leaves the SML and how it survives the descent through the water column, thereby affecting the regeneration depths of organic and inorganic carbon as well as the other nutrients. Shaffer (1993) concludes that these changes in deep-sea processes demand equal attention in carbon cycle studies to those occurring at the surface since they may become significant on a century-time-scale. This is further supported by Honjo (1996), who divided different oceanic regions into silicate and carbonate oceans on the basis of the relative importance of $CaCO_3$ to SiO_2 and POC in export production collected in sediment traps. His conclusion was that carbonate oceans such as the North Atlantic and the equatorial Pacific may not lead to immediate removal of excess CO_2, but on larger time-scales, vigorous $CaCO_3$ dissolution could increase the importance of this 'alkalinity pump' in removing excess CO_2.

1.4. ALKALINITY AND ITS RELEVANCE IN GLOBAL CARBON CYCLE STUDIES

1.4.1. DEFINITIONS OF ALKALINITY

A thorough historical account of the evolution of the alkalinity concept is presented by Dickson (1992). The currently accepted definition of total alkalinity of a seawater sample originates from a previous paper by the same author (1981). Dickson defines TA of a natural water "as the number of moles of hydrogen ion equivalent to the excess of proton acceptors (bases formed from weak acids with a dissociation constant $K \leq 10^{-4.5}$, at 25 °C and zero ionic strength) over proton donors (acids with $K > 10^{-4.5}$) in one kilogram of sample". The units used for TA are equivalents (eq) expressed as either per dm^3 or kilogram.

If one considers the common acid-base systems in seawater such as

$$\mathbf{CO_3^{2-}} + 2\,H^+ \overset{K_2}{\Leftrightarrow} \mathbf{HCO_3^-} + H^+ \overset{K_1}{\Leftrightarrow} H_2CO_3 \qquad (K_2 \approx 10^{-8.4}\,;\, K_1 \approx 10^{-5.9}) \qquad (1.16)$$

$$\mathbf{B(OH)_4^-} + H^+ \Leftrightarrow H_3BO_3 + H_2O \qquad (K \approx 10^{-8.7}) \qquad (1.17)$$

$$\mathbf{OH^-} + H^+ \Leftrightarrow H_2O \qquad (K \approx 10^{-13.3}) \qquad (1.18)$$

$$SO_4^{2-} + H^+ \Leftrightarrow HSO_4^- \qquad (K \approx 10^{-1.1}) \qquad (1.19)$$

$$F^- + H^+ \Leftrightarrow HF \qquad (K \approx 10^{-2.6}) \qquad (1.20)$$

the appropriate proton condition defining the equivalence point for an alkalinity determination is

$$[H^+] + [HSO_4^-] + [HF] = [HCO_3^-] + 2[CO_3^{2-}] + [B(OH)_4^-] + [OH^-]. \qquad (1.21)$$

Correspondingly, the expression for TA is

$$TA = [HCO_3^-] + 2[CO_3^{2-}] + [B(OH)_4^-] + [OH^-] - [H^+] - [HSO_4^-] - [HF]. \qquad (1.22)$$

The $[OH^-]$ here includes OH^- bound to magnesium. The species in bold script are the ones which contribute to TA as defined by Dickson (1981). When TA is measured, HF and HSO_4^-

can contribute to the actually measured TA, which makes it necessary to subtract their concentrations from the measured TA.

Under certain conditions, further acid-base systems may significantly influence TA:

$$\mathbf{PO_4^{3-}} + 3\,H^+ \overset{K_3}{\Leftrightarrow} \mathbf{HPO_4^{2-}} + 2\,H^+ \overset{K_2}{\Leftrightarrow} H_2PO_4^- + H^+ \overset{K_1}{\Leftrightarrow} H_3PO_4$$

$$(K_3 \approx 10^{-14.9};\ K_2 \approx 10^{-6.1};\ K_1 \approx 10^{-1.7}) \qquad (1.23)$$

$$\mathbf{SiO_2(OH)_2^{2-}} + 2\,H^+ \overset{K_2}{\Leftrightarrow} \mathbf{SiO(OH)_3^-} + H^+ \overset{K_1}{\Leftrightarrow} Si(OH)_4$$

$$(K_2 \approx 10^{-12.6};\ K_1 \approx 10^{-9.5}) \qquad (1.24)$$

$$\mathbf{S^{2-}} + 2\,H^+ \overset{K_2}{\Leftrightarrow} \mathbf{HS^-} + H^+ \overset{K_1}{\Leftrightarrow} H_2S \qquad (K_2 \approx 10^{-13};\ K_1 \approx 10^{-7}) \qquad (1.25)$$

$$\mathbf{NH_3} + H^+ \Leftrightarrow NH_4^+ \qquad (K \approx 10^{-9.3}) \qquad (1.26)$$

The complete TA term becomes therefore:

$$\begin{aligned} TA = {} & [HCO_3^-] + 2[CO_3^{2-}] + [B(OH)_4^-] + [OH^-] \\ & + [HPO_4^{2-}] + 2\,[PO_4^{3-}] + [SiO(OH)_3^-] + [HS^-] + [NH_3] + \ldots \\ & - [H^+] - [HSO_4^-] - [HF] - [H_3PO_4] - \ldots \end{aligned} \qquad (1.27)$$

The ellipses stand for additional or yet unidentified acid-base species, for example, pH indicators used in colourimetric analyses or organic acids.

A Bjerrum plot as shown in figure 1.3 helps to give an idea which species of the major acid-base systems are important at a given pH and which ones contribute to TA.

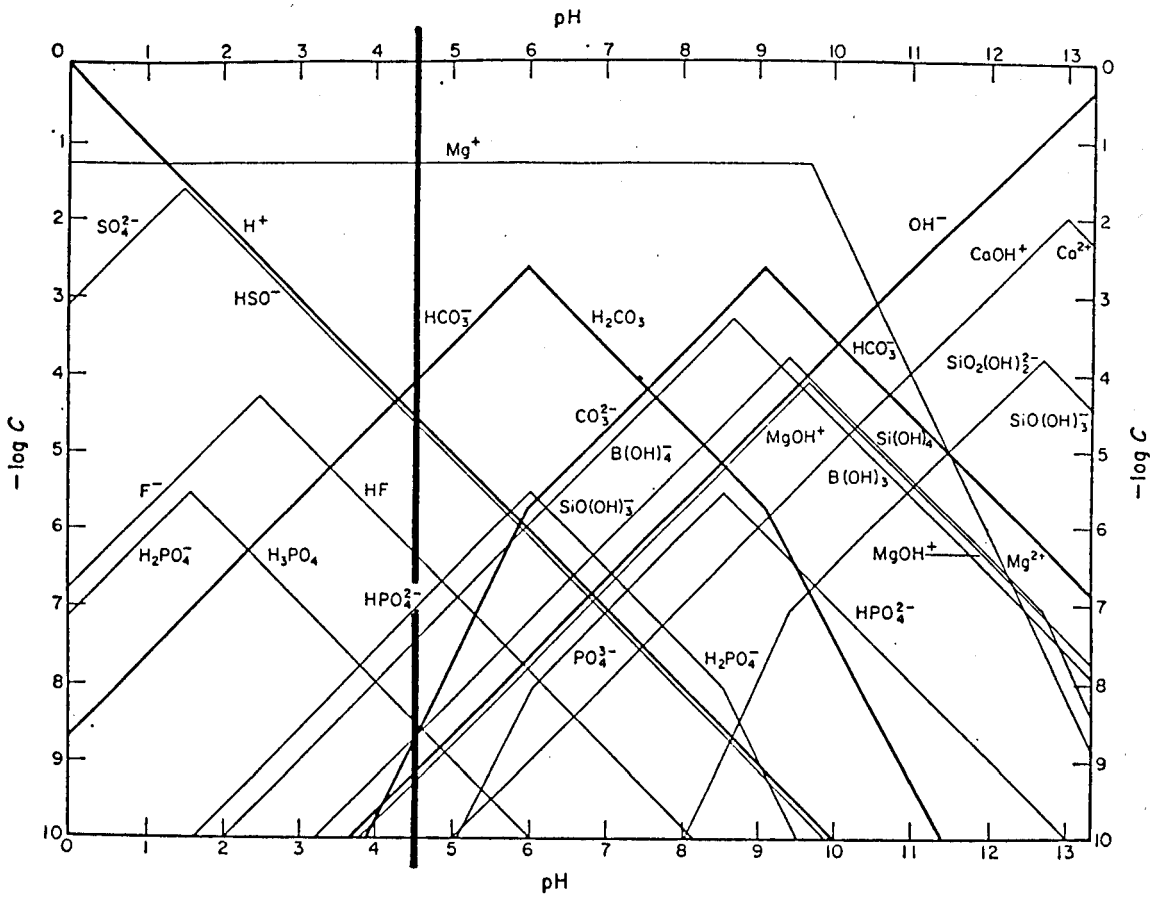

Figure 1.3: Bjerrum plot for seawater adapted from Edmond (1970) showing the inorganic protolytes occurring in total concentrations greater than 10^{-6} M. The representation for species of acids other than carbonic, boric, and phosphoric is only diagramatic owing to uncertainties in the constants. Species of proton acceptors which show an increase in concentration to the right hand side of the bold vertical line will contribute to TA as defined by Dickson (1981). The -log C term is the -log of the concentration of the protolytes.

When carbonate precipitation/dissolution is of interest the carbonate alkalinity (CA) may be a more useful concept than TA:

$$CA = [HCO_3^-] + 2\,[CO_3^{2-}] \qquad (1.28)$$

Carbonate alkalinity has to be calculated from TA. The equation is given by Skirrow (1975).

To facilitate the detection of TA changes induced by factors other than dilution of seawater by pure water, the concept of 'specific alkalinity' (TA_S) has been introduced in which the measured TA is normalized to a constant salinity of usually 35.000 psu, i.e.

$$TA_S = TA_{measured} \times 35.000 \,/\, salinity_{measured}\,. \qquad (1.29)$$

However, due to the potential uncoupling of salinity and TA changes and variations in the past history of different water masses, the above correction for salinity is only an approximation and does not apply universally. This is explained in more detail in section 1.4.2.3 below.

Instead of calculating carbonate alkalinity in $CaCO_3$ precipitation/dissolution studies, the so-called 'potential alkalinity' (TA_{NO3}) is frequently used, which simply includes the concentration of dissolved nitrate in the seawater:

$$TA_{NO3} = TA + [NO_3^-]. \qquad (1.30)$$

The reasoning behind corrections for nitrate is explained in section 1.4.2.6. In the original proposal of potential TA by Brewer et al. (1975) it was pointed out that changes in the concentration of dissolved inorganic phosphate and of other acid-base species should, strictly speaking, be included. However, they are usually ignored since their contributions to changes in TA are regarded as insignificant. Potential alkalinity is the simplest means of correcting for TA increases during phytoplankton growth when nitrate is utilized. Therefore, TA_{NO3} is frequently assumed to change only as a result of formation or dissolution of particulate $CaCO_3$. This concept is, however, inadequate when comparisons are conducted between different water masses which are characterized by different concentrations of original, or 'preformed', nitrate (Redfield et al., 1963). In this case it may be more appropriate to measure a change in oxygen concentration and to use this change to calculate the change in biological nutrient reduction on the basis of the Redfield ratio, e.g. in the case of nitrate,

$$TA_{NO3}' = TA + 16/138\,[O_2]\,. \qquad (1.31)$$

This latter approach of oxidative correction is based on a concept proposed by Broecker (1974) to overcome problems associated with different preformed nutrient concentrations, and it can be applied similarly for phosphate. This concept is inadequate under sub-oxic conditions.

1.4.2. FACTORS INFLUENCING TA

1.4.2.1. Global alkalinity cycle

Volcanism introduces acidity to the atmosphere which leads to weathering of continental rocks. The dissolved alkaline constituents tend to outweigh the acidic constituents thereby introducing alkalinity to the ocean. This occurs via catchment areas of freshwater systems and river transport during which the alkalinity will be further transformed. The nature of the catchment area and the transfomations that occur before the water reaches the oceans will mark the preformed TA of the recipient water mass in the ocean. Due to supersaturation in the surface ocean with respect to calcium carbonate, the main sedimentation process for calcium carbonate is mediated by biological calcification. This eventually results in sedimentation of calcium carbonate and incorporation into the sediments. The alkalinity is further regulated by acidic introductions from hydrothermal vents and ocean fissures.

1.4.2.2. Temperature and pressure

Total alkalinity is temperature and pressure independent if expressed in equivalents-per-kilogram units.

Indirect temperature effects on TA are reflected in empirical relationships between potential temperature and TA in ocean surface waters. These have been established by Edmond (1974) and extended on a constant salinity basis by Chen and co-workers for different oceanic regions. For example, Chen and Millero (1979) found that surface TA in the South Atlantic decreases as temperature increases, but only up to 17°C above which TA remains constant. Proposed possible explanations include changes in biological activity, current flow patterns, or other physical processes. The effect of $CaCO_3$ dissolution which is temperature-dependent has been disregarded as a possible explanation, since the surface waters are almost everywhere supersaturated with respect to $CaCO_3$ (Shiller, 1981).

Exceptions to this temperature relationship also apply for seawater in the vicinity of pack ice which cools the seawater but does not affect some of the chemical properties. This may, for example, have resulted in a slight break at 0.5°C in the relationship for winter data from the northern North Atlantic, more specifically the Norwegian and Greenland Seas. The overall relationship for those regions was found to be

$$TA_S\ (\mu eq\ kg^{-1}) = 2314.6 - 0.6\ T\ (°C)\ ; \qquad 1\sigma = 5.7 \tag{1.32}$$

where T is the temperature in °C and σ is the standard deviation. The latter is similar to the measurement error for TA (Chen et al., 1990). No such relationship was found by Broecker et al. (1985b) for summer data from the same region.

1.4.2.3. Salinity

If NaCl salt were added to water, this would increase the salinity but not TA according to equation (1.27). So, the commonly assumed proportionality between salinity and TA as reflected in the use of the specific alkalinity concept is merely an empirical approximation to account for the effect of evaporation and precipitation of pure water. This is justified because the relative fractions of ions which influence TA in any way remain unaffected by these processes. Therefore, specific alkalinity has been used in glacial-interglacial studies, since any significant growth in the volumes of glaciers would have been caused by increased precipitation over the glaciers relative to the loss term from melting (e.g. Broecker, 1982). As a special consideration, some laboratory work has indicated that the formation of sea ice may lead to fractionation of TA (e.g. Thompson & Nelson, 1956). However, this has not been confirmed in the case of natural conditions (Anderson & Jones, 1985).

In more current studies, specific alkalinity is also commonly used in mapping or time series excercises. However, the above proportionality may be insufficiently accurate because of the potential uncoupling of salinity and TA changes combined with variations in the past histories of different water masses. Consequently, it has been preferred to establish regional functions for the relationship between these two parameters from winter time surface waters, i.e. when biological effects are minimal. These functions have been called upon in subsequent studies, such as those investigating the penetration depth of excess CO_2 (e.g. Brewer et al., 1997), when data from either one of the parameters was absent. Since the reduction in TA

arising from calcification is partially offset by increases from nitrate utilization (see sections of 1.4.2.6), these functions are rather well constrained (Brewer et al., 1997).

1.4.2.4. $CaCO_3$

The effects of $CaCO_3$ production and dissolution on total alkalinity are well established (e.g. Stumm & Morgan, 1981), and may involve bicarbonate or carbonate. The net reactions have already been demonstrated in equations 1.12 and 1.13, i.e. TA is reduced by 2 equivalents for each mole of $CaCO_3$ precipitated, and vice versa. This applies to biological as well as non-biological processes. In the absence of biological precipitation, TA is largely determined by the degree of $CaCO_3$ supersaturation.

1.4.2.5. CO_2

Equations 1.4 and 1.16 demonstrate that the net effect of molecular CO_2 addition or removal, whether it results from abiotic or biotic factors, does not alter the TA of seawater *per se* . As already shown in equation 1.9, carbon dioxide addition will increase the concentrations of HCO_3^- and CO_3^{2-} and thus TA, but the simultaneous release of equivalent amounts of H^+ has the reverse effect, thereby rendering TA unaltered. The only way changes in the concentration of CO_2 could have an affect on TA is by contact with particulate $CaCO_3$ in the water column or in sediments.

However, when looking at TA alterations due to biological activity, an understanding of the overall uptake or release reactions is essential. This is demonstrated below.

1.4.2.6. Nitrogen

Ammonia is present in much lower concentrations than carbonic or boric acid and has a higher pK value, i.e. it is mostly present in form of ammonium (NH_4^+) which does not contribute to TA (see equation 1.26). On the other hand, variations in the concentration of ammonium are usually indicative of biotic changes, and therefore associated with proton exchange, which does affect TA. The same applies to some other forms of dissolved nitrogen.

Nitrogen may be taken up in various forms by photosynthesizing organisms. The preferred form of nitrogen on energetic grounds is ammonia, most of which is regenerated in the surface layers of the ocean (e.g. Dugdale & Goering, 1967). Another regenerated nitrogen source is urea, which has been shown to play a significant role under certain circumstances, e.g. in some euphotic stratified off-shore waters bordered by tidal mixing fronts during the summer when nitrate concentrations were low (Turley, 1986). Most of the excess primary production is supported by nitrate utilization. Under special circumstances, new production may also be supported by atmospheric input of dinitrogen (Karl et al., 1997) or dissolved organic nitrogen (DON) in rain (Peierls & Paerl, 1997).

Provided the composition of organic matter follows the original Redfield ratio with carbon being present as carbohydrate, nitrogen existing in amino form, and phosphorus being present as orthophosphate, the respective net uptake reactions for nitrate and ammonium may be expressed as, e.g.

$$106\ CO_2 + 16\ NO_3^- + 138\ H_2O \Leftrightarrow (CH_2O)_{106}(NH_3)_{16} + 16\ OH^- + 138\ O_2 \qquad (1.33)$$

and

$$106\ CO_2 + 16\ NH_4^+ + 106\ H_2O \Leftrightarrow (CH_2O)_{106}(NH_3)_{16} + 16\ H^+ + 106\ O_2\,. \qquad (1.34)$$

Accordingly, if the production of 106 moles of POC is combined with the uptake of 16 moles of nitrate or ammonia, the respective increase or decrease in TA will amount to 16 equivalents. This net effect of inorganic nitrogen uptake was first pointed out by Brewer et al. (1975) and has been corroborated in laboratory experiments with continuous cultures of *Phaeodactylum tricornutum* , *Dunaliella tertiolecta,* and *Monochrysis lutheri* (Brewer & Goldman, 1976). In subsequent experiments with continuous cultures of *Dunaliella tertiolecta* Goldman and Brewer (1980) found that nitrite (NO_2^-) uptake had the same effect as nitrate, while the use of urea ($H_2N.CO.NH_2$), an uncharged species, was of no consequence to TA.

The above processes are only of relevance in the upper part of the water column where photosynthesis takes place. The respective regeneration processes, which have the reverse effect on TA, may take place anywhere in the water column under oxic conditions. Bacterial nitrification under oxic conditions which reduces TA by two equivalents for each nitrate produced may be summarized as

$$NH_4^+ + 2\ O_2 \Leftrightarrow NO_3^- + H_2O + 2H^+\,. \qquad (1.35)$$

As part of the 'new production' concept developed by Dugdale and Goering (1967) it is however assumed that this process is insignificant in the SML. Under sub-oxic conditions, such as found in microenvironments of surface layers or at greater depths in the oceans, dinitrogen fixation may occur. Taking the reverse equation to denitrification as given by Stumm and Morgan (1981), the initial effect of dinitrogen fixation is a reduction of TA by one equivalent for every mole of nitrate produced, i.e.

$$5\,CO_2 + 2\,N_2 + 7\,H_2O \Leftrightarrow 5\,CH_2O + 4\,NO_3^- + 4\,H^+. \qquad (1.36)$$

If all this nitrate produced will be incorporated into organic matter as demonstrated in equation 1.33, TA would remain unaltered. Since, however, this would imply an unrealistically high fraction of organic nitrogen in the resulting organic matter, John Raven (University Dundee, pers. comm.) has suggested to present the net reaction for phytoplanktonic dinitrogen fixation using the following equation, i.e.

$$10\,CO_2 + N_2 + 24\,H_2O \Leftrightarrow 10\,CH_2O + 2\,NH_3 + 10\,H_2O + 12\,O_2 + H_2. \qquad (1.37)$$

This equation accomodates a more realistic ratio of organic C:N of 5 and implies no change in TA, as for urea. Whether this equation would adequately represent the overall effect on TA under circumstances of high fixation in the upper ocean is still not clear to me for several reasons. First of all, it would not at all reduce the imbalance in the oceanic TA budget caused by denitrification at greater depths, and secondly, it does not include any possible changes in TA due to increased DON release, which has been associated with N_2 fixation. For example, Glibert and Bronk (1994), found that up to half the fixed nitrogen in *Trichodesmium*, which is considered a dominant N_2 fixing taxum in oligotrophic marine ecosystems, was released as DON, mostly in the form of the amino acid glutamate. Further, Karl et al. (1997) have provided supportive evidence for significantly increased DON and PON concentrations in association with N_2-fixing organisms in the subequatorial North Pacific gyre. Therefore, before any theoretical answers can be found with respect to the overall effect of N_2 fixation in surface waters of the oceans, it would be necessary to take account of the overall effect of this excessive DON release. Considering that N_2 fixation was found to support up to half of the new production in the subtropical North Pacific Ocean, it seems appropriate to investigate the overall effect of N_2 fixing phytoplankton species on TA in more detail. There does not seem to exist any published record of such studies having been conducted. If such findings turn out to vindicate the equation suggested by Raven, i.e. no net effect on TA, this would imply that the commonly applied oxidative corrections for nitrate utilization to TA would introduce errors to

derived parameters of a yet undetermined extent. It would also mean that more notice has to be taken of other N_2 fixing organisms such as symbiotic associations with *Rhizosolenia* spp.. Further, any climate induced changes in stratification may change the relative abundance of N_2 -fixing species and may thereby have an associated effect on surface water TA, at least on a short-term basis, i.e. within less than 100 years (Karl et al., 1997).

Denitrification under sub-oxic or anoxic conditions, was found to be of relevance only between 1000 and 3000 m depth in the oxic ocean (Anderson & Sarmiento, 1994). Possible evidence for the reduction of nitrate at depths between 3000 and 3500 m comes from Rommets (1988) in his comparison of different East Indonesian Basins. For one of these basins he observed discrepancies between estimates of $CaCO_3$ dissolution derived from dissolved calcium and potential TA. He suggested nitrate reduction as one possible cause. Based on these findings it seems appropriate to include corrections for the effects of these processes on TA. Furthermore, the proposed reduction in denitrification during glacial periods by Altabet et al. (1995) and Ganeshram et al. (1995) would have brought about an increasing effect on TA, which could account in parts for the glacial-interglacial trends in TA.

The importance of dissolved nitrogen input to the ocean via rain water remains uncertain, but it is recognized by some authors at least on short time scales and in stratified waters. Results by Peierls and Paerl (1997) indicate the potential significance of a previously overlooked contribution of organic nitrogen with respect to enhancing phytoplankton growth. Concentrations of DON varied from undetectable to up to 20 µM, and the contribution of DON reached up to 84% of the total dissolved nitrogen concentration in rain water. It therefore cannot be excluded that these aeolian nitrogen contributions could have an effect on TA, at least on regional and short-term scales. This effect may be direct or indirect via biological uptake mechanisms.

1.4.2.7. Phosphorus

Concentrations of phosphate are generally low in the oceans, so that contributions of dissolved PO_4^{3-} and HPO_4^{2-} to TA in open ocean waters are negligible *per se*.

In the case of biological uptake and remineralization reactions, the exact mechanisms for inorganic phosphate is unknown (Raven, pers. comm., 1993), but the incorporation of one mole of phosphorus into particulate organic matter (POM) is generally assumed to raise TA by one equivalent. This may be demonstrated by net uptake reaction 1.33 from above, once it has been modified to account for phosphorus utilization

$$106\ CO_2 + 16\ NO_3^- + HPO_4^{2-} + 122\ H_2O + 18\ H^+ \Leftrightarrow (CH_2O)_{106}(NH_3)_{16}(HPO_4^{2-}) + 138\ O_2 \qquad (1.38)$$

In this particular case the removal of HPO_4^{2-} lowers TA by one equivalent, but this net charge effect is balanced by a concomitant removal of two protons thereby raising TA by one equivalent. As only a relatively small amount of phosphorus is incorporated into organic matter compared to carbon or nitrogen, phosphorus-induced TA changes are usually of little consequence in seawater, especially, given the precision of the measurements involved. However, significant amounts of particulate organic phosphate may be produced during culture experiments, thereby also having an equivalent effect on TA.

1.4.2.8. Silicate

Concentrations of dissolved silicate are of the same order as those for nitrate, i.e. low in surface layers but may reach several tens of micromoles in the deep ocean. Due to the high dissociation constants for silicic acid, direct impact on TA are nevertheless low in either part of the ocean.

The biological net uptake reaction for silicate by silicifying phytoplankton is still under debate. It remains unresolved whether diatoms, which use silicon to build their frustules, use $Si(OH)_4$ or $SiO(OH)_3^-$. Total alkalinity would not be affected by the utilization of $Si(OH)_4$, which is the main form available to algae at the usual seawater pH. Raven (1986) doubts that silicon is involved in any biochemical mechanisms which could alter TA in the case of land plants.

1.4.2.9. Sulphur

Sulphur is the third most abundant constituent dissolved in seawater. In the presence of oxygen, sulphur can only exist as sulphate rather than sulphide in seawater (Stumm & Morgan, 1981). As demonstrated in section 1.4.1 above, its association with hydrogen ions

has a lowering effect on TA, but this effect is irrelevant in the normal seawater pH range, i.e. it only becomes significant at the microequivalent level when pH conditions are below 6. Due to the constancy of the seawater composition, any corrections for the HSO_4^- effect on TA can usually be derived from the knowledge of salinity. As described below, this relationship may be offset by acidic aeolian input of precipitation containing sulphuric acid. This perturbation may be of global significance but is probably too small to be picked up by any TA method.

The most common form of sulphur used by phytoplankton is SO_4^{2-}. Its uptake is active (Raven,1980). This suggests that for each sulphate ion taken up, TA will be increased by 2 equivalents to balance the electrical charge, and it is thought to be applicable to most sulphur-containing end products such as proteins, cell wall constitutents, and dimethylsulphonium proprionate (DMSP). An exception to this are sulphate esters, in which case TA increases only by one equivalent. The effect of DMSP production on TA has been described by Raven (1993). The production of DMSP by marine phytoplankton from CO_2, H_2O, and SO_4^{2-} takes place according to

$$5\ CO_2 + 6\ H_2O + SO_4^{2-} \Rightarrow C_5H_{10}SO_2 + 8\ O_2 + 2\ OH^- . \qquad (1.39)$$

The sulphur content of algae in terms of the Redfield ratio was estimated by Deuser (1970) as 106:1.6 for POC: POS (particulate organic sulphur). Similarly, Raven (pers. comm., 1998) expects the content to be comparable to that of phosphorus but possibly greater in DMSP producing algae. For example, relatively high concentrations of DMSP have been observed in the prymnesiophyte *Chrysochromulina polylepis,* i.e. 400 mmoles dm^{-3} of cell volume (Keller et al., 1989b), which translates to about 4% of POC concentration on a molar basis (Raven, 1993). Assuming the original Redfield ratio, this would imply that for every 106 moles of carbon fixed into POC, TA would increase by 8 equivalents, which amounts to half the TA increase due to NO_3 utilization. As can be seen from the list of laboratory results for many marine phytoplankton species by Keller et al. (1989a), DMSP production shows considerable variation between species as well as strains of the same species. The latter was demonstrated for *Emiliania huxleyi* by Wolfe et al. (1997). According to the study by Keller et al. (1989a), more important DMSP producers include members of the dinoflagellates, chrysophytes, and prymnesiophytes, the latter including coccolithophorids. The highest value was measured for the dinoflagellate *Amphidinium carterae* with more than 2000

mmoles DMSP dm^{-3} of cell volume. Values for some of the coccolithophorids including *Emiliania huxleyi* ranged between 80 and 200 mmoles DMSP dm^{-3} of cell volume.

Based on estimates above the magnitude of the TA change due to sulphur utilization by non-DMSP producing phytoplankton is approximately twice that due to phosphate utilization. In the extreme case of DMSP producing species like *Amphidinium carterae*, the effect on TA my exceed that of nitrate utilization by two times. However, Keller et al. (1989a) point out that the above values are difficult to extrapolate to natural situations. This is because DMSP production not only depends on the ecological composition but also on environmental conditions such as salinity (e.g. Vairavamurthy et al., 1985), nitrogen limitation (Andreae, 1986), and the association with ice (Kirst et al., 1991). Observations of phytoplankton blooms with elevated coccolithophorid numbers or with a dominance of coccolithophorids in terms of biomass have revealed maximum concentrations of combined dimethyl sulphide (DMS) and DMSP of about 400 nM of seawater (Turner et al., 1989; Matrai & Keller, 1993; Holligan et al., 1993).

It follows that the impact of biological sulphate uptake may be in the order of no more than a few microequivalents during coccolithophorid blooms and therefore on the verge of being detectable. Accordingly, Brewer et al. (1997) have considered any redox reactions involving sulphur as trivial in the oxic ocean. However, in the case of blooms dominated by high DMSP producing species this sulphate effect may be more significant. Its impact on TA is mostly ignored in estimations of potential TA but has been included by some authors. For example, Chen (1978) found that such oxidative sulphate corrections improved the agreement between changes in dissolved calcium concentration and estimated $CaCO_3$ dissolution derived from TA data. Likewise, in the case of some culture experiments which are accompanied by high DMSP production, the omission of this sulphur effect may introduce significant errors in certain parameters derived from TA measurements.

There is still considerable uncertainty as to the synthesis and fate of DMSP and other organic sulphur compounds such as dimethylsulfoxide (DMSO) and DMS. Preliminary results by Matrai and Keller (1993) suggest that most particulate DMSP is remineralized or converted in the surface layer of the ocean and not lost by sedimentation.

On a global and longer-term scale, Raven (1993) has pointed out the possible importance of DMSP production to the oceanic TA budget. The breakdown of DMSP, which is catalysed by a base or enzyme, results in volatile DMS and acrylic acid, i.e.

$$C_5H_{10}SO_2 \Rightarrow (CH_3)_2S + CH_2{=}CHCOO^- + H^+, \quad (1.40)$$

with the latter being broken down to CO_2 and water, i.e.

$$CH_2{=}CHCOO^- + H^+ + 3\,O_2 \Rightarrow 3\,CO_2 + 2\,H_2O. \quad (1.41)$$

Summarizing the above three equations (1.39 - 1.41) results in

$$2\,CO_2 + 4\,H_2O + SO_4^{2-} \Rightarrow (CH_3)_2S + 5\,O_2 + 2\,OH^-, \quad (1.42)$$

which implies an increase in TA by two equivalents for the net reaction of DMS production involving marine phytoplankton. The fraction of DMSP that ends up as DMS is variable, but is not estimated to exceed much beyond 5% (G. Malin, pers. comm.). Its conversion from DMSP may be activated by grazing (Wolfe et al., 1997). The residence time of DMS in the atmosphere is less than one day (Newman et al., 1991; Malin et al., 1992), ultimately leading to the production of sulphuric acid, i.e.

$$(CH_3)_2S + 5\,O_2 \Rightarrow 2\,H_2O + 2\,CO_2 + 2H^+ + SO_4^{2-}. \quad (1.43)$$

The overall reaction of DMS production in the ocean and DMS breakdown in the atmosphere can thus be reduced to:

$$2\,H_2O \Rightarrow 2H^+ + 2OH^- \quad (1.44)$$

where only H^+ is in the atmosphere. If the resulting compounds were all to be precipitated back into the ocean, there would not be a net change in TA due to the production of sulphuric acid in the atmosphere. However, some of the precipitation occurs over the continents, so during pre-industrial times, this would have led to a net increase of the TA in the oceans. Assuming a global annual primary production of 3 Gt C yr^{-1}, or 2500 $\times 10^{12}$ moles, the TA change caused by DMS release to the atmosphere amounts to 1.2 - 3.6 $\times 10^{12}$ equivalents, or about 0.05 - 0.15 % of the carbon production (Andreae & Jaeschke, 1992; Keller et al., 1989b). At present, however, this situation is more likely to be reversed, due to the generation of acid when the reduced sulphur in fossil fuels is oxidised (Newman et al., 1991; Howarth & Stewart, 1992).

With respect to glacial-interglacial changes in DMS release to the atmosphere, Malin et al. (1992) are not aware of direct evidence for changes in DMS production by marine algae. Evidence from ice cores suggests that atmospheric sulphate concentrations were elevated during the glacial period, but the exact reasons for this are unknown. If, in deed, marine DMS production was greater during the glacial period, this would not only have increased the surface albedo but would provide yet another mechanism to cause an increase of TA in glacial oceans.

Under anoxic conditions and once nitrate has been used up as an oxygen source, oxidation of organic matter relies on the reduction of sulfate to hydrogen sulphide, i.e.

$$SO_4^{2-} + 2\,CH_2O + H^+ \Leftrightarrow 2\,CO_2 + HS^- + 2\,H_2O. \qquad (1.45)$$

For each mole of sulphate reduced, TA is increased by two equivalents due to the consumption of one proton and the production of hydrogen sulphide. This process, together with nitrate reduction, may occur in sediments or in the water column in anoxic basins and fjords and may lead to significant increases in specific alkalinity close to the bottom (e.g. Rommets, 1988).

In shallow or deep sediments, the oxidation of hydrogen sulphide by heterotrophic bacteria may take place according to

$$HS^- + 2\,O_2 \Leftrightarrow SO_4^{2-} + H^+. \qquad (1.46)$$

This will reduce TA by two equivalents due to the removal of hydrogen sulphide and the addition of one proton to seawater. Some denitrifying bacteria can carry out this reduction also under anoxic conditions.

1.4.2.10. Organic acid release/ uptake

To what extent organic acids can influence TA is a further matter of uncertainty, mainly due to the problems associated with measuring DOC concentrations and the characterization of the individual substances. Further, the acid-base characteristics of the organic acids as well as the net physiological reactions, are not well known.

The concentration of dissolved organic acids may be increased by lysis of cells and passive and active release by phytoplankton cells. It appears that not much is known about the net reaction which describes the active release of organic acids by phytoplankton cells. Passive release of organic acids occurs down the concentration or electrical potential gradient. The pK values of these organic acids are higher than the pH of the cytosol, so that they are mostly in the dissociated, i.e. charged, form (Raven, 1993). For this reason they contribute to TA.

A. Dickson (pers. comm., 1993) suspected that the effect of the presence of organic acids may increase TA by up to 10 μeq $kgSW^{-1}$ in the open ocean.

1.4.3. VARIATIONS OF TA IN THE OCEANS

Oceanic concentrations of TA tend to range from about 2000 to 2500 μeq kg^{-1}. For the open oceans, the highest TA values are found in the old waters of the deep Pacific and the lowest in the temperate surface waters in general. Since the Pacific is much deeper than the Atlantic Ocean, any $CaCO_3$ in the Pacific will be exposed to dissolution for much longer than in the Atlantic, thus causing the elevated TA in the deep Pacific. The effect of depth- and ocean-related differences in the rates of $CaCO_3$ dissolution relative to organic carbon mineralization and their influences on the TA and TCO_2 of different water masses have been summarized by Broecker and Peng (1989)(figure 1.4.).

Total alkalinity values in lakes show a much greater spread than open ocean waters. The lake TA is determined by the TA generated in the soil, streams, and the watershed, as well as TA generated within the lake itself (e.g. dissimilatory SO_4^{2-} and NO_3^- reduction). The addition of acids from the atmosphere can significantly lower the TA.

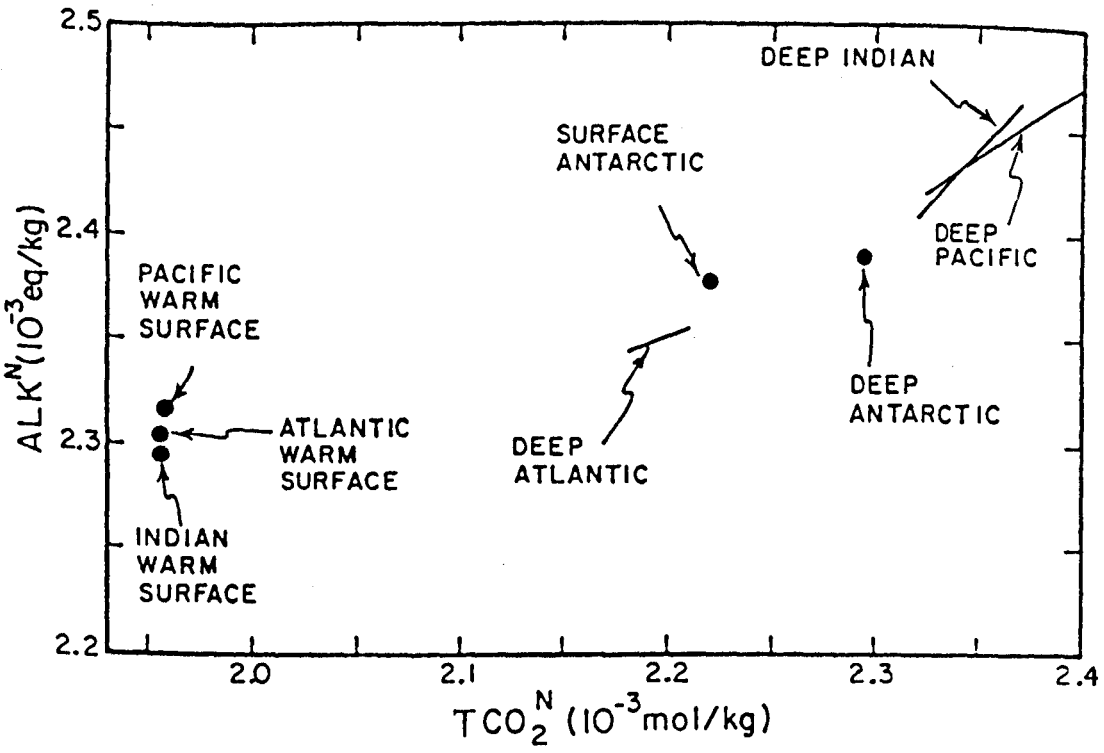

Figure 1.4: Plot of TA against TCO_2 concentration (both normalized to a salinity of 35.00) for major surface or deep water types in the world ocean. Adapted from Broecker and Peng (1989). ALK_N is the term used by the authors for TAs.

1.4.4. APPLICATION OF TA IN CARBON CYCLE AND RELATED STUDIES

Total alkalinity is the main factor determining the capacity of the seawater to absorb atmospheric CO_2. It is therefore a vital parameter in calculations of CO_2 exchanges between atmosphere and ocean for past, present and future. In this context, TA data has been used in various ways to estimate oceanic CO_2 concentrations when no direct pCO_2 data was available. In addition, it is the most appropriate carbonate parameter to identify $CaCO_3$ production/dissolution processes and their effects on pCO_2. In physiological studies it is the most suitable parameter to distinguish between different ways of carbon utilization by calcifying phytoplankton, if used in combination with measurements of one other carbonate parameter. Further interest in TA stems from possible impacts on isotopic fractionations by organisms, which is of great relevance to palaeoceanographic inferences.

1.4.4.1. Direct calculations of pCO_2 using TA

By measuring only two of the four carbonate parameters, i.e. pCO_2, TCO_2, pH and TA, the remaining two parameters and the concentrations of bicarbonate and carbonate may be calculated. The equations are given by Park (1969) and Skirrow (1975), and there are now PC programmes available to carry out these calculations (e.g. Lewis & Wallace, 1995).

1.4.4.1.1. Assumed constancy of TA

In some studies of the carbonate system in which TA has been used to calculate other parameters, TA has been ascribed a constant value assuming that its variability would be insignificant. This assumption may be justifiable for specific TA from open ocean surface waters in certain regions where seasonal changes in pCO_2 have been shown to be predominantly governed by temperature and salinity rather than by biological effects. Calculations of TA from pCO_2 and TCO_2 by Weiss et al. (1982), for example, seem to suggest that this is the case for the North and South Pacific subtropical gyres. In these regions the standard deviations did not exceed $\pm$ 2.0 $\mu eq\ kg^{-1}$ for TA values obtained by calculation from pCO_2 and TCO_2 on several occasions over the course of a year. The same assumption was made for surface waters of the Weddell Sea by Hoppema et al. (1995) on the basis of previously reported conservativeness of TA.

On a global scale, constant TA has been assumed in OGCMs of simplified ocean chemistry, as for example by Sarmiento et al. (1992), and in all three global carbon cycle models used for the IPCC climate predictions. The absolute values of TA are not the same though, e.g. there is a difference of more than 30 μeq kg^{-1} between the Bern model (Joos et al., 1996) and the one by Jain et al. (1995). On the other hand, Maier-Reimer (1993) stresses the importance of using a realistic representation of the carbon cycle in 3 dimensions.

1.4.4.1.2. TA as a variable

Maier-Reimer (1993) introduces TA as one of the principle variables in his OGCM in order to calculate pCO_2. He emphasizes the importance of data sets such as that of the JGOFS study for these purposes. Measuring TA with a reliable method rather than assuming a constant value obviously constitutes an improvement to the accuracy and resolution of the carbonate parameters derived from it. Such data collections have demonstrated considerable regional and spatial variations in TA in different regions of the oceans. Differences in TA between oceanic basins have already been demonstrated in section 1.4.3 above.

Time-series measurements in the Sargasso Sea, i.e. the North Atlantic subtropical gyre, revealed seasonal changes in TA of up to 30 μeq kg^{-1} in the surface layer and at the depth of the chlorophyll maximum (Bates et al., 1996a,b). The even larger variability in the mid- and higher latitudes of the North Atlantic will be treated in more detail in chapters 3 and 5. Other examples of noteworthy measured TA variations include the eastward decrease by about 100 μeq kg^{-1} over about 1500 km along the equatorial Pacific during the 1992 ENSO event (Feely et al., 1994).

Measurements of TA from continental shelves, whose role is still somewhat uncertain with respect to the global carbon cycle, generally show much larger variations in TA than observed in open ocean situations due to the increased biological production and coastal processes caused by upwelling and river input. Changes in specific TA of several hundred μeq kg^{-1} have, for example, been observed over a distance of 100 km along the Straits of Dover, which also varied seasonally by a similar extent (Frankignoulle et al., 1996).

1.4.4.1.3. Check of internal consistency of measured seawater carbonate system

With an increasing need for accurate data of pCO_2 or other parameters of interest one way of testing the accuracy of the measurements is by means of overdetermining the carbonate system, i.e. by measuring more than two carbonate parameters (e.g. Dickson, 1991c). This kind of test can be applied provided certain assumptions are valid, i.e.

(i) the chemical system is internally equilibrated;

(ii) TA is not significantly affected by dissolved organic acids or any other interfering and unquantified species;

(iii) the pCO_2 of atmosphere and seawater are in equilibrium or disequilibria are accounted for.

With typical equilibration times of several minutes for the interconversion of dissolved inorganic carbon species, it can be assumed that errors from disequilibria due to phytoplankton growth can be assumed to be negligible. With respect to the second assumption, it is necessary to know the total concentrations and thermodynamic properties of all the possible acid-base species involved. The possibility of interfering acid-base systems, e.g. in the form of organic acids, has already been mentioned in section 1.4.2.10 above, possibly amounting to differences in the range of 10 $\mu eq\ kg^{-1}$ between measured and calculated TA. This could translate to an error of about 10 μatm in calculated pCO_2. Further complications continue to arise from the discrepancies between thermodynamic constants as determined by different groups of scientists. Dickson (1991c) provided references for the more up-to-date thermodynamic data relevant to the carbonate system. A more recent review has been published by Millero (1995). Brewer et al. (1997) acknowledge that the choice of these constants remains a matter of personal preference. Use of different constants was found to lead to an error range of estimated pCO_2 of about $\pm$ 10 μatm for deep waters and about $\pm$ 25 μatm for surface waters, and the good agreement between the results by Goyet and Poisson (1989) and Roy et al. (1993) may in fact have been due to fortunate coincidence (Brewer et al., 1997). Nevertheless, Brewer et al. (1997) recommend using the constants of either of these groups. Lee et al. (1996) also endorsed the constants determined by Millero (1995) and Lee and Millero (1995) in some cases.

Comparisons in TA results from overdetermination excercises conducted on two cruises to the Northeast Atlantic in the springs of 1990 and 1991 as well as on certified reference material are described and discussed in detail in chapter 2. More recently,

overdeterminations have been conducted in open ocean waters of the Gulf Stream (Lee & Millero, 1995; Lee et al., 1996) and the equatorial Pacific (Millero et al., 1993; Clayton et al., 1995) or with certified reference material (Lee & Millero, 1995), which had been supplied by A. Dickson from Scripps Institution of Oceanography, USA. While an earlier intercomparison of results from different laboratories on samples of reference material reported by Unesco (1990) has revealed significant discrepancies between different methods, the internal consistencies measured on more recent cruises was generally within 14 $\mu eq\ kg^{-1}$ for TA and 10 µatm for pCO_2. Results tended to vary with the combination of constants and parameters and specific methods used (see authors above).

For the remaining uncertainties and the yet limited number of internal consistency checks it is generally recommended to measure the parameter of interest directly whenever possible (Park, 1969). Unfortunately, the measurement of pCO_2 requires the most sophisticated equipment of the measureable carbonate parameters and is therefore not always feasible on cruises or in laboratory experiments. This is one of the reasons why TA continues to be chosen as one of the remaining carbonate parameters in order to calculate pCO_2. Its use, together with TCO_2, also has the advantage of being temperature and pressure independent.

1.4.4.1.4. Identification and quantification of causes for pCO_2 disequilibria

Measurement of TA further allows to narrow down the reasons for any disequilibria of pCO_2 between atmosphere and ocean. Baes (1982) suggested to use TA versus TCO_2 diagrams to identify the three main processes causing such disequilibria, i.e. air-sea exchange, photosynthetic growth/ remineralization, and $CaCO_3$ precipitation/dissolution. This is demonstrated in figure 1.5 below.

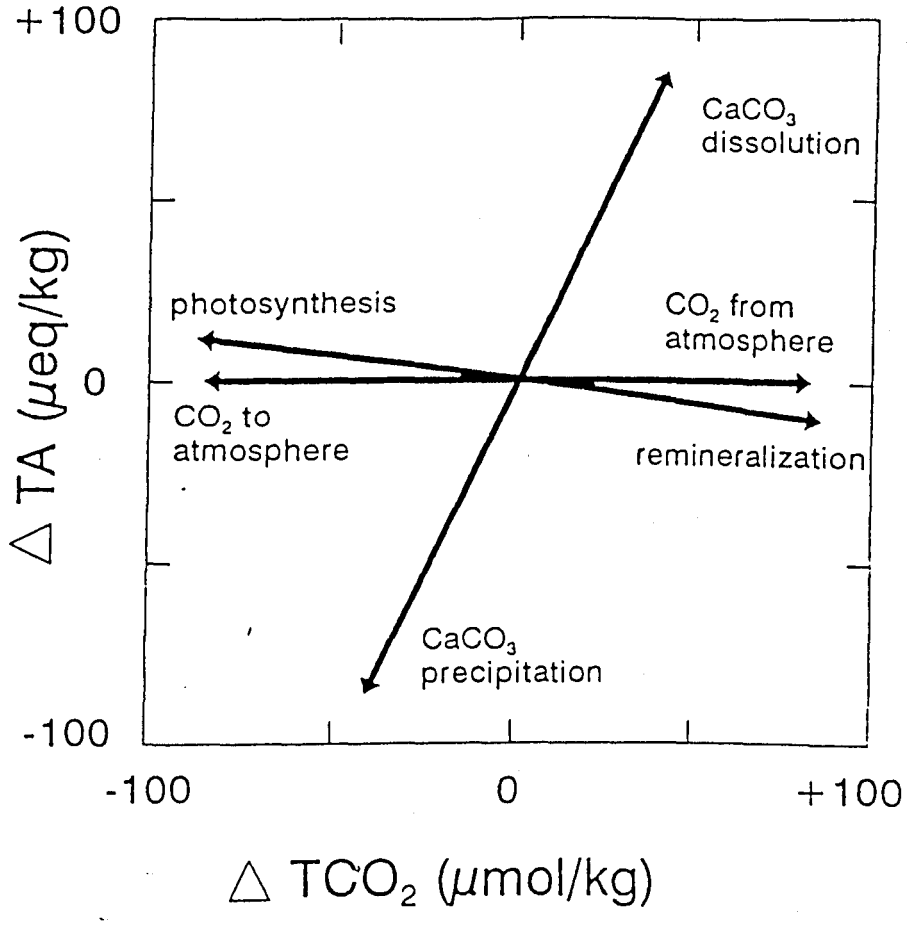

Figure 1.5.: Vector diagram showing the impact of the three major processes influencing TA and/or TCO_2 (photosynthesis and remineralization involve NO_3^- here, whereas NH_4^+ would affect TA in the opposite directions).

In the case of Broecker and Peng (1989), for example, this kind of plot as shown earlier in figure 1.4 demonstrates that the relative importance of $CaCO_3$ dissolution is least relevant in deep Atlantic and most pronounced in deep Indian ocean water.

Brewer (1986) warns, however, that for oceanic surface waters of strongly varying temperature and salinity the simple assumptions used by Baes (1982) may no longer hold. Kinetic factors associated with seasonality, ocean mixing and gas exchange are not accounted for in the scheme by Baes (1982).

One example of a more systematic approach to identifying any causes for changes in TA is the time series study of TA and TCO_2 in the Sargasso Sea by Bates et al. (1996b). Over the course of two years they found a generally close relationship between TA and salinity, suggesting that TA was mostly influenced by changes in evaporation/freshwater precipitation or other physical processes such as convection and mixing. This was further confirmed by a similar relationship obtained by Brewer et al. (1986) for a wider hydrographic range in the North Atlantic. The observed seasonal range at the site in the Sargasso Sea of about 20 $\mu eq\ kg^{-1}$ could be accounted for by reduced evaporation during the summer months (Bates et al., 1996a).

During the above mentioned measurement series, there was however one exceptional period of about one month, i.e. February 1992, during which the TA values were reduced by up to 30 $\mu eq\ kg^{-1}$ below the level expected from the TA versus salinity relationship. This could be easily observed on plots of TA versus salinity as well as of specific TA versus time. Depth profiles of TA show that reductions in TA were most pronounced at two depths which coincided with vertical maxima of primary production and chlorophyll concentration. These depths were also characterized by TCO_2 reduction and an increase in calculated pCO_2. Furthermore, the average reduction of TA within the SML of 10 $\mu eq\ kg^{-1}$ was no longer observed below the SML, where TA varied according to the previously established relationship with salinity (Bates et al., 1996b). Bates et al. (1996b) calculated the SML-integrated change of TA in the SML during this special period. This was done by using the TA/salinity relationship to derive baseline values for TA below the SML. By comparing this TA change to the similarly derived change in TCO_2, Bates et al. (1996b) estimated an increase in the ratio of TA: TCO_2 depletion of 1.8 in the SML relative to the sub-SML baseline values during that month. This translates to a POC: PIC production ratio of 0.1 (see section 4.4.2.2 for conversion). In the alternative approach of regressing the individual depth values of TA

change against those of TCO_2 change, an increase in the TA: TCO_2 depletion ratio of 1.4 was obtained, which implies a decreased POC:PIC net production ratio of about 0.4. In spite of the fact that the TA samples were not filtered before analysis (D. Purdie, pers. comm.), both estimates of the production ratio in the SML are lower than those from previously reported studies with coccolithophorids (e.g. Bleijswijk et al., 1994; Purdie & Finch, 1995; Paasche & Bruback, 1994). In the absence of verifying biological observations, it was concluded that coccolithophorids were the most likely cause for this short-lived phenomenon although foraminifera or pteropods were not ruled out.

A slightly different approach has been preferred by, for example, Anderson and Dyrssen (1994), who examined the effect of calcification and POM production in the Arabian and contributory Seas. In contrast to the specific TA concept describe in section 1.4.1, they simply used the ratio of the two parameters, i.e. TA: salinity. Reduction of this ratio was indicative of calcification in much the same way as for the usual specific TA concept. In addition, these authors also used the difference between TA and TCO_2 as a means of detecting POC production/regeneration on the basis that POC production reduces the concentration of TCO_2 and increases the TA due to nitrate utilization. The fact that this (TA- TCO_2) term did not change significantly in spite of a notable change in the TA:salinity ratio led to the conclusion that the production of PIC was approximately balanced by POC production.

1.4.4.2. Estimation of changes in $CaCO_3$ for pCO_2 back-calculations

1.4.4.2.1. Study of glacial/interglacial changes in atmospheric pCO_2

Present day TA data from surface waters of various regions and mean deep water values have been used by Broecker (1982) to derive glacial pCO_2 values by making various general assumptions. Similarly, Broecker and Peng (1989) used TA data as a basis for their 'polar alkalinity hypothesis' (section 1.3.2.2.1). Heinze et al. (1991) used TA as a variable input parameter in their models.

1.4.4.2.2. Study of anthropogenic CO_2 fluxes in the oceans since pre-industrial times

Detection of penetration depth for anthropogenic CO_2 in the ocean

The detection of a globally averaged disequilibrium of 8 µatm between atmosphere and surface ocean CO_2, which would be necessary to drive a higher estimate of oceanic excess CO_2 uptake, is complicated by natural variations of ± 100 µatm (Tans et al., 1990). So far this disequilibrium has not been unequivocally detected (Brewer et al., 1997).

To determine the ultimate extent of oceanic uptake of excess CO_2, ocean models are being used which generally rely on ^{14}C or tritium data to calibrate carbon fluxes. These tracers are so far the best solution to the detection of this excess CO_2 signal. However, there are some doubts over the accuracy of these calibrations, since both tracers have sources and atmospheric equilibration times which are different to those of excess CO_2, and the possible uncertainties relating to an imbalance in the ^{14}C budget have been mentioned earlier in section 1.3.1. In addition, qualitative calibrations from bomb ^{14}C and tritium are only possible for the last 50 years or less (Chen, 1982b). So, various attempts have been made to detect and estimate the excess CO_2 penetration more directly by means of back-calculations.

Application of the above inverted signals may be limited when it comes to the recovery of a time-record of the past CO_2 chemistry or the quantification of the integrated amount of excess CO_2 entry into the oceans (Broecker et al., 1985b; Brewer et al., 1997). On the other hand, Wallace (1995), who conducted a survey of strategies to monitor global ocean carbon inventories, and Broecker et al. (1985b) acknowledge this method as a useful means to provide model-independent estimates of spatial variability of excess CO_2 distribution, which in turn can be used to validate models. Brewer et al. (1997) have provided a useful review of the approaches used in the back-calculations based on TCO_2 and TA estimates.

The underlying concept of the back-calculation method relies on contemporary chemical observations from samples along isopycnal surfaces below the mixed layer depth (MLD) to estimate their 'original' TCO_2 from the time of subduction from the SML. Assuming complete equilibration, this seawater will carry the imprint of the atmospheric CO_2 concentration prevailing at the time in question, unless this parameter is altered by biogeochemical processes. To account for these processes, corrections are generally made for any exchange of freshwater and the regeneration of POM and PIC. The derived

'original' TCO_2 ought to decrease down to a certain depth, in line with atmospheric CO_2 concentrations of the past 200 years or so. Below this penetration depth of excess CO_2 the back-calculated TCO_2 should remain relatively unchanged. The pCO_2 as calculated from 'original' TCO_2 and 'original' TA ought to resemble the pre-industrial value of about 280 µatm. Deviations from this value may be indicative of an incomplete atmospheric imprint of the original water sample, errors in the measurements, unrepresentative sampling, and incorrect or incomplete assumptions used in the back-calculations.

Brewer (1978) and Chen and Millero (1979) independently applied the above concept with subsequent refinements to study the penetration depth of excess CO_2 in different oceanic regions (Chen & Pytkowicz, 1979; Chen, 1982a, b, c; Poisson & Chen, 1987; Chen et al., 1990; Chen, 1993; Chen et al., 1996; Brewer et al., 1997). However, their approaches differ somewhat with respect to the assumptions used and the normalization procedures applied to the measured data.

To estimate the original TCO_2 of a deep sample, the current TCO_2 needs to be corrected for evaporation/precipitation effects, metabolic CO_2 release during remineralization of POM and for $CaCO_3$ dissolution. The first two corrections are generally achieved by applying salinity and oxidative corrections to the measured TCO_2 data. Estimates of $CaCO_3$ dissolution are obtained from the difference between TA_S measured in the deep sample and the 'original' or 'preformed' TA_S value (TA_S^0). To derive a value for TA_S^0, Brewer (1978) used a somewhat subjective but relatively constrained value for the 'original' TA and salinity on the basis of recent observations at the oceanic site at which the water parcel of interest was subducted, i.e. at the isopycnal outcrop. Subsequently, Brewer et al. (1997) employed the empirical ratio of salinity to TA as a baseline and used this ratio also to correct for subsequent mixing with different water masses. The data had been obtained from the Transient Tracers in the Ocean (TTO) survey (see section 3.2) for winter time surface waters in the region of interest. Chen and co-workers (see various references above) relied usually on another empirical relationships with TA, i.e. between salinity-normalized TA and potential temperature (see also section 1.4.2.2). These relationships had also been established using relatively recent data, e.g. from the GEOSECS expeditions (see section 3.1), and they, too, vary between oceanic regions. By using any of these procedures it is assumed that the TA_S^0 values have not changed significantly since the eve of the industrial revolution. The decrease in TA due to nitrate and phosphate release is derived by

measuring the oxygen deficiency, or apparent oxygen utilization (AOU), and using this parameter to apply oxidative corrections. In the following example for an estimate of $CaCO_3$ dissolution, this is done with the original Redfield ratio, but alternative ratios have been preferred, e.g. by Brewer et al. (1997):

$$\Delta [CaCO_3] = \{ (TA_S - TA_S^0) + (16/138\ \Delta[O_2]) - (1/138\ \Delta[O_2]) \} / 2 . \quad (1.47)$$

The above oxidative corrections to TCO_2 and TA assume that the partial pressure of O_2 in seawater was in equilibrium with the atmosphere at the time of subduction and rely on the accurate knowledge of the original temperature for the calculation of the 'original' concentration of O_2 according to Weiss (1970). So, these above assumptions introduce a certain extent of uncertainty into the estimation of $CaCO_3$ dissolution and preformed TCO_2. However, Brewer et al. (1997) stress that this approach is preferred to a simple correction using measured nitrate concentrations as was shown in equation 1.30 because of the presence of a significant non-metabolised fraction, i.e. the preformed nitrate. The effect of other redox changes on the above calculations are not thought to be significant because the study by Anderson and Sarmiento (1994) indicates that denitrification is only of relevance between 1000 and 3000 m depth and reactions involving sulphur have been considered trivial in the oxic ocean (Brewer et al., 1997).

Major causes for errors and uncertainties in the estimation of excess CO_2 penetration into the oceans include

(i) accuracy of Redfield ratio;
(ii) regional disequilibria in pCO_2 of subducted water;
(iii) accuracy of thermodynamic constants;
(iv) subsurface mixing of water mass with others from different sources;
(v) strong regional and seasonal variations and the representativeness of individual studied sites.

Some of these points may also have a significant effect on the $CaCO_3$ estimates for which TA measurements have been used. Shiller (1981) questioned the reliability of the proton flux corrections applied to the TA data on the basis of work by Bishop et al. (1978) and Shiller and Gieskes (1980), but Chen et al. (1982) argue that these corrections are at least a step in

the right direction. Brewer et al. (1997) compared the effect of using the original Redfield ratio as opposed to the one by Anderson and Sarmiento (1994) and found that the former value yielded lower deeper 'original' pCO_2 values by 30 μatm. Brewer et al. (1997) recommend the value by the latter authors. It is not possible to be entirely confident as to the correct value, due to possible regional disequilibria in pCO_2 during subduction of the water parcel, which in turn introduce uncertainty (Shiller, 1981). However, Chen et al. (1982) have argued that this latter uncertainty may not significantly affect the estimation of the penetration depth provided the disequilibrium is of a constant degree in the source water, since the final results are derived from the difference between two values from the same region. In a reply, Shiller (1982) maintains that a disequilibrium of e.g. 75% would translate to a similar error in the excess CO_2 signal.

As already mentioned earlier in this section, the accuracy of the thermodynamic constants used to calculate the pCO_2 remains controversial, giving rise to an uncertainty similar in extent to that associated with the Redfield ratio (Brewer et al., 1997). The interference of the original chemical signals due to diffusion and mixing with other water masses was a further major concern of Shiller's (1981, 1982), who pointed out that the use of concentration-salinity ratios by Brewer (1978) was inadequate since ratios do not mix in a linear fashion, there was considerable scatter in the data, and the corrections would be complicated if more than two end members were present. Chen et al. (1982) argued that this uncertainty does not translate into major errors after all, and were more concerned about the incompatability of summer and winter data sometimes used in comparisons of surface and deeper water.

Brewer et al. (1997) conclude that the detection of the excess CO_2 signal by the method considered here is easy, providing a robust signal of 45 μmol kg^{-1} in present day surface ocean waters. Results by Brewer and Chen and their respective co-workers are comparable in spite of the differences in approach, and they have been corroborated by data from ^{14}C, tritium and other tracers such as F-11 CFC (Chen et al., 1982; Goyet & Brewer, 1993). In order to achieve the ultimate goal of providing integrated basin scale values which can be used to improve the understanding of long-term CO_2 uptake, it is obviously necessary to improve the understanding of the Redfield ratio and the thermodynamic constants. There is also a need to take more account of possible regional and seasonal variations, and to collect more surface winter TA data. Consolidation of the salinity-TA relationship may then open

up better spatial and temporal coverage of TA in surface waters by means of satellite derived salinity data (Brewer et al., 1997).

Apart from determining the overall flux of excess carbon into the oceans, accurate determinations of the penetration depth are important in predicting whether the excess CO_2 can alter the natural rate of $CaCO_3$ dissolution in sediments. This may, for example, apply to a band of shallow sediments in the North Pacific which contains aragonite and has become exposed to $CaCO_3$ undersaturated waters due to anthropogenic CO_2 entry into the ocean. However, the area estimated to be affected in such a way does not constitute more than 0.1% of the sea floor (Broecker et al., 1979). It has been estimated that deep sea sediments of the North Atlantic which are the most vulnerable to dissolution will remain unaffected for another century yet (Broecker & Takahashi, 1977). However, Chen and Millero (1979) presented a latitudinal profile of penetration depths based on their back-calculation method showing a notable increase in the western basin of the North Atlantic north of 40°N and reaching a penetration depth of about 4550 m at 47°N, thus penetrating the entire water column. This could imply that the strength of the oceanic solubility carbon pump will be significantly increased in the future. In subsequent work, Chen et al. (1990) found that it would not be straight forward to estimate pre-industrial CO_2 concentration in the Greenland and Norwegian Seas because of the absence of sufficiently old waters which are needed to provide the baseline for the absolute excess CO_2 signal.

Pre-industrial fluxes of CO_2 in the oceans

Broecker and Peng (1992) have attempted to estimate to what extent NADW formation acted as a counterflow for the proposed northward atmospheric CO_2 flux of about 1 Gt C yr^{-1} from the Southern Hemisphere in pre-industrial times. In order to estimate past CO_2 exchange between atmosphere and ocean for a given water sample, they back-calculated the TCO_2 of NADW using TCO_2 data measured during the TTO and earlier surveys. The TCO_2 was corrected for fossil fuel additions, freshwater exchange, biological CO_2 exchange, and $CaCO_3$ precipitation/dissolution. The $CaCO_3$ corrections were obtained by correcting measured TA data for freshwater and nitrate metabolism. The format they used to account for the $CaCO_3$ effect on TCO_2 concentrations, which is shown in equation 1.48 and which has been slightly adjusted for comparative purposes here, was different than the one presented in equation 1.47:

$$\Delta [CaCO_3] = \{ \Delta(TA + [NO_3] - (2310 \times salinity_{measured}/35.000))\} / 2. \quad (1.48)$$

The main point here is the fact that Broecker and Peng (1992) used nitrate concentrations instead of oxidative corrections for the effect of nitrate metabolism on TA. The use of the arbitrary constant of 2310 is of no relevance in the discussion here. Broecker and Peng (1992) found that the pre-industrial transport of CO_2 by the NADW to the Southern Hemisphere amounted to approximately 0.6 Gt C yr^{-1}.

1.4.4.3. Estimation of changes in $CaCO_3$ for studies of its distribution, thermodynamics and kinetics

The redistributions of TCO_2 and TA are generally assumed to have played a major role in the glacial/interglacial changes of atmospheric pCO_2. Apart from changes in ocean circulation (e.g. Broecker & Peng, 1989), these rearrangements may have been related to shifts in the biological pumps (Archer & Maier-Reimer, 1994) as described earlier.

Changes in the chemical distributions will take place due to the increasing penetration of anthropogenic CO_2, and the anticipated climate change may also lead to shifts in ocean physics and biology. In order to accurately estimate the effects of these changes in carbon cycle models, it is necessary to improve the understanding of the factors which currently determine the production and dissolution of particulate $CaCO_3$ at various depths in the oceans as well as in pore water of sediments.

The most direct means of estimating the amount of $CaCO_3$ precipitation/dissolution is to measure changes in the concentration of particulate or dissolved $CaCO_3$. Apart from possible methodological problems associated with the analysis of the particulate form, any rapid removal or sinking of particulate $CaCO_3$ may lead to erroneous results in the surface layers. Estimates of particulate $CaCO_3$ flux at greater depths are logistically not straight forward and their accuracy remains to be questionable. The analysis of dissolved $CaCO_3$ has posed analytical problems in the past, because the signal change is small compared to the background concentration in seawater, which is in the range of 10^5 µmol kg^{-1} (Brewer et al., 1975). As the next most related carbonate parameter, TA is therefore frequently chosen to estimate changes in $CaCO_3$.

Brewer et al. (1975) compared changes in TA with depth to those in the concentration of dissolved calcium and demonstrated the importance of making the nitrate corrections. The authors also pointed out the incorrect use of carbonate alkalinity in this context, since this parameter varies with temperature and pressure. Chen (1990) further questioned the validity of such vertical investigations unless corrections are made for possible differences in the concentrations of preformed concentrations of dissolved calcium and TA between surface and deep waters. His solution was to apply an arbitrary adjustment to the deep water values from his investigations of depth profiles. He used winter values of dissolved calcium and TA from the Weddell Sea as a baseline and calculated the flux of these parameters between the Southern Ocean and the site of interest in the North Pacific. The TA data had been corrected for nitrate as well as sulphur effects (Chen, 1985), and was in agreement with data for dissolved calcium.

Biological calcification in oceanic surface waters and the resulting export of particulate $CaCO_3$ to greater depths are largely determined by factors which influence the dominance of coccolithophorids and the remaining ecological structure of secondary producers in the upper part of the water column. These factors vary with oceanic region (Honjo (1996); see section 1.3.2.2.4), but also on much smaller scales. For example, the areal and vertical variability of calcification in surface waters of the Northeast Atlantic have been described in more detail in chapter 5 and by Holligan et al. (1993). The relationship between foodweb structure and export of particulates is dealt with by e.g. Fiadeiro (1980), Peinert et al. (1989), Angel (1989), Lampitt et al. (1993), and Harris (1994).

The range of 4 to 5 for POC:PIC ratios used in global carbon cycle models and the even wider range observed in nature and in a recent biogeochemical OGCM by Yamanaka and Tajika (1996) introduce a degree of uncertainty into any calculations that rely on accurate POC: PIC values. Ratios of POC:PIC export production have been mostly based on the comparison of the chemical composition, including TA, of seawater from surface and deep waters.

Further, on thermodynamical grounds, it remains unclear why, in spite of $CaCO_3$ supersaturation in the surface layers of the oceans, there is no evidence of abiotic precipitation in all but a few regions such as the Bahama Banks. Reasons for this have not been completely clarified, and suggestions have been reviewed by Skirrow (1975).

Of greater importance, though, is the improved understanding of the relationship between saturation and compensation depths for $CaCO_3$ (Edmond, 1974), i.e. why particulate $CaCO_3$ falls below the saturation depth where it would be expected to dissolve on the basis of thermodynamics. Estimation of dissolution rates for particulate $CaCO_3$ are complicated in nature, since this process may be retarded by surface coatings of a composition different from those of the bulk phases (Chave & Suess, 1970). Accordingly, Carter (1978) showed that biogenic and non-biogenic carbonate surfaces selectively adsorb aspartic-acid- rich organic matter. Fagerbakke et al. (1994) found supportive evidence for associated carbohydrates but not nucleic acids or proteins in their elemental analysis of coccoliths. However, inhibitory effects of dissolved organic matter (DOM) have not always been observed. In fact, it has also been proposed that DOM associated with particulate $CaCO_3$ could enhance respiratory dissolution anywhere in the water column, if the DOM provides substrate for heterotrophic organisms (e.g. Milliman et al., 1999). Alternatively, dissolution of liths may occur in acidic zooplankton guts (Harris, 1994).

Increased knowledge of the factors regulating the vertical profiles of POC and PIC are relevant if palaeoclimatic information is to be drawn from observed changes in saturation and lysocline depths. For example, Broecker (1982) used the difference in global lysocline depth between the glacial and interglacial periods to derive glacial TA values, and assumed a fixed POC:PIC rain ratio for both periods to calculate the glacial pCO_2. Further, the exact knowledge of these depths is vital for the identification of buffering processes involving $CaCO_3$ sediments above the lysocline in current oceans. For example, TA and TCO_2 were used by Adams and Mackenzie (1996) to add support to the hypothesis that respiratory calcite dissolution as described by Archer and Maier-Reimer (1994) may be taking place in sediments of the Arabian Sea at present. Since this alkalinity pump mechanism may become increasingly important in removing excess CO_2 in the longer term future in certain oceanic regions (Honjo, 1996), we also need to understand how these depths may be altered in response to anticipated scenarios of increasing CO_2 concentrations, and possibly changes in ocean circulation and biological pumps.

The accurate application of TA in the above studies involving changes in $CaCO_3$ concentrations rely largely on the appropriate corrections necessary to single out the change in carbonate concentration and corrections for differences in preformed concentrations of different water masses. In palaeoceanographic studies it is more complicated to apply and test

elaborate corrections to TA, e.g. Broecker (1982) used the simpler version of the potential alkalinity concept by adding the nitrate concentration to the specific TA value in his glacial/interglacial study. For the estimation of recent or current changes in $CaCO_3$, agreement between data from potential TA and dissolved calcium indicates that salinity- and oxidative nitrate-corrections appear to be largely adequate.

As can be seen from section 1.4.2 there may however be special circumstances under which the commonly applied corrections for nitrate and phosphate according to the original or modified Redfield ratio are insufficient or even incorrect. In surface waters this may apply if, for example, there is a significant amount of organic acid release or DMSP production. Currently, there do not seem to exist reports of field or culture studies in which the effects of these processes on changes in TA and derived estimates of $CaCO_3$ precipitation/ dissolution have been addressed in a systematic way. Such work should be considered bearing in mind that the inclusion of corrections for the oxidation of organic sulphur was found to improve the agreement between calcification estimates from dissolved calcium and potential TA by Chen (1978) in his investigation of vertical profiles in the Pacific Ocean. Chen (1990) included oxidative sulphur corrections in his investigation of $CaCO_3$ fluxes of Pacific deep water. Discrepancies were also observed by Rommets (1988) in one particular East Indonesian ocean basin with much increased specific TA values in the bottom hundred meters. In this case the discrepancy was ascribed to the oxidation of organic matter involving the reduction of nitrate and sulphate rather than oxygen in the upper layers of bottom sediments.

1.4.4.4. Use of TA in phytoplankton culture experiments

Measurements of TA have been used by, for example, Sikes et al. (1980) to determine the type of inorganic carbon source used by coccolithophorid species. They argued that, if the culture experiments are carried out in enclosed vessels, any pH changes can be attributed to movement of CO_2 into the algal cell whereas TA changes indicate HCO_3^- utilization.

1.4.4.5. TA effect on isotopic fractionation (palaeostudies)

In 1975 Brewer et al. pointed out that the isotopic carbon ratios may be affected by concentrations of dissolved $CaCO_3$. It has been demonstrated above that any changes in $CaCO_3$ concentrations may be incorrectly estimated by TA, if insufficient account is taken of

other reactions which may affect TA such as biological nitrate exchange, DMSP production, organic acid release, etc.. In most published works, corrections are only made for the first of these processes, which suggests that possible inferences with respect to isotopic fractionations may also be inaccurate.

1.5. AIMS OF THIS STUDY

The aims of this study were to

(i) develop a photometric TA method which would be precise and accurate enough to detect phytoplankton-induced TA changes in surface open ocean water samples and in algal cultures;

(ii) conduct methodological intercomparisons with other TA methods;

(iii) measure TA changes in the surface open ocean and investigate the most likely factors which influence the variability;

(iv) add to the information available for spatial and temporal variations of TA within the Northeast Atlantic;

(v) compare changes in TA to those measured for PIC production in the open ocean and in *Emiliania huxleyi* cultures.

2. TOTAL ALKALINITY METHOD

2.1 AIM

The aim was to set up a relatively simple spectrophotometric TA method, which would have the required precision and accuracy to measure phytoplankton-induced TA changes in seawater and culture samples. This method should also be suitable for use on board ship and the sample volume should not exceed 150 cm^3.

2.2. INTRODUCTION

A number of approaches are described in Almgren et al. (1983) which are based upon

(i) the backtitration method (Gripenberg, 1936);

(ii) the single point pH method (Anderson & Robinson, 1946);

(iii) the potentiometric or spectrophotometric pH titration method (Dyrssen, 1965; Graneli & Anfalt, 1977).

Since their introduction, all of these approaches have been considerably refined. A modified single point method by Perez and Fraga (1987) has an improved precision compared to the original method. Recently, Dickson's group at the Scripps Institute for Oceanography (SIO), U.S., has been working on the development of a highly accurate and definitive TA method in order to achieve greater accuracy (Dickson, 1991b). It is essentially a coulometric backtitration method based on the procedure used at the U.S. National Institute for Standards and Technology to certify primary standard acids and bases.

A titration approach was chosen for the present work because it is

(i) less time-consuming and more convenient than the backtitration method;

(ii) more precise than the single point method of Anderson and Robinson (1946);

(iii) the necessary sample volume is smaller than the one needed by Perez and Fraga (1987).

2.2.1. ANALYSIS OF THE TITRATION CURVE

There are two different statistical approaches for estimating the equivalence point from the titration data to calculate TA. For the linear least squares regression analysis the pH values are converted to modified Gran functions as described by Dickson (1981) and Anderson and Wedborg (1983). The various non-linear least squares or curve fitting approaches are all based on the same mass balance and equilibrium relationships but differ in how the experimental data are weighted in the fitting procedure. The currently most commonly used curve fitting method for seawater titrations derives from a modified Marquardt procedure as described by Dickson (1981) and Johansson and Wedborg (1982). When Anderson and Wedborg (1985) examined the effect of these different statistical approaches upon the photometric TA results, they found that the results from the linear approach were more than 1% smaller than those from the non-linear method. In this study the linear least squares approach was chosen because of its simpler computation.

2.2.2. THEORY OF THE TA DETERMINATION

Total alkalinity is determined by adding increments of strong acid of known strength to a sample of known volume and recording the respective pH or hydrogen ion concentration. Hydrochloric acid is commonly used for this purpose. The pH values are usually measured before or after the equivalence point for TA which is at a pH of around 4.4 in oceanic seawater.

In order to detect the equivalence point in an acid-base titration, Gran (1952) suggested plotting the so called Gran function (denoted F_G here) against the volume of titrant added. In the context of TA determinations F_G is plotted against the volume of acid (va) added and is defined as:

$$F_G = 10^{k-pH} * (vb+va) \qquad (2.1)$$

where k can be any convenient number which is used as a scaling factor and vb is the volume of the sample. The term (vb+va) accounts for the change in volume of the sample due to the addition of the acid. If k is taken to be zero and the volume correction term is adjusted, this original Gran function represents the volume-corrected free hydrogen ion concentration ($[H^+_{free}]$) per litre. It can be rewritten as $F_{G'}$:

$$F_{G'} = [H^{+}_{free}] * \frac{vb + va}{vb}. \qquad (2.2)$$

Once the sample has been titrated sufficiently beyond the equivalence point, most of the bases will have been neutralized. Upon further acid addition, the concentration of the base will become negligible and almost all protons added from the hydrochloric acid will stay unassociated, i.e. their increase in the sample is almost proportional to the volume of acid added. The plot of the modified Gran function against added titrant should, therefore, approximate a straight line. The intercept of this line with the x-axis reveals the equivalence point, i.e. the amount of acid needed to neutralize all the base of that sample. In order to obtain a perfectly straight line, the measured $[H^{+}_{free}]$ would have to be corrected for the small amounts of untitrated base still present in the sample.

Since the original Gran function was only intended for use with simple solutions, it requires refinement if applied to seawater which contains several interfering acid-base systems. Dickson's definition of TA provides the guideline for these modifications (Dickson, 1981) (see section 1.4.1). In a seawater solution containing water, carbonic acid, boric acid, hydrogen sulphate, and hydrogen fluoride Dickson defines the modified Gran function (C_H) as:

$$C_H = ([H^{+free}] + [HSO_4^-] + [HF] - [HCO_3^-] - 2[CO_3^{2-}] - [B(OH)_4^-] - [OH^-]) * \frac{(vb + va)}{vb}. \qquad (2.3)$$

If there are still unneutralized proton acceptors (i.e. HCO_3^-, CO_3^{2-}, $B(OH)_4^-$, and OH^-) left in the sample at a given point during the titration, these will reduce the increase in the free H^+-concentration of the sample as they will react with some of the protons added. In graphical terms, they will reduce the slope of the Gran plot which leads to a reduced equivalence point. For Gran's basic assumption to remain valid, the concentration of these unneutralized bases has to be subtracted from the measured free H^+-concentration. If HF or HSO_4^- are formed at any point during the titration, they will also reduce the increase in proton concentration in the sample. However, according to the operational TA concept they represent proton donors just like the free hydrogen ions. Their concentrations, thus, have to be added to the free hydrogen ion concentration.

When the readings are taken within the pH range of 3.9 - 2.8, one only needs to account for the following reactions:

$$HCO_3^- + H^+ \_ H_2CO_3 \quad (2.4)$$

$$SO_4^{2-} + H^+ \_ HSO_4^- \quad (2.5)$$

$$F^- + H^+ \_ HF. \quad (2.6)$$

The original Gran function F_G, has to be corrected at each point of the titration for the presence of HCO_3^-, HSO_4^-, and HF, so that the modified Gran function becomes:

$$C_H = ([H^+_{free}] - [HCO_3^-] + [HSO_4^-] + [HF]) * \frac{vb+va}{vb}. \quad (2.7)$$

The effect of unassociated proton acceptors and the formation of proton donors in seawater upon the original Gran function in the pH range between 3.9 to 2.8 is shown in figure 2.1. The modified Gran functions are also included to show the general effect of these corrections at different pH ranges.

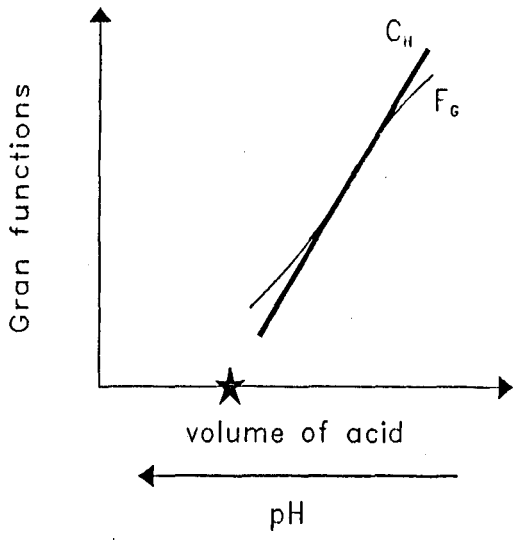

Figure 2.1: Schematic diagram of the effect of unassociated proton acceptors and the formation of proton donors in seawater upon the original Gran function $F_{G'}$ (thin line) in the pH range of about 3.9 - 2.8. The modified Gran function C_H (full line) is included. The star on the x-axis indicates the position of the equivalence point.

The diagram shows that the corrections tend to increase the equivalence volume in the pH range close to the equivalence point which is largely due to the presence of unneutralized bicarbonate ions. At a lower pH some of the protons will react with F^- and SO_4^{2-} ions. The corrections for this tend to decrease the equivalence volume.

2.2.3. THE MEASUREMENT OF PH

Measurements of pH are usually carried out potentiometrically with a glass electrode or photometrically with a pH indicator dye. Anderson and Wedborg (1983) suggested that a photometric system may bear advantages over a potentiometric method due to the response time of a glass electrode and the greater sensitivity to voltage transients in the case of potentiometry. These authors used a sample volume of only 12 cm^3 and the time required to obtain one titration point was only 5 seconds. In a later study the same authors conclude, however, that the potentiometric method is to be preferred to the photometric one because potentiometric measurements can be made over a wider pH range while indicators can only be used in their much narrower colour transition range within ±1.5 pH units of the indicator pK (Anderson & Wedborg, 1985). King and Kester (1989) obtained photometric TA values which they quoted as 0.03 meq kg^{-1} lower than their potentiometric results.

In photometric titrations the pH measurements have most commonly been determined by measuring the absorption of an indicator in the sample with a spectrophotometer at either one or more wavelengths.

pH indicators are weak acids which change their colour when the indicator molecule (Ind^-) gets protonated or deprotonated. The acid-base equilibrium can be defined by

$$HInd \overset{K_{Ind}}{\rightleftharpoons} H^+ + Ind^- \qquad (2.8)$$

where K_{Ind} is the dissociation constant of the indicator.

$$K_{Ind} = \frac{[HInd]}{[H^+] + [Ind^-]}. \qquad (2.9)$$

The total indicator (Ind_T) concentration is then

$$[Ind_T] = [HInd] + [Ind^-]. \qquad (2.10)$$

The pH of a solution can be determined from the pK of the indicator (pK_{Ind}) and the concentration ratio of Ind^- and HInd:

$$K_{Ind} = [H^+] + [Ind^-]/[HInd]. \qquad (2.11)$$

The ratio of Ind^- to HInd is determined colourimetrically by measuring the optical absorbance of the indicator either at one or more wavelengths.

For the single wavelength method

$$\frac{[Ind^-]}{[HInd]} = \frac{A1_{(HA)} - A1}{A1 - A1_{(A^-)}} \qquad (2.12)$$

where A1 is the absorbance of the indicator in the sample during the actual measurement of the pH. The term $A1_{(HA)}$ represents the absorbance value taken when all the indicator is assumed to be in the acidic (i.e. associated) form which is usually the case when the sample pH is three units below the indicator pK value. Conversely, $A1_{(A^-)}$ is measured at a pH three units above the indicator pK when all the indicator is assumed to be in its basic, (i.e. unassociated) form. The single wavelength procedure is described in most text books on photometry and specifically by Anderson and Wedborg (1983).

For the dual wavelength procedure

$$\frac{[Ind^-]}{[HInd]} = \frac{\frac{A1_{(HA)}}{A2_{(HA)}} - \frac{A1}{A2}}{\frac{A1}{A2} - \frac{A1_{(A^-)}}{A2_{(A^-)}}} \qquad (2.13)$$

where A1/A2 is absorbance ratio of the indicator at two different wavelengths. The denotations for the A2 terms have the same meaning as for A1 above. The dual wavelength procedure is explained by Byrne (1987) and King and Kester (1989). When the pH is calculated from absorbances at two wavelengths, an additional correction term has to be added, thus

$$pH = pK_{Ind} + \log \frac{\frac{A1_{(HA)}}{A2_{(HA)}} - \frac{A1}{A2}}{\frac{A1}{A2} - \frac{A1_{(A^-)}}{A2_{(A^-)}}} - \log \frac{A2_{(A^-)}}{A2_{(HA)}}. \qquad (2.14)$$

Different dilution corrections have to be applied to some of the absorbance values and ratios due to the addition of the indicator solution and the titrant (see appendix 1 for the details).

The absorbances are usually read at the wavelength of maximum absorption of the unassociated and/or associated indicator forms (e.g. Byrne, 1987). Thus, the pH-related absorbance changes will be most pronounced. However, King and Kester (1989) use the isosbestic point wavelength as their second wavelength. This is the wavelength at which different pH-solutions of an indicator have the same absorbance value. Consequently, the absorbance of an indicator solution at this wavelength does not change upon acidification, and its use as the second wavelength justifies the omission of the additional correction term in equation 2.14 (King & Kester, 1989).

The absorbance ratio method can potentially give more accurate pH results since any instabilities in the photometric instrument are more likely to affect the absorbance readings at one wavelength but not the ratio of two readings. This is, however, not true when the second wavelength gives low absorbance readings which tend to be less accurate. This might be the case for absorbance readings at the isosbestic point wavelength. When developing the method for the present work, it had to be established experimentally whether to adopt the single or dual wavelength method.

In order to ensure that the slope of the modified Gran plot is correct, it is vital that Beer's law is applicable for the indicator and the photometric set up. This law implies that the indicator concentration and the absorbance are proportional.

For TA determinations, the titrations are usually carried out within a pH range close to the equivalence point, i.e. at a pH of around 4.4. In this pH region it is necessary to know the exact TCO_2 concentration because corrections have to be applied to the original titration data for any

bicarbonate which has not been neutralized at any given point during the titration. At a pH lower than 3.2 these bicarbonate corrections have less impact upon the final TA result, so that an approximated TCO_2 concentration will create only a negligible error in the final TA result. King and Kester (1989) determined the pK values for several sulphonephthalein indicators with different operational pH ranges in seawater of 35 psu (practical salinity units) at 25°C. One of these, bromophenol blue, has a pK value of about 3.7. In order to avoid any bicarbonate interferences, an indicator with a pK of around 3.0 would be the most appropriate choice. Unfortunately, the pK values in seawater have not been determined for indicators such as quinaldine red or p-nitrophenylhydrazine, which change colour in this pH region. Accurate pH measurements are increasingly difficult to make when the pH values are below about 2.8 because the solution is buffered by a large excess of protons (Wedborg, pers. comm.). Since these indicators can only provide reliable pH values over a limited pH range, King and Kester (1989) suggest the use of a combination of two or more indicators in a sample, if a wider pH range is to be analysed.

If an indicator with a pK smaller than 4.5 is added to the sample in its acidic form, the indicator will dissociate in the alkaline seawater sample (see equation 2.8). This does not alter the TA according to Dickson (1981). However, since the Ind^- has to be treated like F^- and SO_4^{2-} throughout the titration, the concentration of HInd has to be added to the modified Gran function. On the other hand, the addition of the indicator solution introduces protons into the sample, i.e. it acts like HCl. The protons of the indicator thus have to be subtracted from the modified Gran function. Since the concentration of protons from the indicator can be assumed to equal Ind_T, the final correction for the indicator in the modified Gran function is derived from equation 2.10. The modified Gran function then becomes:

$$C_H = ([H^+_{free}] - [HCO_3^-] + [HSO_4^-] + [HF] - [Ind^-]) * \frac{vb + vi + va}{vb + vi}, \quad (2.15)$$

where vi is the volume of the indicator solution added to the sample. This is the function that was used in this work.

For high accuracy the titration should be carried out in a closed titration cell without any headspace above the sample. This prevents cumulative pH shifts throughout the titration due to CO_2 loss from the sample to the atmosphere or headspace. Dickson (1991b) recommends a thermostatted Lucite® cell as presented by Bradshaw and Brewer (1988a). If this type of setup is not available, it is possible to reduce the problem of CO_2 loss by minimizing the surface/volume ratio of the sample. Theoretical and experimental evidence for this is provided by Perez and Fraga (1987).

2.2.4. PRECISION AND ACCURACY OF TA MEASUREMENTS

A precision of better than 0.1% has been obtained with the potentiometric and photometric titrations (Johansson & Wedborg, 1982; Anderson & Wedborg, 1983) as well as with the single point method of Perez and Fraga (1987). Dickson (1991a) quotes a precision of 0.02% for the coulometric approach.

At the time of the work described here, reliable TA standards were not readily available. Dickson (1991a) expects the coulometric backtitration method to reach an accuracy of 0.05% once it has been compared with completely independant approaches. These include assaying the acid against pure silver and analysing the certified reference material 'tris' which can be obtained from the U.S. National Institute for Standards and Technology. Since no work seems to have been published in any of the major scientific journals in which these types of standardizations have been carried out, it seems that nobody is in the position at this point to claim a high degree of accuracy. Until now only intercomparisons have been carried out. The results of an intercalibration exercise between different laboratories reveal maximum differences between mean TA values of 1.4% using different analytical methods (UNESCO, 1990). This is about 5 or 10 times greater than the reproducibility of individual laboratories.

Since TA was initially not thought to vary much in the open ocean, some people held the view that a focus on a reproducibility of 0.2% would be essential for the investigation of TA changes, while the accuracy was not considered as important. However, if interannual trends are to be picked up within the greenhouse context, then the accuracy would have to match the desired precision of the method.

2.2.5. SPECIFIC ANALYTICAL PROBLEMS

Calcite has a -log K_{sp} value of around 6.1 (UNESCO, 1983). If the TA titrations are carried out in a pH range below the equivalence point, at least some of the $CaCO_3$ is expected to dissolve. The dissolution reaction rate increases with decreasing pH, i.e. during the course of the titration. The release of CO_3^{2-} ions into solution alters the pH of the sample and thus the equivalence point and final TA result. Since the solubility product cannot be predicted with certainty when the $CaCO_3$ particles are coated with organic compounds, it had to be established experimentally whether the dissolution of the $CaCO_3$ will affect the final TA results.

The size of intact coccoliths has been found to be between about 0.8 and 1 μm, but rarely smaller (D. Harbour, pers. comm.). If the samples are filtered before the titration, it is generally assumed that all the particulate $CaCO_3$ is removed from the solution. However, some types of filters may act as ion exchangers and can change TA either way (Goldman & Brewer, 1980). It is therefore necessary to ensure that the filters used for the pre-treatment of the samples do not have a significant effect upon the TA of the samples.

2.3. MATERIALS AND METHODS

2.3.1. EXPERIMENTAL PROCEDURE AND APPARATUS

Samples for TA analysis were decanted into boro-silicate bottles with ground glass stoppers. The bottles held approximately 125 cm^3 after the bottles were closed with the stoppers and subsequently the stoppers were removed again. The exact volume of each individual bottle had been previously measured to a precision of better than 0.012%. This was done by replicate weighing of the bottles before and after they had been filled with distilled water of a known temperature.

A volume of 4 cm^3 of bromophenol blue indicator solution was added to the sample to give a final indicator concentration of 10 (±1) μM. When this indicator becomes protonated it changes colour from blue to yellow. The indicator stock solution was made up by dissolving 44 mg of the indicator in 5 cm^3 of ethanol, adding 4 g of NaCl dissolved in freshly deionized water, and

adjusting the volume to 100 cm^3. According to the suppliers (Merck Ltd., U.K.), the indicator is in its acidic form. This particular concentration of indicator had been found to be the best compromise between obtaining optimal absorbance readings and avoiding precipitation of the indicator in the indicator stock solution, which occurred when higher indicator concentrations were used. The most reliable absorbance readings tend to be at around 0.4 absorbance units (AU). A magnetic stirrer bar was used to ensured that the sample was mixed in the bottle after about 5 seconds. Hydrochloric acid of about 0.4 N strength was added via a $1cm^3$-Metrohm-Dosimat semi-automated burette. The acid was prepared from a BDH ConvoL® solution with a specified accuracy of 0.1% . An ionic strength of about 0.7 N, similar to that of seawater, was obtained by adding approximately 41 grams of NaCl per dm^3 of the acid solution. This particular acid concentration had been chosen as it is strong enough to acidify the sample to the required pH range which is reached on addition of about 0.8 cm^3 of acid. This is important as the burette readings become more accurate the closer the readings are to the total burette volume. Therefore, the first acid addition was large, followed by 34 small increments of 0.005 cm^3.

Absorbance readings were taken with a Hewlett Packard HP8452 diode array spectrophotometer at 590 nm (A1) and 496 nm (A2). With an instrumental resolution of 2 nm these two wavelengths were found to be the closest it was possible to get to the wavelength of the maximum absorbance of the basic indicator and of the isosbestic point, respectively. By measuring at these two wavelengths, it was possible to calculate the TA results with both the single and dual wavelength method.

The absorbance readings obtained from distilled, deionized or seawater blanks were not significantly different. However, occasionally it was found that they would drift in both directions over time, and this instability could sometimes also be noted in the course of titrations when absorbances at either wavelength changed to an abnormal extent. The design of the titration apparatus did not allow the measurement of optical blanks during the course of a titration and the erratic nature of the variations diminished the usefulness of the application of an optical blank measurement at the end of a titration. Therefore, no corrections were made for optical blanks or instrumental drift, once the instrument had initially been set at optical zero just before the start of the titration. The absorbance minimum values, which are described

below and which were usually close to zero, were used as an additional check on the reliable performance of the spectrophotometer.

The absorbances were read twice upon each addition of acid. The readings were averages of 50 measurements which were taken over a period of 5 seconds. Comparison of the two averaged absorbance values provided some check on disturbances in the system. For the determination of the absorbance maximum and minimum values, readings were taken at the beginning of the titration, before any acid addition, and at the end, after having added 4 cm^3 of 50% HCl. (N.B. Before the 4 cm^3 of HCl could be added, 4 cm^3 of sample had to be removed in order to prevent an overspill of the sample from the titration bottle.) These volume changes were corrected for in the analysis of the data. To ensure that the absorbance maximum and minimum readings were taken sufficiently above and below the indicator pK, these values had been validated in preliminary experiments by adding 50% NaOH and 50% HCl to each sample, respectively. For each individual sample an average of twelve absorbance readings was used for the absorbance maximum and minimum values.

A schematic diagram of the titration system is depicted in figure 2.2.

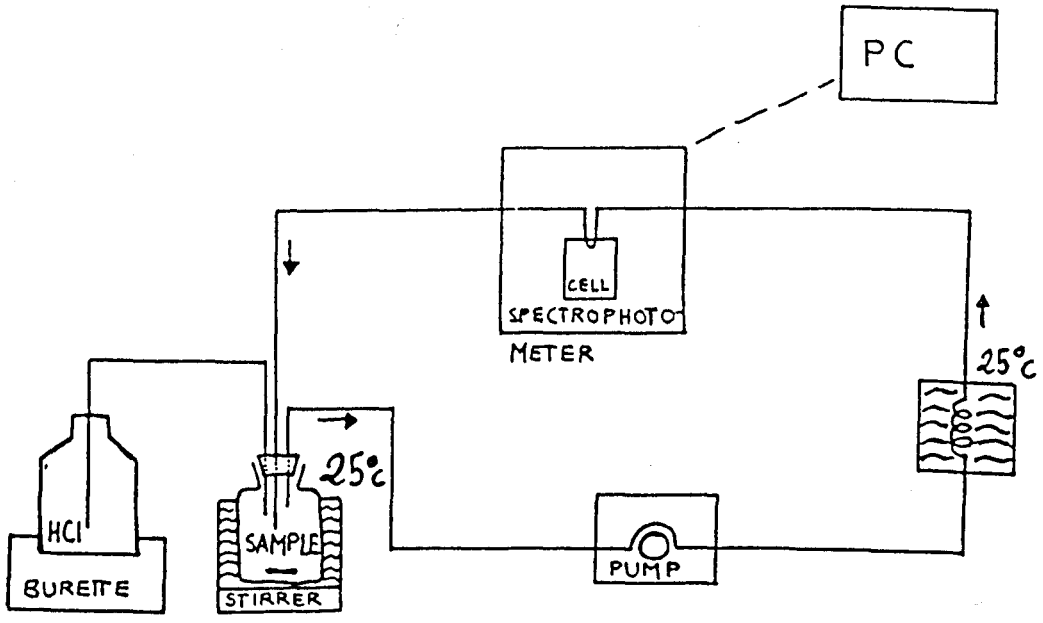

Figure 2.2.: Schematic diagram of the spectrophotometric titration apparatus for TA.

During the titration the sample was continuously pumped from the sample bottle via a peristaltic pump to a flow cell of 1 cm pathlength in the spectrophotometer and back to the sample bottle. The plumbing which preceded the flow cell was kept in a water bath of 25°C (±1°C), i.e. the temperature for which the indicator pK value had been determined by King and Kester (1989). The sample bottle was also kept in a waterbath of the same temperature. The temperatures of each sample were checked before and after each titration. If necessary, the waterbath temperatures were adjusted accordingly. However, it was not possible to check the exact sample temperature in the photocell. Before the inlet and outlet of the flow circuit were inserted into the sample, the tubing was flushed with a sample of similar composition and subsequently drained as thoroughly as possible.

The surface area of the sample which was in contact with the atmosphere or headspace was smaller than 1.5 cm in diameter. The sample bottle was covered firmly with a silicon bung, which held the burette tip and the inlet and outlet of the flow circuit in place. The volume of the headspace between sample and silicon bung was a little more than 1 cm^3 at the onset of a titration to allow for the addition of the titrant. No systematic tests were carried out to assess the extent of possible CO_2 loss over the period of the entire titration, and theoretical calculations of the loss would have been complicated due to the turbulence caused by the stirrer. When acidified samples were left for more than 20 minutes, the variations of absorbance readings were no greater than the variations caused by the normal level of instability exhibited by the spectrophotometer. Even though the titration vessel was not perfectly sealed, the error in the pH readings due to CO_2 loss was assumed to be within the precision limits of the method. It was, therefore, considered to be justifiable to assume that the titration mixture was effectively a closed system and that the results obtained were not appreciably affected by losses of carbon dioxide from solution.

After each acid addition the sample was allowed to mix for 30 seconds before the absorbance was measured in the flow cell. This delay was necessary as the flow circuit held about 2 cm^3 of sample and it took about 8 seconds for the sample to travel through the plumbing and the flow cell.

Provided the spectrophotometer performance was stable, the analysis of one sample took about 50 minutes in total. If the spectrophotometer was found to give continued unreliable readings, the titration was paused until stability was reestablished, or the titration had to be stopped. It was generally not possible to predict the times at which the spectrophotometer would return unreliable readings. In the laboratory, its performance was not improved at night, when the electrical supply could be assumed to be most stable. However, onboard ship the absorbance readings became notable more unstable after a power cut had occurred.

For each titration the temperatures were recorded of the acid and of the sample when it was filled into the titration bottle, so that density corrections could be made. After a titration had been completed, the raw absorbance data was stored on a computer disc.

2.3.2. CHECK ON THE APPLICATION OF BEER'S LAW FOR SOLUTIONS OF BROMOPHENOL BLUE

In order to ensure that Beer's law was obeyed throughout the range of absorbances encountered during the titration, the absorbances of five solutions with different amounts of indicator solution added to them were measured at 590 and 496 nm. This law states that the relationship between indicator concentration and absorbance must be linear, and it implies that both parameters should be zero once corrections for the solvent blank have been applied. The solutions had been made up with seawater which had been filtered (0.2 µm Gelman filter) and UV radiated at 254 nm. The setup of the usual TA titration was used. The indicator concentrations of 2.5, 5.0, 7.5, 10.0, and 12.5 µM were chosen, which covered all the absorbance ranges usually encountered during titrations. Three sets of measurements of the 12.5 µM indicator solution were taken at 5 minute intervals. The seawater had an initial pH of about 8.1. It was, therefore, assumed that the differences in absorbance readings were due solely to the different concentrations of indicator and not due to any alterations of the sample pH as a result of different amounts of indicator solution added. Hence, no buffer was added to the seawater. For comparative purposes absorbances of the same samples were measured immediately afterwards on a Cecil 1010 spectrophotometer which has a resolution of 0.1 nm. The results of the spectrophotometric absorbance readings from solutions of different indicator concentrations are presented in figure 2.3.

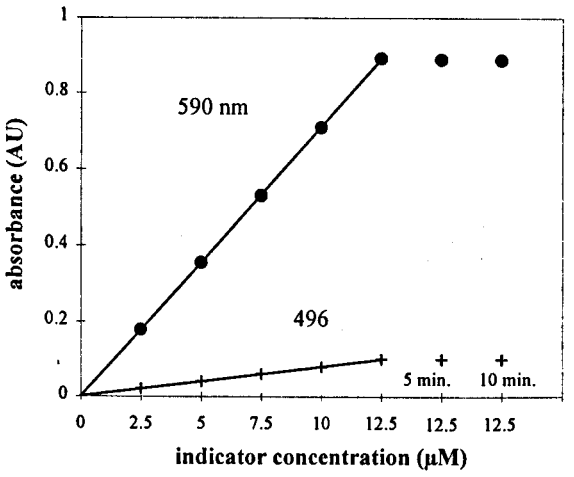

abs(590) = 0.0712 (±0.0001) conc -0.0014 (±0.0018)

$R^2 = 0.9999$
$P < 0.001$

abs(496) = 0.0081 (±0.0002) conc + 0.0002 (±0.0003)

$R^2 = 0.9998$
$P < 0.001$

Figure 2.3.: Absorbance readings at 590 and 496 nm in AU from the HP8452 diode array spectrophotometer plotted against concentration of bromophenol blue (μM). Two additional readings were carried out at 12.5 μM 5 and 10 minutes after the first reading at that concentration. For the results of the regression analysis only the initial 12.5 μM values were used.

The standard errors of the intercepts of the regression lines are within the specified instrumental error and include the origin, thus suggesting that the indicator solution obeys Beer's law over the range of absorbances used. When the intercept values of the regression lines from both wavelengths were compared on a percentage basis, i.e. by dividing these values by the respective slope values, the intercept of the 590 nm regression line was found to be relatively closer to the origin. Similarly, the standard error of the intercept values was relatively smaller for the 590 nm than for the 496 nm readings.

Results from Ancova tests (Sokal & Rohlf, 1981) indicate that there was no significant difference between the absorbance values returned by the two instruments at 590 nm. However, they were different for 496 nm readings at the 95% confidence level (c.l.).

If the measured absorbances of the solutions of the indicator were strictly proportional to their concentrations the ratio A1/A2 should be independent of indicator concentration. Figure 2.4. shows that this ratio tended to increase with increasing concentrations using one spectrophotometer and showed an initial decrease with the other instrument. According to an Ancova test, these results were significantly different between methods (95% c.l.).

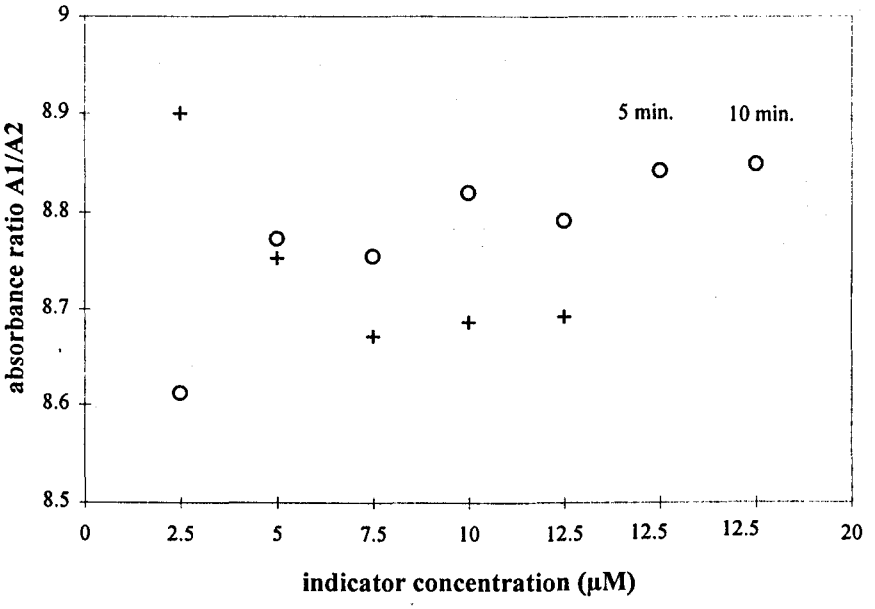

Figure 2.4.: Plot of absorbance ratio A1/A2 (590nm/496nm) against the concentration of bromophenol blue (μM). Absorbance readings were obtained with the HP8452 diode array spectrophotometer (O) and the Cecil 1010 spectrophotometer (+).

Two additional readings were carried out with the diode array spectrophotometer for the 12.5 μM solution 5 and 10 minutes after the first reading at that concentration.

The s.d.(n-1) on the ratios obtained for the diode array spectrophotometer were generally smaller than 0.014.

The largest anomalies occurred with both instruments at the lowest indicator concentrations and with absorbance values in the range when the measurements become increasingly inaccurate. These anomalies may have implications for the application of spectrophotometric methods for the determination of pH with the instrumentation used in this work.

It is noteworthy that all the A2 readings except the ones at 12.5 μM are in an absorbance range of <0.1 AU in which the accuracy of the absorbance readings is largely decreased. The ratio measured for 12.5 μM after 10 minutes gives an idea of how much the ratio can be subject to shifts in the absorbance readings with time. In most instances, the readings taken at 496 nm were found to vary proportionally more than those taken at 590 nm. It is not clear whether this is because readings are generally more unreliable at 496 nm or because the absorbance values at 496 nm were relatively low and therefore less reliable.

2.3.3. COMPUTATION OF TA RESULTS AND ACID STANDARDIZATIONS

The absorbance data was loaded into a Turbo Basic program which had to be written specifically for the apparatus and procedure used in this study. The program was checked with theoretical titration data provided by Dickson (1981). The steps used to calculate TA or the acid strength from the raw absorbance data are illustrated in figure 2.5. The equations and constants used are given in appendix 1. The Turbo Basic program for the determination of TA using the single wavelength method is provided in appendix 2.

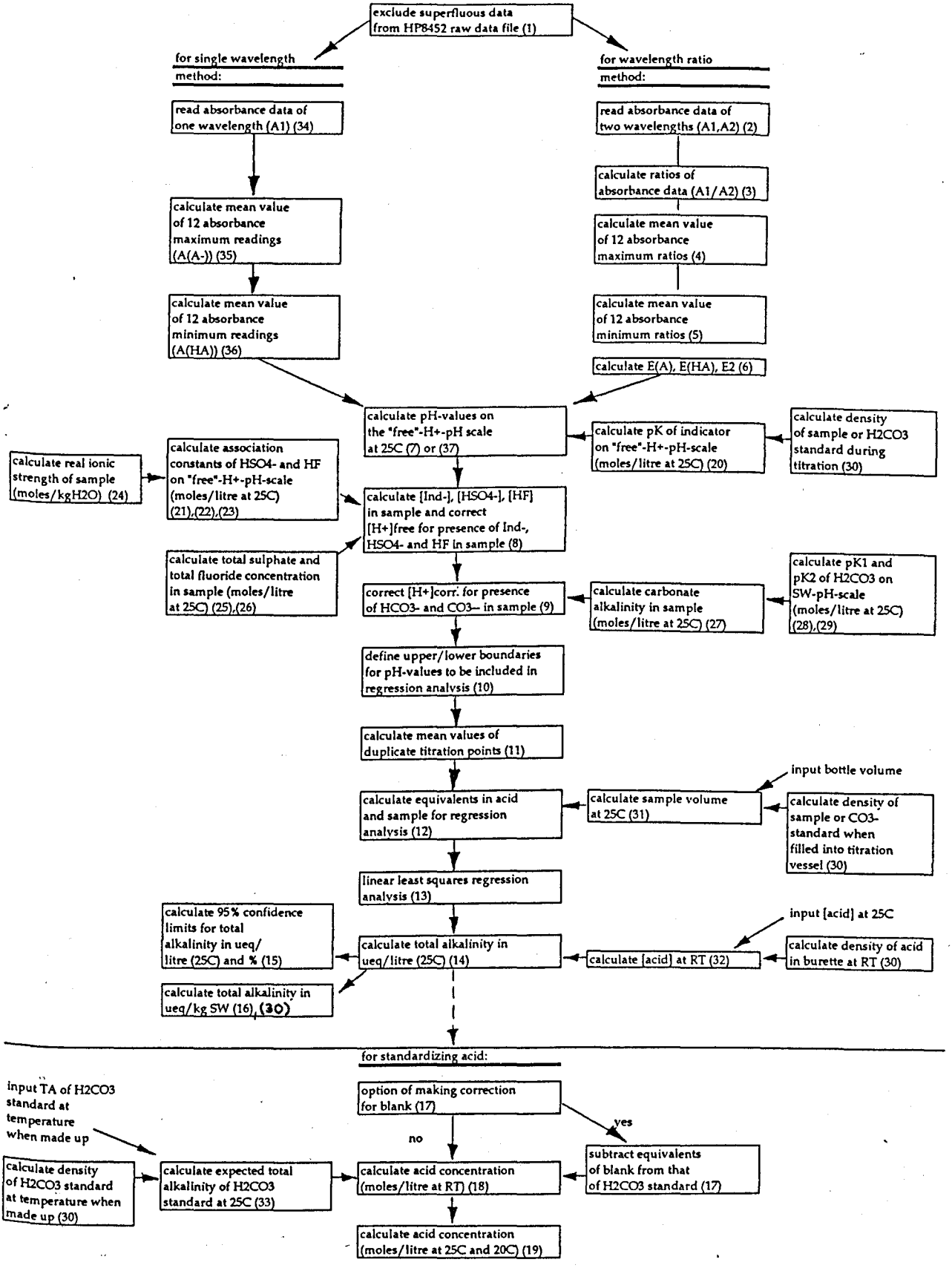

Figure 2.5: Schematic diagram of the steps used to calculate TA and acid strength. The numbers in brackets correspond to the respective parts in the list of equations (appendix 1) and the listing of the Turbo Basic computer program (appendix 2).

The calculations of pH with the single wavelength method were adapted from Anderson and Wedborg (1983) and those with the dual wavelength method were derived from King and Kester (1989). Corrections of the titration data for the presence of sulphate, fluoride, indicator, and carbonate were carried out according to Dickson (1981) and Anderson and Wedborg (1983). The constants or pK values used to calculate the species concentrations were taken from Khoo et al. (1977), Dickson and Riley (1979), King and Kester (1989), and Goyet and Poisson (1989), respectively. Effective ionic strength was determined according to Ramette et al. (1977), and the density of seawater according to Millero and Poisson (1982).

Instead of regressing the modified Gran functions on the volume of acid added, the x-axis was chosen to represent the cumulative amounts of protons added from the acid to a sample of one litre. This allowed direct comparison between the protons added and the equivalent increases in the Gran functions used.

The TA results were initially obtained in $\mu eq\ dm^{-3}$ at 25°C and converted to $\mu eq\ kg^{-1}$ of seawater ($\mu eq\ kgSW^{-1}$) by dividing the initial value by the density of the seawater at 25°C. From the regression analysis of the modified Gran plots the 95% confidence limits of the final TA results were calculated using the method described in Sokal and Rohlf (1981).

2.3.4. STANDARDIZATION OF ACID

Two different batches of HCl were used for the TA determinations. They were standardized against Na_2CO_3 standards of about 1100 µM in deionized water , thus approximating the TA of 2200 $\mu eq\ dm^{-3}$ in seawater. The Na_2CO_3 (BDH AnalaR®) had been dried in an oven for two hours at 285°C and left to cool overnight before weighing. To adjust the standards to the ionic strength of seawater, 40.9 grams of NaCl (BDH AnalaR®) were added to each litre of sodium carbonate solution. The temperature of these standards was recorded when making them up, so that density corrections could be applied (see point 30 and 33 in appendix 1). The density calculations provided by Millero and Poisson (1981) are, strictly speaking, for seawater. However, this was assumed to introduce only a negligible error since the ratio of two density values was used for the corrections. The Na_2CO_3 standards were then titrated with the HCl solutions used for TA determinations in the same way as described for seawater samples.

Determinations of reagent blanks were carried out to correct for any impurities present in the water and in the NaCl used to prepare the standard and the acid solution. Acid I was standardized against four different standards whereas acid II was standardized only against one. Since the reproducibility of the blank determinations was greater than 0.3%, it was decided not to apply any blank corrections, and no blanks were determined for acid II.

2.3.5. ESTIMATING THE EFFECT OF COCCOLITH DISSOLUTION DURING A TITRATION ON TA DETERMINATIONS

In order to find out whether the dissolution of coccoliths during a TA titration significantly alters the TA results, samples of a diluted culture of the coccolithophorid *Emiliania huxleyi* was analysed with and without previous filtration through Whatman cellulose nitrate membrane filters (pore size <0.2 μm). A vacuum pressure of about 0.2 bar was used. The cell density of the culture was adjusted to a more realistic open ocean bloom condition of about 10^7 cells per litre by diluting the original culture with the appropriate amount of pre-screened seawater, which had been pre-filtered through an Gelman filter with a nominal pore/mesh size of 0.2 μm and then UV-radiated at 254 nm. The PIC content of this diluted culture was not determined, but based on the approximate cell number and the ratio of PIC per *E. huxleyi* cell determined during the culture experiments (chapter 6), an approximate PIC concentration of 5 μM could be expected. The pre-screening process is part of the standard treatment for one of the laboratory supplies of large amounts of seawater which otherwise may have a considerable loading of particulates. This process has no bearing on the intended investigation. The results from this comparison are presented in table 2.1.

The unfiltered samples of coccolithophorid cultures led to higher TA results than the filtered samples by approximately 15 μeq dm^{-3}. According to a non-parametric Wilcoxon two-sample test these results were significant at $P = 0.24$. The increase in TA by 10 - 20 μeq dm^{-3} roughly ties in with the presumed PIC concentration. This suggests that the presence of PIC in form of *Emiliania huxleyi* cells led to an equivalent increase in TA of the same order in the case of the photometric TA method of this study.

Table 2.1.: Results from the comparison of TA in filtered and unfiltered diluted cultures of *Emiliania huxleyi* to estimate the effect of coccolith dissolution during the TA titration. Diluted *E. huxleyi* cultures with an approximate final cell density of 10^7 dm^{-3} had been passed through Whatman cellulose nitrate membrane filters with a pore size of 0.2 μm. Note that the standard deviation (s.d.(n-1)) was based on a mean derived from only two replicates.

	TA (μeq dm^{-3}) in	
	unfiltered samples (n = 2)	filtered samples (n = 2)
	2291.7	2270.3
	2282.6	2274.1
mean	2287.1	2272.2
s.d.(n-1)	6.4	2.7

2.3.6. ESTIMATING THE EFFECT OF CELLULOSE NITRATE FILTERS ON TA DETERMINATIONS

In order to examine the possible effects of filtration through Whatman cellulose nitrate membrane filters on the final TA results, filter- and UV-sterilized seawater (see section above) was analysed with and without previous filtration through the filter, which had a pore size of 0.2 μm. The filtration was conducted using a vacuum pressure of about 0.2 bar. The results from this comparison are presented in table 2.2.

The mean results for the filtered samples were slightly lower than for the unfiltered ones. However, this difference was regarded as insignificant within the context of this study and seemed to be within the error range of the method.

Table 2.2.: Results from the comparison of TA in filtered and unfiltered seawater to examine the effect of Whatman cellulose nitrate membrane filters with a pore size of 0.2 μm. Prior to this the seawater had been prefiltered through courser filters and had also been UV-sterilized.
Note that the standard deviation (s.d.(n-1)) was based on a mean derived from only 2 replicates in the case of the unfiltered samples.

	TA ($\mu eq\ dm^{-3}$) in	
	unfiltered samples (n = 2)	filtered samples (n = 3)
		2287.1
	2287.7	2282.6
	2285.9	2281.8
mean	2286.8	2283.8
s.d.(n-1)	1.3	2.9

2.3.7. STORAGE OF THE SAMPLES

Mercuric chloride is frequently added to samples immediately after collection to stop any biological activity. Since none of the TA samples were stored for more than three days, no mercuric chloride was added to any of the samples. Instead, they were kept in 200 cm^3 glass bottles in the dark at a temperature as close as possible to about 4°C. Prior to the titrations the samples were allowed to warm up to 25°C. In the case of samples with high algal cell numbers, i.e. those from the culture experiments and the 1991 cruise, the samples were filtered through Whatman cellulose nitrate filters of 0.45 μm pore size. Filtration took place as soon as possible after collection, usually within one hour. On theoretical grounds, any errors due to biological activity in the above case could be assumed to be within the error limits of this TA method.

2.3.8. DETERMINATION OF PRECISION

The precision of the method was estimated by analysing replicates of

(i) aged seawater;
(ii) TA intercalibration seawater samples;
(iii) Na_2CO_3 standards;
(iv) culture filtrates of *Emiliania huxleyi;*
(v) diluted cultures of *E. huxleyi* (filtered and unfiltered);
(vi) other (un)filtered seawater.

The seawater had been collected from the non-toxic seawater supply (3 m depth) during the 1990 cruise. It had been left to stand for six weeks in the dark. It was assumed that after this time biological activity was reduced to a low level of microbial activity, which had reached a steady state between production and degradation. Hence, any chemical changes occurring between the first and last analyses were taken to be insignificant. At the same time, this seawater was thought to bear more resemblance in terms of complexity to freshly collected seawater than would any artificial seawater.

The TA seawater intercalibration samples had been distributed by Dickson from SIO. It was labelled as batch 2 and was bottled on 1st Octobe 1990. The batch of seawater had previously been filtered, sterilized, and equilibrated with atmospheric levels of carbon dioxide using the

procedure described by Dickson (1990). Details on the preparation of the samples for distribution to various laboratories and the source and chemistry of the seawater are given by Dickson (1991b). The salinity was 33.363 psu and the nutrient levels were below 1 μM.

The preparation of the Na_2CO_3 standards is described in section 2.3.4. on acid standardization.

The algal culture filtrates consisted of *Emiliania huxleyi* batch cultures with a cell density of about 10^8 - 10^9 cells dm^{-3}. In order to remove any particles from the samples, they were filtered through cellulose nitrate filters with a pore size of 0.45 μm and then kept in the dark at 4 to 5°C until they were analysed. The replicates within each set were stored for the same number of hours (between 28 and 54 hours). Concentrations of POC and PIC in the cultures prior to filtration were generally greater than about 200 and 110 μM, respectively, while concentrations of nitrate and phosphate exceeded 450 and 10 μM, respectively.

The diluted cultures of *Emiliania huxleyi* were made up by diluting one of the original batch cultures by a hundred- fold down to about 10^7 cells dm^{-3} using prescreened natural seawater (see section 2.3.5 for further details).

The origin and treatment of the other (un)filtered seawater is described in section 2.3.6.

2.3.9. COMPARISON OF SINGLE AND DUAL WAVELENGTH METHOD

All titrations carried out within this work were analysed using both, the single and dual wavelength methods. The pH values calculated with the dual wavelength method tended to be lower by about 0.010 pH units at the start of the titration and about 0.006 units lower at the end. These differences in pH resulted in lower equivalents points by about 0.3% for the dual wavelength method. A lower equivalence point results in a higher acid strength. This is demonstrated in table 2.3.

Table 2.3.: Comparison between single and dual wavelength method using results of the acid standardizations for two batches of acids. The concentration of acid I was determined on four occasions with a different standard each time. Only one standardization was carried out on acid II. The acid concentrations ([acid]) and standard deviations are expressed in mM at 20°C.

	number of replicates (n)	single wavelength method (1L)			dual wavelength method (2L)			difference between methods (2L-1L)	
		mean [acid] (mM)	s.d.(n)	s.d.(n)%	mean [acid] (mM)	s.d.(n)	s.d.(n)%	mean [acid] (mM)	s.d.(n)
standard 1	6	400.12	0.727	0.182	401.33	0.762	0.19	1.21	0.241
standard 2	6	398.32	0.483	0.121	398.98	0.596	0.149	0.66	0.304
standard 3	3	400.58	0.204	0.051	401.95	0.033	0.008	1.36	0.194
standard 4	4	398.66	0.185	0.046	400.69	0.519	0.129	2.03	0.685
total for acid I	19	399.32	1.058	0.265	400.55	1.280	0.32	1.23	0.626
standard 5 for acid II	6	400.88	0.273	0.068	402.04	0.674	0.168	1.16	0.742

mean difference between methods = 1.21 mM (0.3%)
n= 25
s.d.(n)= 0.656 mM

The discrepancies of 0.3% observed between the results from the single and dual wavelength methods, with their implications for the accuracy of the method, were too large to be acceptable and raised the question of which method to use for subsequent work. The methods were therefore compared in two ways. First of all, standard deviations (s.d.(n)) were calculated for the mean results of replicate analyses and expressed as percentages of the means, or coefficient of variation (s.d.(n)%). Since different replication excercises were carried out, average s.d.(n)% values were calculated for the different replication analyses. Secondly, the 95% confidence limit obtained for each titration result (as described in section 2.3.3) was converted to a percentage of that titration result (95% c.l. %). An average value of this relative 95% c.l. was calculated from the titration data used in this comparison, which included also results from the two cruises. The conversion to relative precision terms was necessary since the comparison involved different sample types such as Na_2CO_3 standards, filtered seawater and culture samples. The results for these comparisons are shown in table 2.4. and were used as criteria for deciding which method to adopt.

Table 2.4.: Results from the comparison of relative precision achieved with the single and dual wavelength methods using
(a) mean standard deviations (s.d.(n)) of replicate analyses expressed as percentages of the mean value for replicate analyses (s.d.(n)(%)) and
(b) mean 95% confidence limits (95% c.l.) calculated for individual titration results and expressed as percentages of each titration result (95% c.l. (%)).
Refer to text for further explanations.

	wavelength method		number of
	single	dual	samples (n)
(a) mean s.d.(n)(%) of replicate analyses	0.111	0.129	73
(b) mean 95% c.l. (%) from each titration result	0.101	0.122	211

The replication between samples as well as the relative 95% confidence limits on each titration result were slightly better for the single wavelength method. This could be expected on theoretical grounds. The second wavelength used in the dual wavelength method provides absorbance values which are in an unreliable absorbance range, i.e. generally below 0.1 AU. Since the A2 readings are used as the denominators when calculating the pH values, any disproportional shifts in the 496 nm readings will be amplified in the ratio method. The absorbances at 590 nm are in the range between 0.3 and 0.1 AU and are, therefore, more accurate. Hence, the single wavelength method should not only provide better precision but also better accuracy with the spectrophotometer used in the work described here.

It was, therefore, decided to adopt the single wavelength method in this work for any intercomparisons with other TA methods and for field and culture studies. However, this decision did not affect the final TA results significantly. This was because the raised equivalence point obtained with the single wavelength method was more or less balanced out by the fact that the results were calculated with a lower acid strength.

It should be emphasized that the choice of the single wavelength approach was brought about by the fact that the absorbance readings for the second wavelength give low measurements. The use of a photometric cell with a greater pathlength, a greater indicator concentration, or possibly the choice of a different second wavelength such as the wavelength of maximum absorbance for the acidic form of the indicator) should theoretically turn the dual wavelength method into the better option.

2.3.10. INTERCOMPARATIVE STUDIES FOR ASSESSING THE PERFORMANCE OF THE SPECTROPHOTOMETRIC TA METHOD

Comparative studies were carried out on four different types of samples:

(i) samples of the two acids used for the TA determinations in the work reported here (for details see section 2.3.4);

(ii) TA intercalibration seawater samples (for details see section 2.3.8);

(iii) unfiltered seawater from CTD casts collected on the 1990 cruise (for details about the cruise see chapter 4); and

(iv) filtered seawater from surface samples collected during the 1991 cruise (for details about the cruise see chapter 5).

The results provided by other workers included in the intercomparison were obtained using the:

(i) coulometric backtitration used by Dickson's group;
(ii) potentiometric titration carried out by Keeling's group (SIO);
(iii) potentiometric titration carried out by Pegler (University of Hamburg, FRG);
(iv) theoretical calculations from TCO_2 and pCO_2 data.

The coulometric standardization of the two acid samples were performed by first adding a little excess acid to a 0.7 molar NaCl background and then neutralizing it with coulometrically generated OH^- ions. The acid sample was then added, and was similarly neutralized. The equivalence point in each case was located using a modified Gran plot. The potentiometric acid titrations included in the intercalibration exercise were all carried out in closed titration cells. Keeling's group used a non-linear least squares program which had been developed by Dickson to fit the titration data, while Pegler used the modified Gran method according to Bradshaw et al. (1981) and Almgren et al. (1983). However, since the potentiometric method from Hamburg was not specifically calibrated, high accuracy was not claimed on those results (Pegler, pers. comm.). Calculated TA was determined according to a modified Haltafall program by Turner (Univ. Gothenburg) based on coulometric TCO_2 measured by Robertson (then University of Wales, Bangor) and pCO_2 determined by Watson's group (then PML) using gas chromatography.

2.4. RESULTS

2.4.1. VARIATIONS IN THE PRECISION OF THE SINGLE WAVELENGTH METHOD IN DIFFERENT TYPES OF SAMPLES

The mean precision recorded from the replicate samples summarized in table 2.4. was 0.11% but this conceals the variations in precision recorded with different types of samples. The precision of the reagent blanks was not included in this average. The replication on the individual sample types are presented in figure 2.6. The figure includes the precision obtained

from the analysis of the reagent blanks. For comparative purposes, it was not expressed as the relative s.d.(n) of the mean result. Instead, the standard deviation was expressed as a percentage of 2200 μeq $kgSW^{-1}$, so that its contribution to the variability of the TA measurements could be assessed.

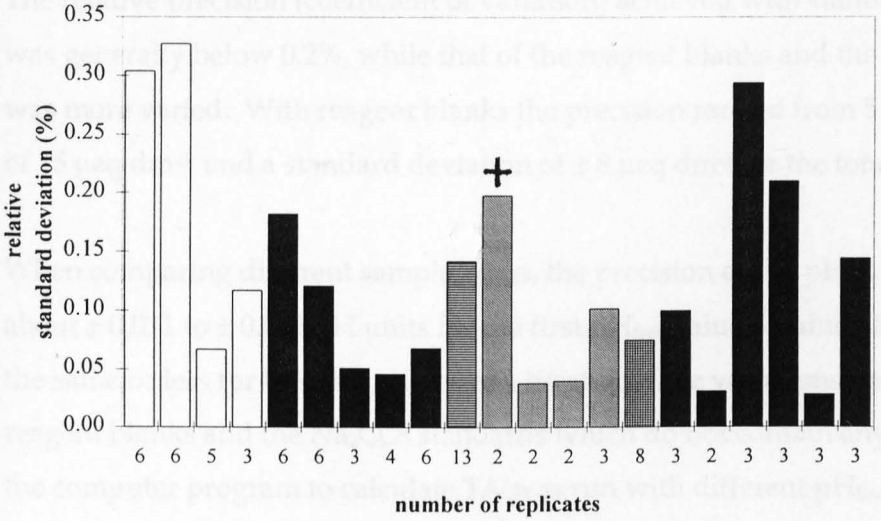

□ reagent blanks
■ standards
▤ unfiltered aged seawater
▨ (un)filtered seawater (+ =incl. diluted E.hux. culture)
▦ filtered intercalibration seawater
■ E. huxleyi culture filtrate

Figure 2.6.: Variations in the relative precision (s.d.(n)(%)) obtained with different types of samples using the spectrophotometric method. The number of replicates varied between the different precision determiniations. They are indicated on the horizontal axis. The relative precision of the reagent blanks was not expressed as the percentage of the mean result. For comparative purposes it was expressed as a percentage of 2200 μeq $kgSW^{-1}$.

The relative precision (coefficient of variation) achieved with standards and seawater samples was generally below 0.2%, while that of the reagent blanks and the coccolithophorid cultures was more varied. With reagent blanks the precision ranged from 5 to 28 μeq dm^{-3} with a mean of 15 μeq dm^{-3} and a standard deviation of ± 8 μeq dm^{-3} for the total of 20 samples.

When comparing different sample types, the precision of the pH_{free} measurements varied from about ± 0.011 to ± 0.002 pH units for the first pH_{free} value obtained for a titration curve and was the same or less for the final values of a titration. The variations tended to be greater in the reagent blanks and the Na_2CO_3 standards which do not contain any sulphate or fluoride. When the computer program to calculate TA was run with different pH_{free} input values, it was found that an error in pH_{free} of about 0.001 units caused an error of about 1 μeq dm^{-3} for the blanks and standards and of about 0.24 μeq dm^{-3} for seawater.

The pH range covered by one titration was about 0.3 to 0.4 pH units. The shift of an absorbance reading by 0.001 AU which is the specified maximum instability of the diode array spectrophotometer, was found to translate to a shift of 0.003 pH units in the pH range of interest here.

In two cases (seawater and culture samples) two replicates were analysed with different volumes of the initial acid addition. This lead to a difference of 0.7 pH units between the initial pH_{free} values obtained for the replicates. Nevertheless, the TA results from both replicates were only 1 μeq $kgSW^{-1}$ apart. This was taken as evidence that the pH range in which the titration was carried out did not affect the TA results of seawater samples with the precision obtained with this photometric method.

2.4.2. INTERCOMPARISONS WITH OTHER METHODS

2.4.2.1. Comparison of acid standardization results

The results of the five acid standardizations using the spectrophotometric method are shown in table 2.3. above. The standard deviation for the final mean value of acid I was much greater than for acid II. This is because acid I was standardized using four different Na_2CO_3 solutions and not just one. Since each of these Na_2CO_3 standards was made up separately, an additional

source of error was introduced which is not contained in the error quoted for the acid II result. When the acid is made up in deionized water, the concentration is specified by the manufacturer as 400 mM at 20°C with an error of 0.1%. The final results from the spectrophotometric and coulometric methods are compared in table 2.5.

With the variances of the results from the two methods being unequal, the combined results of the four standardizations for acid I using the spectrophotometric method were significantly lower than the mean obtained with the coulometric method, but only at the 95.3% confidence level. On the other hand, the spectrophotometrically determined strength of acid II was greater by 2 mM than the coulometric result, i.e. a highly significant result. This difference is large compared to the standard deviations of either method. The reasons for this are unknown.

Table 2.5.: Results of two standardizations of two batches of acid containing 0.7 M NaCl: comparison between photometric and coulometric method. The acid concentrations ([acid]) and standard deviations are expressed in mM at 20°C. The difference in acid concentration is also expressed in percent of coulometric result.

method	photometric			coulometric			difference in [acid] between methods (photometric-coulometric)	
	number of replicates	mean [acid] (mM)	s.d.(n-1) (mM)	number of replicates	mean [acid] (mM)	s.d.(n-1) (mM)	(mM)	(%)
acid I	19	399.32	1.09	7	399.86	0.19	-0.54	= -0.135
acid II	6	400.88	0.30	6	398.01	0.11	+ 2.01	= 0.502

2.4.2.2. Comparison of TA intercalibration results

The results of the TA intercalibration analyses are summarized in table 2.6. The TA results obtained by the spectrophotometric method are 26 and 32 μeq $kgSW^{-1}$ lower than those obtained by the potentiometric determinations by Keeling and the others, respectively. The precision for all three methods ranges around 0.1%.

Table 2.6.: Results from the TA intercalibration excercise.
For the potentiometric results no information was provided about the number of replicates.

method	photometric of this study	potentiometric (Keeling)	potentiometric (other)	difference between methods (Keeling-photom.) (µeq kgSW^{-1})	(other-photom.) (µeq kgSW^{-1})
mean TA result (µeq kgSW^{-1})	2217.9	2243.6	2250	25.7	32.1
number of replicates	8	unspecified	unspecified		
s.d.(n) (µeq kgSW^{-1})	1.7	2.0	2.6		
relative s.d.(n) (%)	0.075	0.09	0.12		

2.4.2.3. Comparison of TA cruise results

The results from the comparison of 34 TA results collected during the 1990 cruise with three different TA methods (spectrophotometric method of this study, a potentiometric method (K. Pegler, Univ. of Hamburg) and theoretically calculated TA (D. Turner, Univ. of Gothenburg)) are shown in figure 2.7. The comparisons and regression analyses were limited to the samples for which data was available from all three methods.

The photometric method gave on average lower results than the other two approaches by about 50 (±7) and 20 (±9) μeq $kgSW^{-1}$ for the calculated and potentiometric methods, respectively. Results from the potentiometric method were generally approximately 30 (±5) μeq $kgSW^{-1}$ lower than those of the calculated method.

While the correlation between the photometric and calculated TA was good with a correlation coefficient of 0.80, the slope of the regression line suggests that changes in the spectrophotometric TA were lower by 30%. The correlation between photometric and potentiometric method was reduced to an R-square value of 0.57, and the relationship suggests that photometric TA changes were lower by 40% than for the potentiometric method. The best relationship was found between the calculated and the potentiometric method with a correlation coefficient of 0.85 and a slope close to unity. Furthermore, the intercept value was close to the origin which was included in the standard error range of the intercept value.

Curiously, in the comparison of photometric and potentiometric results the relationship was significantly negative ($P < 0.05$) for samples limited to the upper 30 m.

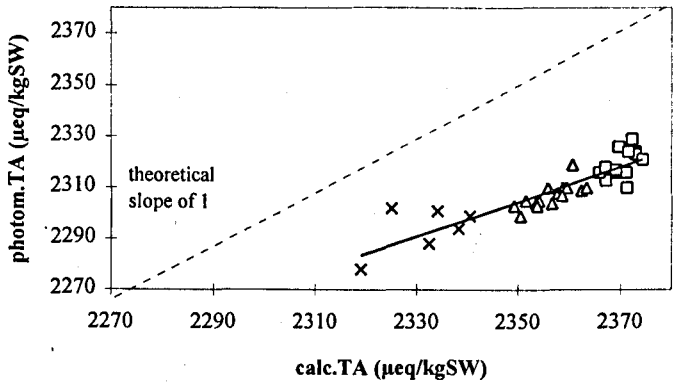

photom. TA = 0.68 (±0.06) calc.TA + 708 (±143)

n = 34
R^2 = 0.80

slope: P<0.001 (H_0 = 1)
intercept: P<0.001

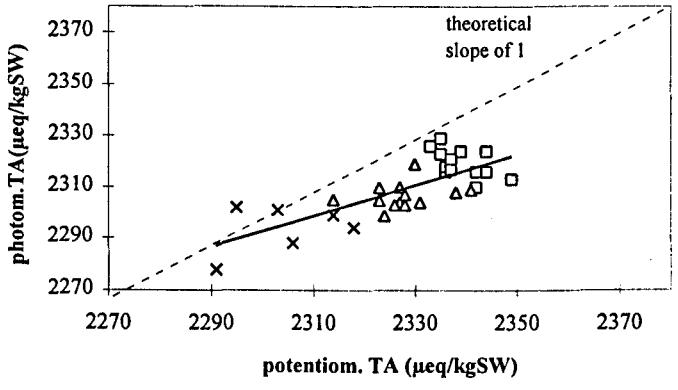

photom. TA = 0.60 (±0.09) pot.TA + 905 (±213)

n = 34
R^2 = 0.57

slope: P<0.001 (H_0 = 1)
intercept: P<0.001

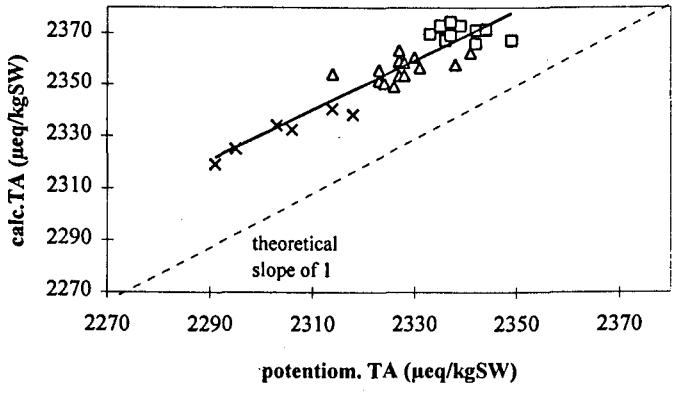

calc.TA = 0.97 (±0.07) pot.TA + 107(±163)

n = 34
R^2 = 0.85

slope: n.s. from 1 at P>0.05
intercept: n.s. at P>0.05

Figure 2.7.: Results from the regression analyses to examine the relationships between different methods to determine TA (phot.TA from photometric method of this study; potentiom. TA from potentiometric method used by K. Pegler (Univ. Hamburg); calc.TA from theoretical calculation from pCO_2 and TCO_2 using a modified Haltafall computation program (D. Turner, Univ. Gothenburg)). The data was collected during the 1990 cruise. Data used in the graphs and statistical analyses is limited to those samples for which corresponding data from the three methods was available. The significance of the slope was tested against the null hypothesis (H_0) of 'slope =1', with H_1 being 'slope ≠ 1'.
The mean differences between the methods and their standard deviations (± s.d. (n-1)), were:

photom. TA - calc.TA	= -47.9 (± 6.79) µeq/kgSW
photom. TA - potentiom. TA	= -18.5 (± 9.02) µeq/kgSW
calc.TA - potentiom. TA	= 29.4 (± 5.51) µeq/kgSW

The results from the comparison between results from two TA methods which were obtained during the 1991 cruise are shown in figure 2.8. The photometric TA results were on average 43 (± 11) μeq $kgSW^{-1}$ lower than the calculated TA ones in a comparison of 56 samples. This discrepancy of absolute TA values is comparable to the one observed for results from the 1990 cruise. However, the slope of the regression analysis indicates that changes in spectrophotometric TA were lower by 15% than for the calculated TA, which is half the discrepancy observed during the 1990 cruise. The correlation coefficient was lower than for the data from the 1990 cruise with a value of 0.64.

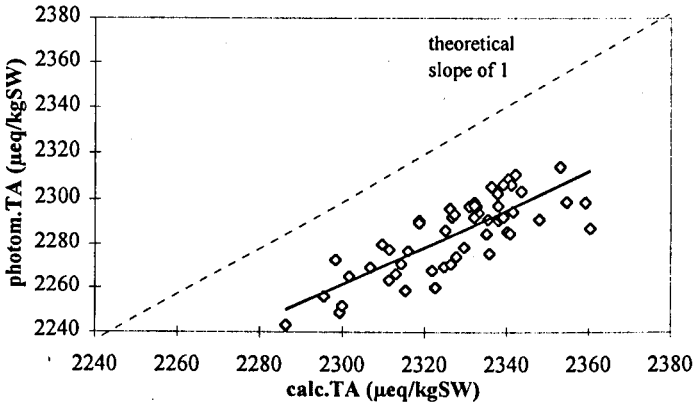

photom. TA = 0.85 (±0.09) calc.TA + 314 (±201)

n = 56

R^2 = 0.64

slope: n.s. from 1 at P>0.05
intercept: n.s. at P>0.05

Figure 2.8.: Results from the regression analysis to examine the relationships between the spectrophotometric method of this study and the theoretically calculated TA from pCO_2 and TCO_2 data (D. Turner, Univ. Gothenburg).
The data was collected from surface (2-3m) samples during the 1991 cruise.
The significance of the slope was tested against the null hypothesis (Ho) of 'slope = 1', with H_1 being 'slope $\neq$ 1'.
The mean difference and standard deviation (n-1) between the methods was:
photom. TA - calc.TA = -43 (± 10.6) µeq/kgSW

2.4.2.4. Summary of results from the intercomparisons

Results from the different intercomparisons between the photometric and other TA methods, which have been presented above in section 2.4.2, are summarized in table 2.7.

The coulometric results are in relatively good agreement with the photometric TA results for the averaged value of Na_2CO_3 standards used for acid I but not so for the standard used for acid II. In the comparison of seawater samples the potentiometric and the calculated results are greater than the photometric ones by about 1% and 2%, respectively. The differences between photometric TA and calculated TA cruise results were comparable for 1990 and 1991.

Table 2.7.: Summary of the differences between results obtained from the photometric and other methods to determine TA.
Results for the Na_2CO_3 standards are expressed as the difference in acid concentration between the photometric and the coulometric method (photometric - coulometric) in percent of the mean photometric acid concentration. The remaining results are expressed as the difference in TA between the other and the photometric method (other - photometric) in percent of the mean photometric TA.

In case of the cruise results, the value in brackets represents the standard deviation (±s.d. (n-1)) from the mean difference from the different cruise samples.

Apart from the intercalibration results for which there is insufficient information to determine the significance, all differences were significant at the 95% c.l. at least.

The original results from the coulometric method were provided by Dickson's group (SIO). The different potentiometric results were obtained by Keeling's group (SIO),an anonymous author, and Pegler (Univ. Hamburg).
Results obtained from calculation using pCO_2 and TCO_2 were provided by Turner (Univ. of Gothenberg).

Further details about the individual comparisons are presented in association with the tables/figures as indicated.

sample type	data adapted from	difference to: coulometry	potentiometry			calculation (pCO_2, TCO_2)
		(Dickson)	(Keeling)	(anon)	(Pegler)	(Turner)
Na_2CO_3 standard for acid I	table 2.5	-0.13				
Na_2CO_3 standard for acid II	table 2.5	0.50				
TA intercalibration samples	table 2.6		1.16	1.45		
cast samples (1990 cruise)	figure 2.7, legend				0.80 (±0.39)	2.08 (±0.29)
surface samples (1991 cruise)	figure 2.8, legend					1.88 (± 0.47)

2.5. DISCUSSION AND CONCLUSIONS

2.5.1. PRECISION AND ACCURACY

With the apparatus available, the photometric TA method used in this study turned out to consume more time and attention in its running than had been anticipated at the outset of this project. The duration of the titration was prolonged by the increased number of titration points needed to obtain the required precision and the time it took before the acid could be assumed to be sufficiently mixed in the flow circuit before any absorbance readings could be made. Throughout the course of an entire titration, full attention was required to check the absorbance readings from both wavelengths for signs of instability in the performance of the spectrophotometer or optical interferences in the light path of the instrument before the next acid addition would be initiated manually.

The precision of about 0.1%, which was obtained from short-term experiments, was generally comparable to that quoted by other potentiometric and the coulometric methods. In spite of the considerable discrepancies between the photometric, potentiometric, and the calculation methods for TA in natural seawater, there was initially little concern about the suitability of the photometric method for the detection of TA changes in seawater and algal cultures. However, a more thorough investigation of the intercomparisons revealed that these discrepancies tended to be significantly lower at reduced TA in the natural seawater samples. Consequently, this casts some doubt over the accuracy of the method *per se* as well as its suitability to accurately measure the TA changes of interest in this study.

Possible causes for incorrect TA values and their impact on single-wavelength spectrophotometric TA are summarized in table 2.8.

Table 2.8: List of factors introducing methodological and instrumental errors and their approximate effects on TA determined by the single-wavelength spectrophotometric TA method of this study.

factor	effect on TA result
precision of sample volume based on replicate determinations of bottle volume	± 0.01 %
accuracy of acid standard affected by absorption of water by Na_2CO_3 salt before and during weighing of the salt	decrease; effect unquantified; assumed negligible
accuracy of acid strength affected by storage in burette bottle	unquantified
precision of the burette (specified)	± 0.1 %
accuracy of the burette (specified)	± 0.3 %
accuracy of temperatures used for density corrections (assuming sample temp. was 2°C too low)	increase 0.05 %
stability of diode array spectrophotometer (simulated decrease in absorbance readings of 0.002 AU throughout the titration)	increase 0.5 %
accuracy of indicator pK value (assuming pK was 0.2 pH units greater)	increase 0.35 %
accuracy of TCO_2 concentration (assuming TCO_2 was 200 µM too low)	decrease 0.05 %
storage of filtered samples causing changes in TA due to continued biological activity	decrease; increase; assumed negligible
introduction of titratable bases into sample during filtration of algal culture sample	increase; unquantified, expected to vary with type and condition of algae and the filtration process
presence of calcified algae in sample	increase of similar order as equivalent amount of PIC present in the sample prior to titration
loss of CO_2 during titration	effect unknown; assumed negligible

The comparison of precision results obtained with different sample types revealed a lower reproducibility on the blanks and the undiluted *Emiliania huxleyi* culture filtrates. In the case of the blanks this phenomenon might be explained by the low buffering of the blanks, which leads to great imprecision of the pH values. This reduces the precision of the TA results. The relatively large imprecision obtained for the coccolithophorid culture filtrates was probably caused by different factors, e.g. the relatively large amounts of POC and PIC present in the coccolithophorid cultures. Phytoplankton cells are more or less easily damaged during the filtration process, which may have led to the release of DOM including titratable bases into the filtrate. In addition, the presence of coccolithophores in unfiltered samples was found to increase the measured TA significantly, i.e. possibly by the equivalent amount of PIC present in the titrated sample. Therefore, variations could have arisen if any PIC of a size smaller than 0.45 μm had passed through the filters. This may happen when the liths have been dissolving or when they were damaged during the filtration process. Although the filtration process can in theory be largely standardized in terms of the filter and vacuum pressure used, in practice it introduces a further source of variability. Apart from this, the precision appears to depend more or less upon the stability of the spectrophotometric absorbance readings, which determines the reliability of the pH readings.

In the TA intercalibration exercise of this study, the precision of the photometric method is slightly better than that obtained by Keeling's group and the other laboratory. However, there was no information available on the number of replicates analysed by these other laboratories. In addition to sample number it would have been useful to know, whether the results were obtained, either, within one run or from separate days. Due to the limited number of intercalibration samples available in this study, the spectrophotometric results were all obtained during one day. Without the availability of other stable seawater reference material, the only information on the spread of the results between separate days derives from the Na_2CO_3 standards. This information is not really reliable, because of the additional uncertainty in the TA of the standards. In any case, these results with the standards indicate that the spread between days/months would not be greater than ± 0.26%. Although a reduction in acid strength with time may affect the long-term precision of a method, if it remains unquantified (D. Purdie, pers. comm.), the variation of the standards did not provide evidence for a reduction of acid strength over the course of several months. The precision obtained by the

spectrophotometric method of this study also compared favourably with those obtained during the earlier intercalibration excercise reported by UNESCO (1990). Ignoring the results from one particularly imprecise method, the precisions obtained by the different participating laboratories ranged between 0.1 and 0.3%.

For the Na_2CO_3 standards the photometric results compared relatively well with the coulometric ones. This is encouraging since the coulometric method appears to be the most promising with regard to precision and accuracy. It is, however, not obvious why the photometric TA results for seawater samples are consistently lower than those obtained using potentiometric and the calculation methods. The results from the cruise samples suggest that the offset is not only an absolute but also a relative one. This implies that there was in fact a problem with the photometric method or the other two methods to determine TA variations accurately.

The offset may depend upon the sample type, i.e. it may only show up in the more complex seawater samples, especially in those of the ocean surface layers. Although there is no actual evidence without a proper seawater standard for TA, it is tempting to assume that the error lies with this photometric rather than with the other three potentiometric or the calculation method, i.e. the photometric TA results were too low.

2.5.2. WHY COULD THE SPECTROPHOTOMETRIC TA RESULTS BE LOWER THAN THOSE OBTAINED BY OTHER METHODS?

The precision and accuracy of the results generally depend upon how precise and accurate the values are determined for the

(i) sample volume;

(ii) acid strength;

(iii) equivalence point.

The error on the reproducibility of the sample volumes is negligible, and if there were an absolute error on the volume, it would be cancelled out for the actual sample results by the fact

that the acid standardizations and the actual sample analyses were carried out in the same titration vessel.

Although the actual acid strength results are in close agreement with the values specified by the manufacturers and those obtained by coulometry, there are several reasons why uncertainties could arise in the acid standardizations carried out in this study. These include:

(i) an error in the Na_2CO_3 concentration of the standard;

(ii) errors due to the experimental apparatus which do or do not get cancelled out by the TA analyses of seawater or culture samples;

(iii) inclusion/exclusion of H_2O blank corrections;

(iv) an error in the titration data; and

(v) an error in the evaluation of the titration data.

The concentration of the Na_2CO_3 salt in standard solutions may be slightly lower than anticipated for two reasons. First, Vogel et al. (1978) warns that the heating of the Na_2CO_3 salt to temperatures above 270°C may lead to CO_2 loss from the Na_2CO_3. Goyet and Poisson (1989), whose instructions have been followed in this study, do however state, that they dry the Na_2CO_3 at 285°C. Secondly, since the Na_2CO_3 is hygroscopic, it may absorb water during the weighing procedure, which on a weight basis reduces its equivalents. These two cases would lead to inflated acid strength results and, subsequently, to inflated TA results of seawater or culture samples. As an alternative to Na_2CO_3, Vogel et al. (1978) recommend the use of sodium tetraborate, which reduces the hydration problem. Most documented TA analyses quote the choice of Na_2CO_3. Most analysts have chosen Na_2CO_3 as a standard for TA determinations and I have not come across any records of reservations about its suitability. Stable seawater reference material for TA determinations, which had been provided by A. Dickson, has been used in subsequent studies to test the longer-term precision of a TA method (Lee & Millero, 1995). However, without a certified TA value, it still does not provide an absolute TA standard for seawater.

If there were instrumental errors, for example, a burette error, these should be cancelled out for the seawater or culture results in the same way as an error on the sample volume, provided the same burette is used for acid standardization and sample analysis. On the other hand, there

may be an error in the experimental apparatus which will affect an Na_2CO_3 standard differently to an actual seawater or culture sample. An example for this is the unknown CO_2 loss from the sample to the atmosphere in this slightly open titration set up. This loss would be smaller in the standard because its TCO_2 concentration is about half that of normal seawater. The overall effect on TA is not obvious, since it is not known how much CO_2 is lost at what stage during the titration. In principle, the pH increase associated with the gas loss from the sample will reduce the modified Gran functions, which tends to lead to an increase of the equivalence point and thus TA. Since however the gas loss will occur thoughout the titration, this tends to reduce the slope of the modified Gran plot and, in turn, tends to lower the equivalence point and TA result. Perez and Fraga (1987) found that the error in TA during their titrations was negligible even though they used an entirely open system with the surface to volume ratio of their sample being 4 times larger than in this study. On one hand, this provides some possible support for the assumption that CO_2 loss had no significant effect on the TA results in this study. On the other hand, in the case of Perez and Fraga (1989) readings were taken in a higher pH range (pH > 4), the duration of their procedure was much shorter, and the turbulence effect on gas exchange across the interface remains unquantified in their as well as in this study.

In order to remove the uncertainty associated with the effect of CO_2 loss, the procedure should ideally have been conducted in a closed system. Alternatively, the monitoring of pH during the entire titrations should be accompanied by TCO_2 measurements to obtain some indication of the possible impact and to implement some correction procedures in the computation of the TA result. A comparison of TA results by using only the first or only the second of the replicate absorbance readings showed no significant difference between the results. Unfortunately, this is not a good indication of CO_2 loss. Instead, it merely confirms that the period between acid addition and absorbance readings was sufficient for the sample to be sufficiently mixed.

The corrections for blanks should ideally be included if the impurities of the NaCl amount to a greater error than the one arising from the experimental apparatus or the imprecision on the blank determinations. Goyet and Poisson (1989) quote TA values for their blanks between 1 and 6 $\mu eq\ kgSW^{-1}$, being close to proportionality with the salinity. Since these values were obtained for a slightly more complex synthetic seawater and not simply the NaCl background as used in this study, they can only give an idea of the significance of the blank corrections.

The level of impurities in the NaCl salt as quoted by the manufacturers should not introduce an error of above 2 μeq $kgSW^{-1}$.

If one assumes that the corrections for sulphate, fluoride, carbonate, and the indicator have been estimated correctly, the error in the equivalence point could arise from incorrect pH values. This error could explain why the discrepancy appears to be less in Na_2CO_3 standards than in seawater. The incorrect pH_{free} values carry a greater bearing on the accuracy of the modified Gran values for seawater than those for the standard since more corrections for interfering side reactions have to be applied in the case of seawater.

The precision of the individual pH readings is generally not a problem as becomes evident from the small 95% confidence limits on the equivalence points. However, the accuracy of the pH measurements is a prerequisite for the accuracy of the TA results. Currently, marine chemists are aiming for an accuracy in the pH measurements of ±0.002 pH units (UNESCO, 1990). In an intercomparison of potentiometric seawater pH measurements between different laboratories, analyses were carried out on NBS buffers (NBS scale), tris buffers, and indirectly from the first measurements of the potential of the samples during the potentiometric titration of seawater (SW scale). The scatter of results from NBS buffers was of the order of 0.3 pH units while the scatter of results from 12 separate bottles obtained by a single laboratory was 0.005 pH units. The scatter of the SWS data ranged from 0.04 to 0.02 pH units for salinities between 30% to 38%. The scatter was thought to be due to standardization problems with buffers used and probably also due to unrecognized liquid junction errors.

With respect to photometric pH measurements, Byrne and Breland (1989) obtained a precision of ± 0.004 pH units using cresol red in a multiwavelength analysis. King and Kester (1989) got photometric pH values for thymol blue which were lower than the potentiometric pH by about 0.005 units at pH 2.6 but not significantly different at pH 3.7 using bromophenol blue. Unfortunately, the latter authors did not compare the photometric pH using bromophenol blue with the potentiometric pH at any lower pH. They quote an error of ±0.007 on the pK value for bromophenol blue and advise determining the indicator pK by direct measurement in the ionic medium of interest because of salt and medium effects upon the dissociation constants of the indicators.

Although the photometer cuvette was not thermostatted, a possible temperature effect on the indicator pK does not seem to be the overriding cause for the discrepancy as in some cases the room and sample temperature were close to 25°C. Robert-Baldo et al. (1985) found that the pK change with temperature was 0.01 pH units per °C in seawater for phenol red, which is another sulphonepthalein indicator. Since, however, an error in the indicator pK does not fully explain the cause of the discrepancy in the TA results, the absorbance readings *per se* need to be improved.

Byrne and Breland (1989) obtained their absorbance readings in the range between 0.4 and 0.8 AU, i.e. in the range where the readings are most reliable. In contrast to King and Kester (1989), their readings at the second wavelength for the absorbance ratio method were not taken at the isosbestic wavelength but at the absorbance maximum of the alkaline form of the indicator, which will give higher absorbance readings than those at the isosbestic wavelength. The comparison between the single and dual wavelength methods gives an idea about the importance of the stability of the absorbance readings. It would be interesting to carry out the titration in a higher absorbance range, by using a greater pathlength of the photometric cell, by using one of the more appropriate pH indicators, or by doubling the concentration of bromophenol blue. The first two cases should generally be favoured because the introduction of any acid-base systems into the samples will always add to the uncertainties.

Byrne and Breland (1989) recommended taking readings at a third wavelength at which the absorbance is negligible. Conjugate measurements at this wavelength with and without the indicator should, ideally, be identical. Consequently, these readings can be used to correct for baseline shifts, which the authors found to be as much as 0.005 AU. In most cases these perturbations were found to be due to physical interferences such as bubbles in the optical path. It is important to bear in mind that the comparison of pH errors from the intercomparative study with those from the spectrophotometric measurements here may not be straight forward, since the former, potentiometric, pH measurements were taken at the usual seawater pH of around 8. These physical interferences posed also a problem with deep water samples during the 1990 cruise. Increased amounts of bubbles developed as the unfiltered samples were warming to room temperature. They led to obstruction of the light path in the

spectrophotometer cell, which tended to give higher absorbence readings. In turn, this results in higher photometric TA estimates.

The statistics applied to the titration data can have a large effect upon the final TA results. This has been demonstrated by Anderson and Wedborg (1985). They analysed potentiometric and photometric titration data from two types of seawater using the modified Gran method and several curve fitting methods. The various curve fitting methods differed by the numbers of parameters and types of variables used. They found no significant differences in the results obtained from the different methods of evaluating potentiometric titration data. However, they obtained differences of up to 1% between results from the modified Gran and the different types of curve fitting evaluations of the photometric titration. Their results are illustrated in figure 2.9.

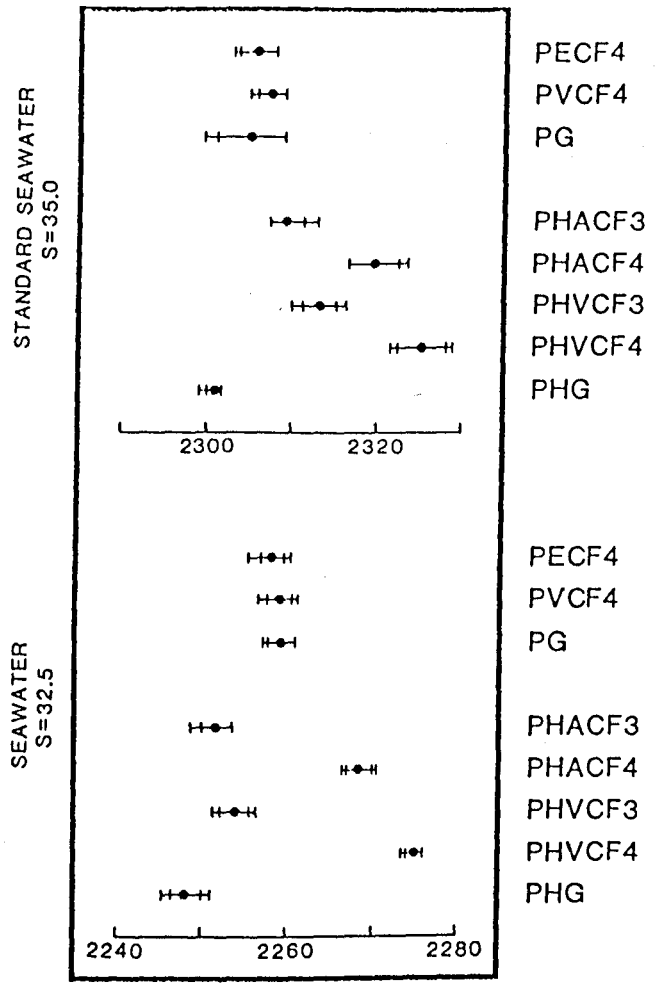

Abbreviation	Experimental method	Evaluation method	Dependent variable	Number of parameters
PECF4	Potentiometry	Curve-fitting	emf	4
PVCF4	Potentiometry	Curve-fitting	Volume of acid	4
PG	Potentiometry	Gran evaluation	–	–
PHACF3	Photometry	Curve-fitting	Absorbance	3
PHACF4	Photometry	Curve-fitting	Absorbance	4
PHVCF3	Photometry	Curve-fitting	Volume of acid	3
PHVCF4	Photometry	Curve-fitting	Volume of acid	4
PHG	Photometry	Gran evaluation	–	–

Figure 2.9.: Plot of results obtained by Anderson and Wedborg (1985) for TA comparing the potentiometric and photometric titration method and different types of evaluation methods on standard seawater and natural seawater (figure from same paper). The mean values are marked with a dot, the inner limits show the standard deviation (± s.d.) and the outer limits show the experimental range; units in μeq $kgSW^{-1}$; abbreviations are explained in the accompanying table.

The Gran method was found to be less sensitive to random errors in the absorbance readings than any of the curve fitting procedures. The authors suggest that the uncertainty in the second dissociation constant introduces the greater deviation between the results from the Gran and the 4 parameter curve fitting approach. The difference between the Gran and the 3 parameter curve fitting method is about 10 μeq $kgSW^{-1}$ in the case of the standard seawater and about half of that in case of natural seawater. This is a further example for methodological discrepancies depending upon the sample type. However, with reference to findings by Butler (1992), it should be noted, that the evaluations were not carried out on the same parts of the titration curve. For the curve fitting the whole curve was used which included part of the region of excess acid for potentiometry but only the values down to pH 4 for photometry. For the Gran evaluation they used the pH range 3.7 to 3.0 for potentiometry and the range 6.6 to 5 for photometry. It is therefore not clear to what extent the deviations in the results are due to the different statistical methods or due to the fact that different pH ranges were used.

In the intercalibration exercise reported by UNESCO (1990) the maximum scatter in TA at a salinity of about 35 psu was 30 μeq $kgSW^{-1}$ (=1.4%) if one excludes the results from the outlying set of results. This puts into doubt a claim by most of the laboratories that they achieve an accuracy of 0.1 or 0.2%.

Without any intercomparisons of coulometric analyses of actual seawater samples or potentiometric analyses of Na_2CO_3 standards, it is not possible to pinpoint the cause for the reported discrepancies between the photometric method of this study and the other methods. The extent of the discrepancies appear to be determined by several possible factors. These include the sample type, the evaluation method, the pH range used, and the analytical method with which the photometric results are compared.

Although the reasons for the discrepancies have been assumed to lie with the photometric method, it should be borne in mind that the other methods also have weak points. The potentiometric results from Pegler have not been claimed to be highly accurate and few details are known about the other two potentiometric analyses. The calculation method may not account for all the acid-base systems present in the samples and is more reliant on the accuracy of several dissociation constants. Such additional acid-base systems may pose a greater

problem in samples taken during phytoplankton blooms. The discrepancy between the potentiometric and the calculated results indicates that at least one of these two methods is not accurate.

The spectrophotometric method used here has been thoroughly checked in order to find possible causes for the discrepancies. The theory behind the data analysis and the computer program have been examined by independent means. Neither, an incorrect indicator pK value nor the specified possible shift in absorbance readings could solely account for the discrepancies of greater than 1%.

2.5.3. IMPROVEMENTS TO THE SPECTROPHOTOMETRIC METHOD

Systematic tests of the longer-term precision of the method should be conducted over the course of an experiment, e.g., by using the stable seawater reference material that has been supplied by A. Dickson in recent years.

The accuracy of the absorbance readings could be improved by using the dual wavelength method with a complementary third wavelength as suggested by Byrne and Breland (1989). The indicator and titration apparatus should allow readings in the absorbance range between 0.4 and 0.8. For the pH values to be accurate, the indicator pK should be determined for the temperatures and salinities likely to be encountered in the subsequent sample analyses. All such measurements should be carried out in the identical apparatus, ideally, by using a thermostattically controlled photocell. If the pathlength of the photocell can be increased, less indicator needs to be added to the sample, thus reducing the uncertainties associated with introducing another acid-base system to the sample.

Any possible errors due to long term shifts in the spectrophotometer readings or CO_2 exchange with the atmosphere could be at least reduced by speeding up the titration procedure. If the titration was carried out within the photocell the time required for one titration point could be reduced from about 50 to 20 seconds. This practice was followed by Anderson and Wedborg (1983), and suggestions for the design of such an apparatus can also be found in Headridge

(1961). In order to avoid any uncertainties with respect to gas loss altogether, the titration cell should be completely closed.

In order to mimic seawater more realistically, at least sulphate and fluoride should be added to the Na_2CO_3 standards and the reagent blanks.

Any chemical reactions other than the neutralization of the bases during storage and the titration can be minimized by filtering samples immediately after sampling. A pore size of 0.45 µm may not be sufficiently small if dissolving or fragmented detached liths are present in the sample. A standardized filtration procedure should be part of the routine analysis for TA. According to findings from preliminary experiments discussed in chapter 6, this filtration should involve only a low vacuum pressure, e.g. 0.2 bar or less, and filters should be exchanged regularly to avoid POC loss from the algal material on the filters.

If unfiltered, cold deep-sea samples should be analysed as quickly as possible, so that bubbles of carbon dioxide, nitrogen, and oxygen which form within few hours do not cause interferences in the optical path.

2.5.4. CONCLUSIONS

In conclusion, this spectrophotometric method provides precise seawater measurements which are lower than potentiometic and calculated TA results by around 1% and 2%, respectively. Further intercomparisons are required to establish with certainty the causes for the discrepancies between methods. There seem to be several ways of improving the reliability of the pH measurements, if it turns out that these are the reason for the deviations. While a consistant inaccuracy of 1% or 2% in the spectrophotometric results would be of no relevant concern, an error in the estimates of TA changes casts some doubt over the quantitative validity of some of the findings in the field and culture experiments of this study.

3. ALKALINITY-RELATED STUDIES IN THE NORTH ATLANTIC PRIOR TO 1990

3.1. GEOSECS

The Geochemical Ocean Section (GEOSECS) programme was the first global survey of geochemical, hydrographic, nutrient and oceanic CO_2 system data throughout the water column. The survey was mainly aimed at studying the

(i) ocean's circulation and mixing processes;

(ii) properties of the ocean's CO_2 system; and

(iii) effect of anthropogenic CO_2.

Areal and vertical profile sampling was carried out in the Atlantic, Pacific, Antarctic and Indian Oceans between 1972 and 1978. The GEOSECS Atlantic Expedition which included measurements of TA, TCO_2 and pCO_2 took place from July 1972 to April 1973. The position of sampling sites for these parameters in the Atlantic Ocean are shown in figure 3.1. Findings of the programme were used to establish some fundamental constraints, e.g. mixing of the world oceans averages around 500 years (Stuiver et al., 1983), and about one third of fossil fuel CO_2 enters the ocean, thereby confirming former modelling results (Broecker et al., 1979). The range of specific alkalinity observed during the study for different parts of the world ocean has already been presented in figure 1.4. The diagram demonstrates the general increase in specific alkalinity with the age of the water mass following bottom water formation in the northern North Atlantic, i.e. it ranges from about 2300 $\mu eq\ kgSW^{-1}$ in North Atlantic surface water to 2500 $\mu eq\ kgSW^{-1}$ in North Pacific Ocean Bottom Water. Unfortunately, the Atlantic Expedition did not cover the northeastern area of this ocean.

The overdetermination of the carbonate system led to further important findings, i.e. significant discrepancies in the results from the Atlantic and Indian/Pacific Ocean carbonate chemistry data set (Takahashi (1977) unpublished in Brewer et al., 1986). A subsequent error search revealed omissions and inconsistencies in the functions and computer programmes used to calculate TCO_2 and TA from potentiometric data such as the omission of corrections for interferences from phosphoric and silicic acid present in seawater and a difference in the pH range analysed. Further errors were associated with

blank corrections (Bradshaw et al., 1981; Bos & Williams, 1982). Amendments of these shortcomings improved the internal consistency of the results. The overall precision of TA measurements reached 0.4% and was better than this at individual stations or cruise sections (Brewer et al., 1986).

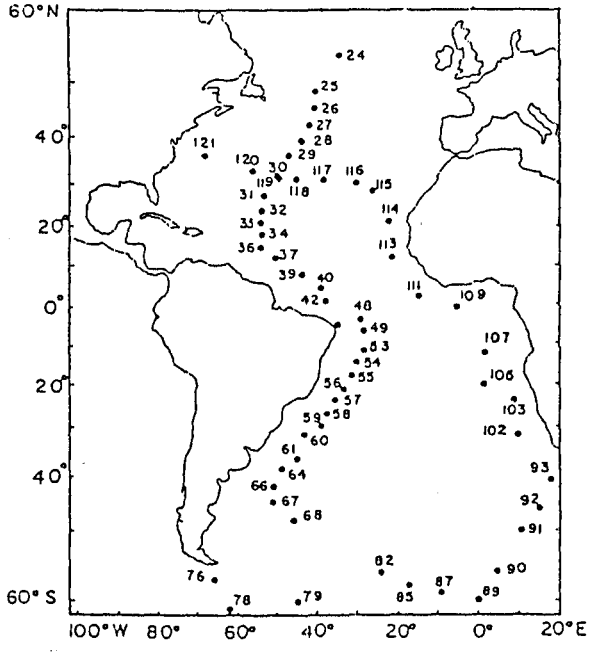

Figure 3.1: Positions of sampling sites during GEOSECS Atlantic Expedition at which carbonate parameters were studied (from Chen, 1982b).

3.2. TTO

The Transient Tracers in the Oceans (TTO) expedition to the North Atlantic from April to October 1981 formed part of the follow-up to the GEOSECS programme (see figure 3.2 for position of sampling sites). In the light of the above methodological problems an additional focus of this expedition was to improve further the precision and accuracy of the carbonate parameter estimates. A protocol of the TCO_2 and TA titration method used for the TTO programme and results were outlined by Brewer et al. (1986). Additions to the procedure included sample preservation for subsequent analyses on shore several months later and a detailed standardization procedure including corrections for blanks. Nevertheless, discrepancies in TCO_2 results became apparent. The titrimetric TCO_2 data set collected on board ship was lower than the one analysed on land by a similar method. At the same time it was higher than TCO_2 values from stored samples using another method involving gas extraction. Since the discrepany in the latter case was smaller and depth-dependent, i.e. less at depths exceeding 1000m, Brewer et al. (1986) concluded that the most likely explanation would be an undiscovered substantial inaccuracy in the basic theory and practice of the potentiometric titration procedure. At the same time, the accuracy of TA determinations achieved at sea was specified as 0.03% with a precision of 0.4%. Further, ship-board and shore-based analyses of TA differed only by 0.8 ($\pm$ 9.5) μeq $kgSW^{-1}$, which is close to the achievable limits for volumetric work. Bradshaw and Brewer (1988 a,b) subsequently provided supportive evidence for the hypothesis that unknown protolytes with pK values in the 6.0 to 8.7 pH range, which masqueraded as carbonic acid, may provide a likely explanation for the discrepant TCO_2 results observed during the TTO expedition, while the TA results remained largely unaffected. An alternative explanation has been subsequently provided by Stoll et al. (1990). They demonstrated that the accuracy of the acidimetric titration procedure largely depends on the calculation routine and the dissociation constants used, both of which may vary between data sets. Since samples were not filtered after collection, Bradshaw and Brewer (1988 a) also considered PIC interference during the titrimetric analyses. However, in this case they were able to discard this possibility on several grounds, especially because it should also have led to discrepant TA results.

The data of TCO_2 and TA and their relationship (Deffeyes, 1965; Baes, 1982) was used by Brewer et al. (1986) to demonstrate graphically variations of oceanic pCO_2 within the North Atlantic. Latitudes north of 55°N act predominantly as sinks, those south of 45°N function

mostly as sources for atmospheric CO_2, and the meridional band in between acts as a sink east of about 30°W (see figure 3.3). The data for TA, TCO_2, salinity and temperature revealed some useful correlations between these parameters in the North Atlantic in spite of the large seasonal range covered during the TTO expedition. Most notably, a strong correlation (correlation coeff. = 0.99; $s.e._{regr.}$ = 9.14 μeq kg^{-1}) could be established between surface TA (0-15 m) and salinity, with the relationship becoming a bit weaker for samples collected at lower salinities (figure 3.4). This correlation was, for example, used by Brewer (1978) to establish the penetration depth of excess CO_2 in the North Atlantic as outlined in section 1.4.4.2.2. In contrast, Chen and co-workers generally used the somewhat weaker correlations between salinity-normalized TCO_2 and potential temperature with the same intention (e.g. correlation coefficient = - 0.885; s.d. = 30 μmol kg^{-1}).

Figure 3.4 indicates that TA for surface water in the Atlantic area studied during TTO ranged from about 2100 to 2450 μeq kg^{-1}. Data from TTO was also used by Glover and Brewer (1988) to estimate the distribution of TA in the SML of the North Atlantic Ocean during winter. Their map with a resolution of 1° x 1° suggests that TA ranges from below 2320 μeq kg^{-1} near Iceland to about 2340 μeq kg^{-1} 15° further south at that time of the year (figure 3.5).

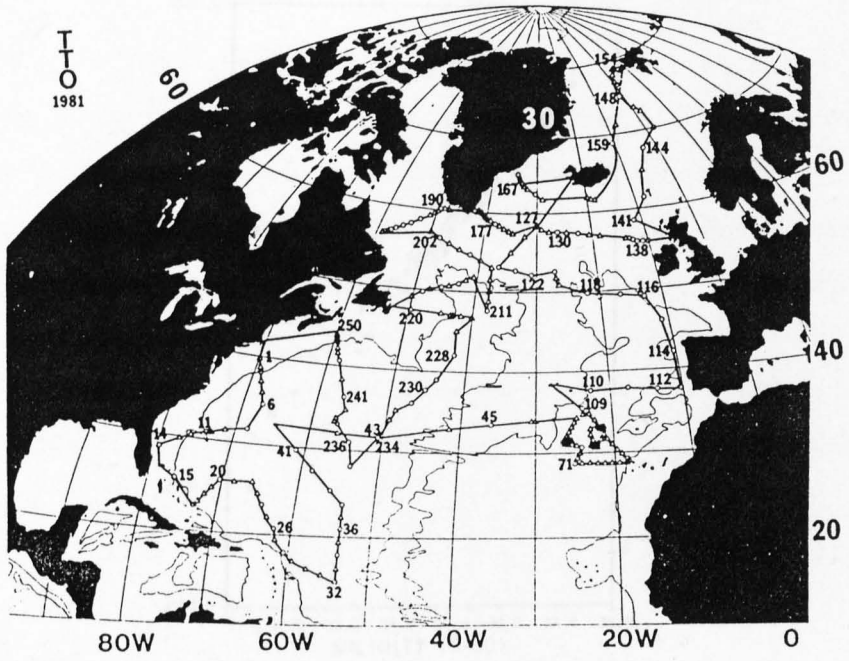

Figure 3.2: Position of sampling sites during TTO expedition to the North Atlantic (from Brewer et al., 1986).

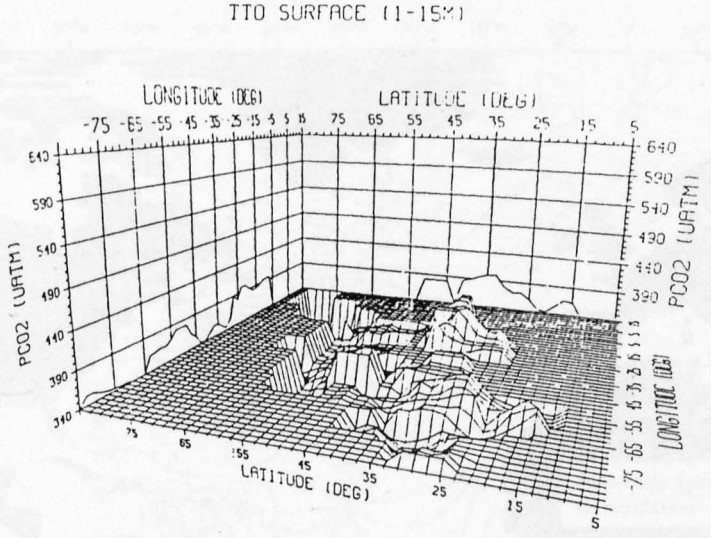

Figure 3.3: Diagram of North Atlantic surface water pCO_2 values as calculated from potentiometric titration data collected during TTO. The pCO_2 field is shown with a "floor" of 340 ppm, i.e. the atmospheric value in 1981. Invasion of CO_2 in the ocean takes place in the "holes" and evasion occurs in the "hills" (from Brewer et al., 1986).

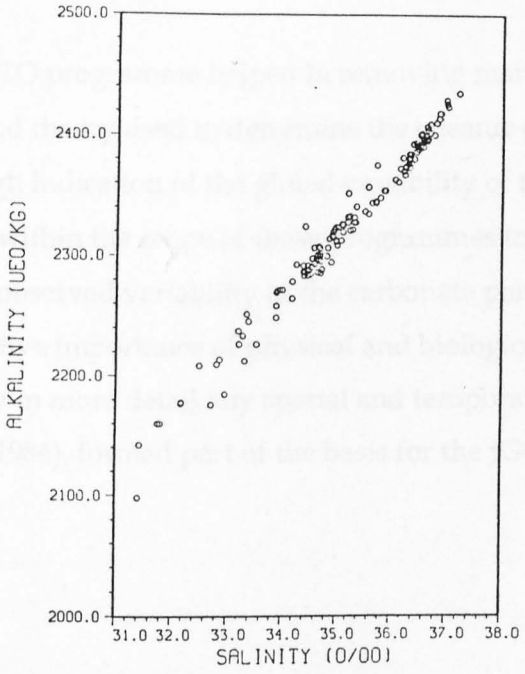

Figure 3.4: Relationship between TA and salinity for data from North Atlantic surface (0-15 m) waters (Brewer et al., 1986) with a regression equation of TA = 547.05 + 50.560 × sal.; corr. coeff. = 0.99; s.d.regr. = 9.14 μeq kg^{-1}

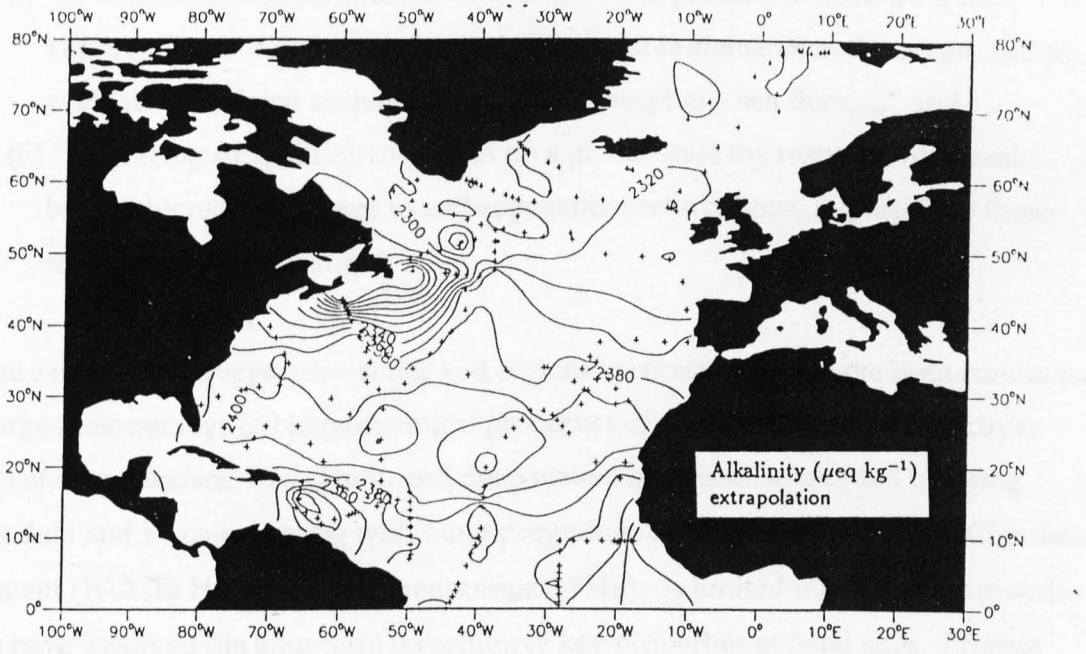

Figure 3.5: Estimate of TA distribution (μeq kg^{-1}) in the SML of the North Atlantic during winter (from Glover & Brewer, 1988)

The GEOSECS and TTO programme helped in removing many of the disagreements about the methodologies and theory used to determine the oceanic carbonate system, and they have provided a rough indication of the global variability of the carbonate chemistry. However, it was not within the scope of these programmes to address the question of which factors influence the observed variability of the carbonate parameters in the surface ocean, in particular, the relative importance of physical and biological controls. Further, they were not designed to study in more detail any spatial and temporal variability. This recognition, outlined by Brewer (1986), formed part of the basis for the JGOFS programme described in the next section.

3.3. JGOFS

The international Joint Global Ocean Flux Studies (JGOFS) programme is a core project of the International Geosphere-Biosphere Programme (IGBP). This programme has included field work from 1988 until 1999, and data synthesis and modelling are still continuing. Its goals have been specified by SCOR (1987) as

(i) "to determine and understand on a global scale processes controlling time varying fluxes of carbon and associated biogenic elements in the ocean, and to evaluate the related exchanges with the atmosphere, sea floor, ..." and

(ii) "to develop a capability to predict on a global scale the response of oceanic biogeochemical processes to anthropogenic perturbations, in particular those related to climate change."

A mixture of global surveys, time-series and regional process studies have been conducted, since large-scale surveys of biogeochemical properties cannot meet all these objectives. Surveys of ocean surface, mid-depth, and deep waters have been attempted by using satellite data and by co-operating with other programmes, e.g. the World Ocean Circulation Experiment (WOCE) Hydrographic Programme (WHP). A limited number of time-series studies have involved the long-term recording of key properties at fixed sites. Process studies, each of which has some unique goal reflecting the characteristics of the site, have all aimed to examine in detail key variables which control carbon fluxes on seasonal or shorter time scales. They do however, require some combination of spatial and Lagrangian observations, since biogeochemical processes move and evolve within advecting water masses.

For the above objectives to be met, it was recognized throughout the course of the programme that methodological aspects could not be ignored, such as the need for:

(i) a procedure of observing the ocean in a routine, synoptic manner to detect possible changes in the ocean carbon cycle in response to climate change; and

(ii) a well-cared for data set, comprising observations made according to standard protocols.

3.3.1. 1989 NABE

The first JGOFS process study was conducted by several countries in the North Atlantic in the period between 1988 and 1991. The aims of this North Atlantic Process Study included

(i) measuring "seasonal and geographical variability of CO_2 exchange between surface water and atmosphere" and

(ii) characterizing the "biological component of drawdown of carbon from the atmosphere to the ocean and from the surface of the ocean to its interior".

Apart from logistical reasons, the North Atlantic had been chosen as a study area because of its conspicuous, extensive, and predictable spring bloom north of about 40°N. Further, it has a fundamental impact on ocean biogeochemistry, because it is the main global site of deep water formation carrying CO_2 derived from fossil fuel (Watson & Whitfield, 1985), and because noticeable annual sedimentation of phytodetritus to bathyal and abyssal depths has been observed there (Billet et al., 1983; Pfannkuche, 1993).

The study started off in 1989 with the North Atlantic Bloom Experiment (NABE), which was the first large-scale internationally coordinated study of ocean biogeochemistry. The locations of the major sampling sites and transects sampled in the North Atlantic from April until August of that year are shown in figure 3.6. Two stations in the Northeast Atlantic received the greatest attention because of the relatively high nutrient concentrations, reached at the onset of stratification in early spring, which is one of the prerequisites for the development of the spring bloom (figure 3.6). The boreal station was near 47°N and the subarctic one near 60°N 20°W. Since the Northeast Atlantic has been found to be physically dynamic (Krauss & Käse, 1984), it has been recognized that changes in the physical field

need to be accounted for when trying to understand changes in carbon biogeochemistry associated with spring bloom events.

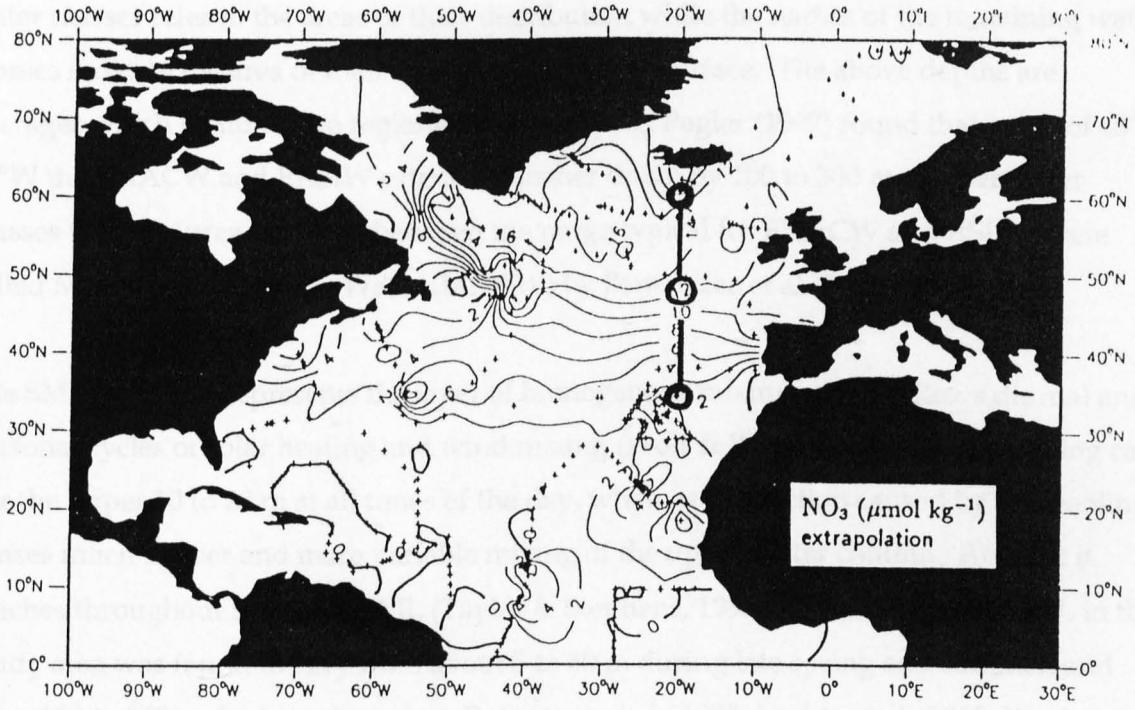

Figure 3.6: Location of major sampling sites and transects sampled during NABE 1989 with estimated winter maximum surface nitrate concentrations (μM) (adapted from Glover & Brewer, 1988)

3.3.1.1. General hydrography of the Northeast Atlantic JGOFS study area (45-65°N 10-25°W)

Water masses of the world ocean can be divided vertically into three types according to Emery and Meincke (1986), i.e.

(i) upper (0 - 500 m)

(ii) intermediate (500 - 1500 m)

(iii) deep and bottom (1500 - bottom).

Typical water masses of the Northeast Atlantic, their acronyms, and their characteristic ranges of potential temperature and salinity are given in table 3.1. The names of the upper water masses refer to the areas of their distribution while the names of the remaining water masses indicate the area of their formation at the sea surface. The above depths are averages which exhibit large regional variations, e.g. Pegler (1997) found that north of 45°N 20°W the ENACW and EASIW extended further down by 100 to 300 m. Upper water masses with features falling in between the range typical for ENACW and ASUW were called Mixed North Atlantic Water (MNAW) by Fernandez et al. (1993).

The SML generally represents the layer of homogenous mixing which follows diurnal and seasonal cycles of solar heating and wind mixing (Wolf & Woods, 1988). Wind mixing can stir the upper 10 to 20 m at all times of the day, whereas convection caused by SST cooling causes much deeper and more variable mixing of the upper water column. At night it reaches throughout the entire SML (Taylor & Stephens, 1993). The depth of the SML in the study area was found to vary from about 5 to 40 m during late spring and summer, and from 150 to 250 m during winter (e.g. Robertson et al., 1993; Lochte et al., 1993; Weeks et al., 1993; Glover & Brewer, 1988).

Table 3.1: Typical water masses of the Northeast Atlantic with typical depth, potential temperature and salinity ranges according to Emery and Meincke (1986).

water mass		depth range (m)	pot. temperature range (°C)	salinity range (psu)
upper water		0 - 500		
Atlantic Subarctic Upper Water	ASUW		0.0 - 4.0	34.00 - 35.00
Eastern North Atlantic Central Water **	ENACW		8.0 - 18.0	35.20 - 36.70
intermediate water		500 - 1500		
Arctic Intermediate Water	AIW		-1.5 - 3.0	34.70 - 34.90
Eastern Atlantic Subarctic Intermediate Water**	EASIW		3.0 - 9.0	34.40 - 35.30
Mediterranean Water	MW		2.6 - 11.0	35.00 - 36.20
deep and bottom water		1500 - bottom		
Arctic Bottom Water	ABW		-1.8 - -0.5	34.88 - 34.94
North Atlantic Deep Water	NADW		1.5 - 4.0	34.80 - 35.00
Antarctic Bottom Water *	AABW		-0.9 - 1.7	34.64 - 34.72

* the AABW is not typical for the North Atlantic but has an influence on the NADW close to the bottom

** Pegler (1997) found that north of 45°N 20°W these water masses extended further down by 100-300 m

The circulation of surface water in the study area covered during NABE and experiments in the following two years is largely characterized by the North Atlantic Drift (NAD). This is a collective term for northern sub-branches of the North Atlantic Current (NAC), which are masked by shallow and variable wind-drift surface measurements (figure 3.7). As the NAC crosses the Mid Atlantic Ridge at about 30°W, its surface waters form a broad easterly flow between 44° - 54°N. On approach of the Eastern Boundary, the NAC moves mainly towards the northeast, ultimately terminating as the Norwegian Current in the Norwegian Sea (Sverdrup, 1942). Using TTO data, the northern margin of the NAC in the Northeast Atlantic was located at 50° - 55°N (Pegler, 1997). This coincides with the front between ASUW and ENACW, i.e. the Polar or Subarctic Front, which is evident from the surface to about 600 m (Harvey, 1982). Some of the northeastward flowing water branches off again further north to join the Irminger Current, which moves in a westerly direction along the southern coast of Iceland (Sverdrup, 1942). However, the main branching of the NAC in the study area occurs east of 20°W near 51°N (Pingree, 1993). In this region some of the current moves in a southeasterly direction to join the Portugal Current (Sverdrup, 1942), which forms part of the Subtropical Gyre (Pingree, 1993). Generally, the area east of 20°W and west of the British Isles, which includes the boreal JGOFS study site, is a relatively stagnant part of the North Atlantic, since it falls between the main branches of the NAC at these longitudes. The exact positions of the sub-branches and their strength are difficult to establish due to, for example, seasonality, undesirable windage effects, and the presence of deep-reaching eddies (Pingree, 1993).

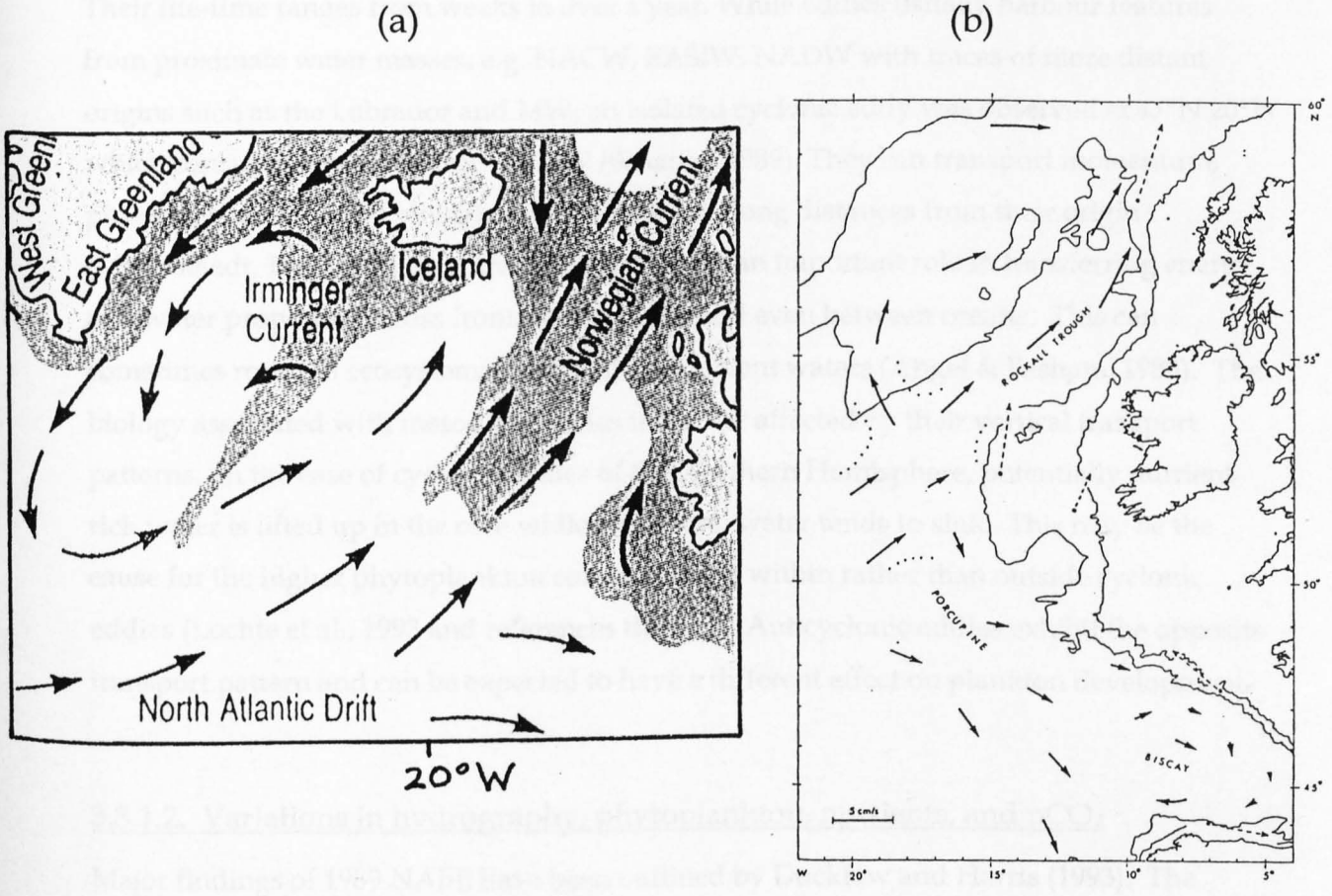

Figure 3.7: Surface flow in the Northeast Atlantic
(a) from OU (1991)
(b) from Pingree (1993)

Earlier studies have shown that mesoscale eddies, typically with 50 - 200 km diameters, are common features in the Northeast Atlantic. They are generally formed in regions with a strong density contrast and vertical current shear which give rise to wave-like perturbations, e.g. along the Subarctic Front with its associated NAC. Vertical displacement of the temperature surface inside eddies has at times exceeded 300 m (Robinson et al., 1993). Their life-time ranges from weeks to over a year. While eddies usually harbour features from proximate water masses, e.g. NACW, EASIW, NADW with traces of more distant origins such as the Labrador and MW, an isolated cyclonic eddy was observed at 47°N 20°W which consisted almost entirely of MW (Schauer, 1989). They can transport momentum, physical, chemical, and biological properties over long distances from their origin (Mittelstaedt, 1987), and they are expected to play an important role in transferring energy and water properties across frontal boundaries and even between oceans. This can sometimes result in ecosystems distinct from ambient waters (Angel & Fasham, 1983). The biology associated with mesoscale eddies is further affected by their vertical transport patterns. In the case of cyclonic eddies of the Northern Hemisphere, potentially nutrient-rich water is lifted up in the core while peripheral water tends to sink. This may be the cause for the higher phytoplankton concentrations within rather than outside cyclonic eddies (Lochte et al., 1993 and references therein). Anticyclonic eddies exhibit the opposite transport pattern and can be expected to have a different effect on plankton development.

3.3.1.2. Variations in hydrography, phytoplankton, nutrients, and pCO_2

Major findings of 1989 NABE have been outlined by Ducklow and Harris (1993). The positions and dates of the investigations by the participating scientifc groups during NABE are indicated in figure 3.8. Most issues covered in this and the following section are based on findings from the U.S., U.K. and Dutch teams.

3.3.1.2.1. Links between hydrography, biology, and pCO_2

Hydrographic studies by Robinson et al. (1993) confirmed that the Northeast Atlantic is a region with highly dynamic heterogeneous eddy fields and complex horizontal advection patterns. Eddies were mostly of 100 - 300 km diameter.

The development and refinement of the method for the analysis of pCO_2 enabled real-time detection of spatial and temporal variations (Watson et al., 1991). This included horizontal

gradients in surface water of 5 to 10 μatm over a distance of 10 km (Robertson et al., 1990) and diurnal and day-to-day variations (Robertson et al., 1993). Concomitant measurements of chlorophyll a, salinity, and temperature on board ship and by remote sensing revealed strong links between pCO_2, ocean circulation, and changes in phytoplankton biomass (Robertson et al., 1993; Yoder et al., 1993). Observations from the Airborne Oceanographic Lidar (AOL) confirmed lateral trends of chlorophyll, i.e. an increase from south to north as time progresses, but no east-west trends (Esias et al., 1986). They also revealed significant co-variation in temperature and chlorophyll on spatial scales ranging from 10 to 290 km. The smaller-scale variations were interpreted as evidence that physical processes such as upwelling and mixing associated with eddy dynamics were the dominant factors influencing spatial variations in chlorophyll in mid-May. The larger-scale reflected the difference between the cyclonic eddy core with higher chlorophyll and the surrounding waters.

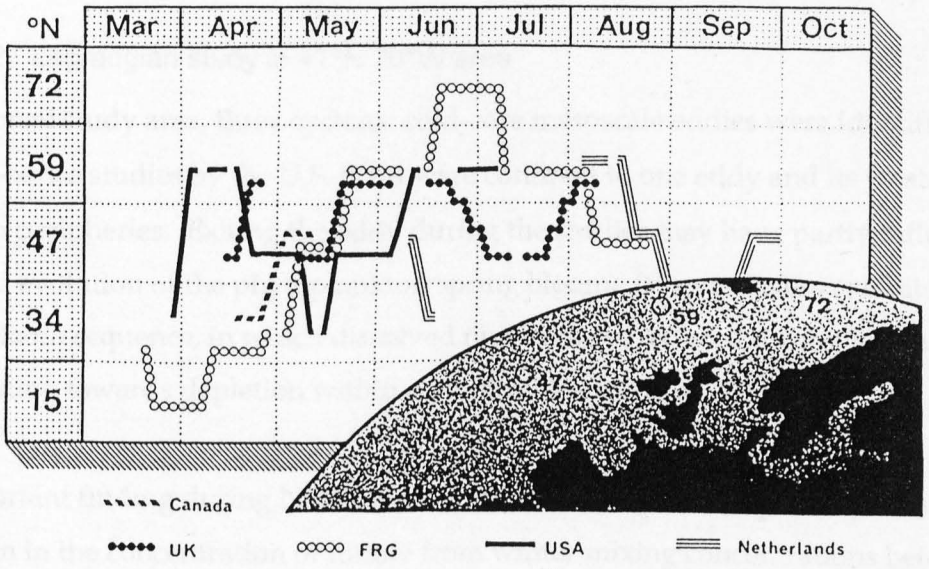

Figure 3.8: Positions and dates of ship coverage by the participating scientific groups during the 1989 NABE (from JGOFS, 1990a).

The hydrographic heterogeneity observed during this study implies that resulting small-scale variations in biomass and pCO_2 need to be accounted for by the appropriate models, i.e. eddy-resolving coupled circulation/ biogeochemical models. For example, Yoder et al. (1993) reported a high amplitude variation in chlorophyll of 2.4 μg dm^{-3} over a distance of 36 km near 60°N 20° at the start of June. With an assumed horizontal advection of 10-15 cm sec^{-1} (Robinson et al., 1993), Yoder et al. pointed out that this change could be erroneously attributed to the rapid dynamics of phytoplankton blooms.

3.3.1.2.2. Lagrangian study in 47°N 20°W area

In the boreal study area, three cyclonic cold-core mesoscale eddies were identified. Most of the time-series studies by the U.S. team were confined to one eddy and its western and southern peripheries. Exiting the eddy during the studies may have partly influenced the observed evolution of the phytoplankton spring bloom. It nevertheless exhibited the classic spring bloom sequence, in which dissolved nutrients are reduced during formation of the SML leading towards depletion within a month (Newton et al., 1994).

An important finding during NABE was the distinct increase in chlorophyll a and a reduction in the concentration of nitrate from winter mixing concentrations before the onset of stratification and the development of the main spring phytoplankton bloom at the end of April (Ducklow, 1989). Williams (1974) and Williams and Hopkins (1975) had recorded typical background values of chlorophyll in the range of 0.1 - 0.2 μg dm^{-3} at Ocean Weather Station India at 59°N 19°W. Concentrations of nitrate in the winter mixed layer at 47° and 60°N 20°W were about 12 μM at both stations according to modelling done by Glover and Brewer (1988), whereas Garside and Garside (1993) derived NO_3 values of 13 and 17 μM for the respective stations. The latter authors found that at least half of the seasonal production predicted by their model had occurred before stratification.

At the end of April, when the experiment started, the thermocline was about to develop, thus allowing the initiation of the main spring phytoplankton bloom. By that time, chlorophyll a concentrations exceeded 0.4 μg dm^{-3} (Lochte et al., 1993) and nitrate concentrations had fallen to 6 μM (Chipman et al., 1993). The start of the bloom occurred in form of a shift in phytoplankton community structure from a balance of diatoms and coccolithophorids to one entirely dominated by diatoms (Marra quoted in US JGOFS, 1989).

The species composition of this diatom population was mixed. The > 5 μm size class was prevalent (Savidge et al., 1995). Peak concentrations of chlorophyll in the surface exceeded 2.5 μg dm^{-3} (Lochte et al., 1993). By mid-May, the supply of silicate and nitrate were depleted in the SML causing a shift in dominant phytoplankton species from diatoms to coccolithophorids and later in June to flagellates and dinoflagellates (Weeks et al., 1990). A similar pattern of phytoplankton species succession has been observed at all latitudes between 47°N and 60°N. However, the start date of the bloom was delayed towards the north, e.g. at 60°N it did not start until early June (Boyd et al., 1990).

Since phytoplankton growth was rapidly succeeded by microzooplankton following the onset of the bloom, some simple models of bloom dynamics have been put into question. In these models it is assumed that there is a distinct period of low grazing, microbial activity, and high export production of uningested larger phytoplankton cells, while nitrate is still in sufficient supply. This would imply that biological CO_2 drawdown is necessarily associated with new production (Ducklow & Harris, 1993). Accordingly, these models also assume that most of the primary production would be supported by nitrate, i.e. the f-ratio (ratio of new to total production) exceeds 0.5. Instead, this scenario was only observed briefly in the upper 10 m of the water column during the peak bloom period in the first half of May (Bury et al., 1990). Otherwise, the regeneration of nutrients such as NH_4 and urea by large and active stocks of microbes including ciliates, nano- and dinoflagellates (Burkill et al., 1993; Verity et al., 1993) resulted in estimated f-ratios of 0.20 - 0.45 (Sambrotto et al., 1993a; Martin et al., 1993).

Results from different types of parameters indicate that primary production rates of more than 80 μmol C m^{-2} day^{-1} were reached in the SML during NABE. This rate was almost doubled during peak time. By the end of May pCO_2 was reduced by up to 80 μatm down to about 260 μatm at 47°N (Robertson et al., 1990). TCO_2 in the SML was notably lowered by about 33 μmoles kg^{-1} at 47°N 20°W over the main two weeks of the phytoplankton bloom. This rate of reduction, i.e. 2.3 μmol kg^{-1} day^{-1}, amounted to 75% of primary productivity (Chipman et al., 1993).

3.3.1.2.3. Latitudinal and seasonal variations

Latitudinal changes between 47° and 60°N 20°W were investigated by Taylor et al. (1992). The observations took place between 20 and 24 May. In spite of considerable variation at the southern end, there was an overall trend in chlorophyll to decrease towards the north. Chlorophyll ranged between 1 and 4 $\mu g\ dm^{-3}$ at the boreal site, while it remained below 1.5 $\mu g\ dm^{-3}$ at the subarctic site. This general trend was accompanied by an overall increase in pCO_2 from about 300 to 340 µatm, and could largely be explained by the delayed onset of the spring bloom at higher latitudes at that particular time of the year. This as well as unpublished observations by D. Harbour (PML) of changes in the species composition of the phytoplankton along the 20°W transect led Taylor et al. (1992) to conclude that the sampling track had covered areas which exhibited different stages of the typical phytoplankton spring bloom. Accordingly, it had started off in an area of bloom decay at the southern end, then passing through a bloom maximum, and ending up in the north where the bloom was about to start. Coccolithophorids were not named as the dominant group in May. In June, however, it was shown that their contribution to phytoplankton biomass became more important at 60°N 20°W with *Coccolithus pelagicus* being the dominant species (Weeks et al., 1993). In August, *Emiliania huxleyi* was found to constitute more than 90% of the ultraplankton size group (here ≤ 5 µm diameter) which, in turn, contributes 50 to 80% to daily primary production during summer stratification (Veldhuis et al., 1993; and references therein).

3.3.1.3. Estimates of surface TA and their variations

3.3.1.3.1. Temporal changes in the 47° and 60° 20°W areas

Between 25 April - 8 May and 18 May- 1 June 1989 TA was measured by the U.S. team on full-depth casts over 24 hours at drifting stations between 46° to 48°N and 18° to 20°W using potentiometric titrations. The data has not yet been fully published (P. Brewer, 2000, pers. comm.). However, another data set from those cruises which is based on TA calculated from pCO_2 and TCO_2 indicates that TA decreased from 2344 to 2338 $\mu eq\ kg^{-1}$ between the end of April and 8 May (Chipman et al., 1993). At the same time salinity decreased by 0.1 psu and the nitrate concentration fell by 3 µM. This implies that the salinity reduction had lowered TA by about 7 $\mu eq\ kg^{-1}$ and nitrate uptake led to an increase by 3 $\mu eq\ kg^{-1}$. The reduction in TA_{NO3} by 3 $\mu eq\ kg^{-1}$ implies that a negligible amount of calcification had

occurred over that period. This estimate may be compared to potentiometric TA results by Takahashi et al. (1990), which suggest that TA_{NO3} based on the potentiometric measurements had decreased slightly more, i.e. by about 5 μeq kg^{-1}. By the end of May, the steady decline in potentiometric TA_{NO3} led to a reduction by about 12 μeq kg^{-1}, i.e. the PIC production had reached about 6 μmol dm^{-3} within that month. From the ratio of TA_{NO3} against salinity-normalized TCO_2, the above authors worked out that the POC:PIC production ratio was about 9. This estimate included a correction for CO_2 entry from the atmosphere.

Although not strictly Lagrangian, measurements of potentiometric TA by the Dutch team in August 1989 and at the end of May 1990 may give some indication of changes in TA over the summer period, which are shown in figure 3.9. Assuming that interannual changes are negligible, this suggests that TA did not change notably at 47°N. In contrast, at 60°N it fell by 10 to 30 μeq kg^{-1} between those months (Stoll, 1994). In principle, this ties in with the increased importance of *Emiliania huxleyi* at that latitude in August (Veldhuis et al., 1993).

3.3.1.3.2. Spatial variations in TA

Results for variations of TA calculated from pCO_2 and TCO_2, which were measured between 12 May and 5 June by the U.K. team have been presented by Taylor et al. (1992) and are shown in figure 3.10. In their latitudinal survey from 47° to 60°N, which took 4 days, calculated TA fell from about 2355 to 2330 μeq kg^{-1}. Potentiometric TA measured by the Dutch fell slightly less by 10 to 20 μeq kg^{-1} (Stoll, 1994). However, this latitudinal trend observed in the calculated TA set from the U.K. team exhibited considerable noise, i.e. it varied within about 20 μeq kg^{-1} at either latitude. This noise was ascribed to advection and other variability (Taylor et al., 1992). The general effects of salinity, nitrate uptake, and calcification on this calculated TA were not specified in the work by Taylor et al.. Regional small-scale latitudinal and longitudinal variability of 10 to 20 μeq kg^{-1} was also observed over distances of 100 to 200 km, which in principle match the variability associated with meso-scale eddies.

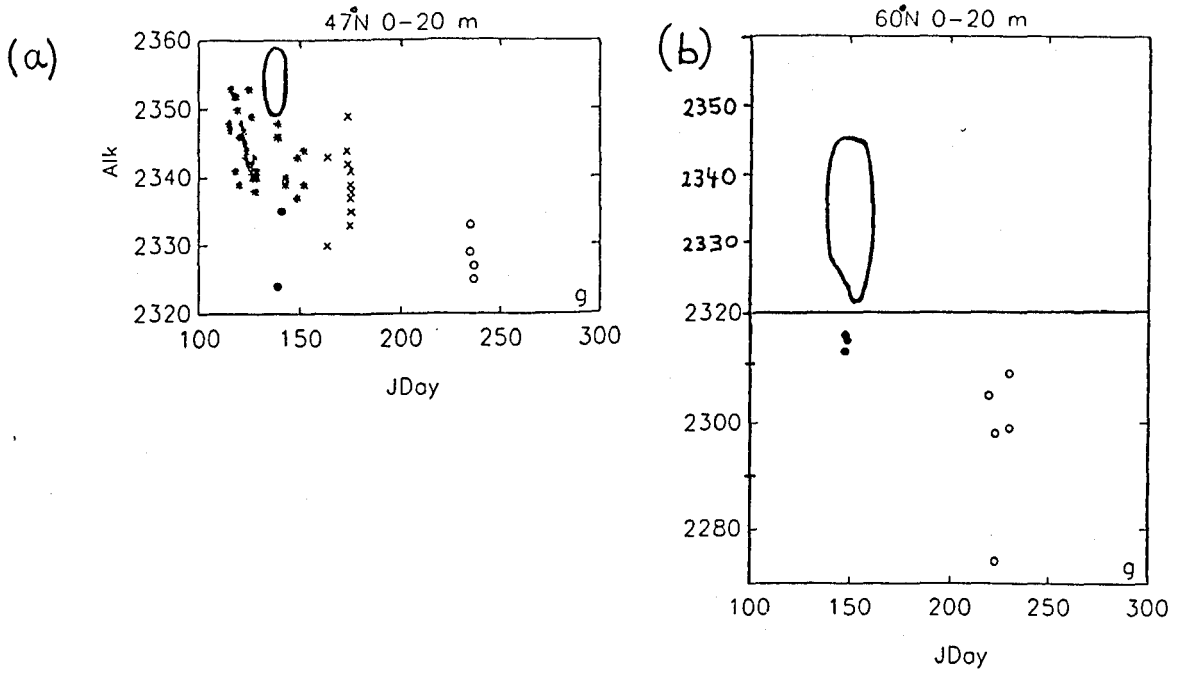

Figure 3.9: Results of potentiometric TA measurements conducted by the Dutch team at (a) 47°N and (b) 60°N 20°W during the 1989 NABE (open circles) and the 1990 Spring Bloom Experiment (full circles) described in chapter 4. Units are μeq kg^{-1}. Measurements of TA by other teams are also shown, i.e. potentiometric TA by the U.S. team (stars), and the encircled areas mark the TA ranges calculated from pCO_2 and TCO_2 by the U.K. team as shown in figure 3.10 below. (adapted from Stoll, 1994)

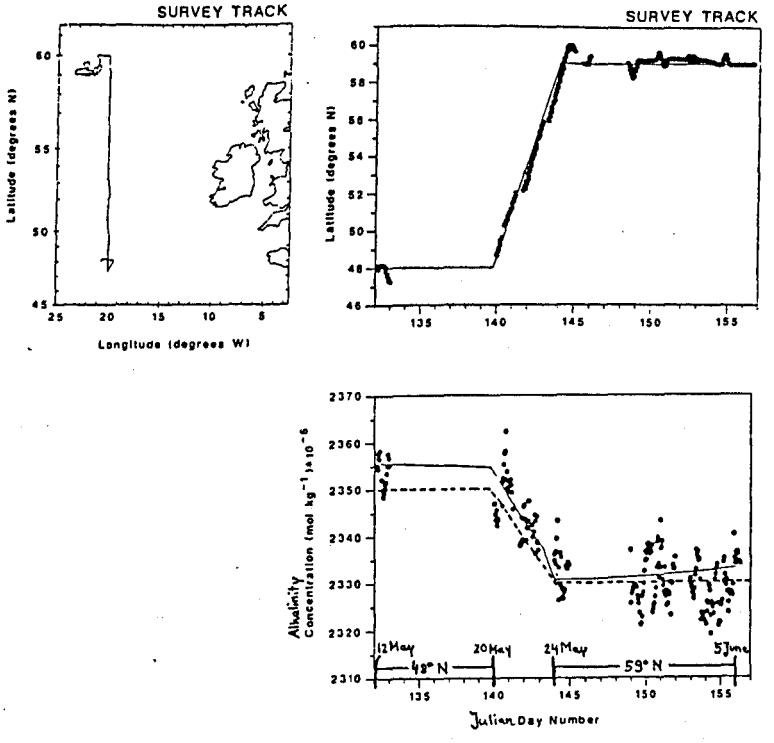

Figure 3.10: Change in alkalinity between 47°N and 60°N along 20°W over the period between 12 May and 5 June 1989. Modelled alkalinity was calculated from temperature and salinity in and below the SML including (solid line) and excluding (broken line) modelled influence of biological NO_3 uptake. Alkalinity derived from measured pCO_2 and TCO_2 in the SML is shown as dots. Values were corrected for borate. Information on sampling positions and cruise track are included. (figures adapted from Taylor et al. 1992)

3.3.1.3.3. Modelled TA

Taylor et al. (1992) also presented a modelled TA data set which had been calculated from temperature and salinity in and below the SML (figure 3.10). Its calculation assumed that concentrations of NO_3 below the SML decreased from 6 to 3 μeq kg^{-1} between 48° and 59°N 20°W. Modelled TA largely agreed with calculated TA from the U.K. team with respect to the latitudinal decline towards the north. A comparison of modelled TA with and without corrections for nitrate suggested that TA decreased with time at 47°N due to vertical mixing gradually introducing water from below the SML with lower preformed alkalinity concentrations while the bloom was decaying (Taylor et al., 1992). This ignores the fact that preformed TA may in fact have been higher at greater depths due to calcification in the SML.

It is not obvious to what extent changes in salinity would have caused variations in alkalinity. The observed change in composition of phytoplankton species, i.e. large numbers of flagellates and dinoflagellates at 48° and 59°N and dominance of diatoms at intermittent stations, was not considered important. This ties in with the tight correlation between pCO_2 and TCO_2 which was observed by Watson et al. (1991), and which suggests that there were no obvious areas of elevated calcification. However, calcification was shown to become more important one month later at 60°N (Weeks et al., 1993), i.e. the model would not have represented biological TA changes accurately at that point in time. Especially with respect to alkalinity it would seem important to consider the potential effect of calcification on alkalinity and pCO_2. This had also been advocated in the JGOFS Science Plan (JGOFS, 1990a).

According to the model by Taylor et al. (1992) the dominant factor determining the difference in alkalinity between the southern and northern stations at that time of the year was the difference in preformed alkalinity from below the SML, which accounted for 20 μeq kg^{-1}.

As a further check on their model, Taylor et al. (1992) compared TCO_2, O_2, and alkalinity values used below the SML of the model to those measured during the TTO expedition. The positions were not identical but as close as possible to the NABE stations, with sampling depths ranging from 180 to 670 m (Takahashi, T., pers. comm. in Taylor et al., 1992). Taylor

et al. concluded that the values are in general agreement. This does not seem to be justified in the case of alkalinity, i.e. modelled alkalinity values were considerably larger than those measured during TTO surveys in 1981. The discrepancies ranged from 12 to 50 μeq kg^{-1}.

3.3.1.3.4. Discrepancies between TA data sets

The interpretation of spatial and temporal variations in TA has been complicated by apparent discrepancies between some of the TA data sets.

On one hand, good agreements were reported between TA calculated by the U.K. team from all three combinations of pCO_2, TCO_2, and pH. These data sets also agreed with potentiometric TA data from the U.S. team at 47°N 20°W in May (JGOFS, 1990b). On the other hand, figure 3.9.a demonstrates that the average range of calculated TA was about 10 μeq $kgSW^{-1}$ greater than the potentiometric TA values from the U.S. Although this comparison is not based on exactly the same water samples, the same area was covered.

A consistent offset of about 20 μeq $kgSW^{-1}$ between potentiometric TA data from the Dutch and the U.S. teams was observed in a direct comparison of cast samples collected down to 4500 m (JGOFS, 1990b). This discrepancy led to investigations into the causes such as the use of different standards, the dissociation constants used to transform titration data into TA results, and the omission of PIC removal prior to the acid titrations. Stoll et al. (1993) found that the choice of dissociation constant for carbonic acid played a minor role. The interference of PIC, which in theory may lead to increased TCO_2 and TA results, was discarded as a fully viable explanation in this case, since coccolith counts suggested that this factor was insignificant. While filtration of samples prior to the TA analysis is not possible when the sample is also analysed for TCO_2, it was nevertheless concluded that further work on filtered and unfiltered samples should be conducted (JGOFS, 1990b). The reason for the discrepancy was not found (Stoll, 1994).

The problem associated with accurate TA measurements will also emerge in the following chapters.

3.3.1.3.5. Overview of seasonal and latitudinal variations of TA in the Northeast Atlantic

In spite of the above discrepancies, some general trends in TA seem to have emerged from the NABE.

With respect to seasonal changes, the investigation period may be split into four parts based on hydrographic and biological changes, i.e.

(i) winter-mixing conditions with negligible phytoplankton growth;
(ii) period of increased phytoplankton growth some time before the onset of stratification;
(iii) spring diatom bloom; and
(iv) subsequent phytoplankton growth involving non-calcifying or calcifying algae.

Baseline TA values for winter-mixing conditions were established by Glover and Brewer (1988). According to the reduced nitrate concentrations, phytoplankton growth may have already increased TA before the development of the thermocline by up to 6 $\mu eq\ kg^{-1}$. It is not clear how important calcification can become during that second phase, i.e. the overall effect of biological activity on TA remains unquantified. However, according to observations by Marra (quoted earlier) and sediment trap data (Newton et al., 1994) significant coccolithophorid growth may occur at that time of year. During the main diatom bloom phase which lasts approximately one month, TA was raised by a further 6 $\mu eq\ kg^{-1}$ due to nitrate uptake and lowered by 12 $\mu eq\ kg^{-1}$ due to calcification. The overall effect of biology on TA at the end of the bloom would have been either insignificant or somewhat reduced. This uncertainty depends on the amount of calcification that had occurred before the start of the diatom bloom.

During the post-bloom phase, increases due to nitrate can be assumed to become less important since much of the continued growth is assumed to be sustained by regenerated nutrients. At the same time, coccolithophorids may continue to grow moderately at latitudes below about 55°N whereas further north their increased importance after the main diatom bloom phase may have been the principle cause for the reduction of 20 to 40 $\mu eq\ kg^{-1}$, which was observed by Stoll (1994).

During winter time, TA presumably depends upon the amount of export production of POC and PIC from the upper 200 m or whatever depth constitutes the winter mixed layer depth.

Latitudinal changes can be assumed to depend first of all on the preformed TA values which according to Glover and Brewer (1988) decrease by about 10 to 20 $\mu eq\ kg^{-1}$ towards the north. In April and May, latitudinal differences will be further enhanced due to the time-lag in the onset of the bloom, i.e. it starts about 5 weeks later at 60°N than at 47°N. Once all the latitudes have experienced the main spring bloom, another latitudinal gradient can be expected when favourable conditions for coccolithophorid blooms lower TA by considerable amounts north of 55°N. This aspect will be investigated further in chapter 5.

4. ALKALINITY IN THE NORTHEAST ATLANTIC DURING THE 1990 BOFS SPRING BLOOM EXPERIMENT

4.1. INTRODUCTION TO THE 1990 EXPERIMENT

As a follow up to NABE, in 1990 the U.K. launched the Spring Bloom Experiment in the vicinity of 48°N 20°W. One particular aim was to gain a better understanding of the factors influencing the development of the phytoplankton spring bloom and associated changes in carbon and other nutrient fluxes and pools from well-mixed winter to stratified summer conditions. This was attempted by conducting time-series observations adjacent to a Lagrangian marker buoy, which was drogued at a depth of 30 m, and which was deployed within the closed circulation of an anticyclonic mesoscale eddy. This warm-core eddy had been identified in a 200 x 200 km (about 2° long. x 3° lat.) spatial survey of the hydrographic field in the upper 300 m of the target area one week before the deployment. The hydrography was studied using a SeaSoar, i.e. a towed CTD (conductivity, temperature and depth) and chlorophyll sensor which undulated within the upper 300 m. One week after this Seasoar survey, a CTD survey was conducted more narrowly around the position of the buoy.

The Lagrangian study continued almost uninterruptedly from 1 May until 15 June. Towards the end of the time-series study, between 12 to 19 June, a second SeaSoar survey was carried out in the area through which the buoy had recently passed. This was followed by a second CTD survey on 22-24 June along two of the legs covered by the SeaSoar survey. These two transects were about 120 km apart with the northern and southern transect passing through 48° and 47° N, respectively. Four shallow and one deep CTD cast were conducted along each of the transects. The SeaSoar survey and shallow CTD casts were aimed at providing information about mesoscale variability of hydrographic and biogeochemical parameters in the waters surrounding the buoy. Samples from deep casts served chiefly for methodological intercomparisons. Shallow casts usually covered the approximate depths of 2, 10, 30, 70, 150, and 300 m. Deep casts were sampled at depths from 500 m down to the ocean floor at approximately 4000 and 5000 m. The distance between neighbouring stations was about 20 km. Positions of the casts are marked in figure 4.1. Timing and location of the Experiment allowed some interannual comparisons with results from the previous year.

The following section aims to provide a background in the hydrographic and bloom dynamics that were observed before the final areal surveys in June, and this is put into a biogeochemical context.

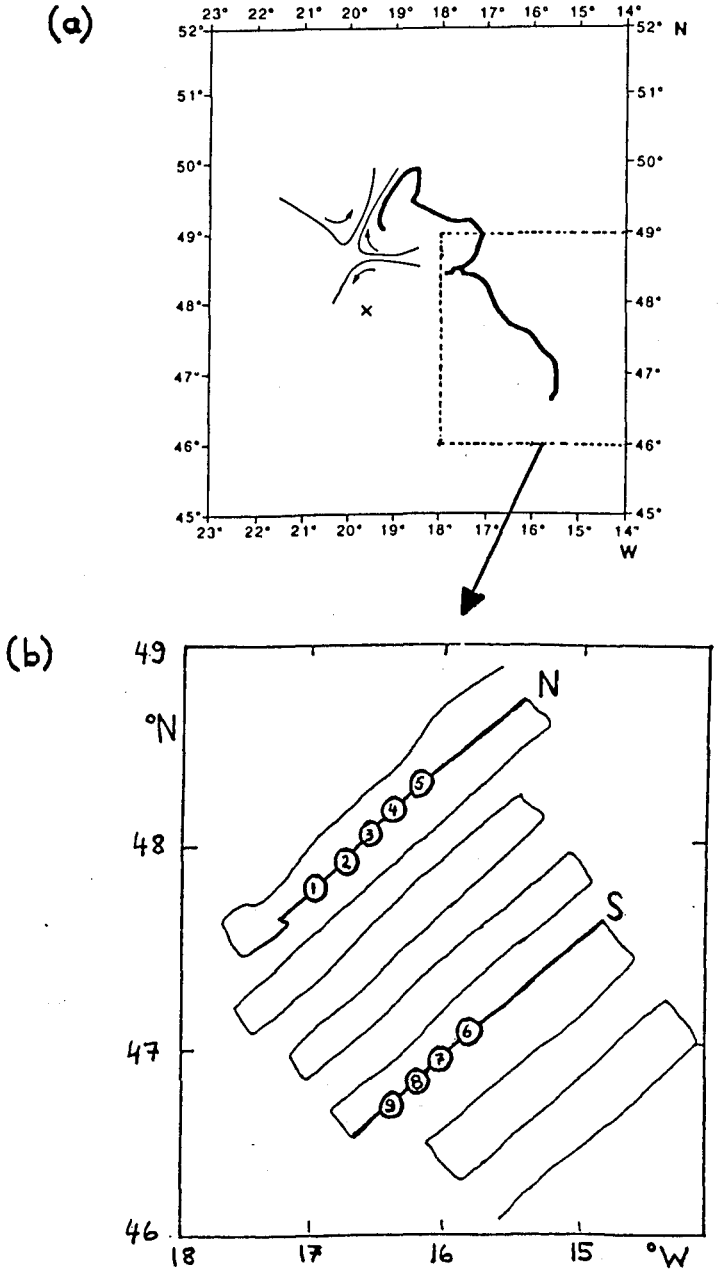

Figure 4.1: Study sites during the 1990 Spring Bloom Experiment conducted in the Northeast Atlantic between April and June indicating
(a) mesoscale eddy structure in second half of April with sense of eddies indicated by arrows; drift pattern of Lagrangian drogue (1 May to 16 June) progressing from northwest to southeast; and area of final SeaSoar and CTD survey (adapted from Newton et al. (1994)); and (b) positions CTD stations along the northern (N) and southern (S) transects studied during the final CTD survey between 22 and 24 June. Deep cast stations are marked with a 'D'.

4.2. HYDROGRAPHY, BLOOM DEVELOPMENT, NUTRIENTS BEFORE AND DURING LAGRANGIAN STUDY

4.2.1. GENERAL WATER MASSES

According to Emery and Meincke (1986), all the water sampled in the upper 400 m during the Experiment showed temperature and salinity characteristics typical of ENACW. Profiles from the deep cast along the northern transect exhibited characteristics of ENACW and/or MW at 500 m, MW at 1000 m, EASIW at 1500 m, and NADW at the greater depths. This pattern was almost the same at the deep cast along the southern transect. However, temperatures and salinities in the 500 to 1500 m depth range were higher at this station, and at 1500 m also matched the characteristics of MW. This may have reflected the closer proximity to the source region of MW. Profiles of these hydrographic parameters are provided in section 4.4.3.7 (figures 4.15; 4.16).

The hydrography of the upper 300 m has been covered extensively by Savidge et al. (1992) and the phytoplankton and nutrient dynamics by Savidge et al. (1995).

4.2.2. SPATIAL VARIATIONS AT 48°-50°N 18°-21°W IN APRIL 1990

Between 19 and 25 April 1990 a hydrographic structure of juxtaposed warm- and cold-core eddy systems was observed which was more complex than in the preceding years. The target eddy had a diameter of about 100 km. Its boundaries were delineated by a sharp vertical gradient of the isotherms while vertical stratification within the eddy was minimal, i.e. less than 0.3°C within the upper 300 m. Temperatures within the eddy core were about 1°C warmer than to its south. At the same time, a cyclonic cold-core eddy southeast of the target eddy exhibited greater lateral structure which marked the beginning of stratification. Further eddies were observed in the survey area. The general picture was complicated by tongues and lobes of these water masses extending into neighbouring regions.

Within the warm-core eddy, concentrations of chlorophyll were generally low, i.e. less than 0.4 μg dm^{-3}. Savidge et al. (1992) concluded that in spite of some phytoplankton growth in the warm-core eddy, the bloom had not started there. In contrast, in the cyclonic cold-core eddy the onset of stratification was notably reflected in elevated chlorophyll concentrations of up to 1.5 μg dm^{-3} near the surface and still in excess of 0.4 μg dm^{-3} at 60 m. This indicated that the main spring bloom was in progress. It showed typically increased numbers of *Chaetoceros* spp. (D. Harbour, unpubl. data, in Savidge et al., 1995). Average nitrate concentrations were around 6 μM within the target eddy, i.e. similar to values of the same date in 1989 (Savidge et al., 1992).

One week later, the average temperature had increased by 0.8°C within the target eddy, probably due to solar heating. As this increase was not universally observed, the SSTs within the target eddy had also increased in a relative sense. The temperature rise within the warm-core eddy was accompanied by an approximate doubling of surface chlorophyll a concentrations. Again, this was not universally observed. Consequently, this change in the general distribution of chlorophyll over one week provided further evidence of the importance of eddies on the spatial development of the phytoplankton bloom in spring, when the balance of heat input and stability is critical (Angel & Fasham, 1983).

4.2.3. LAGRANGIAN STUDY IN MAY/JUNE

Savidge et al. (1995) split the biological observations during this Lagrangian study into three phases which were partially linked to the hydrographic changes.

Between 1 and 11 May the initial north- and eastward movement of the buoy ties in with the anticipated closed anticyclonic circulation around the centre of the eddy. During this period the weather was largely overcast preventing the development of the seasonal thermocline. Meanwhile chlorophyll a concentrations increased gradually to 1.5 - 1.8 μg dm^{-3} in the upper 10 m. The biomass increase was largely due to the small diatom *Nanoneis hasleae* with a typical size of 5 μm (D. Harbour, pers. comm. in Savidge et al., 1992). Towards the end of this phase the relative importance of small (1 - 5 μm) and larger diatoms (>5 μm) had reached its peak. This was accompanied by the maximal decrease in the concentration of dissolved silicate to below 1.0 μM and a reduction in nitrate concentration from 6.7 to 3.5 μM.

On 11 May vertical hydrographic changes indicated that the buoy was leaving the original target eddy. It led to the development of the thermocline and the shallowing of the SML, which was generally enhanced by rising SSTs due to increased insolation after 13 May. This also introduced the second biological phase which lasted until 17 May. It led to peaks in the growth curves of smaller and larger nanoflagellates and of *Nanoneis hasleae*. Chlorophyll a concentrations rapidly increased over four days and briefly exceeded 3 $\mu g\ dm^{-3}$ within the upper 10 m. Satellite-images of reflectivity suggest that this bloom was associated with the front or discontinuity and thus with the buoy track (Savidge et al., 1992). The reduction of this bloom back to a chlorophyll range of 1.0 - 1.5 $\mu g\ dm^{-3}$ coincided with the decrease in the concentrations of dissolved nitrate and silicate to below 0.5 µM. Savidge et al. (1992) provided a quantitative argument that the decline in nitrate concentration was predominantly due to advection of reduced-nitrate water rather than phytoplankton uptake. Substantial grazing by zooplankton was put forward as an additional possible factor (P. Burkill, pers. comm. in Savidge et al., 1992).

Between 11 May and 12 June the buoy followed a relatively consistent course towards the southeast, i.e. the typical net direction of surface currents in this part of the Northeast Atlantic. This as well as the observed changes in vertical temperature distribution over this period led to the conclusion that the buoy probably tracked along a front between the original warm-core and a cyclonic cold-core eddy, and that the drogue grazed the eddy core waters during frontal convolutions. The front or discontinuity was defined between 50 and 200 m, i.e. by the depth of the 11.5 °C isotherm in the cold- and warm-core eddy, respectively. A close congruence of this isotherm and the 35.60 psu isohaline was observed.

During the third biological phase after 17 May, counts of *Nanoneis hasleae* fell rapidly. In terms of phytoplankton biomass, dinoflagellates became increasingly important, contributing up to 50% of the total. Chlorophyll a concentrations rarely fell below 1.0 $\mu g\ dm^{-3}$, while concentrations of dissolved nitrate and silicate remained largely below 0.5 and 1.0 µM, respectively.

On 12 June the buoy abruptly adopted a southwestern course, which implied that the buoy was leaving the warm-core eddy again. Along this southwestern course, a weak chlorophyll a maximum was measured in the subsurface between 20 and 30 m. This was contrasting the vertical pattern of the preceding weeks during which concentrations had

monotonically decreased with depth. Savidge et al. (1992) suggested the complex thermal structure as a possible explanation for this. However, the sinking of this particulate matter to greater depths in the case of advanced bloom stages in the warmer waters may provide an alternative or at least additional explanation. This may also be supported by the generally lower surface chlorophyll concentrations recorded one to two weeks later during the spatial surveys described below.

Throughout this entire time-series study, estimates of species-specific contributions to TPC by phytoplankton at 10 m depth suggest that coccolithophorids did not contribute much more than 10% to total phytoplankton carbon, since their TPC remained below a concentration of 1 μM. This implies that calcification was relatively insignificant at this particular depth when compared to coccolithophorid bloom situations. The main coccolithophorid species were *Ophiaster hydroides* and *Syrcosphaera pulchra*. Counts of *Emiliania huxleyi* and *Coccolithus pelagicus* stayed below 10^3 cells dm^{-3} (Savidge et al., 1995).

4.2.4. COMPARISONS WITH 1989 AND BIOGEOCHEMICAL IMPLICATIONS

In both years nitrate concentrations measured before the onset of stratification were well below the estimates for winter mixed conditions, thereby implying that a significant amount of primary production had already taken place before the end of April. Also, as for 1989, observations were largely consistent with the classic bloom sequence regarding nutrient depletion during and following formation of the SML (Newton et al., 1994). Diatoms formed the dominant group during the main bloom. Counts of coccolithophorids remained generally below 10^6 cells dm^{-3}. Primary production rates and the reduction in TCO_2 and pCO_2 were all comparable to values in 1989 (Savidge et al., 1995; C. Robinson, unpubl. in Boyd & Newton, 1995; Williamson, 1991). Further, there was little interannual difference in the range of observed micro- and mesozooplankton grazing activities and bacterial production (several references in Boyd & Newton, 1995). Sediment trap data from 3100 m showed that in both years a major flux event was recorded in autumn in addition to the spring event. This demonstrated that it is not always the spring bloom which dominates export of carbon to greater depths.

In spite of the above similarities in the two years, major interannual differences were observed in the export of carbon to greater depths. The amounts of POC and PIC collected

in sediment traps at 3100 m during spring were about two times greater in 1989 than in 1990. Also, the POC collected in autumn of 1989 was, in turn, two times greater than in the spring of the same year and notably enriched with mucopolysaccharides (Newton et al. 1994). Boyd and Newton (1995) proposed that the interannual difference in POC flux during spring was related to the changed size-structure of phytoplankton during the main spring bloom, i.e. the dominance of larger diatoms such as *Chaetoceros* and *Nitzschia* spp. in 1989 and of the smaller *Nanoneis hasleae* in 1990. The authors proposed that the reduced size of the dominant species led to reduced coupling between surface primary production and carbon export to greater depths, so that the biological pump was less efficient in 1990.

Since the dominance of larger diatoms during vernal spring blooms had so far been regarded as typical for temperate waters, the results from 1990 raised the question as to how representative blooms of smaller diatom species are. On one hand, changing climate conditions may lead to a shift in favour of these smaller species, thereby reducing the impact of the biological pump (Aebischer et al., 1990). On the other hand, Savidge et al. (1995) pointed out that small diatoms and their blooms may have been underestimated previously due to methodological complications in identifying smaller phytoplankton species. It is also possible that the growth of larger diatoms was restricted in 1990 due to their infection by chitrid fungi, thus enabling smaller species to become dominant within the diatom group.

A further noteworthy finding in 1990 was the considerable flux, particularly of PIC, which began to reach the sediment traps at 3100 m by the end of April. The assumed settling rate of approximately 100 m per day provides further evidence that significant primary production had occurred in the SML prior to the main spring bloom (Newton et al., 1994). This is in contrast to 1989, when no major pre-bloom flux was recorded in the traps. Accordingly, pre-bloom production was apparently regenerated within the SML (Garside & Garside, 1993). However, Newton et al. (1994) have also drawn attention to the uncertainty as to the origins of material found in sediment traps and the considerable spatial variability of fluxes at these greater depths.

4.3. SHORT-TERM CHANGES BETWEEN THE SEASOAR AND CTD SURVEYS IN MID-JUNE 1990

The above section has provided an insight into the considerable horizontal, vertical and temporal variability in hydrography and biology in that boreal region of the Northeast Atlantic during May and the first half of June. Similar variability was also observed between the final SeaSoar and the final CTD surveys over the course of 4 to 10 days. This is described below and made it difficult or impossible to ascribe features observed in CTD casts to those observed in the Seasoar survey. However, on the basis of isotherm depths such an attempt has been made below, so that TA variations described in section 4.4. could be put into some context with the preceding hydrographic and biological developments.

4.3.1. SEASOAR SURVEY: 12-19 JUNE

During the final SeaSoar survey the general trend of SST was found to be similar to that of the initial survey. A thermal discontinuity separated cooler water with an average SST of 15.4 °C in the northwest from warmer water with mean SST of 16.1 °C in the southwest and east (figure 4.2.a). As observed earlier, intruding lobes and tongues of different water masses complicated the hydrographic scenario. The distribution of surface salinity, although more complex, was largely found to reflect that of SST. Figure 4.2.b shows that the thermal discontinuity was only a feature of the SML, since it was not clearly distinguishable at 100 m. However, most of the smaller scale features were also recognizable at this depth.

Surface concentration of chlorophyll a had generally fallen to below 1.0 $\mu g\ dm^{-3}$ and did not show much spatial variation. However, the thermal discontinuity was clearly reflected in chlorophyll concentrations. Cooler water in the northwest was associated with higher chlorophyll concentrations of typically 0.6 - 0.7 $\mu g\ dm^{-3}$, while they had largely fallen to below 0.5 $\mu g\ dm^{-3}$ in the warmer waters of the southwest and the east. The inverse relationship between SST and chlorophyll concentration also marked smaller-scale hydrographic features. Surface concentrations of nitrate did not show any correlation with physical parameters and chlorophyll.

No vertical profiles of hydrographic or biological parameters along the southern transect were presented by Savidge et al. (1992; 1995).

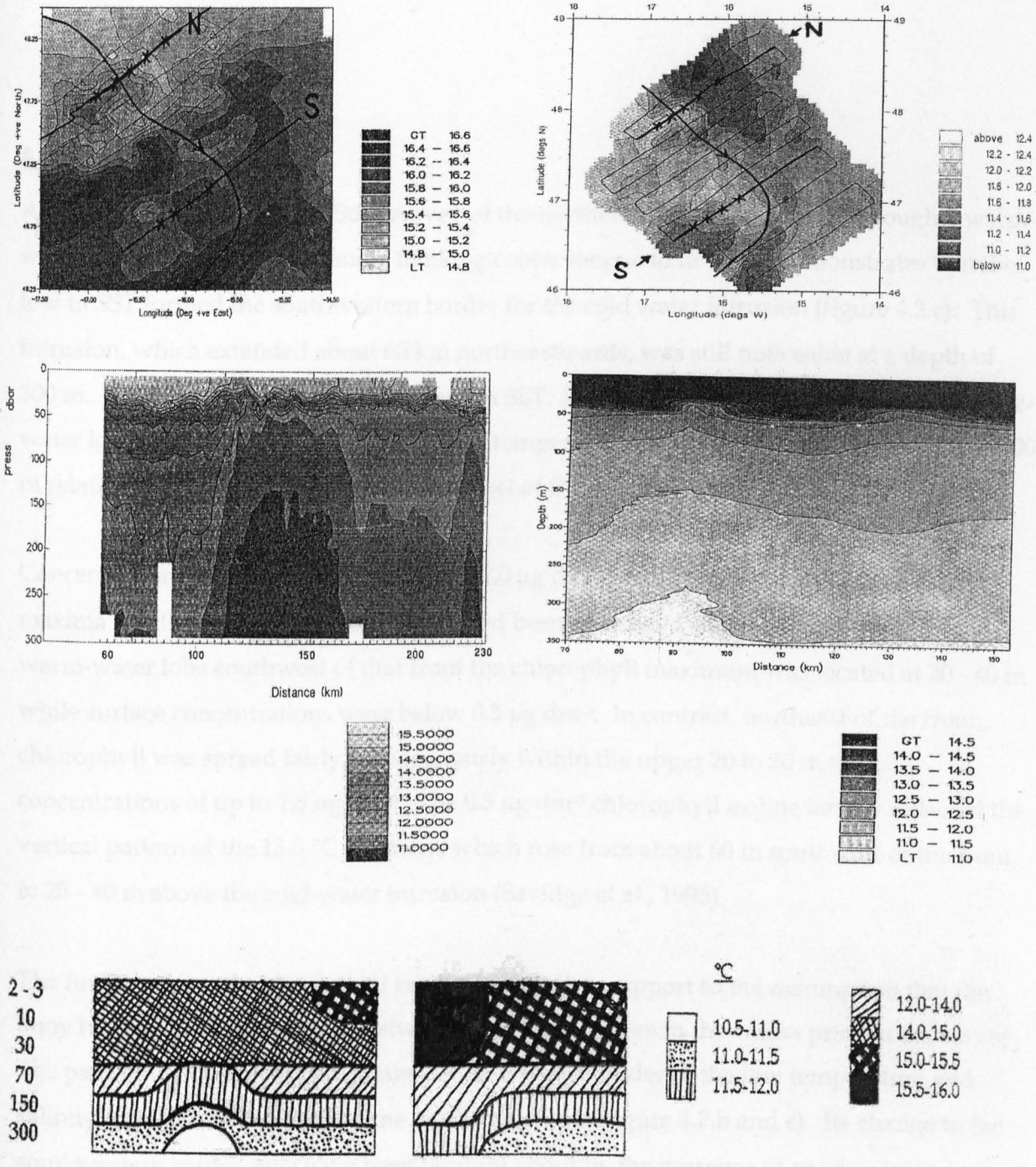

Figure 4.2.: Temperature profiles (°C) obtained during the final SeaSoar (12-19 June) and CTD surveys (22 - 24 June) conducted during the 1990 Spring Bloom Experiment in the Northeast Atlantic. The northern (N) and southern (S) transects, the CTD stations, and the track of the Lagrangian marker drogue are marked in horizontal profiles (adapted from Savidge et al.,1992). The positions of the CTD stations are not marked in the vertical profiles, since it was not entirely clear how the distance which was provided as a reference point in the vertical profiles (c) and (d) could be related to the geographical positions in figures (a) and (b). It should be noted that the shading is not consistent throughout the diagrams.

(a) surface distribution during SeaSoar survey;
(b) mean distribution from 98 - 106 m depth during SeaSoar survey;
(c) vertical profile from N transect during SeaSoar survey (from Savidge et al., 1992);
(d) vertical profile from N transect during CTD survey on 22-23 June (from Savidge et al.,1992);
(e) schematic vertical profile from N transect during CTD survey on 22-23 June (this study);
(f) schematic vertical profile from S transect during CTD survey on 24 June (this study).

4.3.1.1. Northern transect

A depth profile from the SeaSoar survey of the northern transect which cut through a warm-water lobe in the northwest and a flanking cooler tongue to its north demonstrates that the low in SST formed the southwestern border for the cold water intrusion (figure 4.2.c). This intrusion, which extended about 60 km northeastwards, was still noticeable at a depth of 300 m. It had however no obvious effect on SST. Southwest of the SST minimum a warmer-water lobe was also mirrored in the higher temperatures at depths throughout the upper 300 m relative to the waters within and northeast of the intrusion (Savidge et al., 1992; 1995).

Concentrations of chlorophyll a exceeded 1.0 $\mu g\ dm^{-3}$ within the vertical chlorophyll maxima at either side of the front which had been associated with the buoy track. In the warm-water lobe southwest of that front the chlorophyll maximum was located at 20 - 40 m while surface concentrations were below 0.5 $\mu g\ dm^{-3}$. In contrast, northeast of the front, chlorophyll was spread fairly homogenously within the upper 20 to 30 m with concentrations of up to 1.5 $\mu g\ dm^{-3}$. The 0.5 $\mu g\ dm^{-3}$ chlorophyll isoline largely reflected the vertical pattern of the 13.0 °C isotherm, which rose from about 60 m southwest of the front to 25 - 40 m above the cold-water intrusion (Savidge et al., 1995).

The findings from the above areal survey lent further support to the assumption that the buoy had tracked along a front between two water masses in the weeks prior to the survey. The path of the buoy had run alongside the western border of the low temperature and salinity intrusion which formed the northern tongue (figure 4.2.b and c). Its change to the southwestern course may have been brought about by the presence of another intrusion which formed the low temperature and salinity tongue in the south (Savidge et al., 1992).

4.3.2. CTD SURVEY: 22 - 24 JUNE

The CTD survey was conducted to obtain more detailed information on biogeochemical parameters across the frontal feature mentioned above. However, a major storm event occurred just before which may have contributed to the observed changes between the two spatial surveys.

4.3.2.1. Northern transect

A temperature profile of the northern CTD transect, which was conducted 22 - 23 June, is shown in figure 4.2.d. Although there was only a gap of four days between covering the same transect, the comparison was complicated by the intermittent storm event on 19 and 20 June (Turner, 1990) and by the highly dynamic nature of intermediate depth intrusions (Savidge et al., 1992). With respect to the SML, its depth had increased to more than 30 m, average temperatures were lowered by 0.5 °C and salinity was slightly increased. These changes may have been brought about by the storm event causing increased mixing with water from the thermocline and advection. Subsequent improved weather conditions may have contributed to the rising SSTs as sampling progressed in a northeastern direction along this transect. Regarding intermediate depths, the distinct cold-water intrusion observed on the 19 June was no longer present four days later. Savidge et al. (1992) presume that it had moved north- or eastwards. Instead, a small, 10 to 20 km wide, and more moderate cold-water intrusion was recorded further to the southwest. Its reduced temperature and salinity were observed at 70 m down to 300 m with temperatures being about 0.5 °C lower than those at the surrounding stations. This was also observed in the schematic temperature profile used in this study (figure 4.2.e).

If the depth range of the 11.0 to 12.0 °C isotherms are used for comparative purposes between the SeaSoar and CTD survey, it may be concluded that three of the CTD stations were in areas typical of the cooler water encountered northeast of the earlier cold-water intrusion. Remaining station 2 represented a moderate cold-water intrusion. Thus, none of the CTD casts along that transect covered the warm-water lobe captured four days earlier.

Limited chlorophyll a data indicates that the concentration range had fallen to 0.4 - 1.0 $\mu g\ dm^{-3}$ (section 4.4.3.1, figure 4.3). While concentrations were relatively homogeneous within the SML southwest of the new cold-water intrusion, northeast of this feature chlorophyll

concentrations at 2 - 3 m were twice as high as those at 10 m. A further notable change over the four-day period involved surface nitrate concentrations that had risen by about 0.7 μM to approximately 1.3 μM. A more likely explanation for these marked changes in chlorophyll and nitrate concentrations over these few days was horizontal advection since vertical mixing would presumably have tended to decrease salinity. The advected water would have introduced the higher nitrate-water.

4.3.2.2. Southern transect

The southern CTD transect, which was covered ten days earlier in the SeaSoar survey, was positioned just southwest of where the buoy had crossed this transect. During the Seasoar survey, this transect had cut through the cold-water lobe and tongue which were embedded in the warmer water of the south (figure 4.2.a). Figure 4.2.f which covers the three stations immediately southeast of the buoy track, demonstrates similar temporal trends as for the northern transect, i.e. temperature had fallen and salinity had increased over the previous ten days. However, compared to the northern transect, SST and surface salinity were generally higher here. Below the SML, the two northeastern stations 6 and 7 shared their hydrographic characteristics with those typical along the northern CTD transect, whereas station 8 tended to have notably higher temperatures and salinities.

Chlorophyll had apparently not increased much along this transect. At the same time surface nitrate had increased to 0.2 - 0.5 μM, presumably due to advection.

4.3.3. CONCLUSIONS REGARDING EXPERIMENTAL DESIGN

The CTD surveys of temperature distribution no longer identified the frontal feature which was assumed to have influenced the drogue track. Instead, it clearly demonstrated a temperature difference between the northern and southern transects. This may have been related to the main thermal discontinuity in SST observed during the SeaSoar survey which ran in a southwest-northeastern direction (figure 4.2.a). In the investigation of regional TA variations below, it therefore seemed more appropriate to focus on differences between the two transects rather than across them.

4.4. ESTIMATES OF TA AND THEIR VARIATIONS

4.4.1. AIMS

Total alkalinity measurements were conducted during the 1990 Spring Bloom Experiment specifically to

(i) determine the range and spatial variation of TA in relation to influencing hydrographic, chemical and biological factors, with a particular focus on the effect of phytoplankton growth;

(ii) carry out an intercomparison between the various techniques used for the analysis of the carbonate system; and

(iii) add the findings to the picture of spatial and seasonal TA variations in the Northeast Atlantic.

4.4.2. MATERIALS AND METHODS

4.4.2.1. Coverage of TA determinations during the 1990 Experiment

No direct measurements were conducted during the first spatial surveys in April and the time-series study in May and June. Potentiometric TA data was obtained during the final SeaSoar survey in June, while analytical problems precluded estimates by photometry. The final CTD survey was covered by all three types of TA techniques, i.e. including calculations using pCO_2 and TCO_2.

4.4.2.2. Presentation and interpretation of the TA results

An overview of results from photometric TA and other hydrographic, biological and chemical parameters is presented in section 4.4.3.1. It also provides detailed results from depth profiles for these parameters.

General ranges of photometric TA, TA_S, and TA_{NO3} within the SML, i.e. from the upper 30m, are presented in section 4.4.3.2. The overall effect of freshwater exchange on TA was estimated from the difference between the TA and TA_S ranges. Similarly, the effect of nitrate uptake by phytoplankton was estimated from the difference between TA_S and TA_{NO3}. The range of TA_{NO3} was assumed to represent variations in net calcification within

the SML. For a regional investigation of TA variations and its causes in the SML, a comparison between the northern and southern transect was conducted using mean values from each transect. The statistical significance of the findings were evaluated by applying t-tests for two samples of equal variances (Sokal & Rohlf, 1981).

The relationships between TA or its derived parameters and hydrographic, nutrient, or biological parameters are presented in section 4.4.3.3. They were quantified using the method of least squares regression analysis, and the significance of the relationships was evaluated using a t-test (Sokal & Rohlf, 1981).

Estimates of POC: PIC net production are presented in section 4.4.3.4. They were derived from the slope of the relationship between photometric TA_{NO3} to salinity-normalized TCO_2 (TCO_2S, 35 psu), i.e. if

a change in $TA_{NO3} = x$, and
a change in $TCO_2S = y$, then
the amount of PIC production = $x/2$, and
the amount of POC production = $y - x/2$, and
the production ratio of POC: PIC = $(y-x/2) / (x/2)$.

Accordingly, a slope of zero implies that a change in photosynthesis was not accompanied by a proportional change in calcification, and a slope of 2 means the reverse. It is important to bear in mind that the ratio *per se* does not provide information about the absolute amounts of net POC and PIC production that have occurred.

General ranges of TA and related parameters at two sub-thermocline depth ranges are presented in section 4.4.3.5, which also includes estimates of the effect of variations in salinity, nitrate metabolism, and PIC production/dissolution on TA. These were obtained in the same way as was done for SML ranges, which is described above. Equally, results were compared for the northern and southern transects. However, in some cases the t-test had to account for unequal variances of the two samples that were compared. A couple of small-scale changes in TA were identified. The thermocline was generally taken to represent the depth range which corresponded to a temperature change of greater than 0.02 $°C\ m^{-1}$ (Lochte et al., 1993).

In section 4.4.3.6 differences in TA between the SML and the sub-thermocline depth range of 70 -150 m are compared. The change in TA across the thermocline was determined separately for each CTD station by subtracting the mean sub-thermocline TA from the mean TA in the SML. In turn, averages of these changes were calculated to estimate the overall change in the area of the final CTD study and to compare results from the two transects. The statistical significance of the change across the thermocline and its difference between transects was investigated using a two sample t-test. The same procedure was repeated for TA_S, TA_{NO3}, ($TA-TA_S$), and (TA_S-TA_{NO3}). The latter three parameters provided respective estimates for the impact of net calcification, evaporation, and biological nitrate utilization on the seasonal change in TA within the SML.

For the above seasonal inferences to be justified, several assumptions had to be made, e.g.

(i) winter mixing occurred down to at least 150 m;

(ii) the overall chemical and biological conditions had not changed significantly at 70 and 150 m since the onset of stratification and were accurately representing the pre-stratification state;

(iii) no mixing across the thermocline and differential advection above and below the thermocline had taken place;

(iv) changes in nitrate concentration accurately represented the net effect of nitrate uptake on TA, and similarly, changes in TA_{NO3} provided an accurate quantification of the amount of net calcification that had occurred; and

(v) phytoplankton growth occurred only in the SML.

Vertical profiles of TA from the two deep casts are presented in section 4.4.3.7. Due to the shortage of photometric results, general vertical and horizontal trends were inferred from all three TA methods. Results from other parameters were used to get some idea of the main factors which had influenced TA at these greater depths.

A comparison of results from the different TA methods is presented in section 4.4.3.8.

4.4.2.3. Sample collection and analyses of TA

Details of sampling and the analyses have already been provided in section 2.3.10. Due to the early stage in the development of the TA method, none of the samples for TA were filtered before they were analysed. Specific alkalinity was generally calculated using a constant salinity value of 35.000 psu. Potential alkalinity, in turn, was determined from such TA_S values.

Spectrophotometric analyses of TA were carried out using the single wavelength method specifically set up for this study. Analysis of the samples took place within 72 hours of sample collection. The temperature of the samples was adjusted to 25°C in a waterbath prior to the titration.

Potentiometric TA was determined by K. Pegler (University of Hamburg), and TA estimates calculated from pCO_2 and TCO_2 were provided by D. Turner and his group (then PML). Potentiometric titration analyses were conducted within 24 hours after sampling.

4.4.2.4. Sampling and determinations of other parameters

Descriptions of the technical analyses employed for estimating other parameters, which were all carried out by other scientists, have been provided by Turner (1990) and are outlined below. All seawater samples were collected from the same Niskin bottle as the TA samples.

Salinity and temperature were obtained with a CTD. Density (sigma-t) data was computed from CTD data and obtained from the British Oceanographic Data Centre (BODC).

For the analysis of chlorophyll a, samples were collected on Whatman GF/F glassfibre filters, extracted in acetone and analysed on a Turner Designs bench fluorometer. For the determination of TPC and TPN a volume of 500 cm^3 was filtered onto non-combusted Whatman GF/F glassfibre filters. These were folded in foil and stored for several months before being analysed by high temperature combustion using a Europa Roboprep CN

analyzer. Results of TPN which were below the detection limit of the analytical method were taken to equal zero. The TPC and TPN were used to calculate particulate C/N ratios.

Samples for TCO_2 were analysed using a coulometric titration system as described by Robinson and Williams (1991). The pCO_2 in seawater was determined using a gas chromatographic method as described in Robertson et al. (1994). Sample temperatures of 15 °C were usually achieved by placing the samples in a waterbath prior to analysis. Samples of one cast were analysed at 8 °C. Adjustments of the results to 15 °C or in situ temperatures were carried out according to the DOE (1994) using the computer model by Lewis and Wallace (1995). Dissociation constants used for the conversions were adopted from Roy et al. (1993).

Dissolved oxygen analyses were carried using the Winkler titration method as described by Williams and Jenkinson (1982).

Nutrients were measured using a Technicon AA2 autoanalyser. Nitrate was reduced to nitrite by Cu/Cd coil. The nitrite then reacted with sulphanilamide in acidic conditions to form a diazo compound which then coupled with N-(1-napthyl-) ethylenediamine dihydrochloride to form an azo dye. Phosphate was measured by reducing a phosphomolybdate complex in acid solution to 'molybdenum blue' by ascorbic acid with sensitivity enhanced by the catalytic action of antimony potassium tartrate (Strickland & Parsons, 1972).

4.4.3. RESULTS

Throughout much of this section results of photometric TA are presented alongside those obtained by potentiometry and the calculation method. The comparison of results from different methods will be dealt with in section 4.4.3.8. Unless stated otherwise, TA refers to photometric results.

4.4.3.1. Profiles of TA and other parameters

An overview of results for TA and other parameters from shallow CTD casts along the two transects is given in figure 4.3. Detailed results from individual shallow casts are presented in figures 4.4 to 4.10.

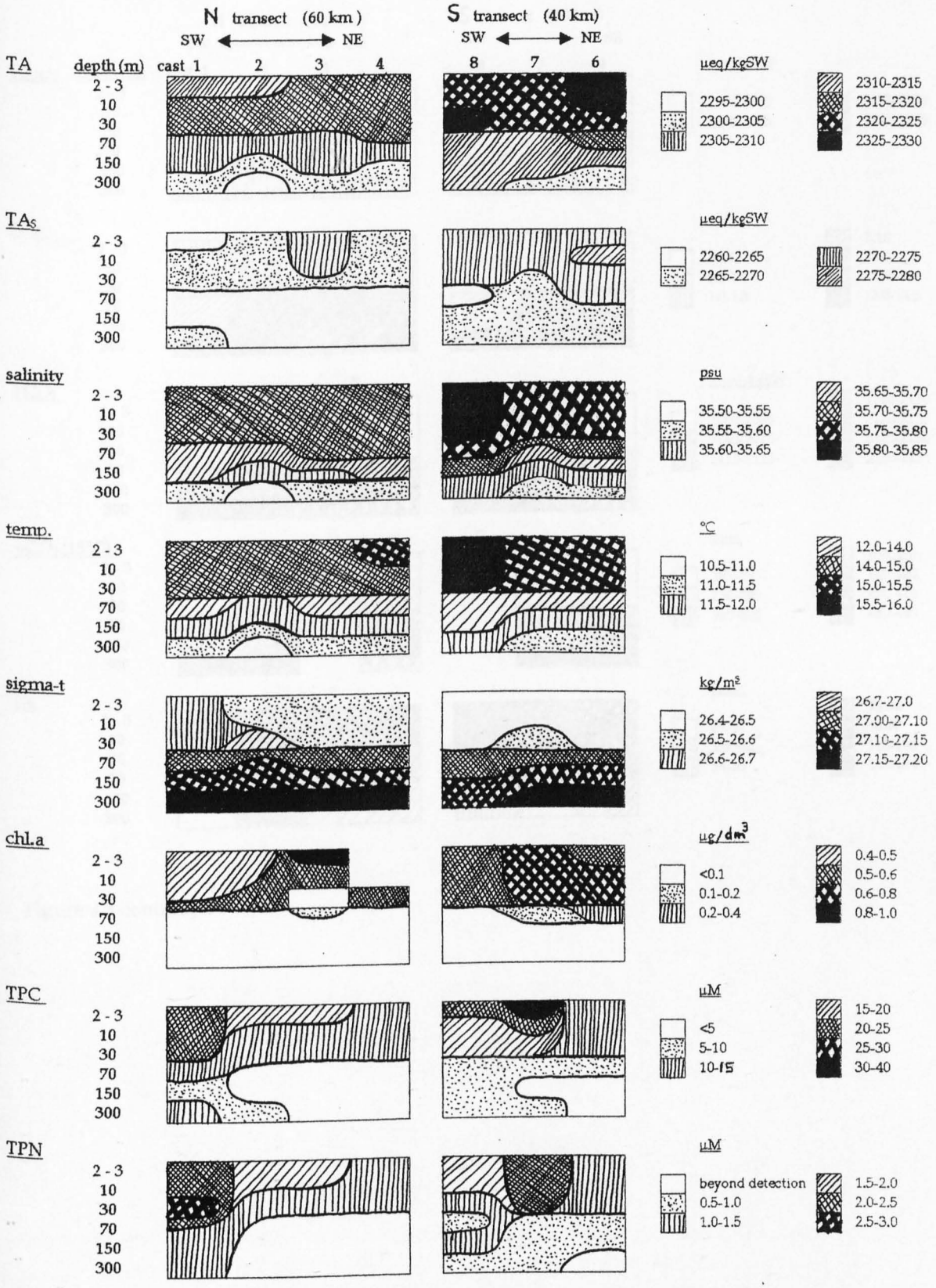

Figure 4.3: Overview of results obtained from seven shallow CTD casts along the northern (N) transect around 48° N 16.5°W and the southern (S) transect around 47°N 16°W on 22-24 June 1990 as part of the final CTD survey of the BOFS Spring Bloom Experiment. Numbers refer to CTD stations. More exact positions of the casts are given in figures 4.4 - 4.10. TA, TA_S, and TA_{NO3} refer to photometric results. This figure continues on the next page.

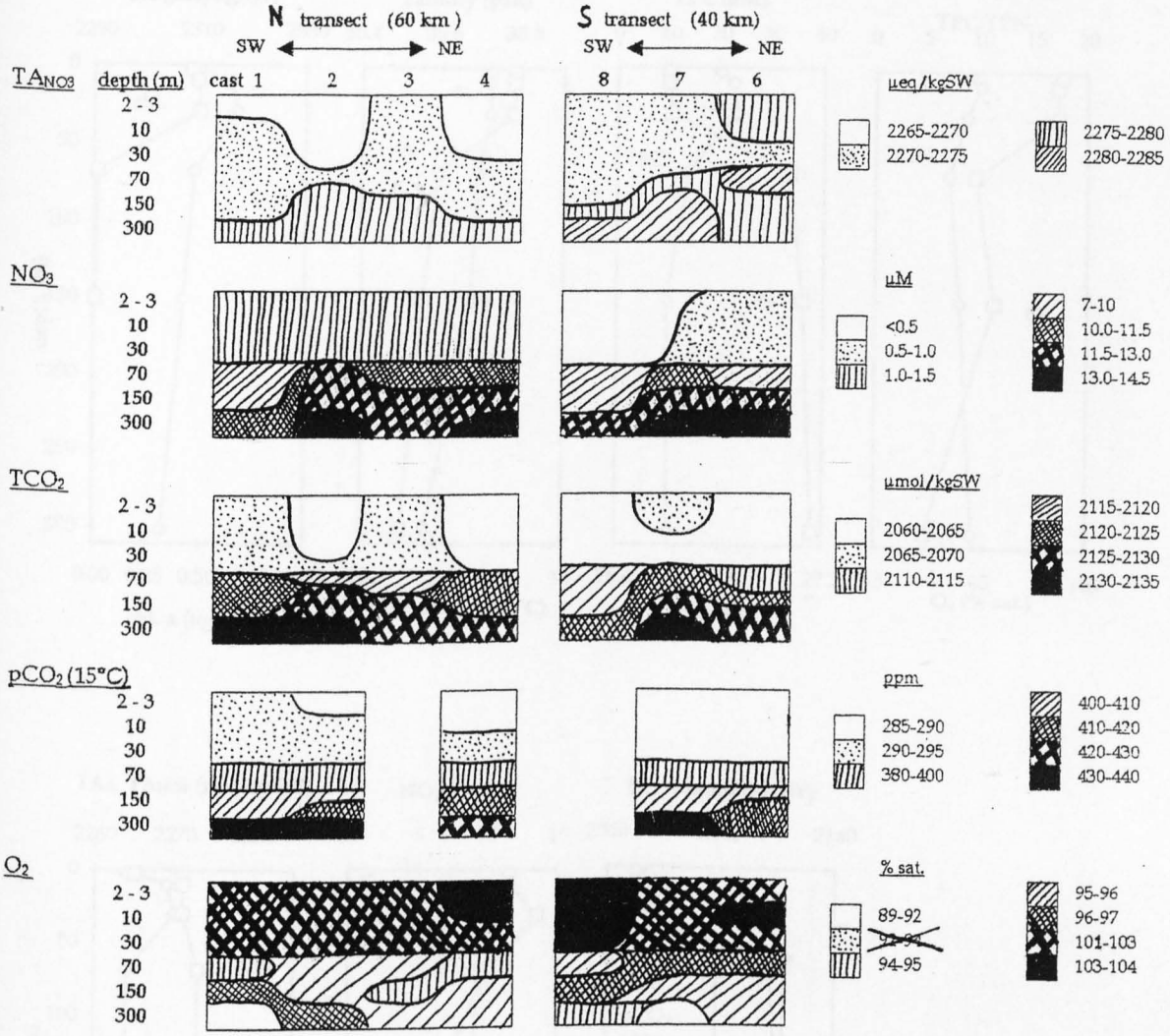

Figure 4.3 continued

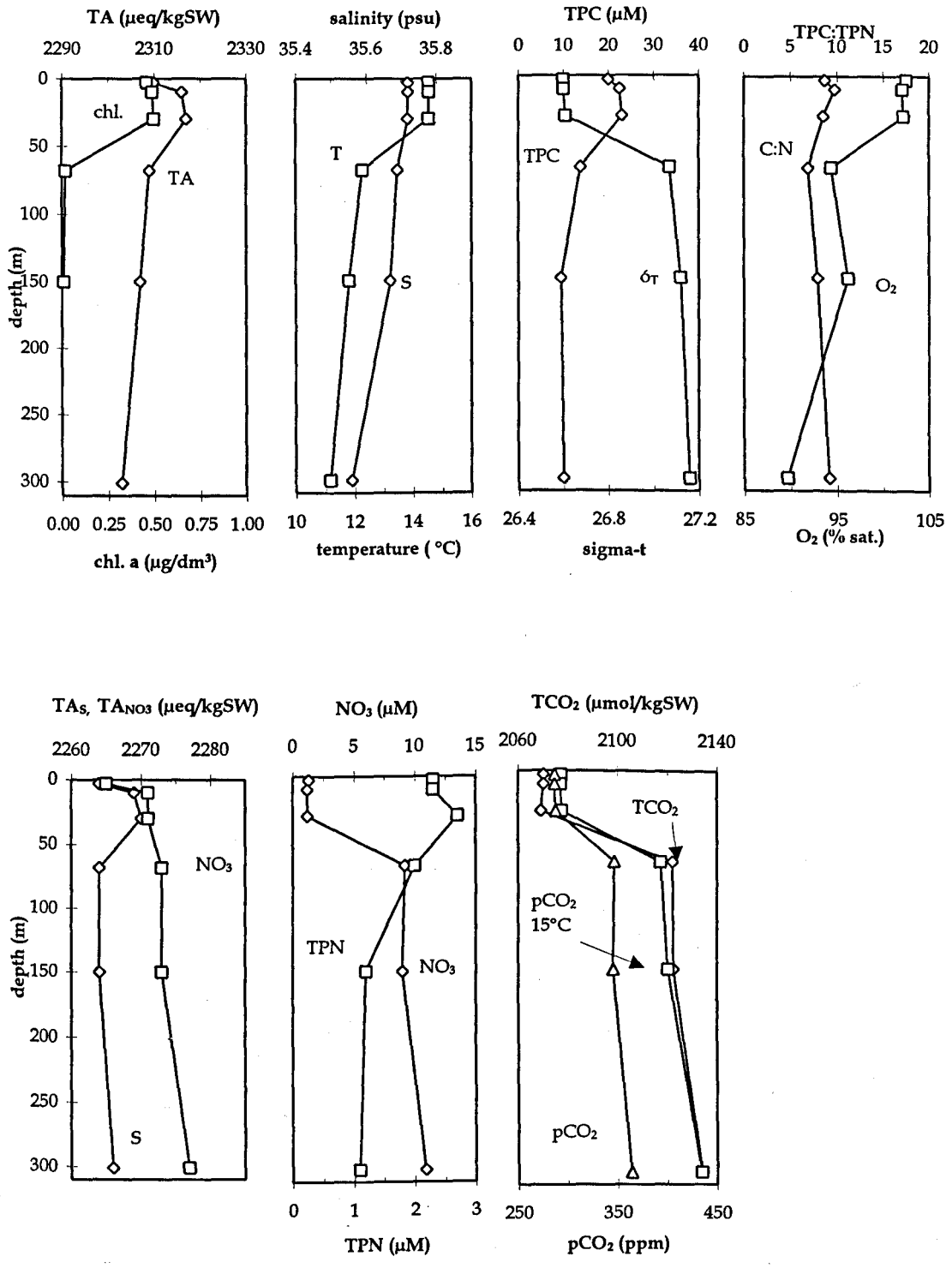

Figure 4.4: Vertical profiles of various in situ parameters obtained from station 1 along the northern transect around 47°49'N 16°57'W on 22 June 1990 as part of the final CTD survey of the BOFS Spring Bloom Experiment. Further parameters include pCO_2 at 15°C. TA, TA_S, and TA_{NO3} refer to photometric results.

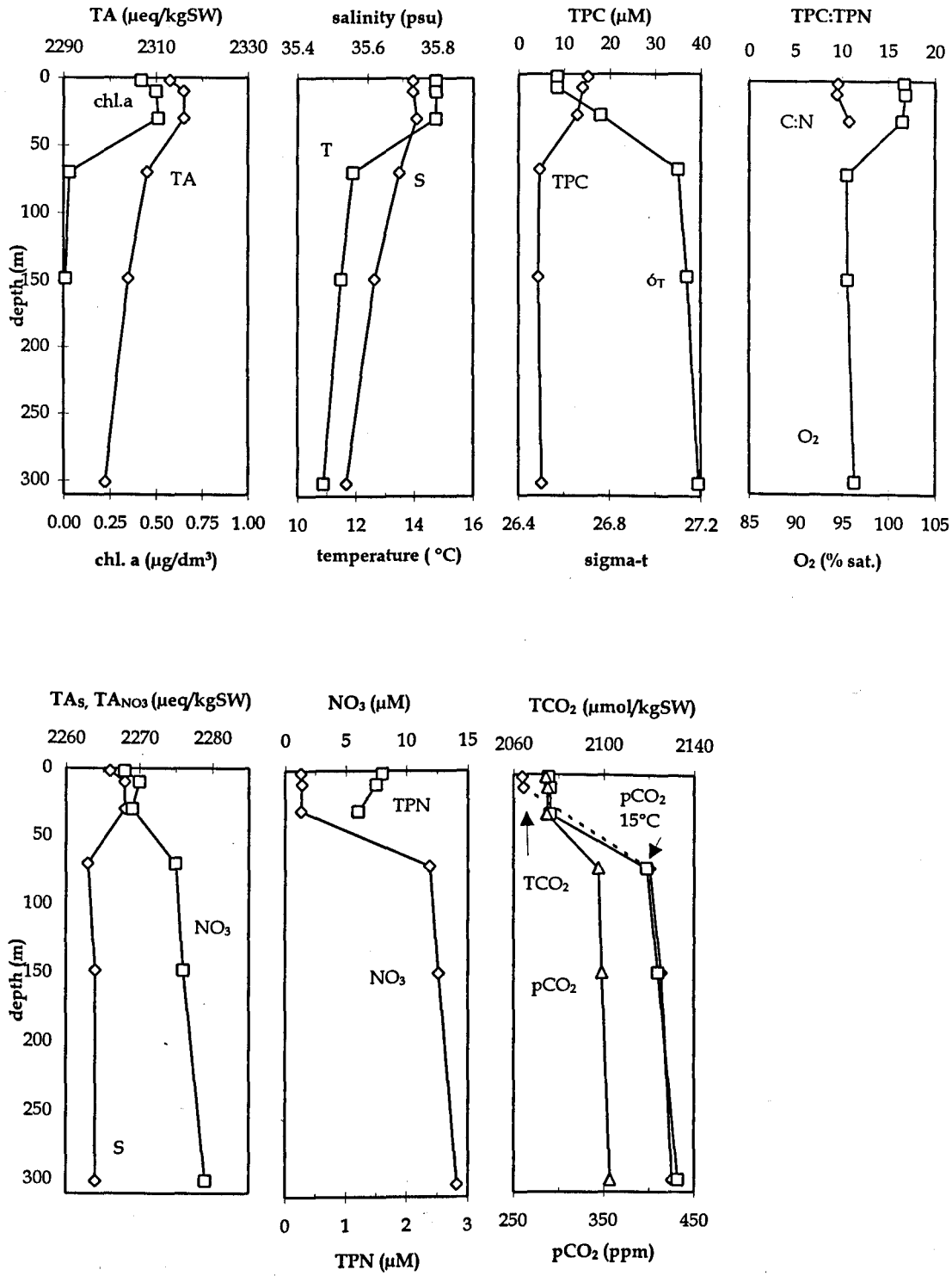

Figure 4.5: Vertical profiles of various in situ parameters obtained from station 2 along the northern transect at 47°56'N 16°46'W on 23 June 1990 as part of the final CTD survey of the BOFS Spring Bloom Experiment. Further parameters include pCO_2 at 15°C. TA, TA_S, and TA_{NO3} refer to photometric results.
The broken line indicates that the result for one sampling depth is missing.

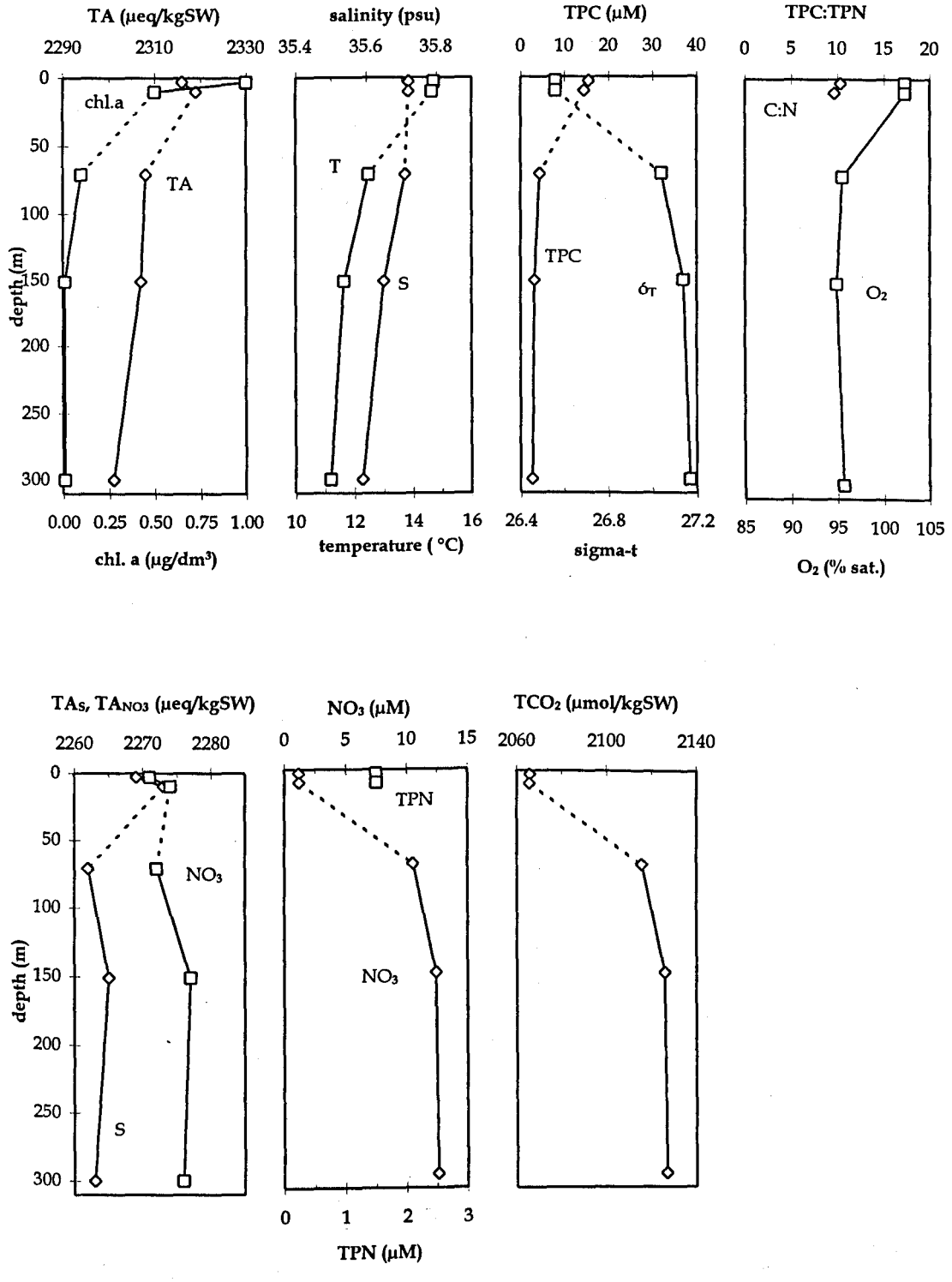

Figure 4.6: Vertical profiles of various in situ parameters obtained from station 3 along the northern transect at 48°03'N 16°30'W on 23 June 1990 as part of the final CTD survey of the BOFS Spring Bloom Experiment.
TA, TA_S, and TA_{NO3} refer to photometric results.
Broken lines indicate that results for certain sampling depths are missing.

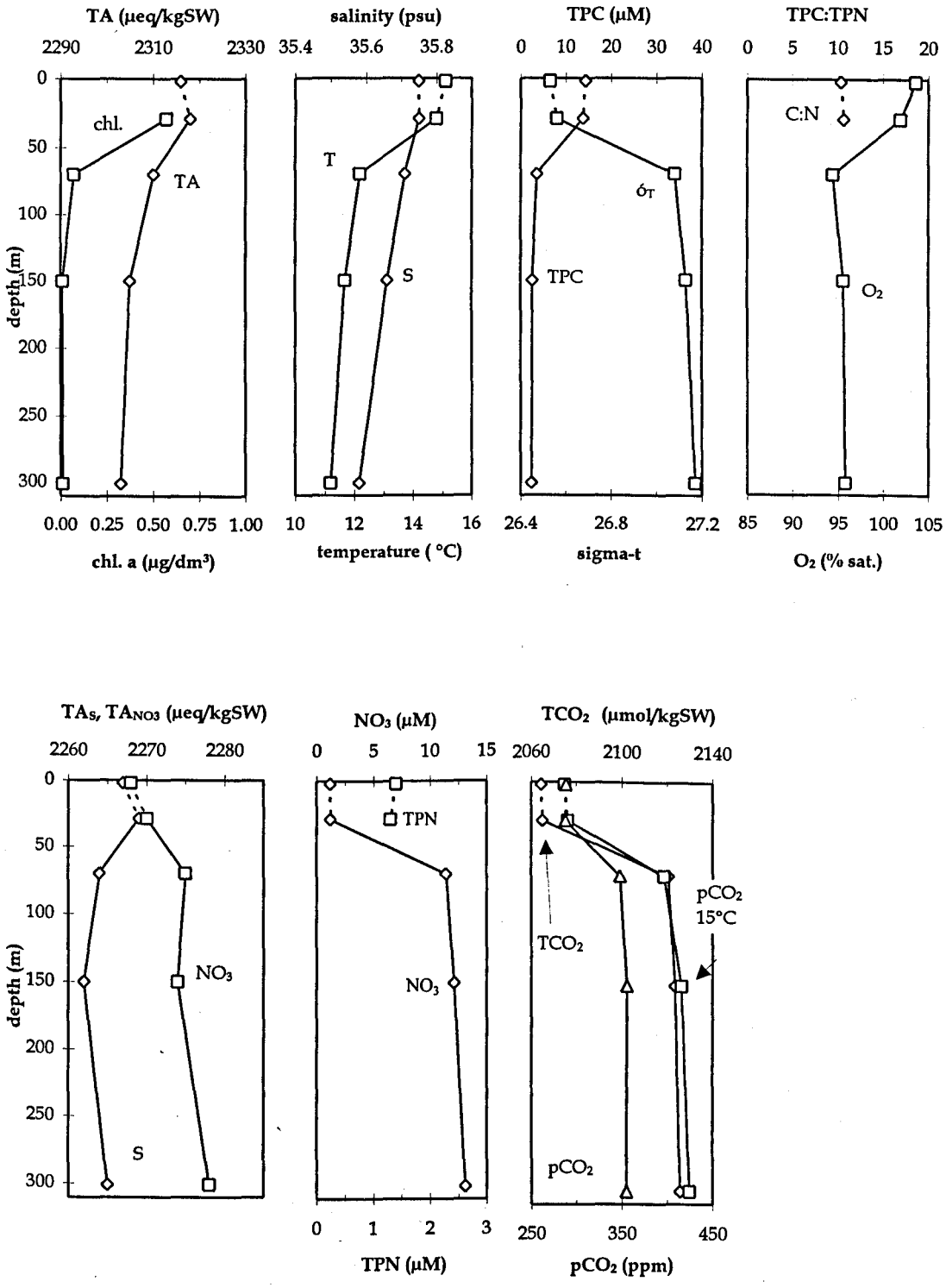

Figure 4.7: Vertical profiles of various in situ parameters obtained from station 4 along the northern transect at 48°11'N 16°20'W on 23 June 1990 as part of the final CTD survey of the BOFS Spring Bloom Experiment. Further parameters include pCO_2 at 15°C. TA, TA_S, and TA_{NO3} refer to photometric results. Broken lines indicate that results for certain sampling depths are missing.

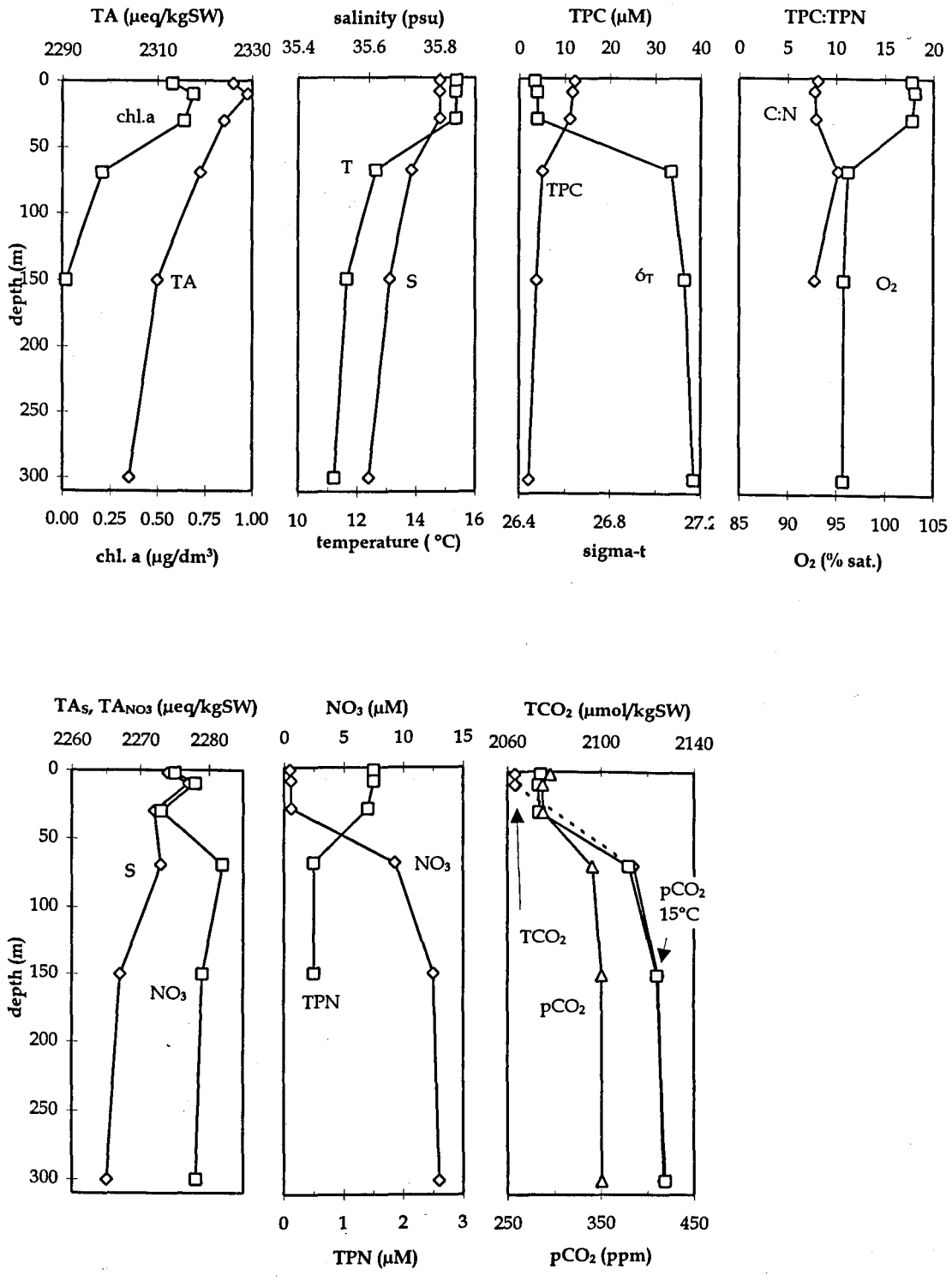

Figure 4.8: Vertical profiles of various in situ parameters obtained from station 6 along the southern transect at 47°04'N 15°50'W on 24 June 1990 as part of the final CTD survey of the BOFS Spring Bloom Experiment. Further parameters include pCO_2 at 15°C. TA, TA_S, and TA_{NO3} refer to photometric results. The broken line indicates that the result for one sampling depth is missing.

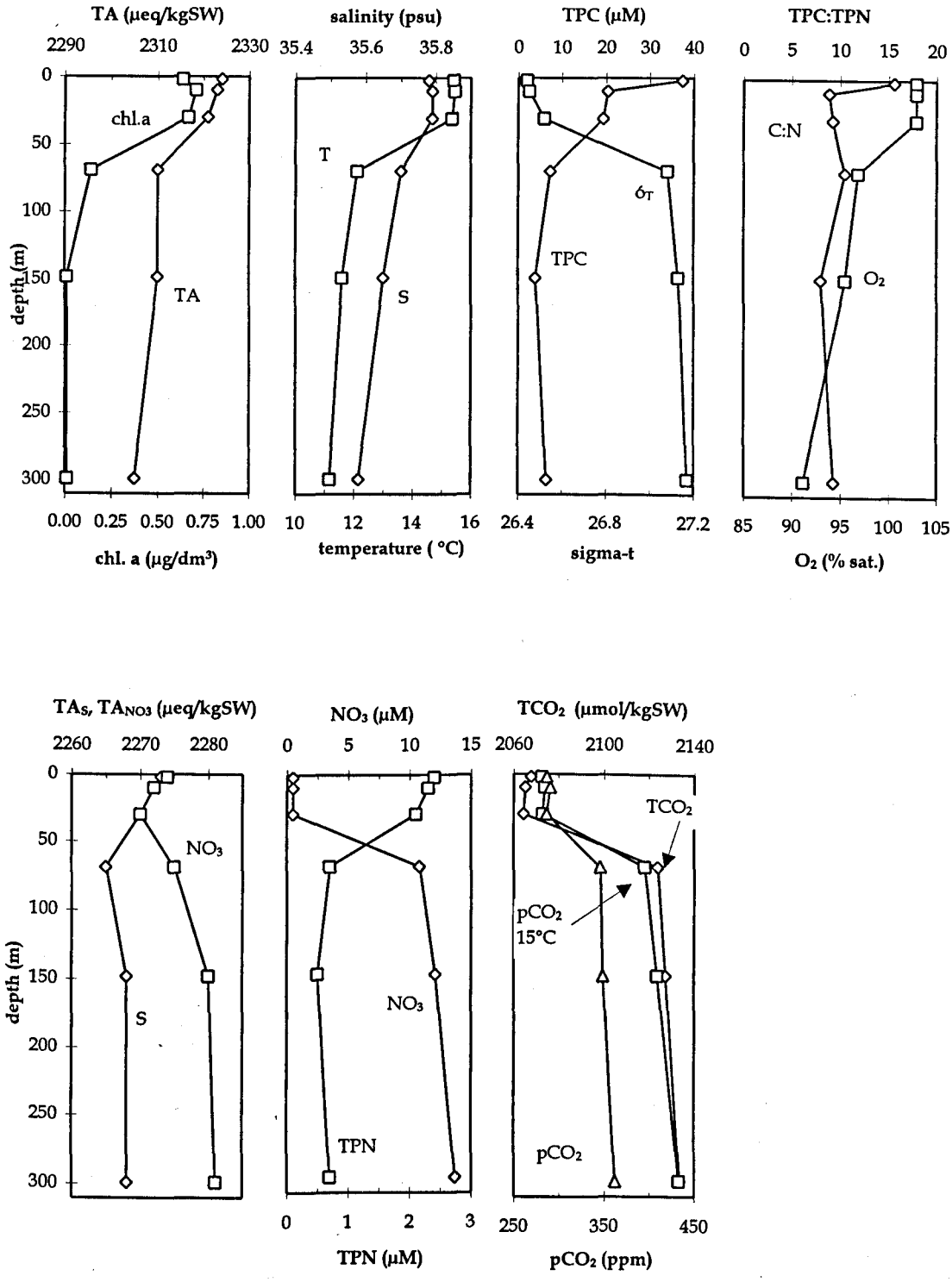

Figure 4.9: Vertical profiles of various in situ parameters obtained from station 7 along the southern transect at 46°57'N 16°02'W on 24 June 1990 as part of the final CTD survey of the BOFS Spring Bloom Experiment. Further parameters include pCO_2 at 15°C. TA, TA_S, and TA_{NO3} refer to photometric results.

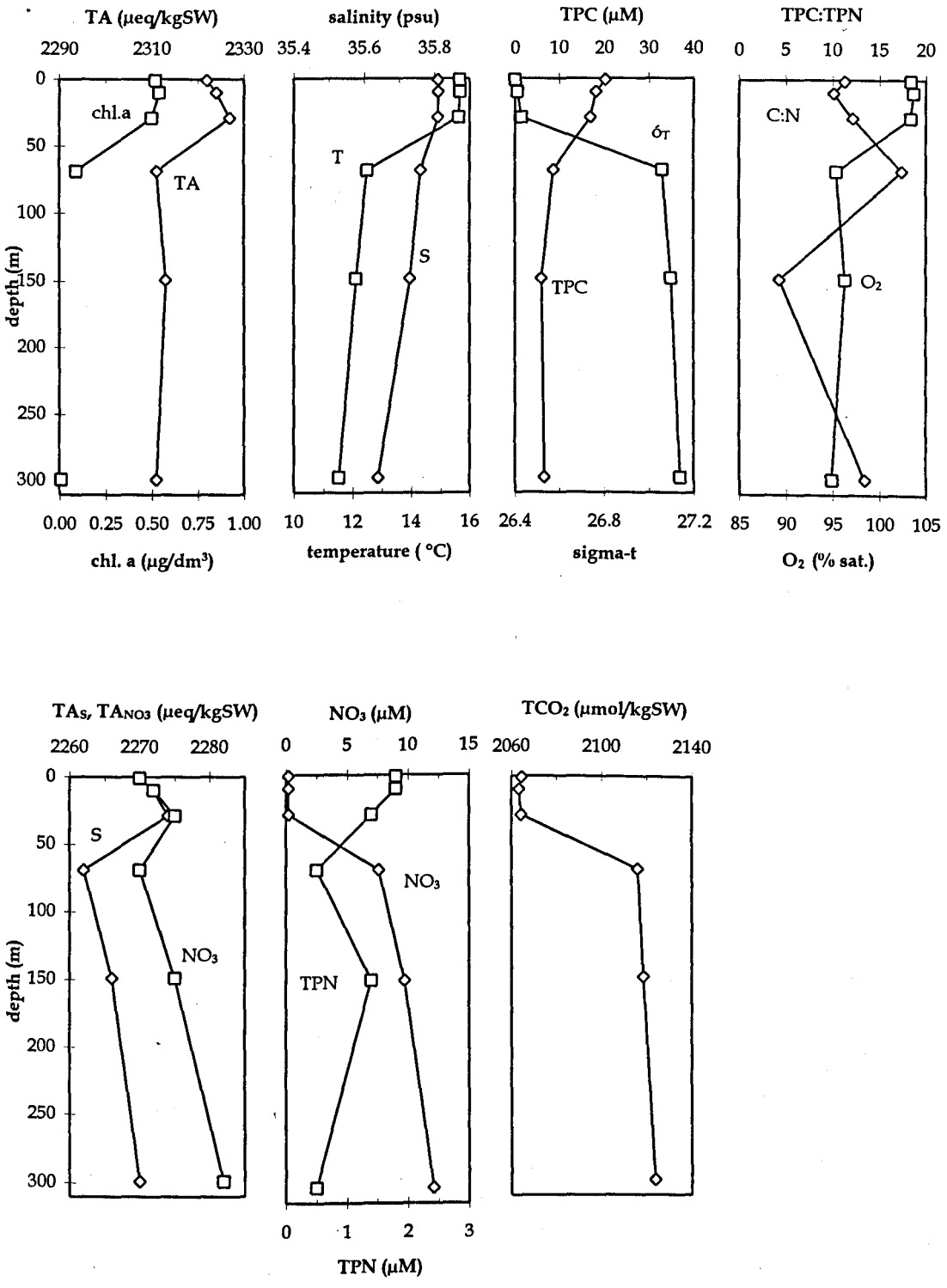

Figure 4.10: Vertical profiles of various in situ parameters obtained from station 8 along the southern transect at 46°50'N 16°12'W on 24 June 1990 as part of the final CTD survey of the BOFS Spring Bloom Experiment.
TA, TA_S, and TA_{NO3} refer to photometric results.

4.4.3.2. TA ranges within the SML

General results of TA within the SML are presented in table 4.1.a. Photometric TA averaged 2320 μeq $kgSW^{-1}$, covering a range of about 20 μeq $kgSW^{-1}$. Variations in salinity had contributed up to 6 μeq $kgSW^{-1}$ to this range. Since nitrate concentrations did not exceed 1.5 μM in the SML, it appeared that the effect of variations in nitrate uptake was negligible. The measured TA_{NO3} range suggests that variations in net calcification had led to a TA variation of 13 μeq $kgSW^{-1}$ in the study area. The standard deviation of the TA_{NO3} estimate was slightly larger than the precision of the method.

Results from the comparison of TA and derived parameters between the two transects, i.e. over a distance of one latitudinal degree or about 110 km, are shown in table 4.2.a. Total alkalinity was significantly higher along the southern transect by an average of 9 μeq $kgSW^{-1}$. The comparison of ($TA-TA_S$) and TA_{NO3} between transects suggests that this regional difference was caused by higher salinity and less net calcification along the southern transect. The effects of these two factors appeared to have a comparable impact on TA, i.e. about 4 μeq $kgSW^{-1}$ each, while any differences in nitrate uptake seemed to have a negligible effect on the regional difference in TA.

Figures 4.3 - 4.10 reveal that depth-related variations within the SML amounted to 7 μeq kg^{-1}. This was largely due to a tendency for TA to increase between the surface and 10 and/or 30 m. Also, surface TA increased by about 5 μeq kg^{-1} over a distance of 40 km towards the northeast. Similar trends in TA_S and TA_{NO3} imply that net calcification tended to be higher in the upper 2 to 3 m and towards the southwest of each transect.

Table 4.1: Ranges of TA and derived parameters (μeq $kgSW^{-1}$) observed in the SML around 47-48°N 16-17°W during the final CTD survey of the Spring Bloom Experiment conducted 22 - 24 June 1990. Data was obtained by (a) photometry, (b) potentiometry, and (c) calculation from pCO_2 and TCO_2.
Values marked in bold are used to discuss the effect of salinity (difference in range: TA-TA_S), nitrate utilization (difference in range: TA_S - TA_{NO3}), and net calcification (range of TA_{NO3}) on the observed ranges of TA.

	(a) photometry (n = 19)			(b) potentiometry (n = 19)			(c) calculation (n = 13)		
	TA	TA_S	TA_{NO3}	TA	TA_S	TA_{NO3}	TA	TA_S	TA_{NO3}
average	2320	2270	2271	2339	2290	2290	2370	2320	2321
s.d.(n-1)	5.1	3.2	3.0	4.1	5.7	6.0	2.6	2.1	2.4
range	19	13	13	16	20	21	8	6	8
difference (range)		**6**	**0**		**-4**	**-1**		**2**	**-2**

Table 4.2: Differences in TA and derived parameters (μeq $kgSW^{-1}$) observed in the SML between the northern (N) transect around 48°N 16.5°W and the southern (S) transect around 47°N 16°W during the final CTD survey of the Spring Bloom Experiment conducted 22 - 24 June 1990. Data was obtained by (a) photometry, (b) potentiometry, and (c) calculation from pCO_2 and TCO_2.
The value in brackets is the probability (P) obtained from a t-test to estimate the significance of the differences between transects.
The differences in results from 'S-N' refer to the effect of salinity (from TA-TA_S) and the effect of nitrate uptake (from TA_S-TA_{NO3}) on the observed difference in TA between the two transects. The 'S-N' value for TA_{NO3} represents the effect of net calcification.
A positive value implies that there was less calcification along the southern transect.

(a) photometry

		TA		TA_S		TA_{NO3}	
transect	n	mean	s.d.(n-1)	mean	s.d.(n-1)	mean	s.d.(n-1)
N	10	2315.7	2.5	2268.4	2.5	2269.7	2.4
S	9	2324.4	2.5	2272.7	2.2	2273.3	2.5
S-N		8.7 (<0.001)		4.3 (<0.01)		3.6 (<0.01)	
difference (S-N)			4.4		0.7		

(b) potentiometry

		TA		TA_S		TA_{NO3}	
transect	n	mean	s.d.(n-1)	mean	s.d.(n-1)	mean	s.d.(n-1)
N	10	2337.6	4.2	2293.3	4.5	2294.4	4.6
S	9	2324.4	3.4	2285.3	3.4	2285.7	3.4
S-N		-13.2 (n.s. at 0.05)		-8.0 (<0.001)		-8.7 (<0.001)	
difference (S-N)			-5.2		0.7		

(c) calculation

		TA		TA_S		TA_{NO3}	
transect	n	mean	s.d.(n-1)	mean	s.d.(n-1)	mean	s.d.(n-1)
N	7	2368.6	2.0	2320.3	2.1	2321.7	2.6
S	6	2372.3	1.4	2319.8	1.8	2320.2	1.9
S-N		3.7 (<0.01)		-0.5 (n.s. at 0.05)		-1.5 (n.s. at 0.05)	
difference (S-N)			4.2		1.0		

4.4.3.3. Correlations of TA with other parameters within the SML

Figure 4.11.a demonstrates significant positive relationships of TA with salinity and temperature and a significant negative relationship with nitrate concentration. No correlation was observed between TA and the concentration of chlorophyll a.

Relationships of TA_S with other parameters are presented in figure 4.12.a. The salinity corrections had led to an approximate halving of the slopes with temperature and nitrate concentration, but they were still clearly significant. The relationship with nitrate concentration indicates that TA_S decreased by about 5 μeq $kgSW^{-1}$ while nitrate increased by 1 μM. This suggests that more net calcification had occurred at sites where less nitrate had been taken up. Further, the relationship with temperature implies that this increased net calcification was more typical of colder waters. The relationship of TA_S with chlorophyll a was inconclusive. In figure 4.13.a the relationship of TA_{NO3} versus temperature of 3.5 suggests that calcification was increased by almost 2 μmol dm^{-3} in the water which was 1°C colder. Again, this apparent calcification effect could not be linked to concentrations of chlorophyll.

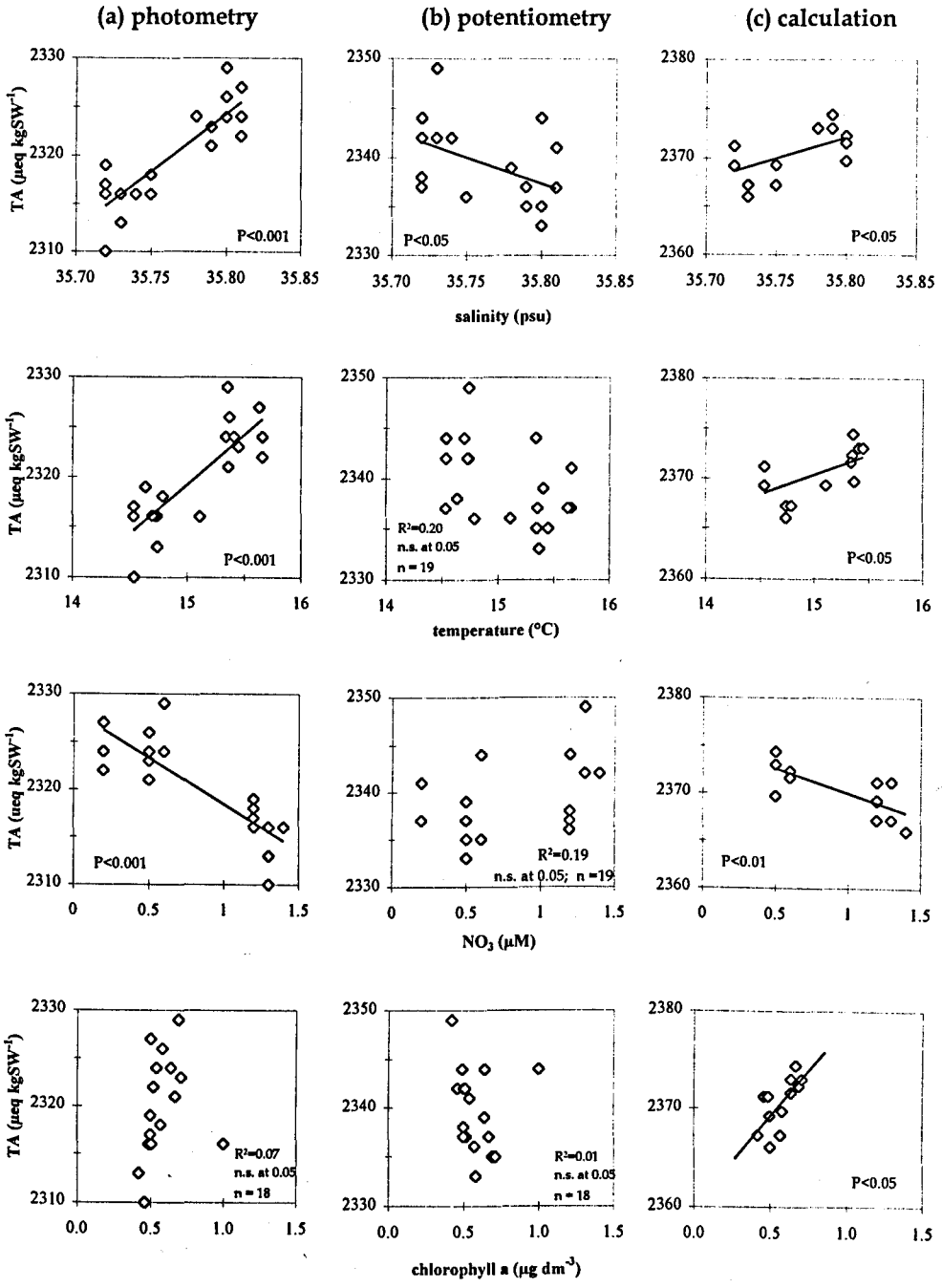

Figure 4.11: Results from linear least squares regression analyses to examine the relationships between TA and other parameters in the SML around 47-48°N 16-17°W during the final CTD survey of the Spring Bloom Experiment conducted 22 - 24 June 1990. Data for TA was obtained by (a) photometry, (b) potentiometry, and (c) calculation from pCO_2 and TCO_2. P refers to the slope of the regression line. Regression equations and additional statistics for significant relationships are:

photometric TA = 112 (± 16) sal. - 1965 (± 590.8); n = 19; R^2 = 0.76; $s.e._{regr}$ = 2.6;
potentiometric TA = -52 (± 23) sal. + 4200 (± 852.7); n = 19; R^2 = 0.22; $s.e._{regr}$ = 3.7;
calculated TA = 44 (± 18) sal. + 813 (± 666.0); n = 13; R^2 = 0.33; $s.e._{regr}$ = 2.2

photometric TA= 10.1 (± 1.7) temp. - 2168 (± 25.0); n = 19; R^2 = 0.68; $s.e._{regr}$ = 3.0;
calculated TA = 4.0 (± 1.7) temp. + 2310 (± 24.9); n = 13; R^2 = 0.35; $s.e._{regr}$ = 2.2

photometric TA = -9.8 (± 1.5) NO_3 - 2328 (± 1.4); n = 19; R^2 = 0.72; $s.e._{regr}$ = 2.8;
calculated TA = -5.1(± 1.3) NO_3 + 2375 (± 1.3); n = 13; R^2 = 0.58; $s.e._{regr}$ = 1.7

calculated TA = 18.8 (± 6.2) chl.a + 2360 (± 3.6); n= 12; R^2 = 0.48; $s.e._{regr}$ = 2.0

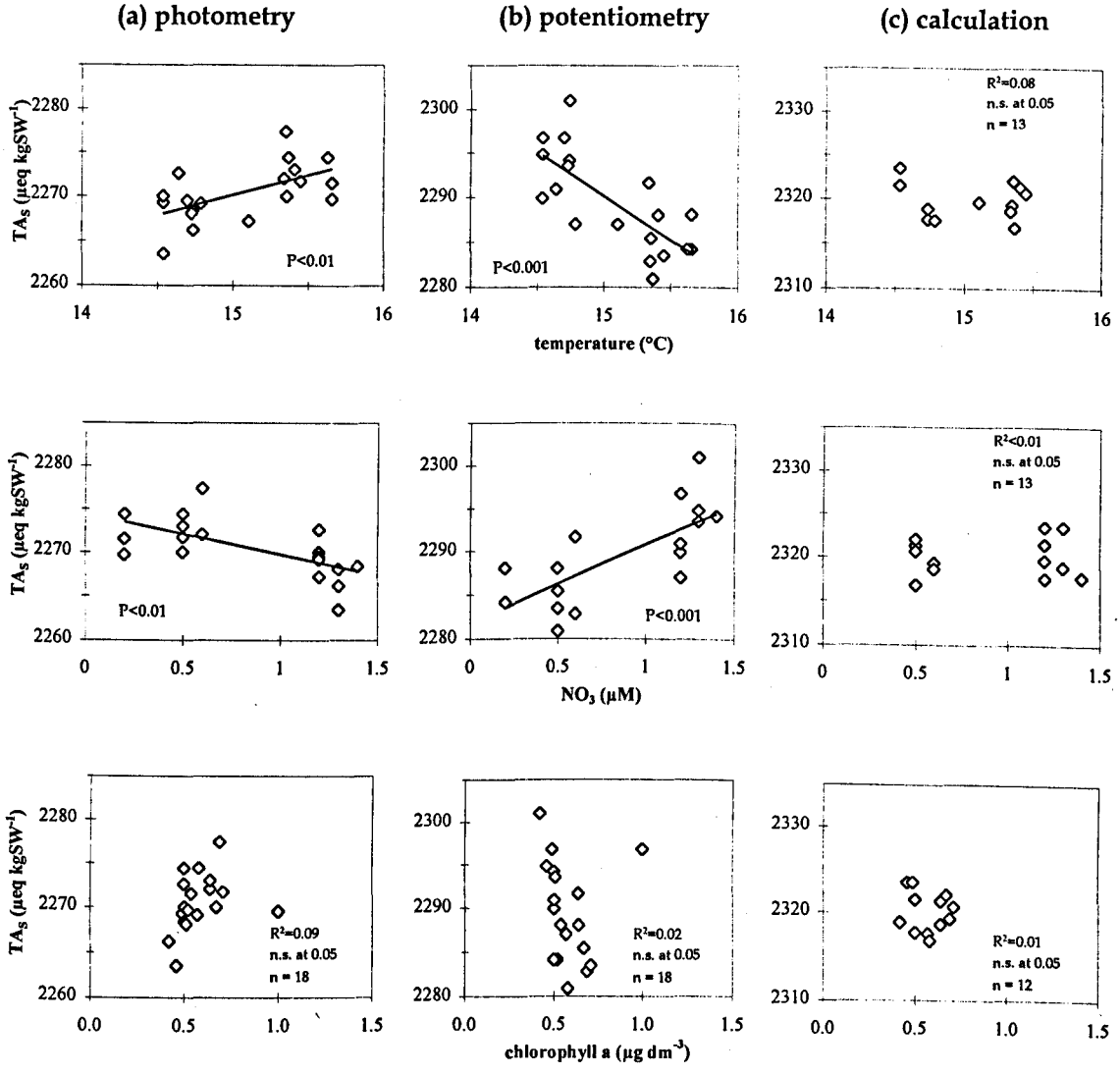

Figure 4.12: Results from linear least squares regression analyses to examine the relationships between TA_S and other parameters in the SML around 47-48°N 16-17°W during the final CTD survey of the Spring Bloom Experiment conducted 22 - 24 June 1990. Data for TA_S is based on (a) photometry, (b) potentiometry, and (c) calculation from pCO_2 and TCO_2. P refers to the slope of the regression line. Regression equations and additional statistics for the significant relationships are:

photometric TA_S = 4.5 (± 1.5) temp. - 2203 (± 22.8); n = 19; R^2 = 0.34; $s.e._{regr}$ = 2.7;
potentiometric TA_S = -9.8 (± 2.1) temp. + 2437 (± 32.5); n = 19; R^2 = 0.55; $s.e._{regr}$ = 3.8

photometric TA = -4.6 (± 1.4) NO_3 - 2274 (± 1.3); n = 19; R^2 = 0.41; $s.e._{regr}$ = 2.6;
potentiometric TA = 9.1 (± 2.1) NO_3 + 2282 (± 2.0); n = 19; R^2 = 0.52; $s.e._{regr}$ = 4.0

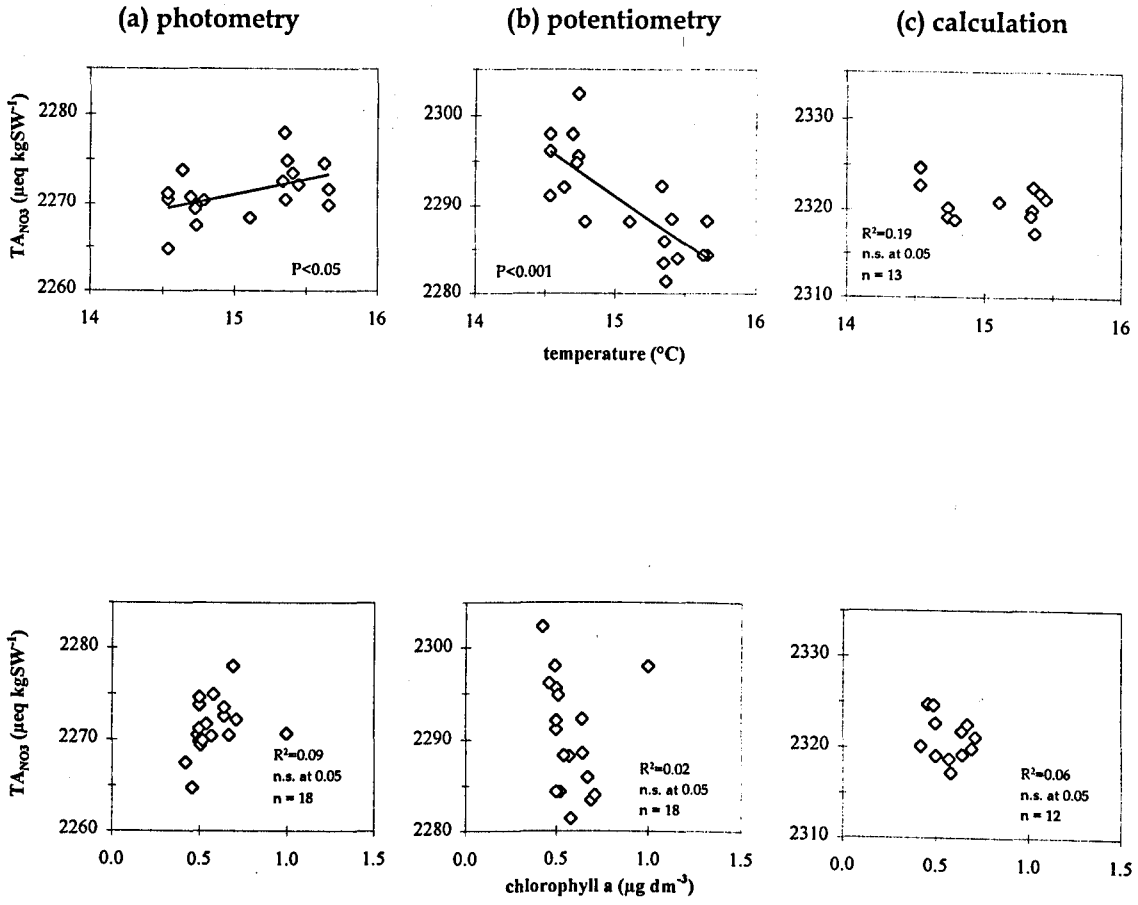

Figure 4.13: Results from linear least squares regression analyses to examine the relationships of TA_{NO3} with temperature and chlorophyll a in the SML around 47-48°N 16-17°W during the final CTD survey of the Spring Bloom Experiment conducted 22 - 24 June 1990. Data for TA_{NO3} is based on (a) photometry, (b) potentiometry, and (c) calculation from pCO_2 and TCO_2. P refers to the slope of the regression line. Regression equations and additional statistics for the significant relationships are:

photometric TA_{NO3} = 3.5 (± 1.49) temp. - 2219 (± 22.4); n = 19; R^2 = 0.24; $s.e._{regr}$ = 2.7;
potentiom. TA_{NO3} = -10.8 (± 2.17) temp. + 2453 (± 32.7); n = 19; R^2 = 0.59; $s.e._{regr}$ = 3.9

4.4.3.4 Estimates of POC:PIC net production

Results from the estimate of POC:PIC net production are shown in figure 4.14.a. They suggest that the absolute amount of net PIC production was less in samples where POC production was increased.

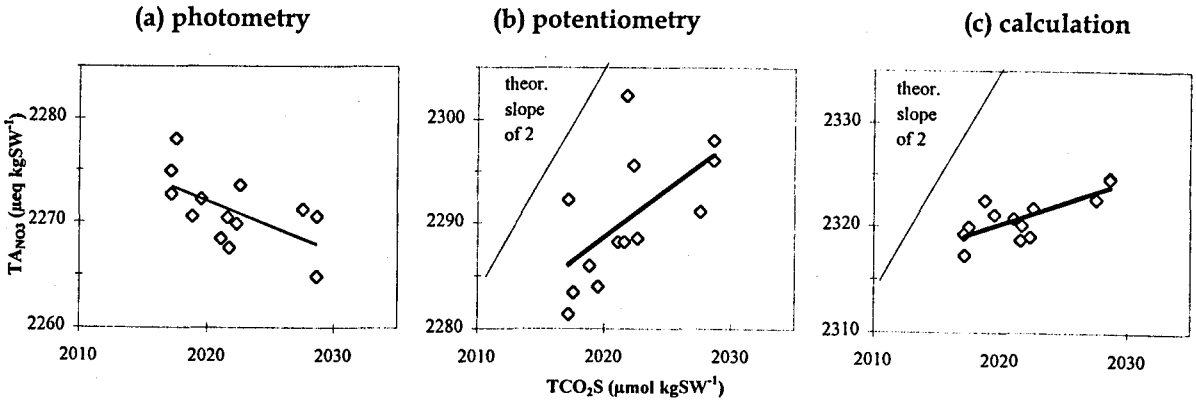

Figure 4.14: Estimates of POC:PIC net production ratios based on the relationship of TA_{NO3} against salinity-normalized (35 psu) TCO_2 using TA estimates from (a) photometry, (b) potentiometry, and (c) calculation from pCO_2 and TCO_2. Samples were collected from the SML during the 1990 Experiment in the Northeast Atlantic.

The relationships were determined using linear least squares regression analyses.
P refers to the slope of the regression line.
Regression equations and additional statistics are:

photom. TA = **-0.48** (± 0.20) TCO_2S+ 3239 (± 400); n = 13; R^2 = 0.35; s.e.regr. = 2.8; $P < 0.05$
potentiom. TA = **0.92** (± 0.36) TCO_2S - 422 (± 731); n = 13; R^2 = 0.37; s.e.regr. = 5.2; $P < 0.05$
calculated TA = **0.42** (± 0.10) TCO_2S + 1470 (± 211); n = 13; R^2 = 0.60; s.e.regr. = 1.5; $P < 0.01$

A slope of zero implies that an increase in photosynthesis was not accompanied by a proportional increase in calcification, and a slope of 2 means the reverse.
A negative slope suggests that the amount of absolute net calcification was less in samples where photosynthesis was higher.

Based on the above slope values, the resulting POC:PIC net production ratios are:

(a) photometry	(b) potentiometry	(c) calculation
-3.2	**1.2**	**3.8**

The negative value of the ratio above implies that POC net production was not accompanied by PIC net production but by net dissolution instead.

4.4.3.5. Variations of TA in sub-thermocline depth ranges

Mean TA values and their variations below the thermocline at (i) 70 to 150 m and (ii) 300 m are presented in table 4.3.a. Total alkalinity generally declined with depth. In the upper depth group TA averaged about 2310 μeq $kgSW^{-1}$, covering a range of about 15 μeq $kgSW^{-1}$. The mean and range of TA at 300 m fell to approximately 2305 and 10 μeq $kgSW^{-1}$, respectively. These latter values are based on only half the number of samples, so that the standard deviations ended up being the same for both depth ranges.

Variations of salinity had contributed to variability in TA within both depth groups by about 5 μeq $kgSW^{-1}$, whereas variations in nitrate metabolism had a negligible effect. Spatial changes in PIC precipitation/dissolution appeared to have led to TA variations of 12 μeq $kgSW^{-1}$ at 70 -150 m and half that at 300 m.

Figure 4.3 showed that at 150 and 300m TA tended to be a few microequivalents less at station 2 compared to neighbouring stations. Station 2 was also the site of intruding water of lower temperature, salinity, and higher nitrate concentration. This feature was almost removed in the TA_S profile and slightly reversed in the TA_{NO3} profile. Similarly, TA at station 8 stood out by being higher than those at other stations, which was matched by higher temperature and salinity at 150 and 300 m. This feature was not obvious in the TA_S and TA_{NO3} profiles at station 8.

Results from the comparison between the two transects are presented in table 4.4.a. It demonstrates that, at 70 and 150 m, TA was significantly higher along the southern transect, i.e. by 5 μeq $kgSW^{-1}$. It further indicates a tendency for slightly higher TA_{NO3} values along the southern transect, suggesting that these waters had at some stage been exposed to more PIC dissolution. Effects of differences in salinity and nitrate metabolism had a negligible impact on the difference of TA between transects.

Table 4.3: Ranges of TA and derived parameters (μeq $kgSW^{-1}$) observed at different depth ranges within the upper ocean around 47-48°N 16-17°W during the final CTD survey of the Spring Bloom Experiment conducted 22 - 24 June 1990. Data was obtained by (a) photometry, (b) potentiometry, and (c) calculation from pCO_2 and TCO_2.
Values marked in bold are used to discuss the effect of salinity (difference in range: $TA-TA_S$), nitrate metabolism (difference in range: $TA_S - TA_{NO3}$), and $CaCO_3$ precipitation/ dissolution (range of TA_{NO3}) on the observed variability of TA.

(i) 70 - 150 m:

	(a) photometry (n = 14)			(b) potentiometry (n = 13)			(c) calculation (n = 10)		
	TA	TA_S	TA_{NO3}	TA	TA_S	TA_{NO3}	TA	TA_S	TA_{NO3}
average	2309	2265	2275	2328	2284	2295	2359	2314	2325
s.d.(n-1)	3.7	2.9	3.2	5.6	5.7	6.0	3.2	2.7	2.9
range	15	11	12	19	17	19	11	9	9
difference (range)		**4**	**-1**		**2**	**-2**		**2**	**0**

(ii) 300 m:

	(a) photometry (n = 7)			(b) potentiometry (n = 7)			(c) calculation (n = 5)		
	TA	TA_S	TA_{NO3}	TA	TA_S	TA_{NO3}	TA	TA_S	TA_{NO3}
average	2304	2266	2279	2323	2285	2297	2352	2315	2327
s.d.(n-1)	3.8	2.4	2.1	4.9	5.7	5.7	2.3	2.4	2.1
range	12	7	6	14	15	13	5	6	5
difference (range)		**5**	**1**		**-1**	**2**		**-1**	**1**

Table 4.4: Differences in TA and derived parameters (μeq $kgSW^{-1}$) observed below the thermocline at 70 and 150 m between the northern (N) transect around 48°N 16.5°W and the southern (S) transect around 47°N 16°W during the final CTD survey of the Spring Bloom Experiment conducted 22 - 24 June 1990.
Data was obtained by (a) photometry, (b) potentiometry, and
(c) calculation from pCO_2 and TCO_2.
The value in brackets is the probability (P) obtained from t-tests to estimate the significance of the differences between transects.
The differences in results from 'S-N' refer to the effect of salinity (from $TA-TA_S$) and the effect of nitrate uptake (from TA_S-TA_{NO3}) on the observed difference in TA between the two transects. The 'S-N' value for TA_{NO3} quantifies the net effect of $CaCO_3$ dissolution. A positive value implies that there was more dissolution along the southern transect.

(a) photometry

		TA		TA_S		TA_{NO3}	
transect	n	mean	s.d.(n-1)	mean	s.d.(n-1)	mean	s.d.(n-1)
N	8	2307.3	2.0	2263.5	1.1	2274.4	1.7
S	6	2312.2	3.5	2266.8	3.7	2276.8	4.4
S-N		4.9 (<0.01)		3.3 (n.s. at 0.05)		2.4 (n.s. at 0.05)	
difference (S-N)			1.6		0.9		

(b) potentiometry

		TA		TA_S		TA_{NO3}	
transect	n	mean	s.d.(n-1)	mean	s.d.(n-1)	mean	s.d.(n-1)
N	8	2329.4	6.9	2285.4	6.7	2296.4	6.7
S	5	2327.0	2.6	2281.6	2.4	2292.0	3.9
S-N		-2.4 (n.s. at 0.05)		-3.8 (n.s. at 0.05)		-4.4 (n.s. at 0.05)	
difference (S-N)			1.4		0.6		

(c) calculation

		TA		TA_S		TA_{NO3}	
transect	n	mean	s.d.(n-1)	mean	s.d.(n-1)	mean	s.d.(n-1)
N	6	2357.8	3.3	2313.2	3.3	2324.0	2.8
S	4	2360.0	2.9	2314.5	2.4	2326.0	3.2
S-N		2.2 (n.s. at 0.05)		1.3 (n.s. at 0.05)		2.0 (n.s. at 0.05)	
difference (S-N)			0.2		-0.7		

4.4.3.6. Changes in TA across the thermocline

Estimates of TA changes across the seasonal thermocline are presented in table 4.5.a. Values of TA and TA_S tended to be elevated in the SML by about 11 and 6 μeq $kgSW^{-1}$, while TA_{NO3} was reduced by about 5 μeq $kgSW^{-1}$. This implies that the increase in TA by 5 μeq $kgSW^{-1}$ due to evaporation was counterbalanced by the effect of calcification. The major cause for the elevation in TA appeared to be the uptake of nitrate in the SML, which amounted to 10 μeq $kgSW^{-1}$. The change in TA across the thermocline was slightly higher by about 4 μeq $kgSW^{-1}$ along the southern transect, whereas there were no significant differences with respect to TA_S and TA_{NO3}. Consequently, the salinity effect tended to be slightly greater along the southern transect by about 3 μeq $kgSW^{-1}$, while the impact of nitrate uptake and calcification did not seem to differ significantly between transects.

The above results suggest that since the onset of stratification the effect of evaporation and net calcification on TA in the SML were of similar magnitude, i.e. about 5 μeq $kgSW^{-1}$, but of opposite effects. By leading to a TA increase of about 10 μeq $kgSW^{-1}$, nitrate uptake seemed to be the dominant factor influencing the changes in TA which had occurred in the study area between early spring and late June. Evaporation was slightly more important in warmer waters, i.e. along the southern transect.

Table 4.5: Changes in TA and derived parameters (μeq $kgSW^{-1}$) observed across the thermocline during the final CTD survey of the Spring Bloom Experiment conducted 22 - 24 June 1990.
The changes were calculated from the difference in results between samples from the SML (1-30 m) and those from below the thermocline (70 and 150 m). The impact of variations in salinity, nitrate uptake, and net calcification were estimated from differences between TA, TA_S, and TA_{NO3} (see section 4.4.2.2 for more detail).
Positive results of the salinity and nitrate impact would imply that evaporation and nitrate uptake, respectively, had increased TA, while negative values of TA_{NO3} are assumed to reflect the decrease of TA in the SML due to net calcification.
The sample number, n, represents the number of CTD stations.

Results from the northern (N) transect around 48°N 16.5°W and the southern (S) transect around 47°N 16°W are also investigated. Positive values of the difference (S - N) would imply that changes in TA or derived parameters across the thermocline were bigger along the southern transect.

Data was obtained by (a) photometry, (b) potentiometry, and (c) calculation from pCO_2 and TCO_2.

(a) photometry

		change across thermocline:						impact on TA change across thermocline from changes in:			
		TA		TA_S		TA_{NO3}		salinity		nitrate concentration	
transects	n	mean	s.d.(n-1)	mean	s.d.(n-1)	mean	s.d.(n-1)	mean	s.d.(n-1)	mean	s.d.(n-1)
both	7	10.2	2.2	5.6	1.7	-4.3	2.1	4.6	1.9	9.9	1.2
N	4	8.7	1.6	5.2	1.9	-4.7	1.8	3.5	1.2	9.9	1.4
S	3	12.3	0.4	6.1	1.6	-3.8	2.9	6.2	1.6	9.9	1.3
S-N		3.6		0.9		0.9		2.7		0.0	

(b) potentiometry

		change across thermocline:						impact on TA change across thermocline from changes in:			
		TA		TA_S		TA_{NO3}		salinity		nitrate concentration	
transects	n	mean	s.d.(n-1)	mean	s.d.(n-1)	mean	s.d.(n-1)	mean	s.d.(n-1)	mean	s.d.(n-1)
both	7	10.9	3.3	6.1	4.1	-3.6	4.3	4.7	1.9	9.8	1.5
N	4	11.2	4.6	7.4	4.9	-2.5	4.7	3.8	1.2	9.9	1.4
S	3	10.4	0.4	4.4	2.2	-5.2	4.1	6.0	2.2	9.6	1.9
S-N		-0.8		-3.0		-2.7		2.2		-0.3	

(c) calculation

		change across thermocline:						impact on TA change across thermocline from changes in:			
		TA		TA_S		TA_{NO3}		salinity		nitrate concentration	
transects	n	mean	s.d.(n-1)	mean	s.d.(n-1)	mean	s.d.(n-1)	mean	s.d.(n-1)	mean	s.d.(n-1)
both	5	11.5	1.7	6.1	1.8	-4.1	2.7	5.4	2.0	10.1	1.3
N	3	10.8	2.0	6.7	2.2	-3.0	3.1	4.1	1.2	9.8	1.7
S	2	12.5	0.7	5.0	0.7	-5.6	1.2	7.4	0.1	10.6	0.4
S-N		1.6		-1.7		-2.6		3.3		0.9	

4.4.3.7. TA at 500 m and greater depths

Results for TA and other parameters from the two deep casts are shown in figures 4.15 and 4.16. Although samples were collected at 4000 m and below, spectrophotometric TA results were not obtained for these samples due to methodological problems described and discussed in chapter 2. For these reasons the description of the results includes observations of TA obtained by potentiometry and the calculation method, which generally correlated well at these greater depths.

The little data available from 500 m is not conclusive. Potentiometric TA matched the respective range observed at 300 m, while calculated TA decreased between 300 and 500 m. Between 500 and 1000 m TA generally did not differ much, whereas a decrease of at least 20 μeq $kgSW^{-1}$ was observed between 1000 and 1500 m. Profiles of TA_S and TA_{NO3} suggest that this reduction was largely due to differences in salinity between the two depths. A further common feature was the increase in TA and TA_{NO3} below the 1500 or 2000 m depth range, which suggests increasing PIC dissolution at greater depths. Apart from the above commonalities, TA and derived parmeters from the 1000 to 1500 m depth range tended to be higher at the southern station.

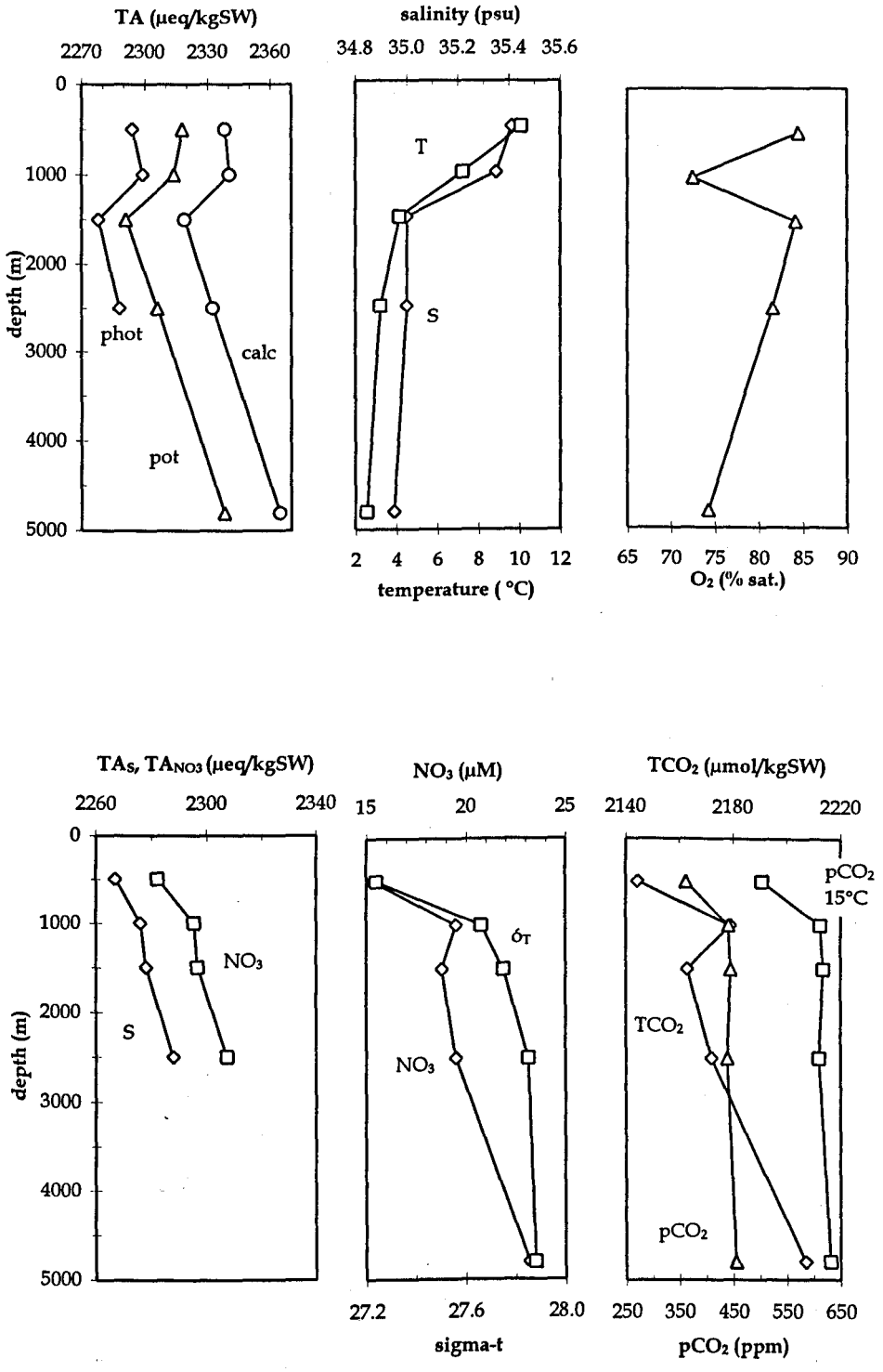

Figure 4.15: Vertical profiles of various in situ parameters obtained from station 5 along the northern transect at 48°17'N 16°07'W on 23 June 1990 as part of the final CTD survey of hte BOFS Spring Bloom Experiment. Further parameters include pCO_2 at 15°C. Results for TA originate from photometric (phot), potentiometric (pot), and calculated (calc) determinations. TA_S and TA_{NO3} have been derived from photometric TA.

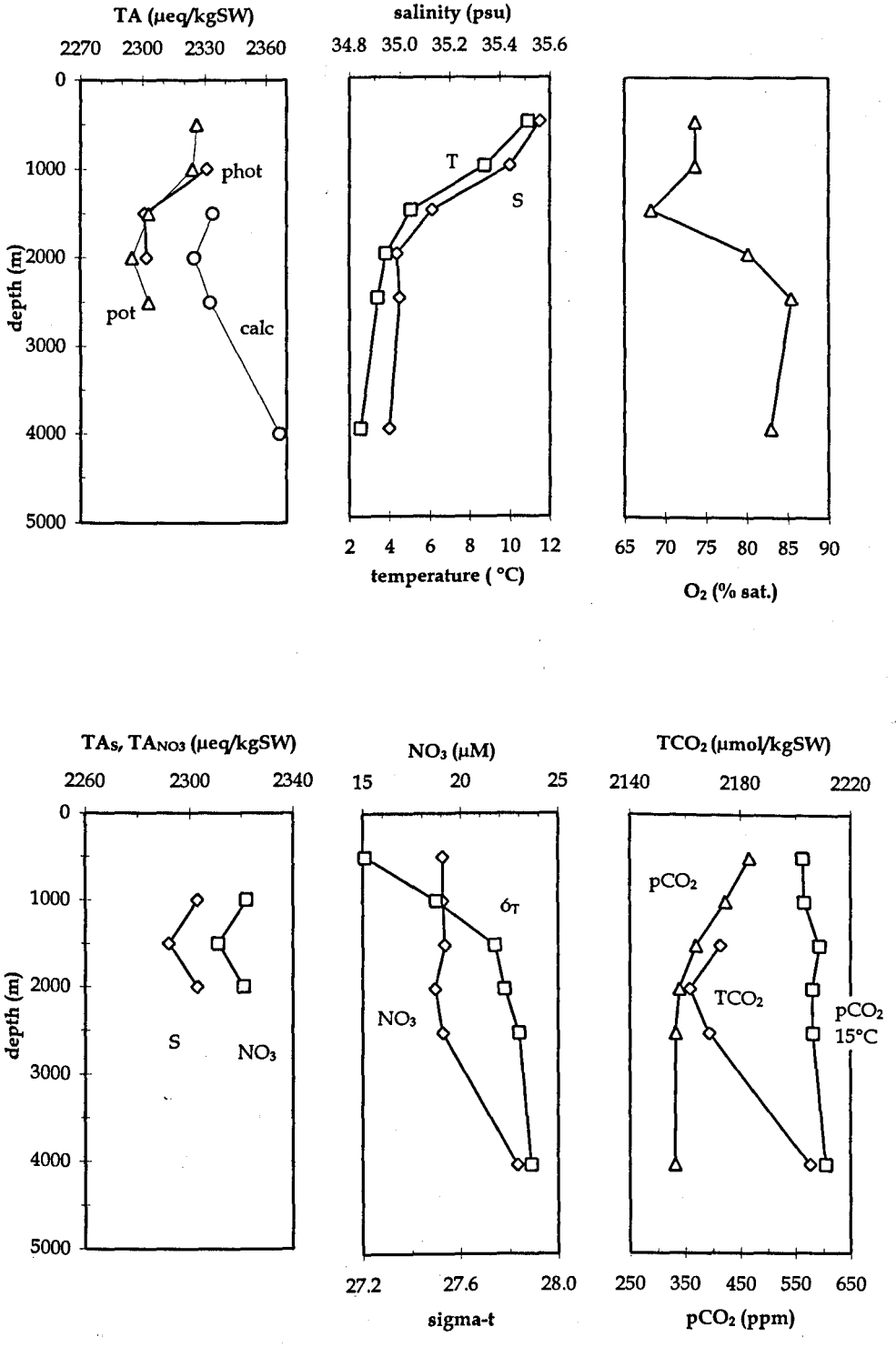

Figure 4.16: Vertical profiles of various in situ parameters obtained from station 9 along the southern transect at 46°42'N 16°26'W on 24 June 1990 as part of the final CTD survey of hte BOFS Spring Bloom Experiment. Further parameters include pCO_2 at 15°C. Results for TA originate from photometric (phot), potentiometric (pot), and calculated (calc) determinations. TAs and TA_{NO3} have been derived from photometric TA.

4.4.3.8. Comparison of TA results from different methods

The general outcome of the intercomparison between the various techniques used for the analysis of the seawater carbonate system has already been presented and discussed in chapter 2. The chief finding was that photometric results were on average about 20 (± 9) and 50 (± 8) μeq $kgSW^{-1}$ lower than the respective potentiometric and calculated TA results. Further, data and observations during the analyses suggest that the discrepancies between the photometric and the other two methods were reduced in samples from deep casts, i.e. from depths exceeding 300 m. This may have been due to methodological problems associated with the photometric technique during that particular cruise. For data from the upper 300 m, the relationship between photometric and calculated TA was the best, while that between photometric and potentiometric TA was poor, and curiously, the relationship between the latter pair was inverse for samples limited to the SML.

An overview of the TA profiles along the transects from all three methods is provided in figure 4.17. Calculated TA exhibited the least and smoothest decrease in TA between the surface and 300 m, while potentiometric TA covered the largest range with the 'noisiest' profile. The more detailed comparison below is conducted separately for different depth ranges.

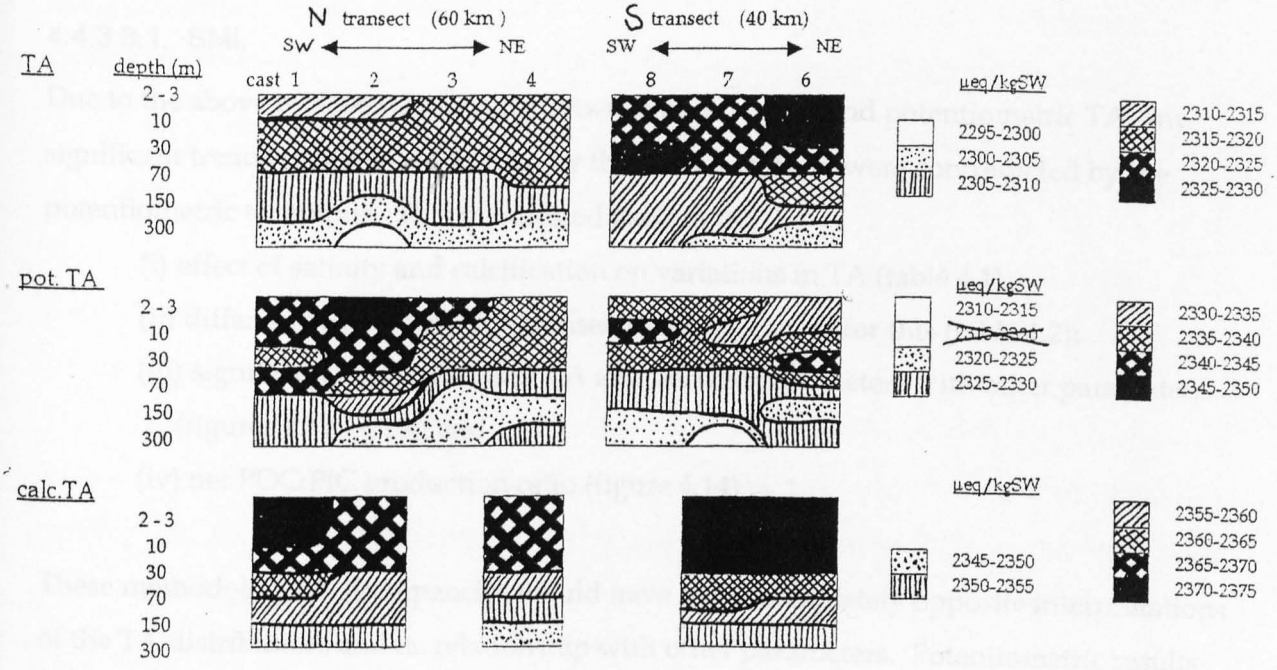

Figure 4.17: Overview of results obtained from seven shallow CTD casts along the northern (N) transect around 48°N 16.5°W and the southern (S) transect around 47°N 16°W on 22-24 June 1990 as part of the final CTD survey of the BOFS Spring Bloom Experiment. Numbers refer to CTD stations. More exact positions of the casts are given in figures 4.4.- 4.10. 'TA' refers to photometric results, whereas pot. TA' was obtained by potentiometry and 'calc TA' by calculation from pCO_2 and TCO_2.

4.4.3.8.1. SML

Due to the above inverse relationship between photometric and potentiometric TA, any significant trends that were picked up by the former method were contradicted by the potentiometric technique. This manifested itself in the

(i) effect of salinity and calcification on variations in TA (table 4.1);

(ii) difference in TA between transects and the causes for this (table 4.2);

(iii) significant relationships of TA and derived parameters with other parameters (figures 4.11 - 4.13); and

(iv) net POC:PIC production ratio (figure 4.14).

These methodological discrepancies would have led to completely opposite interpretations of the TA distribution, and its relationship with other parameters. Potentiometric results also suggested that the relative amount of PIC production was much greater than estimated by photometry, i.e. a POC: PIC net production ratio of about 1.2 was established by potentiometry. The only agreements between the two methods existed with respect to the absence of a relationship with chlorophyll a concentrations, and the negligible impact of nitrate variations on the TA range.

A true comparison between photometric and calculated TA was not possible as there was less data available from the calculation method. The general trends observed by the calculation method seemed to lie in between those observed by the other two techniques. However, the calculation method tended to confirm the general trends observed by the photometric method with respect to

(i) higher TA along the southern transect due to increased salinity (table 4.2); and

(ii) correlations of TA with other parameters (figures 4.11 - 4.13).

The calculation method did not confirm the trends observed by photometric TA_{NO3}. This resulted in a different estimate of the POC:PIC net production ratio of 3.8, which implies that the relative importance of net calcification was much greater than observed by photometry and much lower than observed by potentiometry (figure 4.14).

Small-scale features observed by the photometric method such as the tendency for higher TA in samples from 2-3 m relative to 10 or 30 m and the increase in TA towards the northeast were not observed by either of the other two methods (figure 4.17).

4.4.3.8.2. Sub-thermocline depths (70 - 300 m)

Since the average offsets between methods did not differ between depth groups (tables 4.2 and 4.3), the photometric depth profile from between the SML and 300 m was generally corroborated by the other two methods, i.e. TA decreased similarly with depth. However, the differences between transects which were observed by the photometric method were contradicted by the potentiometric method or not found to be significant by the calculation method (table 4.4). Furthermore, the special photometric features in TA at stations 2 and 8 which could be related to hydrographic features were either not observed or there was not enough data available to draw conclusions (figure 4.17).

4.4.3.8.3. Changes in TA across the thermocline

The photometric estimates of TA changes across the thermocline were largely confirmed by the other two techniques. The same applied to the estimates of the nitrate and calcification effects on these vertical changes in TA (table 4.5).

4.4.3.8.4. 500 m and greater depths

Potentiometric and calculated TA showed similar changes with depth, i.e. the discrepancies were constant between the two methods (figures 4.15; 4.16). The relationship between photometric TA and that of the other two methods appeared to be more or less reduced at these depths. It is not clear whether this was typical for the photometric method or whether this phenomenon was due to problems with the photometric analyses of deep samples during that particular 1990 cruise.

4.4.3.8.5. Summary

The agreement between methods was not good with respect to the horizontal distribution of TA within the SML. This also applied to results from the sub-thermocline layer. However,

the agreement between all three methods was good for seasonal estimates of TA and its contributing factors within the thermocline.

4.4.4. DISCUSSION

4.4.4.1. Variations in hydrography and biology

Considerable spatial and temporal variability in hydrography was observed during the Experiment in 1990. This included marked changes over the course of a few days between the final SeaSoar and CTD surveys which altered the characteristics of the water masses and small-scale features above as well as below the thermocline.

With respect to biology, the waters generally represented post-bloom conditions typical for late June in these latitudes. This was manifested in relatively low chlorophyll a and nitrate concentrations. However, some of the higher chlorophyll values were observed at the surface which may have been triggered by slightly increased nitrate concentrations and improved weather conditions following the preceding storm event.

4.4.4.2. Spatial variations of TA within the SML

Before discussing the photometric TA results from this Experiment in 1990, it has to be borne in mind that due to logistic reasons, no attempt was made to filter the samples prior to the titration. Cell counts of coccolithophorids in the study area of the 1990 Experiment which were carried out up until about one week before the final CTD survey implied that the effect of PIC interference on the outcome of the photometric TA titrations would have been insignificant. On this basis it was generally assumed that interference from PIC had no significant effect on the accuracy of the TA results in 1990. However, without direct information on the abundance of coccolithophorids in the samples from the final CTD survey, the accuracy of the spatial variations of TA and the conclusions regarding calcification could be put into question. As results in section 2.3.5 have shown, the possible presence of PIC in any sample during the titration would have led to overestimates of TA and therefore underestimates of recent net calcification by an amount equivalent to that of the PIC. The following discussion is generally based on the assumption that the amount of PIC in samples collected during the final CTD survey was negligible. If a small amount of PIC was present in the samples, the qualitative conclusions with respect to seasonal and

regional variations in TA and net calcification may still be valid, since the PIC signature of less recent calcification may have been lost from the body of sampled water by sinking or herbivory.

During the study in 1990, the average TA within the SML was 2320 μeq $kgSW^{-1}$ and the general range amounted to about 20 μeq $kgSW^{-1}$. Variations in the effect of nitrate uptake generally appeared to be negligible within the SML due to the generally low concentrations of nitrate. Errors of the nitrate uptake estimates are discussed in section 5.4.4.4.2. According to salinity corrections and the range of TA_{NO3}, about one third of the TA variation was due to hydrographic variability, and the remaining 13 μeq $kgSW^{-1}$ seemed to be due to variations in net calcification. However, this estimate of 6.5 μmol dm^{-3} appears large considering the low abundance of coccolithophorids observed in surface waters all throughout the time-series study. This estimate may well have been an overestimate due to possible variations in pre-formed TA_{NO3} and the error in the TA method. For example, preformed values as taken from the 70 to 150 m depth range varied by 12 μeq $kgSW^{-1}$, although there may, in turn, be other plausible reasons for such variability in the sub-thermocline estimates, which are discussed in section 5.4.4.9. The imprecision of the TA method may have accounted for a range of about 5 μeq $kgSW^{-1}$.

The link between hydrography and TA was established by positive correlations of TA and related parameters with salinity and temperature. The relationship with salinity fitted into the generally observed trend for the North Atlantic during the TTO Expedition (Brewer et al., 1986; figure 3.4). A clear link between TA and biology could not be established. The general absence of any correlation between TA or derived parameters with chlorophyll a concentration does however not necessarily mean that biological influences on TA were insignificant. There are several possible reasons for this, e.g.

(i) the effect of nitrate utilization by phytoplankton may be cancelled out by net calcification;
(ii) the ratio of chlorophyll production to nitrate uptake may vary;
(iii) other biological exchange processes may alter TA significantly; and
(iv) unless sampling takes place at the beginning of a bloom, concentrations of particulates in a sample do not necessarily reflect the amount of original production due to possible loss or gain from sinking or herbivory.

The negative correlation of TA or TA_S with nitrate concentration may be interpreted to reflect the TA increase that occurs when nitrate is utilized by phytoplankton. However, due to uncertainties regarding preformed nitrate values, this relationship does not provide conclusive evidence. The uncertainties regarding preformed nitrate values are discussed further in section 5.4.4.4.2.

The comparison of results from the two transects revealed that TA was about 10 $\mu eq\ kgSW^{-1}$ lower along the colder surface waters of the northern transect due to the lower salinities, more net calcification, and slightly lower preformed TA_{NO3} values there. While the latter factor, again, is not conclusive, increased calcification has generally been associated with more northern and colder waters in the Northeast Atlantic (Aiken & Bellan, 1990).

Small-scale features in TA included the reduction by a few microequivalents between the surface and 10 or 30 m samples, as well as the increase in surface TA along the transects towards the northeast. These features were not recorded by the other two TA techniques. The trends are not based on many samples, and they were not obviously mirrored in any other available parameter. Consequently, these photometric results may

(i) be simply a consequence of the imprecision of the photometric method and therefore coincidental;

(ii) reflect the outcome of a biological or physico-chemical process limited to the surface which the other two TA methods would not have been adequate enough to pick up; or

(iii) reflect some systematic error in the photometric or the other two methods.

Since the above features were also observed in the TA_{NO3} profiles, this could suggest that net calcification was greater in the surface and in the southwest by up to 3 $\mu mol\ kg^{-1}$. Such lateral variations in net calcification of this extent over a distance of 60 km have been observed further north during the 1991 Study, which also revealed depth-related variations of calcification rates within the upper 35 m (Fernandez et al., 1993). With respect to systematic errors in the TA methods, it needs to be born in mind that none of the samples were filtered before their analyses. This implies that any PIC with its varying concentrations, shapes and coatings may have increased the results of the different TA methods depending upon the extent of PIC dissolution during the different acidification

procedures and the theoretical data analysis. The photometric titration set up only operated at the more acidic end of the titration curve, while the potentiometric method also covered the higher pH range. Since the photometric titration took at least as long as the potentiometric one, any PIC would have been exposed much longer to high concentrations of protons. Consequently, the photometric method would have been the more likely method to overestimate TA in the presence of liths. This possible inaccuracy of the photometric method would only be significant and noticeable in the SML where sufficiently high concentrations of PIC can be measured. These may vary with station and depth, depending upon the original growth of the coccolithophorid species and the subsequent fate of the attached and detached liths. With respect to potential errors in calculated TA data, it is not straightforward to evaluate the effect of the presence of liths in the samples. The acidification process applied in the determination of TCO_2 involves much stronger acidification, much shorter exposure time, and final purging of the sample with an inert carrier gas. Without appropriate standards for TA and parallel information on the concentrations of PIC in the samples, it remains unresolved whether these features recorded by the photometric technique were actually real.

In the above discussion of TA variations within the SML, the focus was set on the photometric results. Due to a generally negative correlation between photometric and potentiometric results, a discussion of results by the latter method would obviously have altered the outcome of the interpretation considerably. It remains unresolved why this relative discrepancy emerged. Although not conclusive, it is encouraging that in many cases the calculated results were supportive of the photometric results, e.g. the positive correlations of TA with salinity and temperature, the negative relationship of TA with nitrate concentration, and the general trends of TA between transects. Furthermore, these photometric TA trends fitted into the existing picture of the hydrography of the Northeast Atlantic, i.e. it corroborated the generally positive relationship between TA and salinity observed during TTO by Brewer et al. (1986) (figure 3.4). Also, a negative relationship of TA_S with nitrate concentration indicates that TA changes due to phytoplankton growth were predominantly governed by nitrate uptake rather than net calcification. This ties in with the finding that calcification is relatively unimportant in this part of the Northeast Atlantic at this time of year.

4.4.4.3. Spatial variations in TA below the thermocline

Below the thermocline TA generally decreased with depth down to 300 m. In the 70 to 150m depth range TA was about 10 μeq $kgSW^{-1}$ lower than in the SML while the range was slightly reduced. Variations of salinity, nitrate metabolism, and net calcification/ dissolution on the TA range were similar to those observed in the SML. Also, TA and TA_{NO3} tended to be lower along the colder northern transect, although only by about 5 μeq $kgSW^{-1}$. While salinity and nitrate did not vary much between the two transects, this suggests that preformed TA_{NO3} concentrations may have been lower in the northern waters. However, this is not unambiguous as discussed in section 5.4.4.9 and demonstrated at station 2. Here the moderate sub-thermocline intrusion was reflected in different TA values relative to those from neighbouring stations, which would have led to an overestimate of the preformed TA_{NO3} value.

Results by the potentiometric and calculation methods confirmed the depth related changes, i.e. the decrease in TA from the SML down to 300 m. However, they did not corroborate the significant difference in sub-thermocline TA which was observed by the photometric method between the northern and southern transects. This indicates that the agreement between methods was better for vertical than for horizontal changes in TA.

4.4.4.4. TA changes at 500 m and greater depths

At depths of 500 m or below, TA tends to be determined by the origin of the water mass, the depth, and the total exposure to flux of PIC and POC since the formation of the water mass. Increased particle rain at the study sites may further have an impact on the observed TA. The sporadic nature of these events on a temporal and on spatial meso-scales has been demonstrated by Newton et al. (1994).

Due to the limited amount of TA data available, only a few clear-cut observations have emerged from the 1990 Experiment. The general decrease in TA between 1000 and 1500 m coincided with the decrease in salinity and the change from MW to EASIW as the dominant water mass. Consequently, the decrease in TA by about 20 μeq $kgSW^{-1}$ can at least to some extent be related to hydrographic changes. In contrast, the increase in TA below 1500 or 2000 m is not accompanied by relevant changes in salinity. However, the slight decrease in temperature may reflect some change in the water masses, which in these depths would

presumably be the replacement of the warmer EASIW by NADW. Since the profiles of TA_{NO3} resembled those of TA at these depths, nitrate remineralization can clearly be excluded as an explanation . The results therefore point at increasing importance of PIC dissolution below this depth range. This makes thermodynamic sense, i.e. the estimated lysocline depth is at about 2000 m in the North Atlantic (Edmond, 1974).

4.4.4.5. Seasonal changes in TA within the SML

All three methods agreed on the estimate of TA change in the upper 30 m since winter-mixing conditions, and also on the relative importance of the contributing factors. Accordingly, nitrate uptake had raised TA by about 10 μeq $kgSW^{-1}$, and the 5 μeq $kgSW^{-1}$ increase due to evaporation was counterbalanced by a similar amount of net calcification. This translates to a seasonal calcification estimate of 2.5 μmol kg^{-1}. Although the accuracy of these estimates can be easily questioned because of the various assumptions these estimates are based on (discussed further in section 5.4.4.9), the estimate of nitrate uptake turned out to be similar to the concentration of nitrate during winter-mixing in that part of the Northeast Atlantic (Glover & Brewer, 1988). In addition, the apparently small change of TA due to net calcification, which may be questioned since the TA samples were unfiltered, ties in to some extent with the fact that coccolithophorid counts remained in the order of 10^5 cells dm^{-3} all throughout May and June (Savidge et al, 1995). These cell counts are one to two orders of magnitude lower than those observed under *Emiliania huxleyi* bloom conditions in 1991, where TA_{NO3} was reduced by less than 1 μeq for every 10^5 coccolithophorid cells (section 5.4.3.4).

These observations agree largely with those from 1989, although some possible differences emerged. First of all, sediment trap data gave clear indications that, at some sites in that boreal region of the Northeast Atlantic, increased coccolithophorid growth may have occurred before the onset of stratification. It further appears that PIC net production was twice as large in 1989. It may nevertheless be significant that the estimate from 1989 was obtained about 3 weeks earlier in the year. Thirdly, the interannual difference in the size of the dominant spring bloom diatom species should not affect changes in TA during the following weeks, i.e. in the short-term. However, this size-difference may have an annual effect if it leads to significant differences in export production and therefore nutrients from the upper 200 m. This in turn would lead to annual changes in the concentration of pre-

formed nutrients within the winter-mixed layer. In view of the methodological discrepancies that have emerge in absolute and relative terms between the three methods it is not attempted to fit the photometric TA into the seasonal picture of TA established by Stoll (1994) which was based on 1989 and 1990 data.

With respect to seasonal POC:PIC net production, estimates of the relationship by the photometric method suggest that the absolute amount of net calcification was greater in samples where less photosynthesis had taken place. This can only make sense if two different biological regimes were sampled, which may have been the case between the northern and the southern transects. One of these could be a post-bloom regime where more POC had been regenerated than PIC dissolved, and the other one would have to be a regime of recent POC growth with hardly any PIC production. It has not been further investigated whether such scenarios were actually encountered. The POC:PIC net production ratios by the calculation and potentiometric methods were considerably lower, i.e. 4 and 1, respectively. However, the potentiometrically derived ratio seems unrealistically high considering that coccolithophorid growth was found to be very low throughout the time-series study of the Experiment (Savidge et al., 1995). These values compared to an estimate of about 10 for late-bloom conditions in 1989 by Takahashi et al. (1990).

4.4.4.6. Comparison of TA changes from different TA methods: Conclusion

In neither of the TA methods the PIC was removed prior to analysis. The results from section 2.3.5 showed that this can introduce a significant overestimate in the photometric TA of this study when PIC concentrations are typical of a coccolithophorid bloom. It is not clear to what extent the accuracy of the other two methods would have been affected in a similar excercise. On theoretical grounds, this error may have been reduced or negligible in the case of the potentiometric and the calculated TA. Any variation in PIC concentration may therefore account for at least some of the variability in the discrepancy between the photometric and the other two methods.

All three methods tended to agree on depth-related changes but not horizontal ones. This applied to the depth range above and below the thermocline. This study therefore has presented considerable relative discrepancies between methods which seem to be related to

some horizontally varying parameter which has yet to be identified. While some sources of errors have already been discussed in section 3.3.1.3.4, section 5.4.4.10 deals specifically with causes for relative errors in the methods.

The results highlight the need for caution when accurate TA values are required and when estimates of larger-scale changes are being derived from more than one TA technique. While work should continue on removing potential shortcomings or hidden errors in the different TA estimates, it seems of paramount importance to stick to one well-researched and generally approved method, or at least a combination of well-intercalibrated techniques.

5. ALKALINITY IN THE NORTH EAST ATLANTIC DURING THE 1991 BOFS COCCOLITHOPHORE BLOOM STUDY

5.1. INTRODUCTION TO THE 1991 STUDY

In 1991 the BOFS programme focused on a coccolithophorid bloom to the south of Iceland, where these blooms have been the most intense (Aiken & Bellan, 1990). The general aim was to investigate various biogeochemical aspects within and outside the bloom and to relate the findings to the spatial and temporal distribution of coccolithophorids in the North Atlantic. The biogeochemical aspects in the upper ocean included biological productivity, calcification and concomitant variations in the seawater carbonate system, in particular pCO_2 and TA. The latter parameter was of increased interest in 1991 since it appears to be the most suitable one to estimate calcification and thus its impact on the lessening in oceanic CO_2 drawdown associated with such blooms. An additional goal was to derive algorithms for the calibration of remotely sensed data on calcification by establishing relationships between satellite reflectance, coccolith light backscatter, and TA. The 1991 Study further included DMS-related studies, and was completed by investigations of the breakdown of the bloom in the surface and export of biogenic matter from the SML down the water column.

Satellite imagery from the advanced very high resolution radiometer (AVHRR) for the visible and infrared wavelength bands was transmitted daily to the research ship and used to identify an *Emiliania huxleyi* bloom and to design a ship sampling strategy accordingly. An extensive bloom developed some time in early/mid- June, reaching its maximal extent at 60-63°N 13-28°W between 15 and 23 June 1991. On an east-west scale, the bloom clearly exceeded 1000 km. In early July it extended to 10°W and down to at least 58°N along the Rockall Trough and the shelf waters west of Scotland. By 10 July the bloom was no longer obvious along the 20°W transect north of 60°N (Holligan et al., 1993).

The first cruise of the 1991 Study, which focused on carbonate chemistry, primary production and calcification processes in the SML, took place on the RRS 'Charles Darwin' between 13 June and 3 July. Surface measurements were carried out along six transects and were supplemented by depth profiles from six CTD casts as well as productivity studies in the vicinity of the cast stations. The transects and stations of the CTD casts are shown in

figure 5.1. A wide-ranging account and some of the major findings from this cruise has been produced by the participants of the cruise (Holligan et al., 1993). Robertson et al. (1994) presented a more specific assessment of the calcification effect on pCO_2 during the bloom. In addition, a detailed evaluation of productivity and calcification rates was produced by Fernandez et al. (1993). The breakdown of the bloom and export fluxes from the SML were investigated on a follow-up cruise. The data obtained during the 1991 Study was used to investigate environmental factors which allow *Emiliania huxleyi* to form blooms (Tyrrell & Taylor, 1995; 1996).

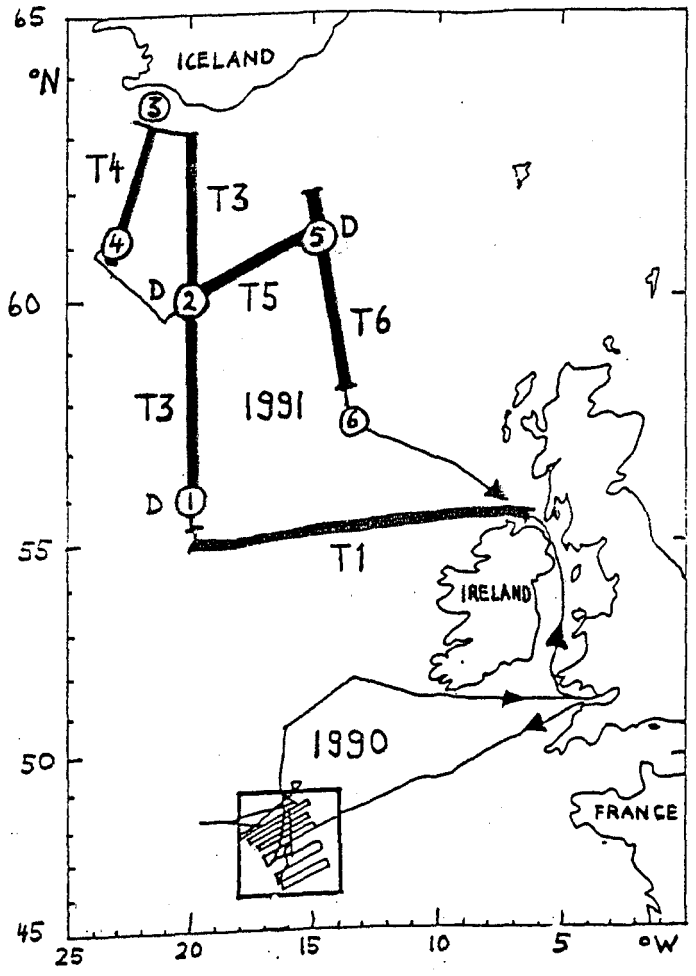

Figure 5.1: Positions of transects (T) and casts (1 - 6) surveyed for TA during the first cruise of the 1991 Coccolithophore Bloom Study in the Northeast Atlantic between 14 June and 1 July. Deep casts are marked with a 'D'.

5.2. HYDROGRAPHY OF THE STUDY AREA (55-64°N 14-23°W)

5.2.1. UPPER 200 M

Between 15 and 24 June 1991 exceptionally cloud-free conditions resulted in extremely warm and calm weather across the North Atlantic north of about 59°N. Infrared band satellite imagery revealed the complex mesoscale eddy structure typical of the Northeast Atlantic in the pattern of SST, with the most obvious features being several cold-core eddies in the Iceland Basin (Holligan et al., 1993). The SST of open ocean water varied by less than 3°C between 10.5 and 13.5 °C. It tended to be lower towards the north and west of the Study area. Two exceptions to this spatial trend were observed within the main bloom area between 61° and 62°20'N 20°W and at the eastern margin of the bloom at around 61°N 15°W where SSTs were increased. Salinity also tended to decrease towards the north and west.

The general pattern of surface water advection for the central part of the coccolithophorid bloom was deduced from a sequence of visible-band satellite images and density profiles established along the transects. Along the 20°W line, the southern margin of the bloom was located in a hydrographic transition zone at 61°N. South of this zone, high density water (sigma-t > 26.8) was identified as NACW which moved in a northeastern direction in line with the prevailing flow of the NAD in this region. North of the transition zone, lower density water was flowing in a westward direction in accordance with the general surface flow off the southern coast of Iceland. This water was identified as MNAW by Fernandez et al. (1993) but would have qualified as ENACW according to Emery and Meincke (1986). In spite of the general flow in the northern areas, some eddies appeared to remain almost stationary, and their sudden appearance or disappearance in terms of reflectance was ascribed to vertical displacement of coccolith-rich water (Holligan et al., 1993).

Figure 5.2 demonstrates how temperature and salinity related to each other along different transects. Six groups of water types were identified on the basis of salinity (Emery & Meincke, 1986), surface flow (Holligan et al., 1993), and temperature. According to Emery and Meincke, three types of water qualified as NACW. These comprised

(i) high-salinity NACW along 55°N and the southern end of the eastern transect 6;

(ii) intermediate-salinity NACW along parts of the eastern transects (T5, T6) and the southern end of the 20°W line (T2);

(iii) intermediate-salinity NACW with elevated temperatures at parts of the eastern transects (T5, T6).

These waters could be assumed to flow in a generally eastern direction. The remaining three water types fell outside the salinity threshold, so that they have been categorized as MNAW in this study. They could be categorized as:

(iv) eastward-flowing higher-salinity MNAW found mainly along the 20°W line between 58°20′ and 61°N (northern part of T2; southern part of T3);

(v) westward-flowing low-salinity and -temperature MNAW along the Iceland coast and in the northwest (northern part of transect 3; western transect 4); and

(vi) westward-flowing MNAW with elevated temperatures along the 20°W line between 61°N and about 62°20′N (middle part of T3).

In general, high-reflectance regions were confined to westward-flowing MNAW.

The thermocline depth as indicated by the 9.5 °C isotherm became shallower towards the north along the 20°W line narrowing from about 50 m at 58° 30′N to 10 m at 62° 30′N (Holligan et al., 1993). As indicated by temperature depth profiles in this study, the 70 - 150 m depth range fell safely below the SML at all the deep water stations.

The depth of the 1% isolume with respect to photosynthetically available radiation, PAR, ranged from > 24 m outside the coccolithophorid bloom to 8 m in the most turbid water due to the presence of detached liths (Holligan et al., 1993).

An important finding arising from this Study was the vast extent of the *Emiliania huxleyi* bloom, which greatly exceeded that of mesoscale features such as eddies or other dynamic surface layer properties generally regarded as relevant influences on phytoplankton distribution (Holligan et al., 1993; Fernandez et al., 1993).

5.2.2. GREATER DEPTHS (≥ 300 M).

According to Emery and Meincke (1986), hydrographic measurements from deep casts indicate that the upper water masses at 300 and 500 m changed from ENACW at 56°N 20°W to MNAW at the more northern stations. Temperatures at these greater depths decreased

towards the north, with station 5 in the northeast being coldest and slightly more saline than stations 2 and 4 further west.

Intermediate and deep water consisted of EASIW and NADW, respectively. None of the cast sites showed signs of MW at intermediate depths.

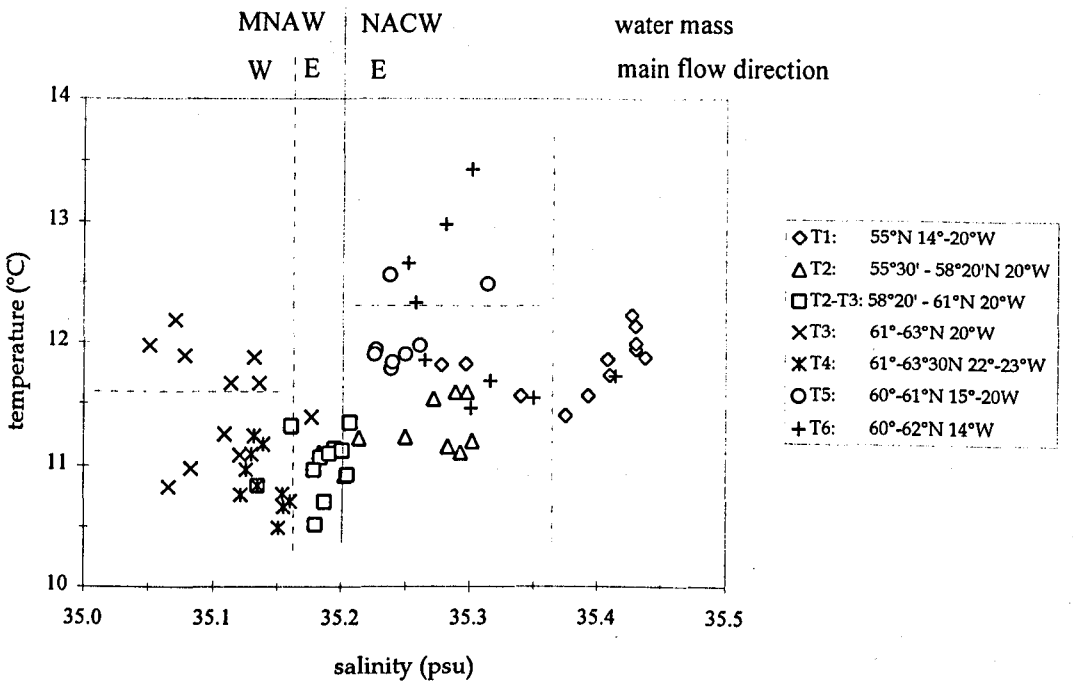

Figure 5.2: Temperature-salinity plot from samples collected during the 1991 Coccolithophore Bloom Study in the Northeast Atlantic. Samples have been marked according to transects (T) and, in the case of the 20°W transects (2 and 3) further distinctions have been made according to fronts associated with density and salinity thresholds set by Fernandez et al. (1993) and Emery and Meincke (1986), respectively. The categories of water types were based on these thresholds, the general direction of flow (E = eastwards, W = westwards), elevated temperatures, and elevated salinity.

5.3. BIOGEOCHEMICAL FINDINGS

5.3.1. SPATIAL VARIATIONS IN BIOLOGICAL STANDING STOCKS AND PRODUCTION RATES

5.3.1.1. Outside the bloom

Outside the *Emiliania huxleyi* bloom area, concentrations of chlorophyll a and POC reached up to 2.5 μg dm^{-3} and 35 μM, respectively. Biomass from *E. huxleyi* and *Coccolithus pelagicus*, PIC concentrations, and PIC production rates were generally low. Station 2 at 60°N 20°W was in such an area. Here proportions of biomass from *E. huxleyi*, *C. pelagicus*, holococcolithophorids, and other small coccolithophorids were similar and very low. The biomass maximum was found at 15 m. Between 20 and 35 m, much of the biomass was made up of diatoms typical of the spring bloom. Some PIC production was measured between 15 and 35 m in association with *C. pelagicus* (Fernandez et al., 1993). Transects 1 and 2, and CTD station 1 were also outside the bloom area.

5.3.1.2. Within the bloom

Within the *Emiliania huxleyi* bloom area, concentrations of chlorophyll a generally remained below 1.0 μg dm^{-3}. Concentrations of POC did not exceed 15 μM. Photosynthetic rates were low compared to the situation of a diatom bloom (Fernandez et al., 1993). Measured concentrations of PIC were relatively high, reaching above 30 μM near 63°N 20°W. A maximum PIC concentration integrated over the upper 35 m of 17 μM was determined by Fernandez et al. (1993). As this concentration is similar to those observed in other oceanic regions, the authors proposed that it may represent an upper threshold for calcification by *E. huxleyi*, which is independent of oceanic regime. Other PIC estimates from surface samples were based on satellite reflectance data calibrated against the beam attenuation coefficient at 532 nm and chlorophyll a. They implied a maximum PIC concentration of 42 μM and an average value for the whole bloom area of 16.5 μM (Holligan et al., 1993).

Ratios of POC: PIC production never fell below 4. Fernandez et al. (1993) found that POC and PIC production rates depended on light regime and region of the bloom. Calcification rates were frequently higher in the surface than in the sub-surface layers, unless the coccolithophorid maximum was further down in the water column. The rates were generally low in areas where *Emiliania huxleyi* was dominant, only exceeding 10% in surface waters at the southern border of the main bloom and in some subsurface populations from within the bloom where *Coccolithus pelagicus* was abundant. Ratios of POC: PIC production rates were in stark contrast to some of the ratios measured for POC:PIC standing stock. Rate ratios decreased to 1 and below at some sites and were more comparable to independent estimates of POC: PIC production in the field and in batch cultures of high-calcifying strains of *E. huxleyi* during the early growth phase (Balch et al., 1992; Nimer & Merrett, 1992).

The discrepancy between the standing stock and carbon incorporation rates with respect to the POC:PIC ratios was presumed to be related to the advanced stage of the bloom. Balch et al. (1991, 1992) found that changes in the ratio of POC:PIC production during the development of an *Emiliania huxleyi* bloom in the field matched those observed in batch cultures. Towards the end of the exponential phase both production rates decline and an increasing number of liths are shed. The absence of a clear relationship between PIC and coccolithophorids was ascribed to the presence of these detached liths and empty coccospheres. It was concluded that the relatively high PIC concentrations within the *Emiliania* bloom were caused by the more efficient removal of POC by sinking or regenerative oxidation, which tends to become more pronounced towards the end of a bloom. This is also consistent with the relatively low concentrations of chlorophyll a and the higher proportion of empty coccospheres in samples containing the greatest numbers of *E. huxleyi*.

At the western 'bloom' region close to station 4, some of the highest amounts of biomass from *Emiliania huxleyi* and *Coccolithus pelagicus* were observed. This occurred in connection with high PIC standing stocks. Coccolithophorids made up more than 60% of total phytoplankton biomass. *Emiliania huxleyi* was the dominant species, reaching a maximum within the thermocline at 15 m. Some of the highest PIC production rates of the 1991 Study were observed in this region reaching 0.12 µmol dm^{-3} hr^{-1} and 0.6 µmol dm^{-3} day^{-1}. Due to these high rates and the few liths in relation to *E. huxleyi* cells this region was taken to

represent an 'early bloom' situation. The POC:PIC production ratio amounted to only 5, which was lower than those measured in eastern parts close to station 5 (Fernandez et al., 1993). These eastern sites, at the periphery of the bloom area, were considered to represent a 'late bloom' situation based on the low production rates and relatively high numbers of liths. While there was a high biomass of flagellates, coccolithophorids were still dominant within and below the thermocline. *Coccolithus pelagicus* was more important than *E. huxleyi* at this site. Absolute production rates of POC and PIC were low here, but reached a high level at the very surface similar to those measured at the western station. The productivity studies by Fernandez et al. also revealed considerable variations over a day in absolute and relative amounts and production rates of POC and PIC.

5.3.1.3. Transitional areas

The transition from non-bloom to bloom situation was most apparent along the 20°W transect 3, western transect 4, and eastern transect 6. North of 58°N 20°W coccolithophorid biomass became increasingly important with *Emiliania huxleyi* being the dominant contributor north of 61°N. Cell and lith counts further revealed parallel increases in dead *E. huxleyi* cells, i.e. coccospheres, as well as in detached liths. Total counts of *E. huxleyi*, i.e. live cells and empty coccospheres, reached up to about 20×10^6 dm^{-3}, half of which was due to coccospheres. Lith counts peaked at around 350×10^6 dm^{-3}. These high values coincided with the high reflectance observed between 62° and 63°N and are believed to be the highest reported at the time for open ocean waters (Holligan et al., 1993). The high proportion of coccospheres may at least partially explain why a notable fraction of phytoplankton was made up of naked flagellates, which appeared to be prymnesiophytes. It has been proposed that the coccospheres arose from the sudden release of naked motile cells which form another part of the *E. huxleyi* life cycle (Green et al., 1990). Transect 4 passed through the centre of the bloom, leaving it at its southwestern end. Along the eastern transect 6 a marked physical front between 59° and 60°N separated *E. huxleyi*-dominated waters in the north from *Coccolithus pelagicus*-dominated waters in the south. The front bore the highest relative PIC production observed during the study reaching 25% of the total (Fernandez et al., 1993). The 60°-61°N transect 5 ran along the southern margin of the bloom crossing different water types. It represented a somewhat mixed and transitional hydrographic and biological situation with 'late bloom' station 5 as its eastern extension.

5.3.2. NITRATE CONCENTRATIONS

Surface nitrate concentrations generally ranged from depletion levels up to 7 μM. They were highest outside the bloom area at 60°N 20°W. The lowest measurements were made in the northwest in the coastal waters of Iceland and in the eastern region, i.e. along transect 6 and the eastern part of transect 5. Within bloom waters, nitrate tended to stay above 2 μM. Along the 20°W line, this spatial pattern led to a steady increase from 55° to 60°N. North of 60°N it declined again. Within the bloom area, considerable small-scale fluctuations were observed with lower concentrations tending to be in low reflectance areas.

5.3.3. PIC NET PRODUCTION

The findings from section 5.3.1.2 demonstrate that chemical measurements of PIC standing stock and production rates based on ^{14}C measurements may not always be adequate in estimating the total amount of PIC production that has occurred over the entire course of the bloom. On this and longer time-scales it is generally more accurate to derive calcification estimates from the TA imprint left behind in the SML. In the 1991 Study a good correlation was established between photometric TA and PIC concentrations (Holligan et al., 1993; this study). Furthermore, TA calculated from pCO_2 and TCO_2 revealed a tight correlation with PIC along the 20°W transect with sharp gradients of these parameters over short distances. For example, just south of 63°N a PIC increase of 20 μM was matched by a decrease in calculated TA of 40 μeq $kgSW^{-1}$ (Robertson et al., 1994).

Neither photometric nor calculated TA have been used to conduct independent investigations into the amount of calcification that has occurred in the bloom area of 1991. Calculated TA was however employed to establish net production ratios of POC:PIC (Robertson et al., 1994). By correlating potential TA to salinity-normalized TCO_2 (35 psu), Robertson et al. (1994) found that the average production ratio of POC:PIC was close to 1 over the course of the *Emiliania huxleyi* bloom. This compared to a slightly lower ratio of 0.75 which was based on estimates from the standing stock of PIC and POC, with the latter being derived from coccosphere counts (Fernandez et al., 1993).

5.3.4. PCO_2

Outside the coccolithophorid bloom area south of 60°N, pCO_2 levels ranged around 300 µatm, i.e. they were on average about 55 µatm lower than the atmospheric pCO_2 at the time (Schneider et al., 1992). Within the coccolithophore bloom area where concentrations of particulate $CaCO_3$ tended to be high, oceanic pCO_2 was reduced much less, i.e. by as little as 5 µatm, but gradients in pCO_2 of up to 90 µatm over a distance of 25 km were reported by Holligan et al. (1993) and Robertson et al. (1994). These authors provided multiple evidence for the link between relative increase in pCO_2 and calcification. Holligan et al. (1993) calculated that calcification of 16.5 µM, i.e. their mean calcification estimate for surface waters in the whole bloom area, led to a mean increase in pCO_2 of 17 µatm. In a somewhat different approach, Robertson et al. (1994) obtained a mean relative increase of pCO_2 of 15 µatm. However, the total increase in pCO_2 was estimated to be even higher due to the SST rise by up to 1°C, which was ascribed to increased reflectivity from liths, but no average value for this temperature effect was provided. Based on the above estimates, Robertson et al. (1994) estimated that the occurrence of such a bloom at that particular time of year could reduce the total air-sea CO_2 flux which occurs during stratified conditions by up to 35%. Calcification was estimated to be responsible for 17% of that reduction. Nevertheless, surface waters in the study area tended to remain a net sink for pCO_2, albeit a much weaker one than in the absence of such a bloom.

5.3.5. METHODOLOGICAL CONCLUSIONS

Holligan et al. (1993) pointed out that accurate field observations are essential in order to obtain reliable estimates of the climatic impact of coccolithophorids. The above studies have shown that calcification is the main process by which coccolithophorids can have a significant impact on the air-sea flux of CO_2 in the short-term as well as on geological time-scales.

5.4. ESTIMATES OF TA AND THEIR VARIATIONS

5.4.1. AIMS

During the 1991 Coccolithophore Bloom Study photometric TA measurements were carried out with the specific aims to

(i) investigate in more detail the TA range and its spatial variations in relation to influencing factors with particular focus on the effect of coccolithophorid growth;

(ii) provide independent measurements of TA than those by the calculation method to estimate the effect of a coccolithophorid bloom on PIC production and the carbonate chemistry in the SML;

(iii) establish algorithms for calibration of optical and biological calcification data;

(iv) continue the intercomparison of TA methods from 1990 in a more diverse range of hydrographic and biological regimes;

(v) add the findings to the available information of seasonal and spatial variations of TA within the Northeast Atlantic.

5.4.2. MATERIALS AND METHODS

5.4.2.1. Coverage of TA determinations during the 1991 Study

Photometric TA measurements in surface (2-3 m) samples were collected along all six transects marked in figure 5.1. Distances between sampling positions ranged mostly between 20 and 40 km upon hourly or two-hourly sampling intervals. Vertical profiles of photometric TA were obtained from the six CTD casts also shown in figure 5.1. Apart from stations 3 and 6, i.e. in Icelandic coastal waters and on the Rockall Bank, respectively, the casts were carried out in areas where ocean depths exceeded 1400 m. At open ocean stations 1, 2, and 4 the casts covered the entire water column with the respective depths of approximately 1500, 2700, and 2200 m. At eastern station 5, where water depth was about 2200 m, the CTD only went down to 500 m. Concomitant results from calculated TA were available for most parts of the six transects, but not for the CTD casts.

5.4.2.2. Presentation and interpretation of the TA results

General ranges of TA, specific, and potential alkalinity are presented in section 5.4.3.1. Overall effects of variations in salinity, nitrate uptake and calcification were approximated by comparing these ranges in a similar way as was done for the 1990 study (section 4.4.2.2). The regional distribution of TA was compared to that of reflectance shown in the AVHRR satellite images.

In section 5.4.3.2 small- and large-scale variations in surface TA along transects are presented in more detail alongside profiles of hydrographic, biological, optical, and other chemical parameters. Accompanying vertical profiles from the CTD casts down to 150 m were used to obtain information about changes that had occurred across the thermocline. This was done using the same assumptions as for the interpretation of data from the 1990 Experiment (section 4.4.2.2). As there was no vertical data for nitrate concentrations, at most stations potential TA for the SML was calculated using nitrate data from the nearest surface samples. Sub-thermocline TA_{NO3} was derived using winter-mixing concentrations of nitrate for the appropriate regions as estimated by Glover and Brewer (1988). On one occasion, on Rockall Bank where no appropriate data for nitrate utilization was available, these corrections were attempted by adding the concentration of TPN to that of TA_S.

A regional overview of TA and derived parameters is presented for surface samples and cast profiles in section 5.4.3.3. Surface samples were plotted against latitude and marked according to transect, thus providing further regional insight into the origin of the samples. A comparison between TA, TA_S, and TA_{NO3} plots was conducted to determine the influence of different factors on surface TA in the different regions of the Northeast Atlantic. This was substantiated by a regional overview of vertical profiles.

General relationships of surface TA and TA_{NO3} with hydrographic, biological, chemical, and optical parameters were investigated in section 5.4.3.4 using linear least squares regression analyses according to Sokal and Rohlf (1981). The deviation of the relationship between TA_{NO3} and PIC concentration from the expected slope of -2 was used to estimate the average percentage loss of PIC from surface samples during the 1991 Study. For this to be justified it has to be assumed that this relationship was not skewed by any differences in preformed TA_{NO3} or other factors which may affect TA. The resulting information was used, in turn, to

estimate how much TA may be lowered by the growth of a given number of *Emiliania huxleyi* cells.

In section 5.4.3.5 the information of TA_{NO3} and PIC concentrations were combined to investigate to what extent PIC production and loss by sinking or herbivory from the surface prior to the sampling date may have occurred in different regions of the 1991 Study area. If one assumes that the concept of potential alkalinity is appropriate to estimate the amount of net calcification in seawater prior to its collection, then the term

$TA_{NO3} + 2\,[PIC]$, where [PIC] is the molar concentration of PIC,

should be the same for all samples if they have lost the same amount of PIC. Lower values of this term imply that more PIC has been lost from this sample, and vice versa. It is important to bear in mind that this term only reflects the loss from the parcel of water that was sampled and not necessarily from the SML altogether.

The mean difference in PIC net production between the *Emiliania huxleyi* bloom area north of 61°N 20°W and the non-bloom area south of this point along the 20°W line was estimated in section 5.4.3.6. This was done by comparing surface TA_{NO3} values from the two regimes. It was assumed that preformed TA_{NO3} levels had been the same in both regimes before the *E. huxleyi* bloom had started.

The net production ratio of POC: PIC was investigated and compared for different regions in section 5.4.3.7. The procedure for this has been described in section 4.4.2.2.

A comparison between TA measured by photometry and calculated from pCO_2 and TCO_2 is described in section 5.4.3.8 on some selected aspects for which a proper comparison was possible, i.e.

(i) regional distributions of TA and derived parameters including the 'PIC loss' term;
(ii) correlations with PIC and backscatter due to calcite using linear least squares regression analyses;
(iii) relative increase of PIC net production within the *Emiliania huxleyi* bloom area;
(iv) net production ratios of POC: PIC.

To conduct a valid quantitative comparison, the latter two aspects were investigated using only samples for which data from both methods were available.

Section 5.4.3.9 briefly deals with results from the four CTD casts at which sampling depths exceeded 150 m, to provide some information on regional differences of TA at greater depths.

In section 5.4.3.10 results of TA and related parameters from the 1991 Study are compared to those obtained from the 1990 Experiment. Final comments on spatial and temporal variations in the Northeast Atlantic are made.

5.4.2.3. Sample collection and analyses of TA

For photometric TA measurements along the transects, surface (2-3 m) samples were collected from the non-toxic seawater supply to the 'wet' laboratory of the ship. Cast samples were collected from Niskin bottles. Analyses followed the same procedure as described for the 1990 Experiment (chapter 2; section 4.4.2.3) with one exception. In 1991, analyses were carried out on samples that had been filtered through pre-rinsed Whatman cellulose nitrate filters with a pore size of 0.45 µm at a vacuum pressure of less than 0.2 bar.

Estimates of calculated TA along the transects were provided by D. Turner and his group (then PML). They were determined from on-line pCO_2 and TCO_2 data in the same way as for the 1990 Experiment (section 4.4.2.4). In contrast to 1990, a potential bias may have arisen from the fact that pCO_2 and TCO_2 samples were taken from different seawater supply systems (Robertson et al., 1994; section 5.4.2.4 below).

5.4.2.4. Sampling and determinations of other parameters

All the parameters mentioned in this section were determined by other scientists directly or indirectly involved with the first cruise of the 1991 Study. Some descriptions of the methodologies are given in more detail by Holligan et al. (1993), Fernandez et al. (1993), and Robertson et al. (1994).

Conductivity and temperature data along transects were obtained from sensors attached to an undulating oceanic recorder (UOR). For vertical profiles salinity and temperature data was obtained from the CTD. Density data was obtained from the BODC.

Discrete samples for the determination of various biological, chemical and optical parameters were taken from the same water supply system that provided samples for photometric TA. Chlorophyll a was determined by fluorometry after filtration onto Whatman GF/F glass fibre filters and extraction for 24 hours at 4°C with 90% acetone. Phytoplankton cells were counted and identified under an inverted microscope. The samples had been preserved with Lugol' iodine and buffered formalin. A distinction was made between live *Emiliania huxleyi* cells and dead ones (here: empty 'coccospheres'). Lith counts referred to detached liths. For analyses of particulate carbon and nitrogen, volumes of 500 cm^3 were collected on Whatman GF/F glass fibre filters and subsequently frozen at -20°C. Measurements for TPC and TPN were carried out on a Carlo-Erba 1500 series 2 CHN analyser. Particulate inorganic carbon was obtained from the calcium content, assuming that all the measured calcium was present in form of calcium carbonate, so that this parameter is referred to as PIC in the text below. No determinations of PIC in the accurate sense, i.e. by acidifying filters containing TPC, were carried out in this Study. Flame atomic absorption spectrometry with an air-acetylene flame at 422.7 nm was used to determine the calcium concentration. Samples were made up with 1% lanthanum chloride as a releasing agent to remove phosphorus suppression of ionisation. Particulate organic carbon was calculated from the difference between TPC and PIC. Light backscatter (b_b') was measured at 550 nm with a light scattering photometer. The backscatter caused by coccolithophorids was determined from the difference between acidified and unacidified samples. The method is described in more detail by Balch et al. (1991).

Samples for the determination of TCO_2 and nitrate concentration were received on-line from the non-toxic seawater supply via a 130 dm^3 header tank. They were pre-filtered using separate on-line filtration units. In the case of TCO_2, this unit held a Whatman cellulose nitrate filter with a pore size of 0.45 µm. Apart from the pre-filtration, the procedure for TCO_2 analysis was the same as for 1990 (section 4.4.2.4). Analysis of samples for nitrate concentration by Technicon AA2 also followed the procedure already outlined for the 1990 Experiment (section 4.4.2.4).

Samples for the determination of pCO_2 were also collected on-line from the non-toxic seawater supply. However, in contrast to the system used in 1990 and the system used for TCO_2 and nitrate samples in 1991, seawater was diverted from the system before passing through the 130 dm^3 header tank. It passed through a separate 10 dm^3 header tank, instead. This may have led to a potential and unquantifyable error in the results from pCO_2 and TCO_2. The actual analytical procedure for pCO_2 was the same as for the 1990 Experiment.

AVHRR satellite reflectance (580-680 nm) images were provided by S. Groom (Univ. of Plymouth).

5.4.3. RESULTS

5.4.3.1. General range of surface TA during the 1991 Study

General results of 95 photometric surface TA measurements conducted during the 1991 Study are provided in table 5.1. Values of specific and potential TA are also included. Photometric TA averaged around 2290 $\mu eq\ kgSW^{-1}$, ranging by about 70 $\mu eq\ kgSW^{-1}$ from 2314 down to 2243 $\mu eq\ kgSW^{-1}$. Salinity normalization of the TA data suggests that part of the overall variation, i.e. about 15 $\mu eq\ kgSW^{-1}$, was brought about by variations in the evaporation/precipitation history of the waters sampled. The effect of variations in nitrate uptake as derived from nitrate concentrations was negligible with respect to the overall TA range. The TA_{NO3} range amounted to about 55 $\mu eq\ kgSW^{-1}$ implying that calcification may have varied by up to 25-30 $\mu mol\ dm^{-3}$ between different samples. Although the ranges of TA, TA_S, and TA_{NO3} were based on different samples sizes, the comparison seemed justifiable as minimum and maximum values tended to come from samples represented in all three parameters.

Areas of higher and lower TA coincided with respective lower and higher reflectance areas in AVHRR satellite images from 19 and 25 June (figure 5.3).

Table 5.1: Ranges of photometric TA and derived parameters (μeq $kgSW^{-1}$) observed in surface (2-3 m) samples during the 1991 Coccolithophore Bloom Study conducted 14 June to 1 July.

	TA (n= 95)	TA_S (n= 88)	TA_{NO3} (n= 66)
mean	2290	2274	2275
minimum	2243	2235	2240
maximum	2314	2290	2296
range	71	55	56
s.d.(n-1)	18.2	14.5	16.0

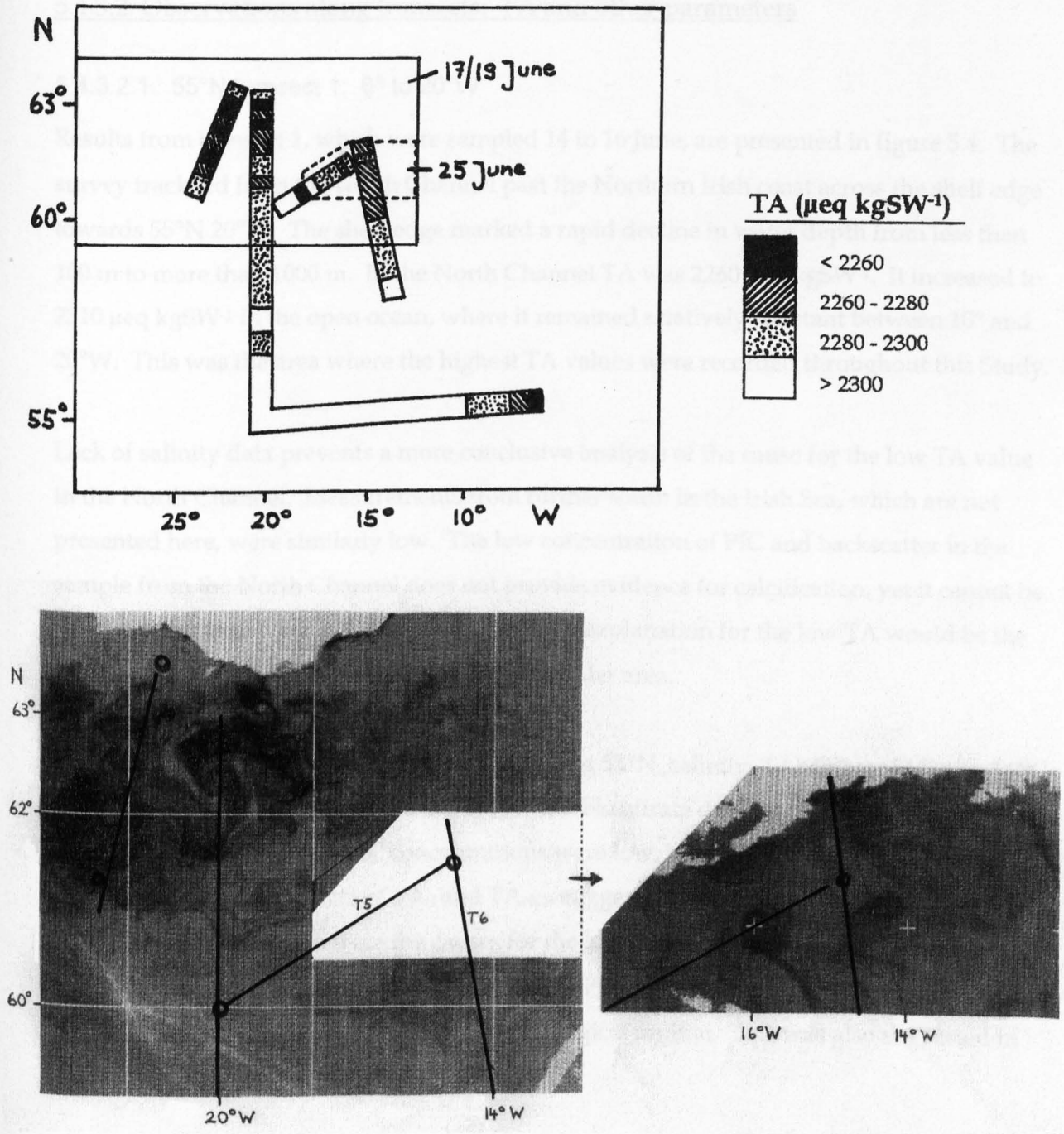

Figure 5.3.: Comparison of the surface (2-3 m) profile of photometric TA with AVHRR satellite reflectance images during the 1991 Coccolithophorid Bloom Study conducted along six transects between 14 June and 1 July. Satellite images were provided by S. Groom (Univ. of Plymouth). Relatively high reflectance shows up as **dark** shades. Very light shades represent land or cloud cover.

(a) Photometric TA. Marked areas are covered by the satellite images.

(b) Satellite image taken on 19 June covering the northern part of the 1991 Study area. Transects or parts of them and CTD stations are marked. Transects 5 and 6 were studied 8 to 12 days after the images were taken. For these two transects figure (c) is more appropriate in terms of the dates.

(c) Satellite image from 25 June covering a small area in the northeastern part of the 1991 Study area. Parts of transects 5 and 6 and station 5 are marked.

5.4.3.2. Observations along transects: TA and other parameters

5.4.3.2.1. 55°N transect 1: 6° to 20°W

Results from transect 1, which were sampled 14 to 16 June, are presented in figure 5.4. The survey track led from the North Channel past the Northern Irish coast across the shelf edge towards 55°N 20°W. The shelf edge marked a rapid decline in water depth from less than 100 m to more than 1000 m. In the North Channel TA was 2260 μeq $kgSW^{-1}$. It increased to 2310 μeq $kgSW^{-1}$ in the open ocean, where it remained relatively constant between 10° and 20°W. This was the area where the highest TA values were recorded throughout this Study.

Lack of salinity data prevents a more conclusive analysis of the cause for the low TA value in the North Channel. Measurements from further south in the Irish Sea, which are not presented here, were similarly low. The low concentration of PIC and backscatter in the sample from the North Channel does not provide evidence for calcification, yet it cannot be ruled out that it had taken place earlier. A likely explanation for the low TA would be the influence of freshwater regimes in this coastal water area.

Throughout much of the open ocean section along 55°N, salinity, TA, chlorophyll a and PIC remained almost constant. While the little available nitrate data did not suggest a limitation of nitrate, chlorophyll and PIC concentrations were low, i.e. around 0.5 μg dm^{-3} and 5 μM, respectively. Available data of TA_S and TA_{NO3} suggest that the relatively high salinity and low levels of calcification were the causes for the high TA along this part. However, nearer to 20°W a notable decrease in salinity and rise in PIC and chlorophyll concentrations reflected a change in the hydrographic and biological regime. This was also suggested in the slightly elevated TA_{NO3} closer to 20°W.

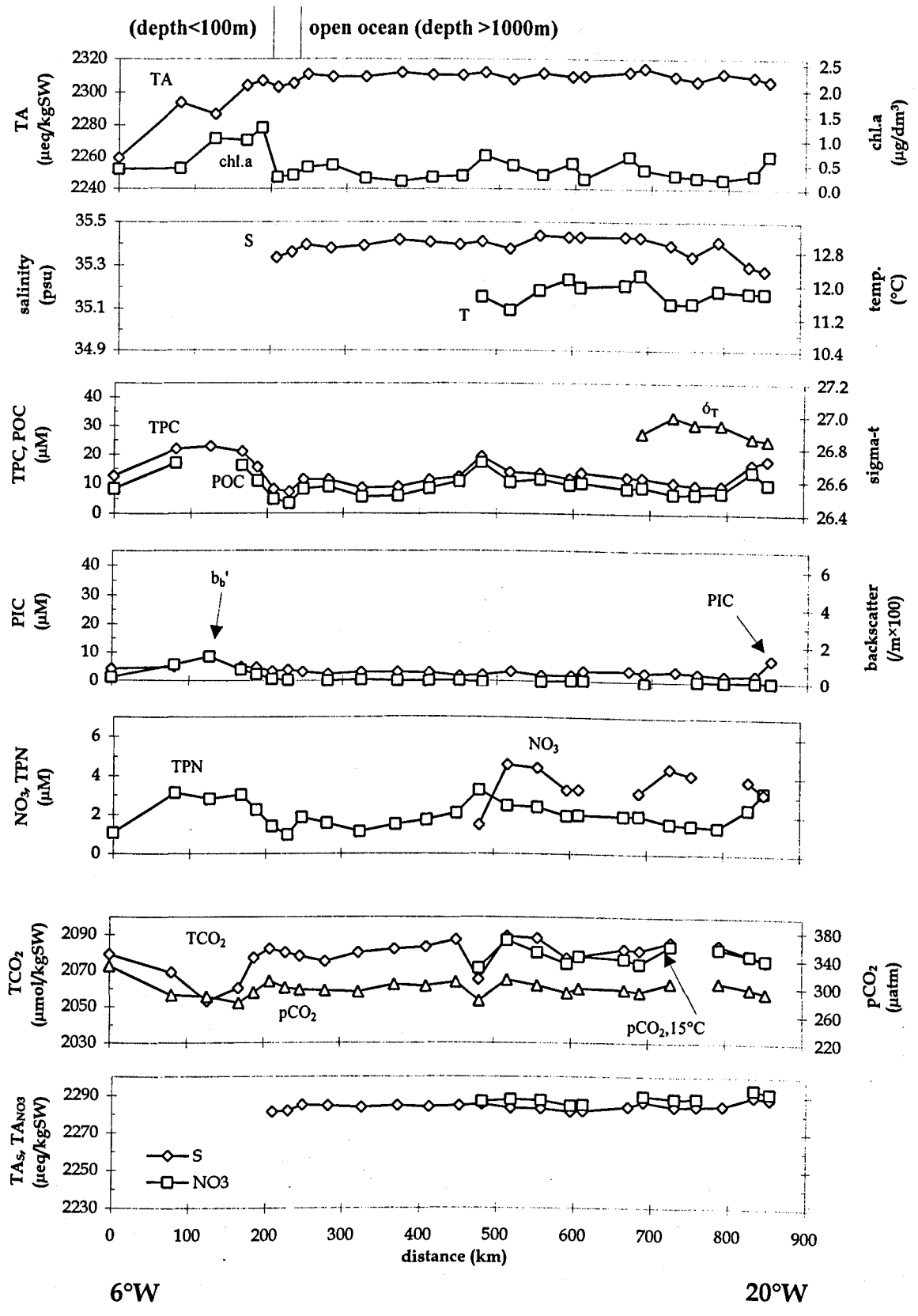

Figure 5.4: Surface (2-3 m) profiles of various in situ parameters along 55°N transect 1 (6° to 20°W) from the 1991 Study conducted 14 to 16 June. TA and derived parameters were determined by photometry. PCO_2 is also expressed at 15°C.

5.4.3.2.2. 20°W transect 2: 55°30' - 60°N

Results from the southern 20°W transect and accompanying CTD profiles 1 and 2 at 56°N and 60°N, respectively, are presented in figures 5.5 - 5.7. The transect, which was surveyed 16 to 19 June, started off just south of the Rockall Plateau, crossed it, and entered the Iceland Basin about halfway along. At the southern end of this transect, TA and other features tended to be similar to those at 55°N 20°W (western end of transect 1). As salinity gradually decreased towards the north, TA fell from 2305 to 2290 μeq $kgSW^{-1}$. The TA_S and TA_{NO3} profiles suggest that this was largely due to the salinity decrease and to a small extent also calcification. However, this latter effect may have been too small to be picked up by the PIC measurements, which showed little change from around 3 - 5 μM. While nitrate concentrations rose from 3 to 6 μM between 55°30' and 60°N, chlorophyll a also increased from 0.5 to 1.0- 2.0 μg dm^{-3} in the Iceland Basin This coincided largely with notable rise in the number of coccolithophorids other than *Emiliania huxleyi* to about 10^7 dm^{-3}. Abundance of *E. huxleyi*, dinoflagellates and diatoms remained relatively negligible, i.e. below 10^6 dm^{-3}.

A small-scale hydrographic feature of about 60 km at 57°N on the Rockall Plateau between 57° and 58°N could be recognized by its increased salinity (figure 5.5). This was accompanied by a TA increase of about 10 μeq $kgSW^{-1}$ and reductions in the concentrations of particulates, thus briefly interrupting the general latitudinal trends observed above. According to Emery and Meincke (1986), this physical feature may have marked the boundary between NACW and MNAW and relates to the changes in chemical and biological parameters.

Depth profile 1

Vertical changes in TA and other parameters measured at CTD station 1 south of the Rockall Plateau at 56°N 20°W on 17 June are depicted in figure 5.6. This station was in the area of high TA typical of the southern end of the 20°W transect. The thermocline was somewhere between 30 and 80 m. Salinity was considerably lower in the SML than at 80 and 150 m, indicating different types of water masses above and below the thermocline and thus a history of differential advection in these two layers. The difference in salinity had led to a reduction of surface TA relative to sub-thermocline levels by about 15 μeq $kgSW^{-1}$. The difference in nitrate concentration of 4 μM in the SML and 14 μM at sub-thermocline depths implies that nitrate uptake in the SML would have raised TA by about 10 μeq $kgSW^{-1}$. The

resulting TA_{NO3} values were higher above the thermocline by about 10 μeq $kgSW^{-1}$. This does not tie in with PIC concentrations of up to 5 μM in the SML, which lead to the expectation that TA_{NO3} should be at least 10 μeq $kgSW^{-1}$ lower in the SML. Some unaccounted factor(s) had therefore raised TA in the SML by about 20 μeq $kgSW^{-1}$. Differential advection is a possible reason for this observation.

Depth profile 2

Results from CTD cast 2 at 60°N 20°W in the Iceland Basin on 19 June are presented in figure 5.7. Without higher resolution temperature data available in this study, the thermocline could only be narrowed down to a depth range of somewhere between 5 and 80 m. Total alkalinity deviated little from 2290 μeq $kgSW^{-1}$ between surface and 150 m except for a slight decrease at 12 m which coincided with a PIC increase to about 5 μM. Salinity had a negligible effect on the TA profile. From the difference between surface nitrate concentrations of about 6 μM in this region and the assumed winter mixing concentration of 11 μM in the sub-thermocline layer, it may be concluded that nitrate uptake had raised TA in the SML by about 5 μeq $kgSW^{-1}$. This, in turn, implies that TA_{NO3} was about 10 μeq $kgSW^{-1}$ lower in the SML than at the sub-thermocline depths. Concentrations of PIC between 2 to 4 μM all the way down to 80 m may be a possible indication that some vertical loss of PIC from the SML had occurred. Assuming that all the PIC present in the upper 80 m was produced in the SML over the preceding weeks, total PIC production within the SML would have amounted to about 4 to 8 μM This would tie in with the calcification estimate derived from TA_{NO3}.

Assuming that some vertical loss of PIC from the SML had occurred, the almost unchanged TA with depth appeared to be a consequence of equally moderate effects of nitrate uptake and calcification which had cancelled each other out.

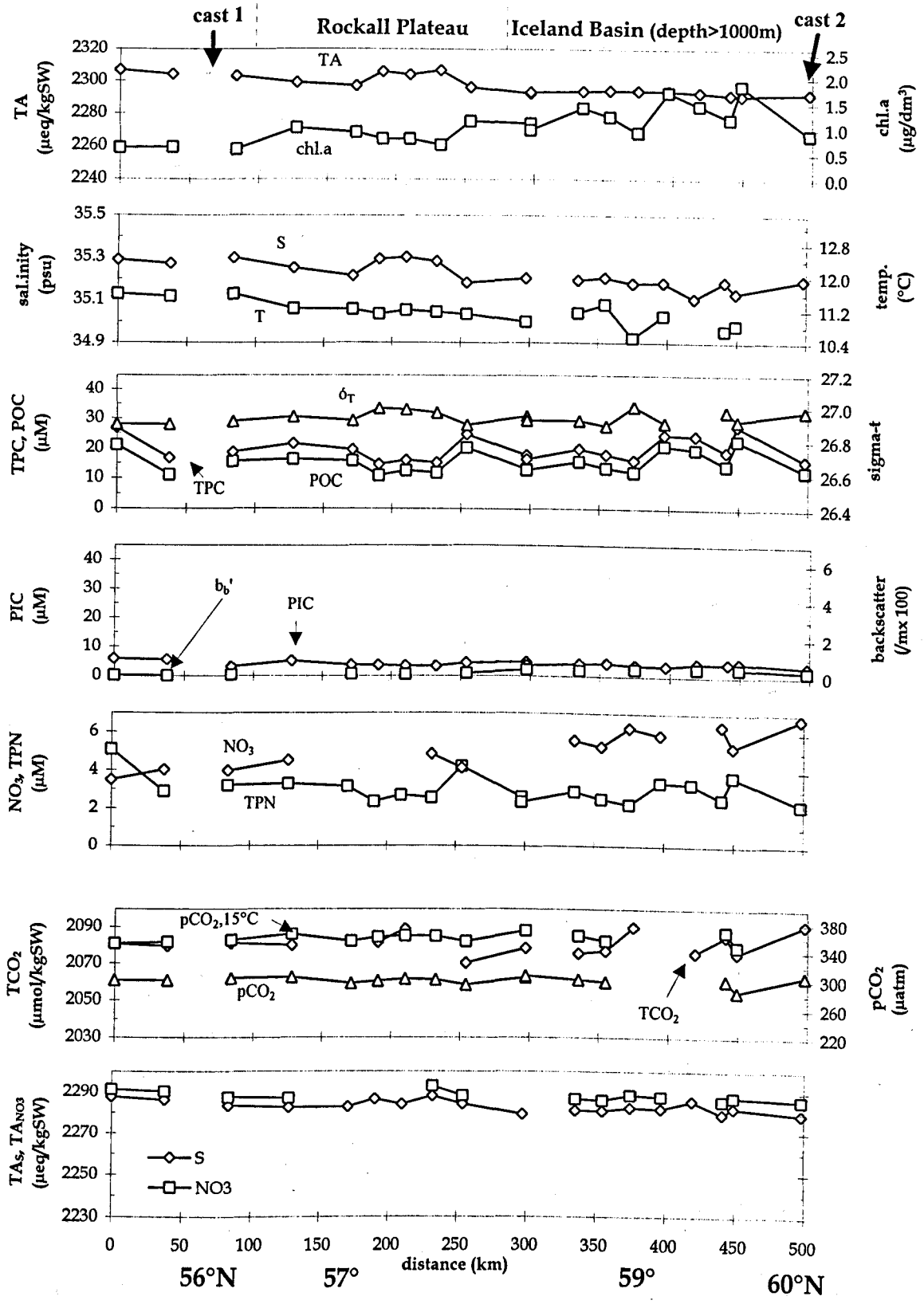

Figure 5.5: Surface (2-3 m) profiles of various in situ parameters along 20°W transect 2 (55°30' to 60°N) from the 1991 Study conducted 16 to 19 June. TA and derived parameters were determined by photometry. PCO_2 is also expressed at 15°C. Topographic references are approximate. Positions of depth profiles are indicated.

Continued on next page.

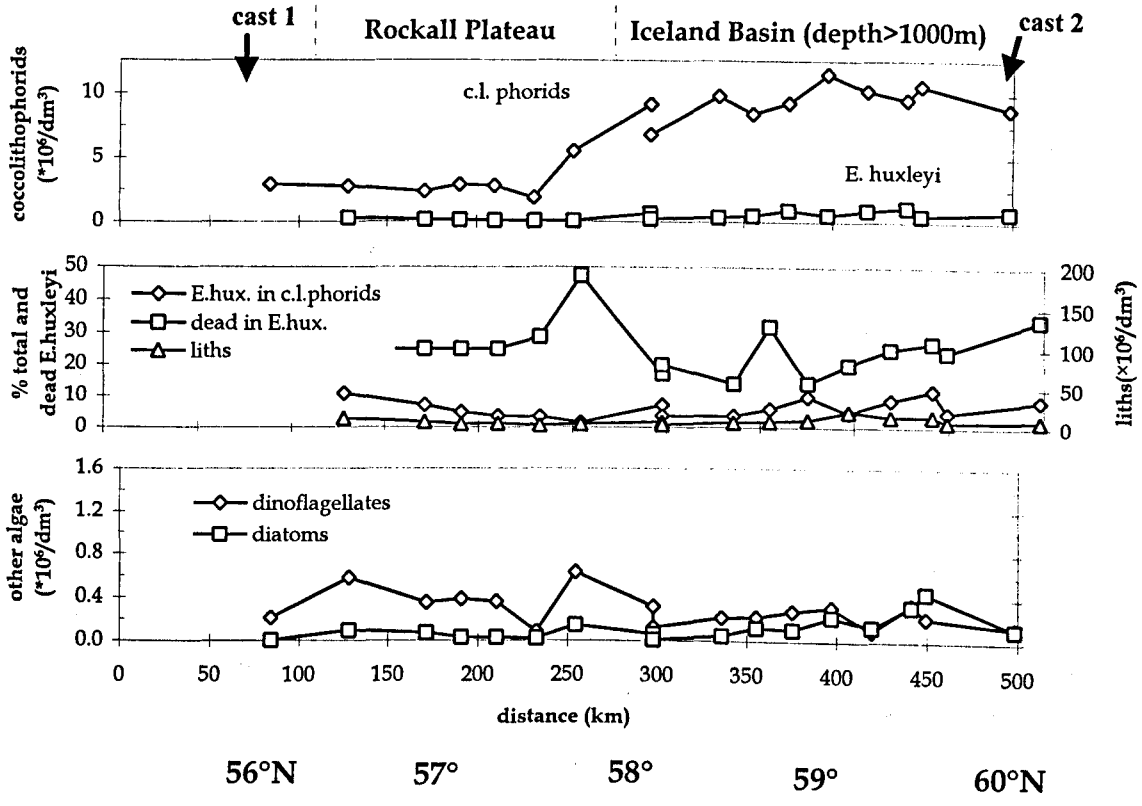

Figure 5.5. continued:

Percentages refer to total (alive and dead) *Emiliania huxleyi* in total coccolithophorid counts, and dead in total *E. huxleyi* counts.

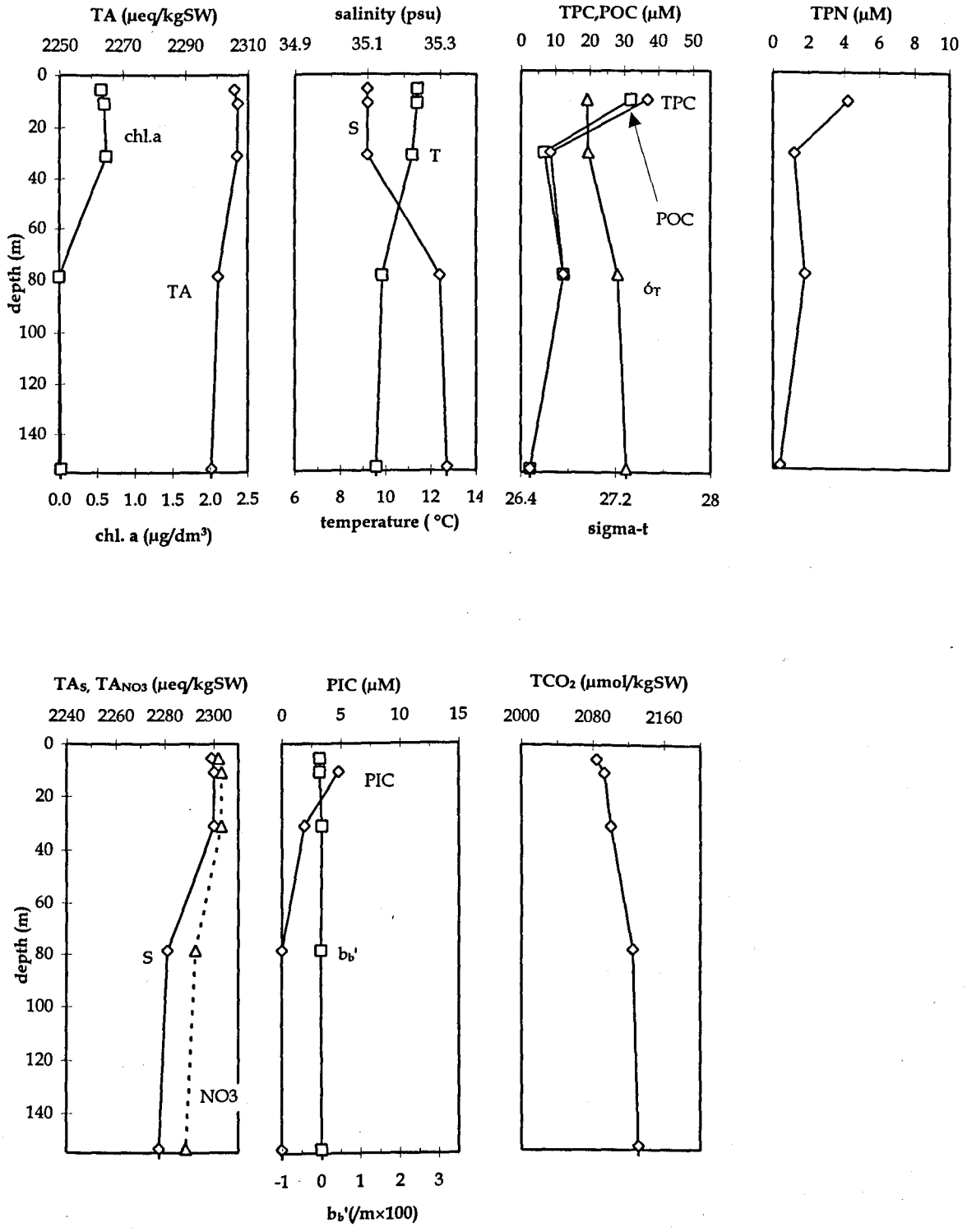

Figure 5.6: Vertical profiles of various in situ parameters measured at station 1 (56°N 20°W) on 17 June during the 1991 Study.
TA and derived parameters were determined by photometry. TA_{NO3} is based on assumed nitrate concentrations of 4 and 14 µM for the SML and sub-thermocline layer, respectively. The assumptions are described in the text. b_b' is backscatter due to calcite.

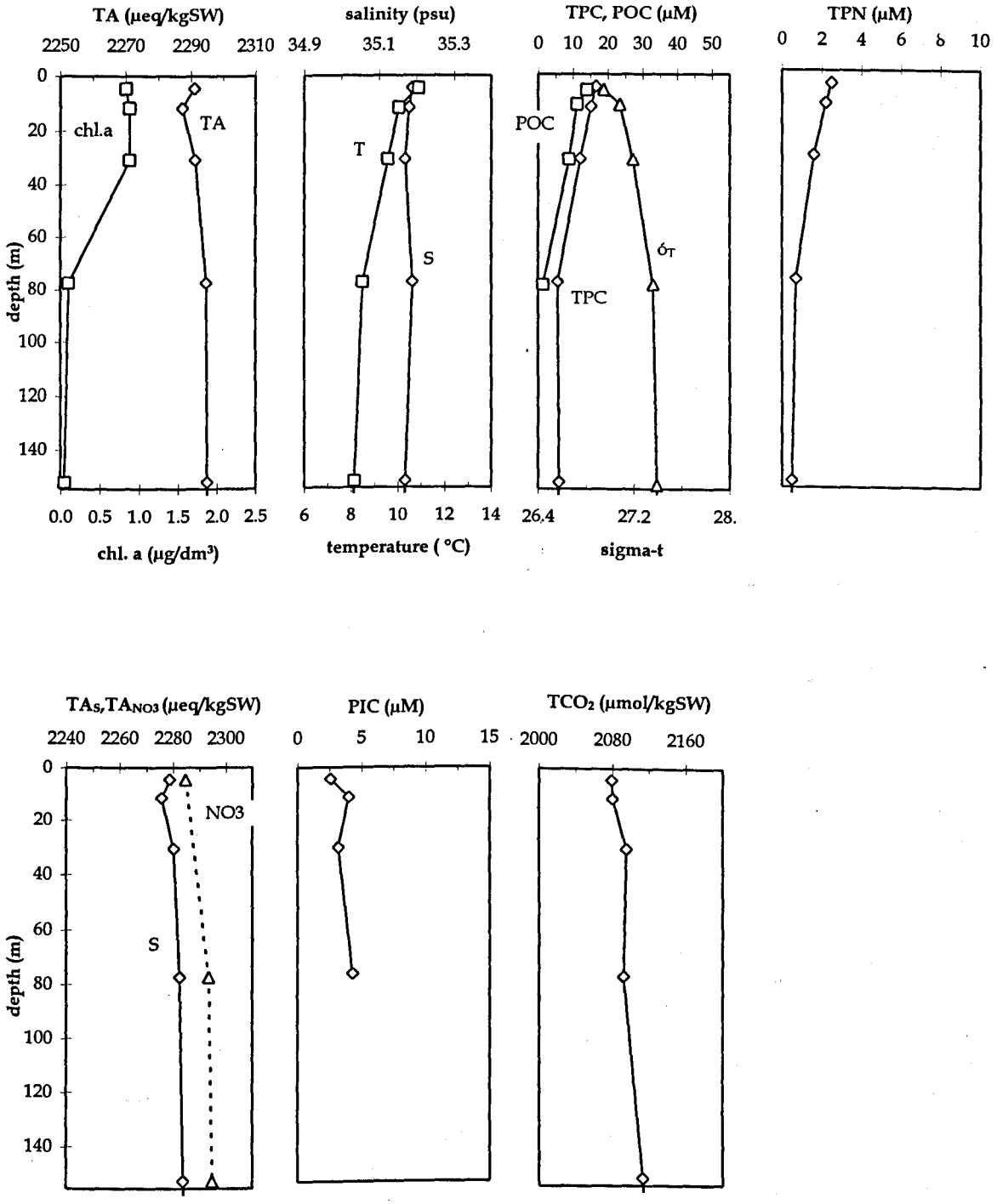

Figure 5.7: Vertical profiles of various in situ parameters measured at station 2 (60°N 20°W) on 19 June during the 1991 Study.
TA and derived parameters were determined by photometry. TA_{NO3} is based on assumed nitrate concentrations of 6 and 11 µM for the SML and sub-thermocline layer, respectively. The assumptions are described in the text.

5.4.3.2.3. 20°W transect 3: 60° - 63°N

Results from the northern 20°W transect are presented in figure 5.8. It was surveyed on 20 to 21 June. This transect led from the Iceland Basin onto the Icelandic shelf after an approximate distance of 150 km. It thereby passed from the eastward flowing NACW regime via the hydrographic transition zone at 61°N into the westward flowing regime of warmer and colder MNAW. The westward flowing zone had already been identified as a high reflectance region in the AVHRR satellite reflectance image and as an area where some of the lowest TA values were recorded during this 1991 Study (figure 5.3.a and c).

Outside the *Emiliania huxleyi* bloom area, i.e. south of 61°N 20°W, TA, salinity, nitrate and PIC were comparable to levels observed towards the northern end of the previous transect just south of 60°N. Upon crossing the hydrographic transition zone at 61°N, salinity decreased slightly, but it remained relatively constant on the Icelandic shelf. It therefore exerted relatively little influence on TA in this region. In contrast, the general northwards increase in PIC, backscatter, and relative and absolute importance of *E. huxleyi* within the coccolithophorid group were well correlated with the notable decrease and fluctuation of TA. The latter amounted to a small-scale decline in TA in the 62°-63°N area of about 40 μeq $kgSW^{-1}$ down to 2240 μeq $kgSW^{-1}$. At the same time, the concentration of PIC reached 30 μM and *E. huxleyi* counts amounted to 2×10^7 dm^{-3}.

This transect clearly demonstrated how a change within the phytoplankton assemblage can have a marked influence on TA. The change from a dominance of other coccolithophorids to one of *Emiliania huxleyi* halfway along the transect is also reflected in the relationship between TA and chlorophyll a, which changed from a positive to a negative one. Furthermore, the negative correlation between TA and pCO_2 in this area further demonstrates the effect of calcification on pCO_2, i.e. pCO_2 showed a relative increase of about 50 μatm while TA decreased by 40 μeq $kgSW^{-1}$. These changes occurred over a distance of about 40 km.

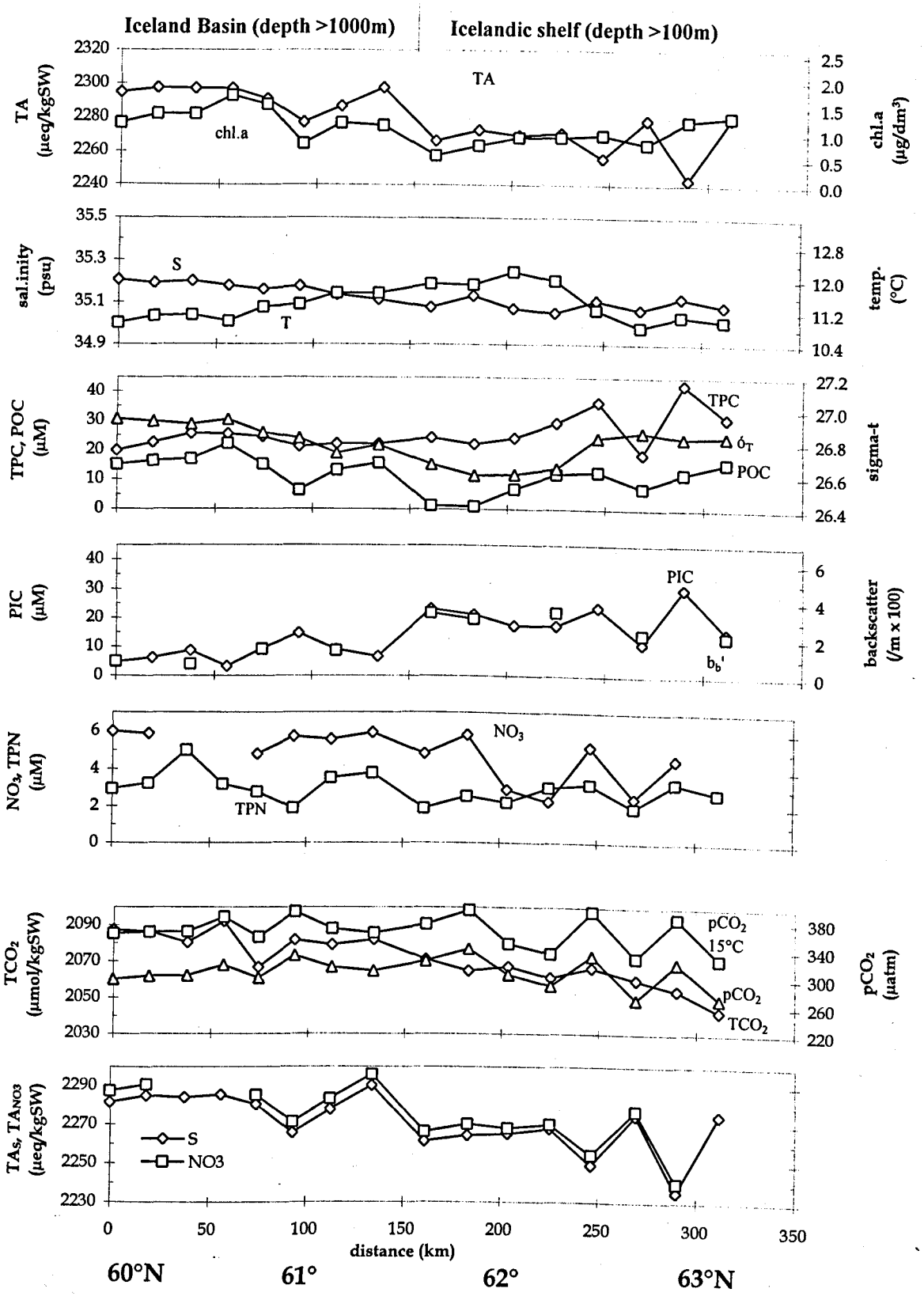

Figure 5.8: Surface (2-3 m) profiles of various in situ parameters along 20°W transect 3 (60° to 63°N) from the 1991 Study conducted 20 to 21 June. TA and derived parameters were determined by photometry. PCO_2 is also expressed at 15°C. Topographic references are approximate. Continued on next page.

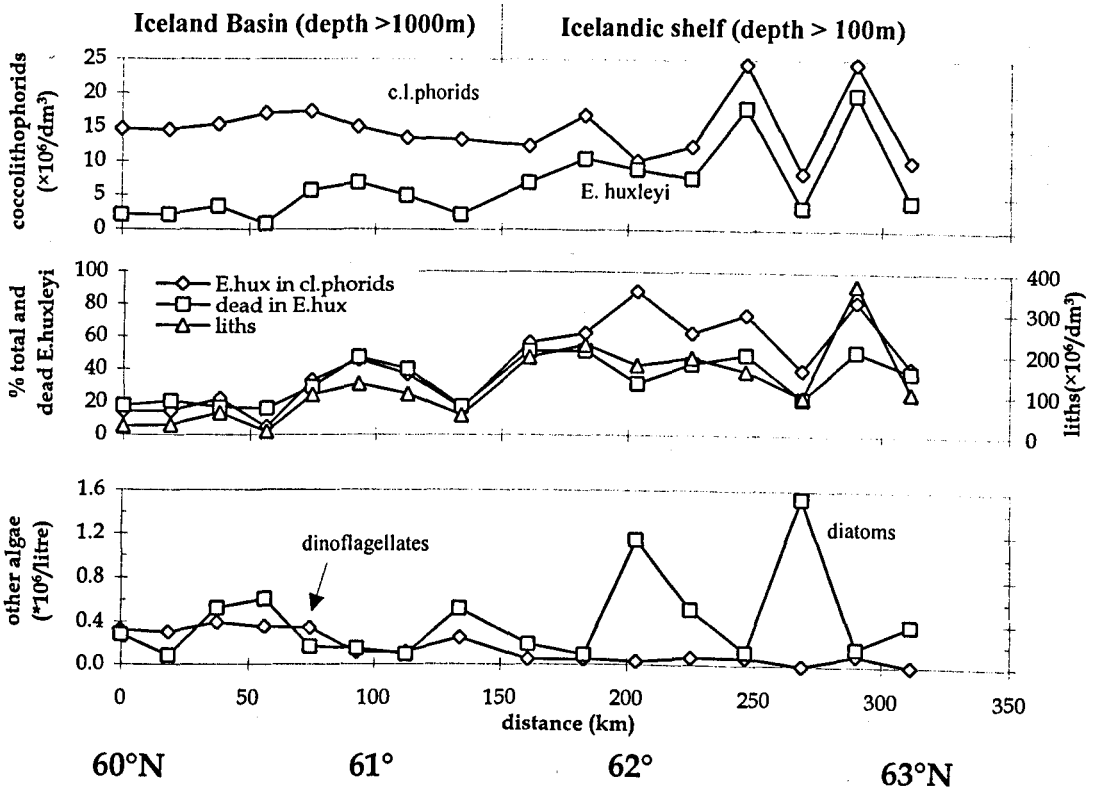

Figure 5.8. continued:

Percentages refer to total (alive and dead) *Emiliania huxleyi* in total coccolithophorid counts, and dead in total *E. huxleyi* counts.

The scales are different to those from transect 2 in the upper two graphs.

5.4.3.2.4. 22°W transect 4: 63°-61°N

This transect, which was investigated on 21 to 22 June, started off in coastal waters on the Icelandic shelf about 100 km west of the Westman Islands where water depth was still less than 100 m. It led into the Iceland Basin about halfway along the transect. Results from this transect are shown in figure 5.9. Compared to similar latitudes at 20°W, the water was about 1°C colder, and therefore more comparable to the low temperature, low salinity MNAW at the northern end of the 20°W survey track.

Reflectance in the AVHRR satellite image from 19 June was low at the shallow end of this transect but increased notably towards 61°N where it declined again. This trend was largely reflected in TA which started off and ended up at around 2280 μeq $kgSW^{-1}$ while ranging between 2240 and 2270 μeq $kgSW^{-1}$ in the high reflectance bloom area. Salinity variations had little effect on the areal TA profile except in the near coastal waters where it was lower. Nitrate concentrations were limiting at stations close to the coast and between 2 to 5 μM along the rest of the transect. These variations had a relatively negligible effect on the observed TA range. In contrast, PIC concentrations were relatively high, i.e. 20 μM or higher along the transect, but declined steadily to zero over the southernmost 50 km. This matches the TA_{NO3} increase of about 40 μeq $kgSW^{-1}$, hereby providing further evidence for the paramount importance of calcification on TA and thus pCO_2 at these latitudes. Accordingly, clear opposite trends between TA and temperature-corrected pCO_2 were observed along this transect.

Depth profile 3

Results from CTD station 3 which was conducted on 21 June are presented in figure 5.10. This site lies about 100 km south of the Iceland coast and about 50 km north of the northern end of transect 4. Temperature was relatively constant within the upper 10 m. A sharp but steady decline occurred between 10 and 50 m. In stark contrast, salinity increased sharply between 10 and 20 m. This resulted in a sharp pycnocline below 10 m, which suggests that freshwater from the coast may have been largely isolated within the upper 10 m. Maxima of PIC and chlorophyll a were measured at sub-SML depths of 20/30 m, where the hydrography was more typical of open ocean sites. Consequently, freshwater influences seemed to have lowered TA in the upper 10 m by about 50 μeq $kgSW^{-1}$. Estimates of the influences involving nitrogen utilization are more complicated at this site without any

nitrate data, but from the TPN profile it may be concluded that nitrogen metabolism did not affect TA by more than a few microequivalents. A comparison of TA_S and PIC profiles suggests that the TA_S decrease of about 15 μeq $kgSW^{-1}$ between 10 and 20 m could be largely accounted for by the increased PIC concentration between these two depths. At 50m PIC declined to negligible concentrations, but TA_S did not change much.

This station was found in a low reflectance area within the AVHRR satellite image from 19 June. Total alkalinity and PIC data have provided evidence for a significant amount of calcification at this site. However, this occurred at greater depths below the low-salinity and low-density SML. In spite of the calcification-induced reduction of TA at 20 m, the main influencing factor on the TA profile was the sharp gradient in salinity between surface and sub-surface depths.

Depth profile 4

On 24 June, two days after completion of transect 4, a high resolution CTD cast was conducted in the Iceland Basin close to 61°N 23°W. The station was about 40 km west of the southern margin of the high PIC patch observed along the transect where also the productivity experiments were carried out. The most proximate sampling site along transect 4 is marked in figure 5.9. Results from the cast are presented in figure 5.11. The thermocline occurred between 10 and 70 m. The TA in the SML was 2260 μeq $kgSW^{-1}$, chlorophyll a exceeded 1 μg dm^{-3} and PIC was 10 μM. However, the highest chlorophyll and PIC concentrations occurred within the thermocline reaching 1.5 μg dm^{-3} and 15 μM, respectively. These maxima were also reflected in slightly reduced TA. Below the thermocline at 70 and 100 m, there was still some chlorophyll and PIC present, albeit in low concentrations. This indicates that some loss by sinking or zooplankton migration from the euphotic zone had occurred. Total alkalinity was higher by 30 μeq $kgSW^{-1}$ at sub-thermocline depths. Profiles of TA and TA_S were similar due to the fairly unaltered salinity with depth. Assuming a nitrate concentration of 4 μM for the SML and a concentration of 11 μM for sub-thermocline depths, nitrate uptake would have raised TA by about 7 μeq $kgSW^{-1}$ in the SML. This was relatively insignificant when compared to the calcification effect. Estimates of TA_{NO3} were about 35 μeq $kgSW^{-1}$ lower in the SML, which approximately ties in with the PIC concentrations in the SML and the small fraction already lost to greater depths.

This station therefore clearly demonstrated the considerable effect of calcification on vertical profiles within the *Emiliania huxleyi* bloom since most of the TA reduction could be accounted for by equivalent amounts of PIC in the SML.

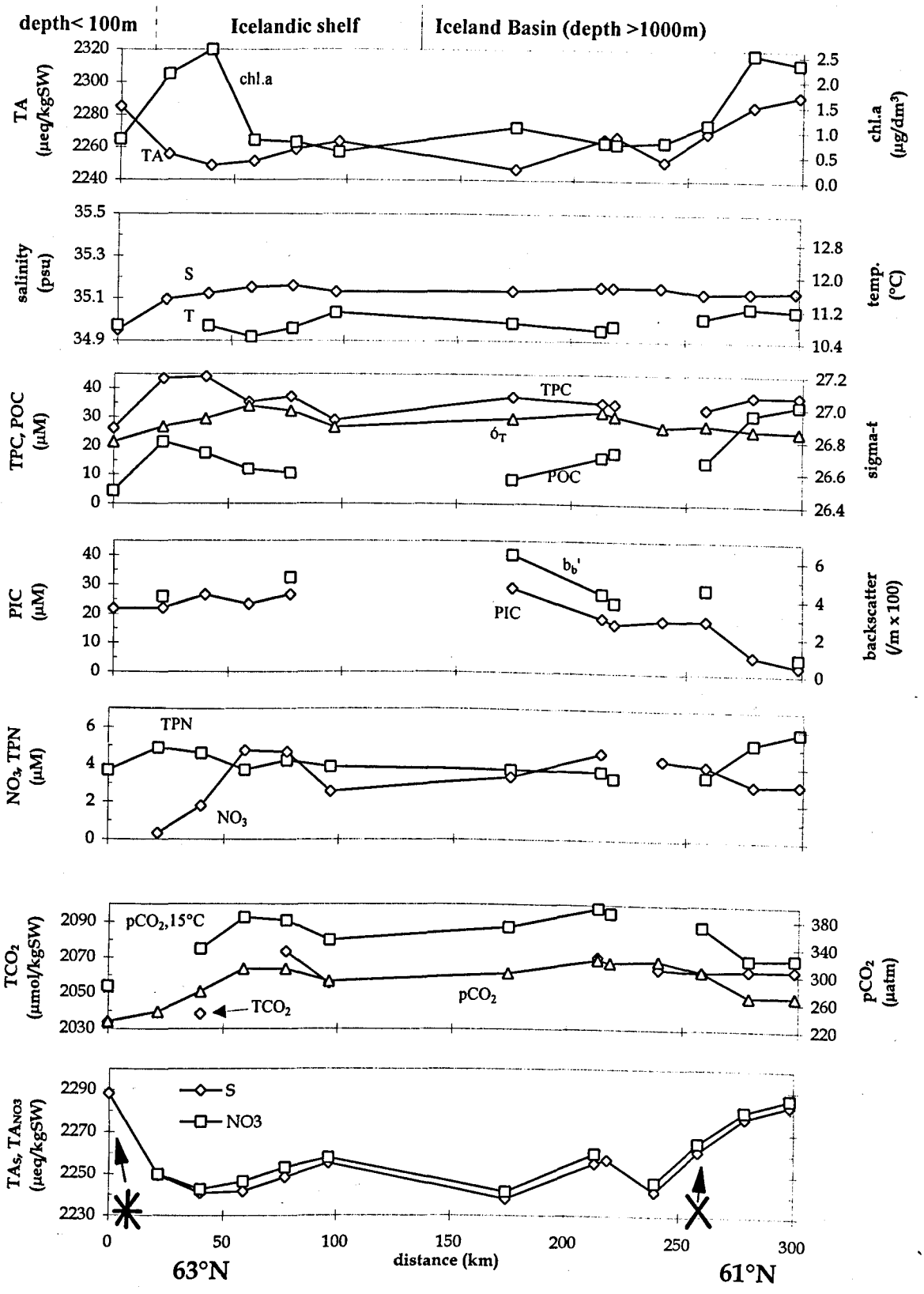

Figure 5.9: Surface (2-3 m) profiles of various in situ parameters along 22°W transect 4 (63°30'N to 60°50'N) from the 1991 Study conducted 21 to 22 June. TA and derived parameters were determined by photometry. PCO_2 is also expressed at 15°C. Topographic references are approximate. Positions marked with a star and cross are close to CTD stations 3 and 4, respectively.

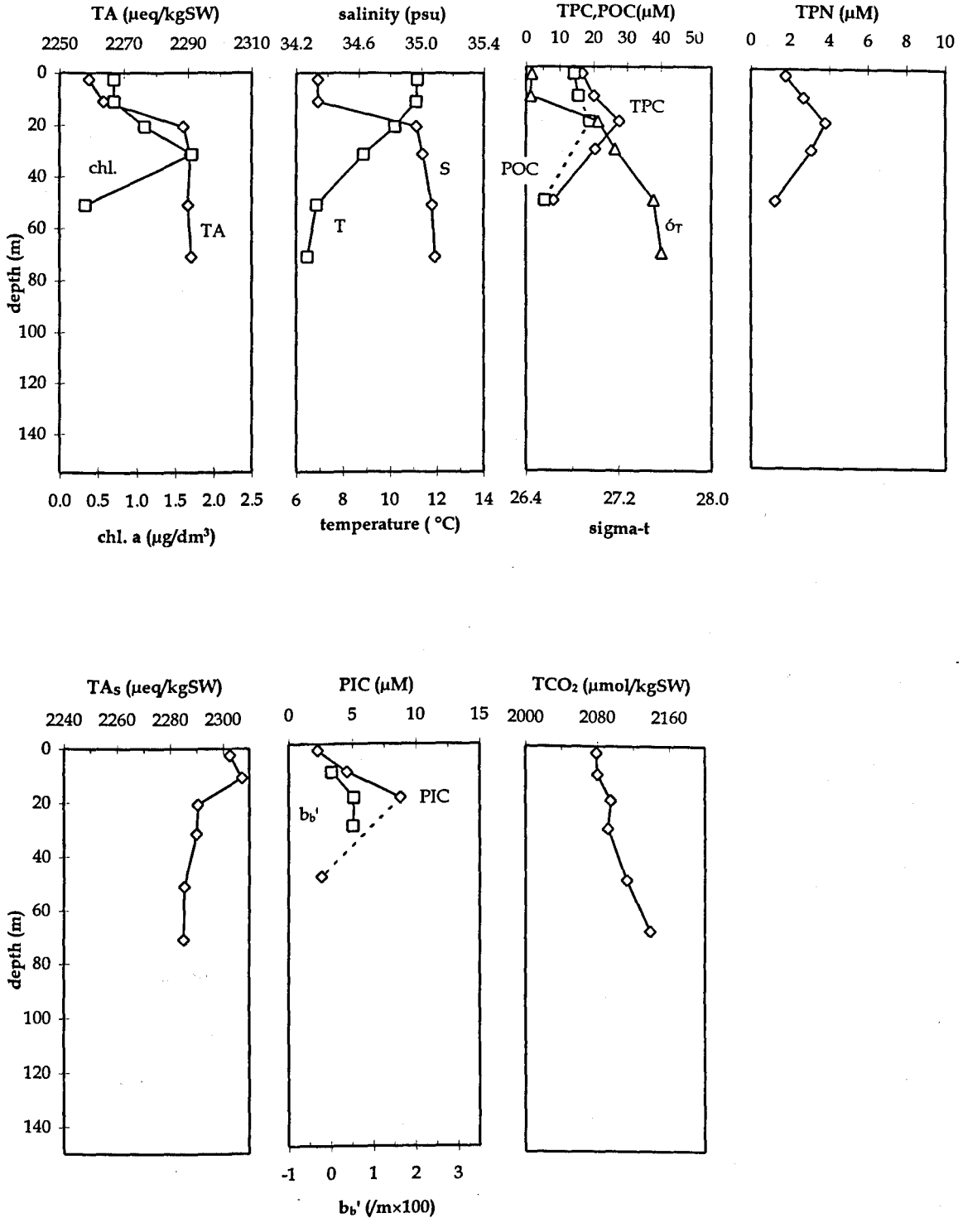

Figure 5.10: Vertical profiles of various in situ parameters measured at station 3 (63°35'N 21°20'W) 21 June during the 1991 Study. Water depth was less than 80 m.
TA and TAs were determined by photometry. b_b' is backscatter due to calcite.
Broken lines indicate that results for certain sampling depths are missing.

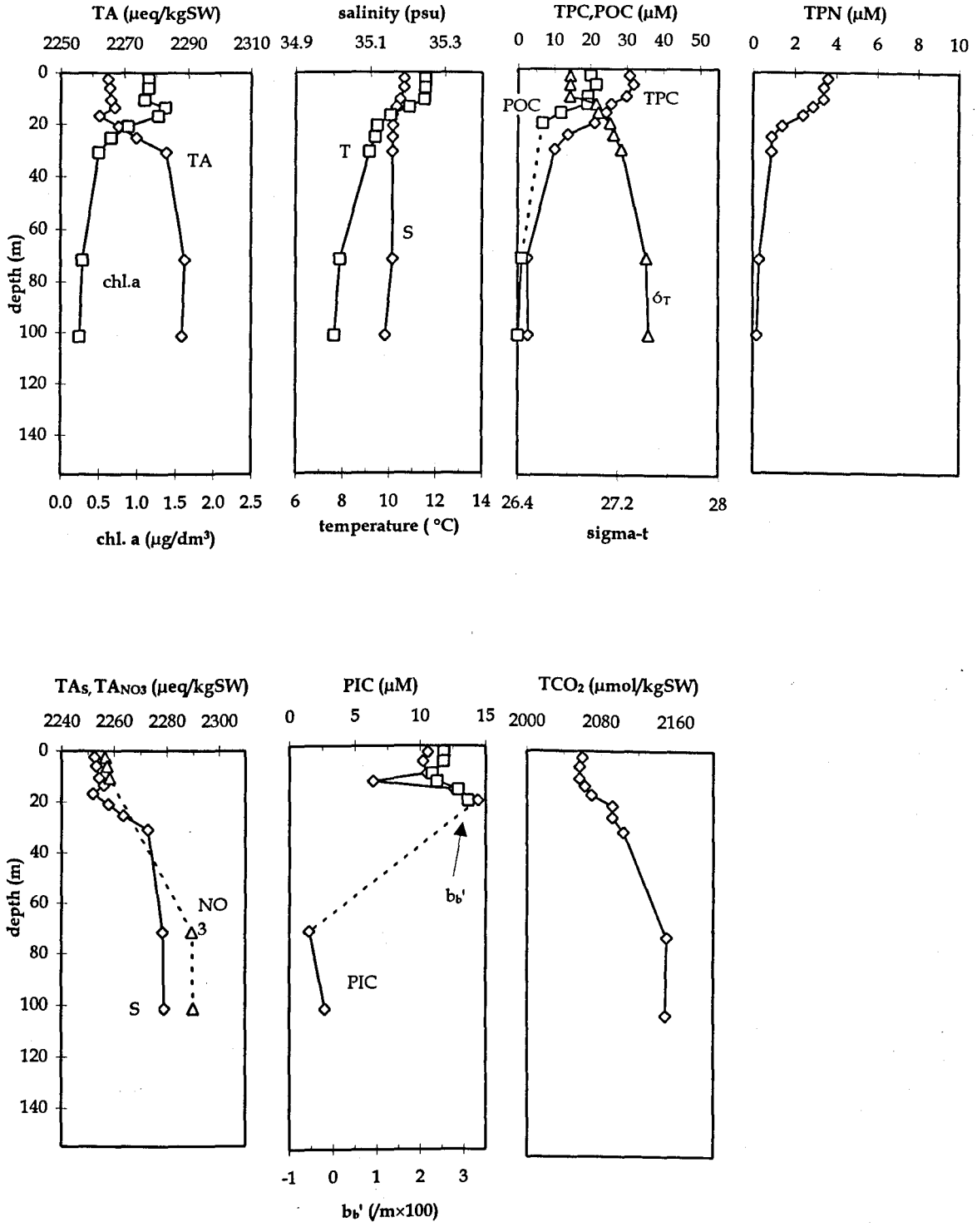

Figure 5.11: Vertical profiles of various in situ parameters measured at station 4 (61°10'N 23°W) on 24 June during the 1991 Study.
TA and derived parameters were determined by photometry. TA_{NO3} is based on assumed nitrate concentrations of 4 and 11 µM for the SML and sub-thermocline layer, respectively. The assumptions are described in the text. b_b' is backscatter due to calcite. Broken lines other than for TA_{NO3} indicate that results for certain sampling depths are missing.

5.4.3.2.5. 61°N transect 5: 20° - 14°W

Results from transect 5 conducted on 27 June are presented in figure 5.12. This transect ran through the eastern part of the Iceland Basin along the hydrographic transition zone which had been identified at 61°N 20°W one week earlier. In contrast to the previous week, salinity was higher, so that all the waters sampled along this transect qualified as NACW. A northward shift of the front between NACW and MNAW seemed to have occurred over one week, at least at the surface. This may explain the changes in temperature and TA near 60°N 20°W since 20 June when this area was first surveyed. Over the course of a week, temperature had increased, density had fallen, and TA had increased by 8 μeq $kgSW^{-1}$. Along the remainder of this transect two patches of high-temperature NACW were crossed.

For much of the transect, TA was comparable to values measured in waters of lower temperature, lower salinity NACW along transects 1 and 2, i.e. it ranged between 2290 and 2305 μeq $kgSW^{-1}$. A notable exception to this was measured at around 61°N 16°W, where it fell briefly to about 2270 μeq $kgSW^{-1}$. This site of high PIC and low TA matched the high reflectance patch in the AVHRR satellite image from 25 June (figure 5.3.c). The available data from salinity and nitrate concentrations suggests that changes in salinity and nitrate uptake were relatively insignificant in determining the TA pattern. Instead, PIC data provided evidence for compatible calcification, i.e. PIC exceeded 15 μM at 61°N 16°W while it remained below 10 μM elsewhere along the track.

Depth profile 5

Depth profile 5 at 61° 10'N 14° 50'W was conducted on 29 June, two days after the completion of transect 5. This site was positioned approximately 30 km further east from the eastern end of the transect. According to the satellite image from 25 June this position was in a low reflectance area. Results from the cast are presented in figure 5.13.

With the resolution of temperature data, the depth of the thermocline could only be narrowed down to somewhere between 2 and 75 m. The considerably higher temperature and salinity at the surface indicated different water masses above and below the thermocline, which indicates that differential advection had occurred. This ties in with the dynamic hydrography already observed along transect 5. At the surface, high concentrations of chlorophyll a suggested considerable recent phytoplankton growth.

Concentrations of PIC and TA were at intermediate ranges of 8 μM and 2290 μeq $kgSW^{-1}$, respectively. These values were similar to the most eastern station of transect 5. Below the thermocline at 75 and 150 m, TA was much the same, while PIC had fallen to below 3 μM and chlorophyll was almost absent. The TA_S profile shows that salinity had raised TA by about 15-20 μeq $kgSW^{-1}$ in the SML. Assuming nitrate depletion at the surface and a winter mixing concentration of 13 μM for sub-thermocline depths, the nitrate effect would have furthered the increase of TA by 13 μeq $kgSW^{-1}$ within the SML. Consequently, TA_{NO3} would have been about 30 μeq $kgSW^{-1}$ lower in the surface. This TA reduction was not matched by the equivalent concentration of PIC. This discrepancy may be partly the result of vertical loss of PIC from the shallower depths which is associated with the advanced stage of the bloom. It is not clear to what extent differential advection had altered this depth profile, though.

The almost constant TA of 2290 μeq $kgSW^{-1}$ with depth down to 150 m is therefore a coincidence as the considerable cumulative effects associated with salinity and nitrate uptake appeared to be cancelled out by the large opposing effect of calcification and/or that of differential advection.

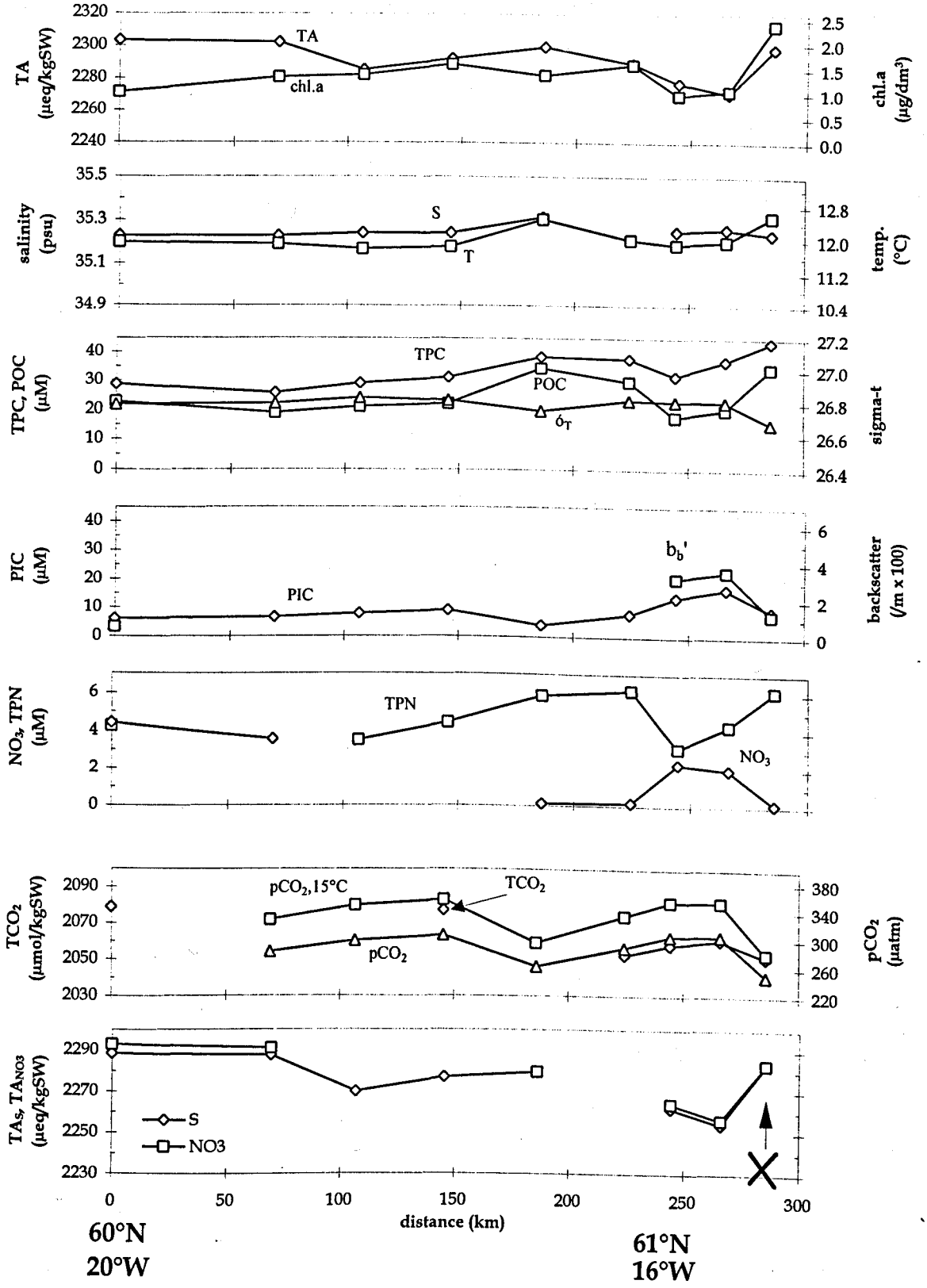

Figure 5.12: Surface (2-3 m) profiles of various in situ parameters along 61°N transect 5 (60°N 19°50'W to 61°10'N 15°10'W) from the 1991 Study conducted 27 June. TA and derived parameters were determined by photometry. PCO_2 is also expressed at 15°C.
The position marked with a cross is close to CTD station 5.

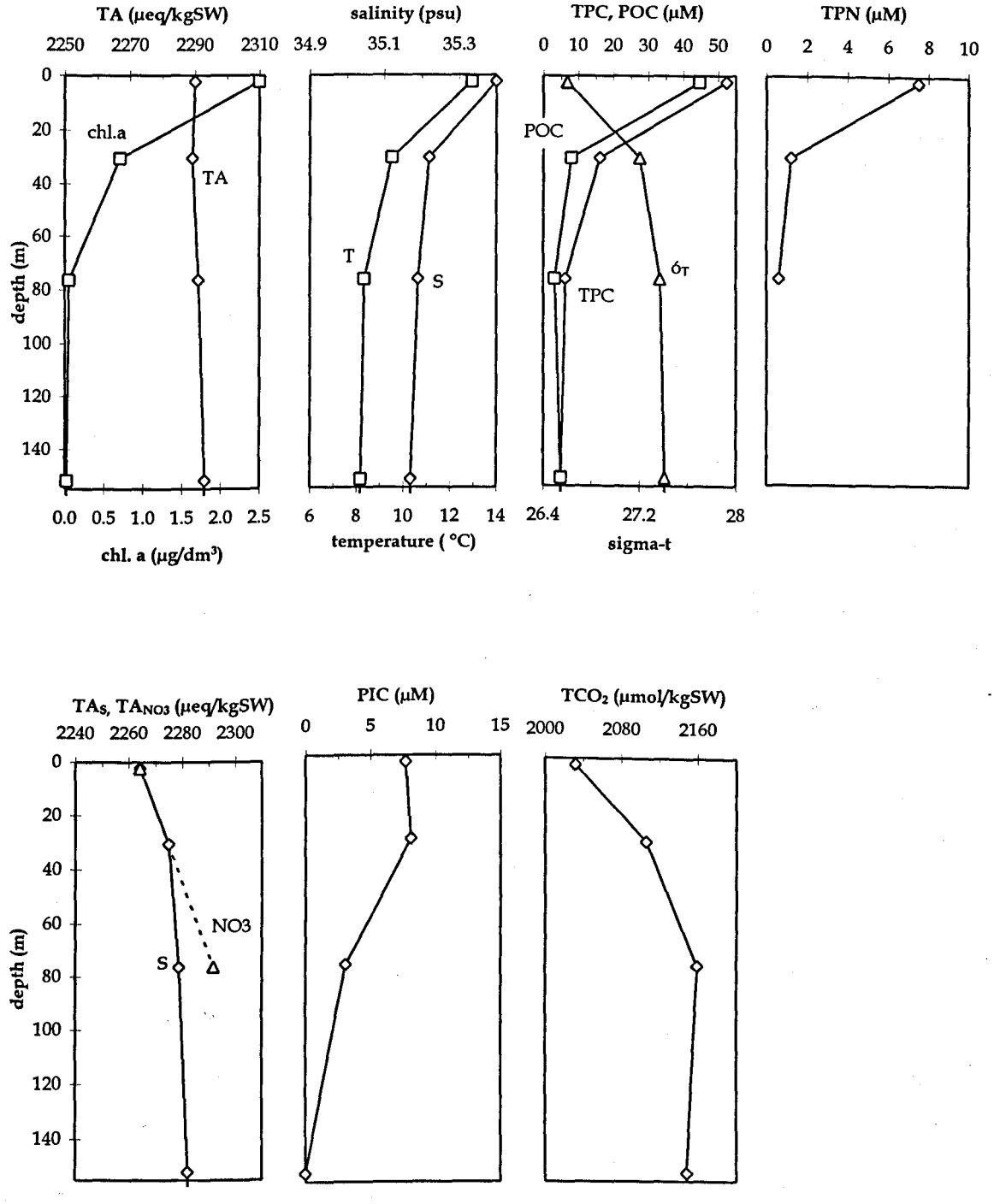

Figure 5.13: Vertical profiles of various in situ parameters measured at station 5 (61°08'N 14°49'W) 29 June during the 1991 Study.
TA and derived parameters were determined by photometry. TA_{NO3} is based on assumed nitrate concentrations of 0 and 13 µM for SML and sub-thermocline layer, respectively. The assumptions are described in the text.

5.4.3.2.6. 15°W transect 6: 62° - 58°N

This eastern transect was conducted 30 June to 31 July leading from the Iceland Basin onto the Rockall Plateau towards Rockall Bank. The AVHRR satellite image from 25 June shows that there were two patches of high reflectance at around 61° and 62°N (figure 5.3 c).

Results from this transect are provided in figure 5.14. Increases in salinity and density suggest a fairly gradual change in the hydrography from the lower to the higher salinity NACW along this stretch, apart from a patch of high-temperature NACW at around 61°N. Both, large and small-scale variations, could also be observed in TA, which showed an overall increase in TA from below 2280 μeq $kgSW^{-1}$ in the northern *Emiliania huxleyi* - dominated waters to 2300 μeq $kgSW^{-1}$ in the southern *Coccolithus pelagicus*-dominated waters. A localized decrease of almost 30 μeq $kgSW^{-1}$ was observed at 61°N in association with the higher-temperature water and high reflectance in the satellite image from 25 June.

The salinity effect only played a minor role in the latitudinal TA trend. Similarly, the effect of nitrate uptake was negligible, as nitrate concentrations remaining largely below 2 μM. The resulting increase in TA_{NO3} between 62° and 58°N of about 20 μeq $kgSW^{-1}$ could partially be accounted for by the decrease in PIC concentrations from approximately 10 to 5 μM. Any remaining discrepancy may have been due to some vertical loss of PIC. This may also provide an explanation for the absence of a localized increase in PIC concentrations at 61°N, which had shown up as a higher reflectance patch in the AVHRR satellite image five days earlier, and where the localized reduction in TA_{NO3} was measured.

Depth profile 6

The final CTD cast during the 1991 study was conducted on Rockall Bank on 1 July. It was positioned about 150 km southeast of the southernmost station of transect 6. Water depth was 180 m. Results from the cast are shown in figure 5.15. The thermocline started at a depth of less than 10 m and ended somewhere between 30 and 100 m. Total alkalinity ranged between 2300 and 2310 μeq $kgSW^{-1}$. Chlorophyll a stayed at about 0.5 μg dm^{-3} at all studied depths down to 50 m, whereas PIC reached a maximum of about 10 μM at the surface and was relatively low at other shallow depths. This peak was discernible in a slight reduction of surface TA, but overall TA changed little with depth. While the almost constant salinity had a negligible effect on the vertical profile of TA, nitrate uptake may

have increased surface TA by 5 to 10 μeq $kgSW^{-1}$, if the surface TPN concentration is used as a measure for this effect. Consequently, potential alkalinity would be about 15 μeq $kgSW^{-1}$ lower in the SML. This gradient was approximately matched by an equivalent increase in PIC in the surface.

Although this station was hydrographically different to the deeper site at station 5, both stations were comparable in having relatively constant TA with depth due to apparently moderate effects of nitrate uptake and calcification which would have cancelled each other out.

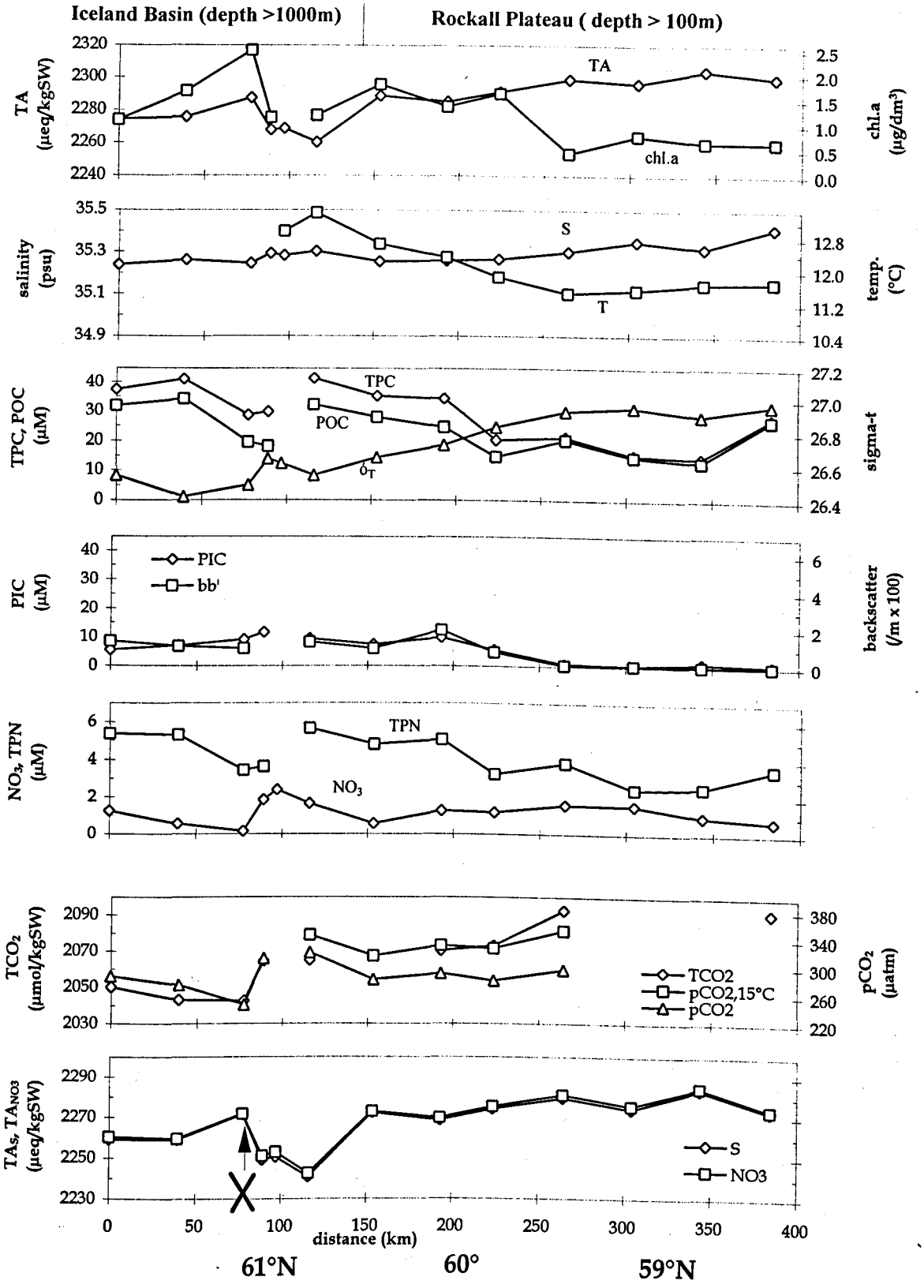

Figure 5.14: Surface (2-3 m) profiles of various in situ parameters along 15°W transect 6 (61°50'N to 58°25'N 14°W) from the 1991 Study conducted 30 June/1July. TA and derived parameters were determined by photometry. PCO_2 is also expressed at 15°C. Topographic references are approximate. The position marked with a cross is close to CTD station 5.

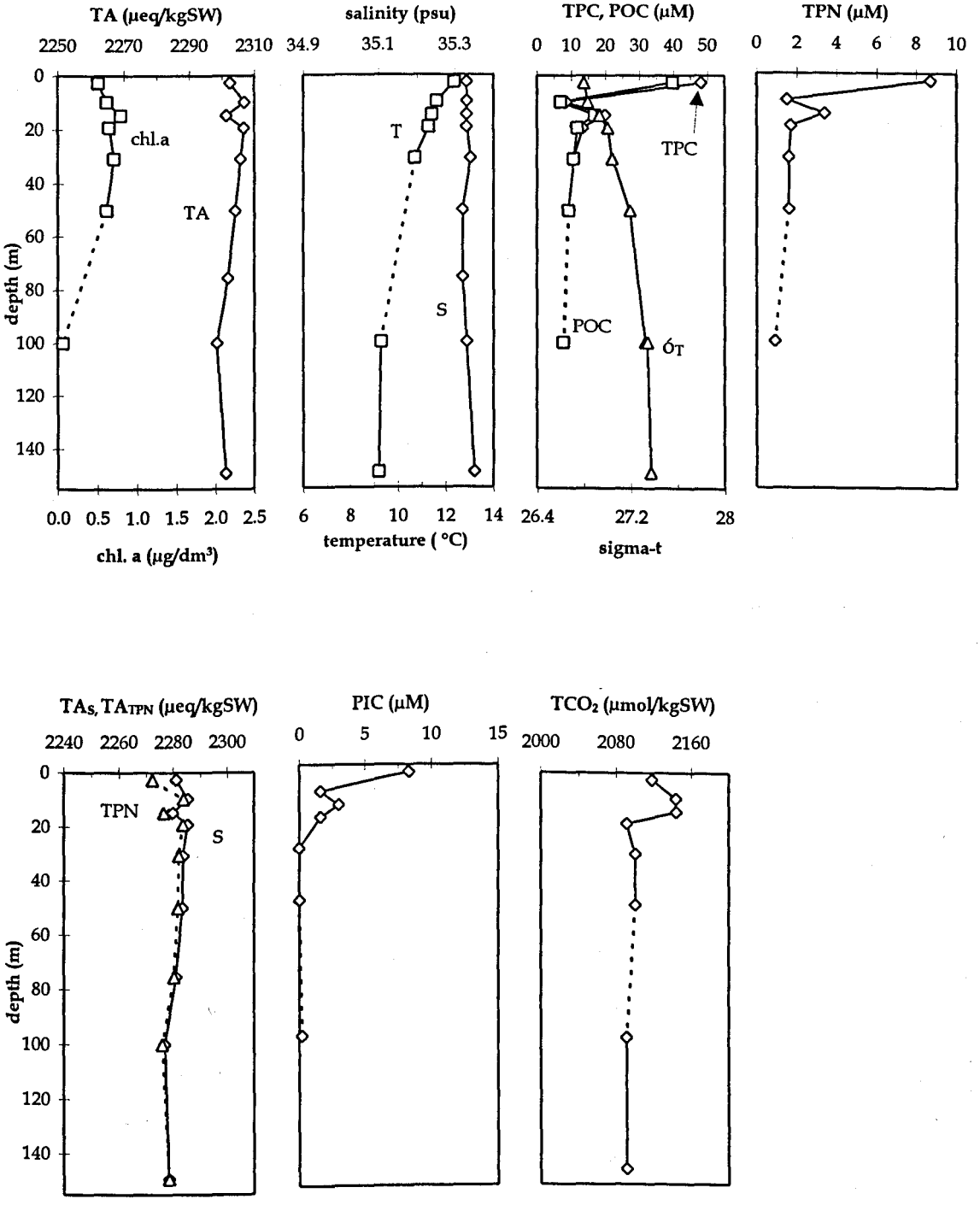

Figure 5.15: Vertical profiles of various in situ parameters measured at station 6 (57°25'N 12°55'W) on 1 July during the 1991 Study. Water depth was about 180 m.
TA and derived parameters were determined by photometry. TA_{TPN} was used instead of TA_{NO3}. It was derived by subtracting the concentration of TPN from TA_S.
Broken lines other than for TA_{TPN} indicate that results for certain sampling depths are missing.

5.4.3.3. Overview of regional distributions of TA, TA_S, and TA_{NO3}

5.4.3.3.1. Surface profiles

The highest TA values during the 1991 Study were encountered in high-salinity NADW along the 55°N transect around 15°W, where also the highest salinities were measured. The highest TA_S and TA_{NO3} were recorded in different water types between 55°-61°N 20°W on 16-20 June and, again, one week later when the area was resurveyed. The lowest TA, TA_S, and TA_{NO3} were observed in different types of MNAW at scattered locations on the Icelandic Shelf at around 63°N 20°-22°W and in the Icelandic Basin at 61°-62°N 22°30'W. At these sites concentrations of PIC exceeded 25 µM. Low TA_{NO3} measurements were also made in NACW along the eastern transects 5 and 6. In the case of transect 6, PIC concentrations amounted to only 10 µM.

The general distribution of photometric TA with latitude and to some extent longitude is summarized in figure 5.16.a. Results from calculated TA shown in part (b) of figure 5.16 will be compared to the photometric results in section 5.4.3.8. A relatively constant decline in TA by about 15 µeq $kgSW^{-1}$ is indicated along the 20°W line between 55° and 61°N, i.e. the area of eastward flowing NACW and MNAW with low satellite reflectance. Results from other transects matched this latitudinal trend, with two exceptions. Average TA along the 55°N transect 1 was generally about 5 µeq $kgSW^{-1}$ greater than would have been expected from the 20°W slope, and TA was up to 30 µeq $kgSW^{-1}$ lower at eastern transect 6. North of 61°N the above latitudinal relationship established along 20°W broke down. Total alkalinity tended to be latitudinally noisy and considerably lower, i.e. ranging from 2300 down to 2240 µeq $kgSW^{-1}$. Within this range, western sites (transect 4) tended to be lower, i.e. below 2270 µeq $kgSW^{-1}$, while eastern sites (transect 6) tended to be higher.

When comparing the areal distribution of TA_S in figure 5.16 with that of TA it becomes evident that the elevated TA along the 55°N transect and the latitudinal decrease along the 20°W line between 55° and 61°N was predominantly caused by the concomitant decrease in salinity. This factor caused a decrease of about 10 µeq $kgSW^{-1}$ between these latitudes. In contrast, salinity had a much lesser effect on the TA further east (transect 6). Here most TA_S values were about 10 µeq $kgSW^{-1}$ lower than along 20°W, and at two of the sites, close to

61°N, TA_S differed from the 20°W trend by 35 μeq $kgSW^{-1}$. North of 61°N, salinity corrections had little overall effect on the spread of TA.

The comparison between areal distributions of TA_{NO3} and TA_S suggests that differences in nitrate uptake had a mostly negligible effect on the regional distribution of surface TA. Nevertheless, increasing nitrate concentrations along the 20°W transect south of 61°N had removed the significant trend observed in TA_S. This implies that the effect of nitrate uptake on TA was slightly lower at latitudes closer to 61°N, and that latitudinal differences in calcification or other TA-reducing factors had been negligible south of 61°N 20°W. However, longitudinal or temporal differences in calcification became apparent along the 15°W transect 6. Here TA_{NO3} was about 10 μeq $kgSW^{-1}$ lower than at 20°W and this difference increased to 45 μeq $kgSW^{-1}$ near 61°N. North of 61°N, small-scale variations along 20°W as well as longitudinal differences in calcification or other factors led to TA variations of up to 60 μeq $kgSW^{-1}$.

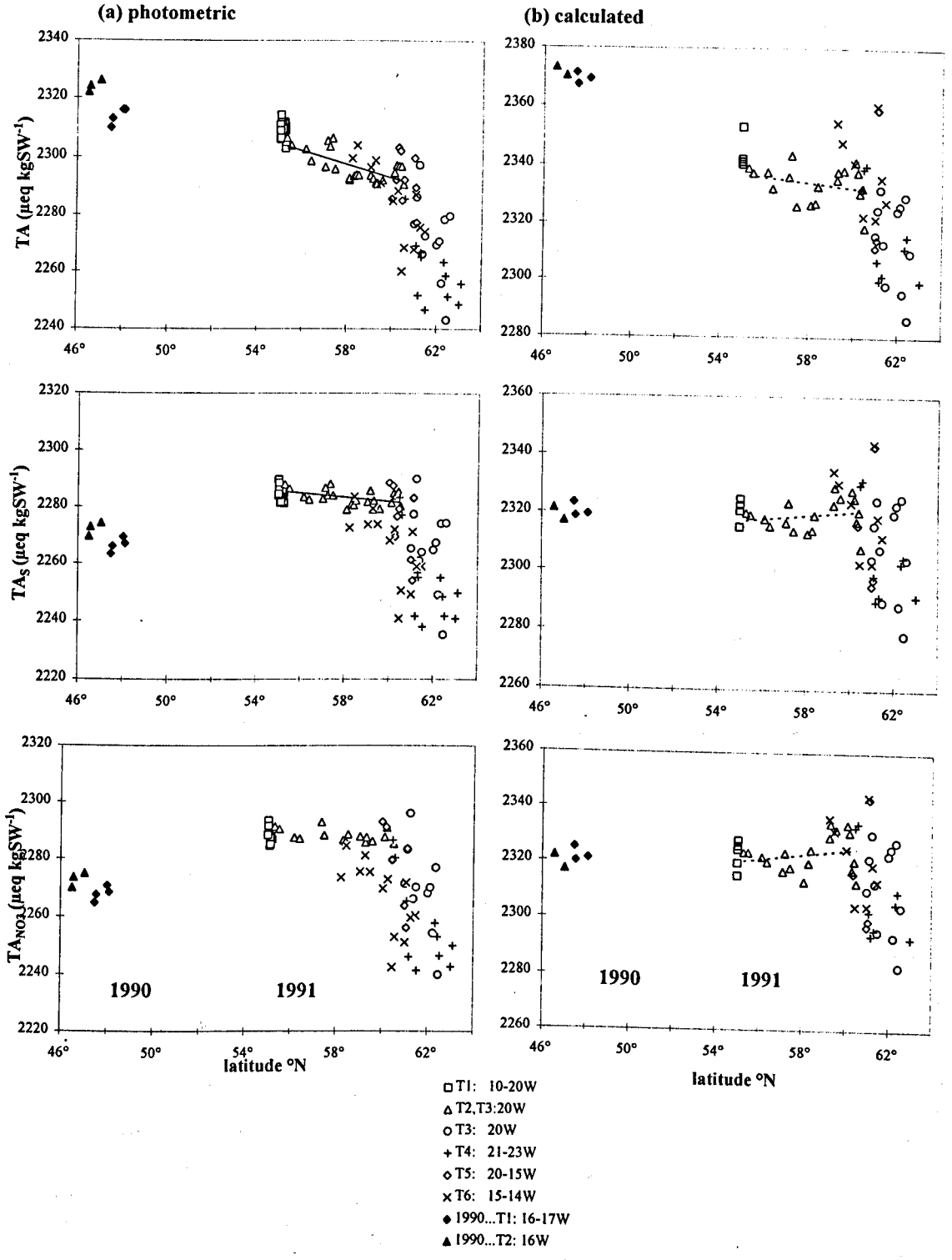

Figure 5.16.: Distribution of TA and derived parameters with latitude from surface samples collected during the 1991 Coccolithophore Bloom Study between 15 June and 1 July and during the 1990 Spring Bloom Experiment between 22 and 24 June. TA was (a) measured by photometry and (b) calculated from pCO_2 and TCO_2. Regional identification was based on transects (T).
Linear least squares regression analyses were carried out on data from the 20°W line south of 61°N (marked as triangles). Only the relationships significant at the 95% confidence level which have been marked with solid lines are given below:

phot.TA = -2.3 (± 0.5) °lat. + 2432 (± 30); n =24; R^2 = 0.48; $s.e._{regr.}$ = 3.8; $P < 0.001$

phot.TA_S = -0.7 (± 0.3) °lat. + 2445 (± 19); n =23; R^2 = 0.18; $s.e._{regr.}$ = 2.5; $P < 0.05$

5.4.3.3.2. Vertical profiles

Regional variation in profiles of TA and related parameters in the upper 150 m are presented in figure 5.17. Results from 1991 show that concentrations of TA below the thermocline were around 2290 μeq $kgSW^{-1}$ between 60°N and Iceland. South of this area, TA was around 2300 μeq $kgSW^{-1}$. Sub-thermocline levels of TA_S and TA_{NO3} were similar at all but the shallow stations, i.e. on the shallow Iceland shelf and on Rockall Bank.

The variability in surface TA and sub-thermocline TA led to equally variable changes of TA across the thermocline. Apart from the two north/northwestern stations 3 and 4 where TA was at least 20 μeq $kgSW^{-1}$ lower above than below the thermocline, TA change across the thermocline did not vary by more than 10 μeq $kgSW^{-1}$ within stations. Comparison of TA and TA_S, and TA_{NO3} profiles demonstrate that nitrate uptake had generally raised surface TA by about 10 μeq $kgSW^{-1}$ at open ocean stations. Apart from that, relative and absolute influences of different factors on TA varied between locations. This is outlined below.

At 60°N 20°W and on Rockall Bank (stations 2 and 6) calcification appeared to be of lesser importance. In addition, vertical changes in salinity and nitrate concentrations were comparatively small, which explains the overall constancy of TA with depth at these sites. At the shallow Iceland shelf station (stations 3), freshwater influences from the nearby coast appeared to have been the main factor for the large reduction of TA in the surface, in spite of considerable calcification within the thermocline which dampened this vertical gradient to some extent. At the 61°N stations (stations 4 and 5) calcification seemed to have occurred in the surface, but this did not become apparent at the eastern station 5 due to compensating effects associated with salinity and nitrate uptake. The only station where high calcification was clearly reflected in the TA and TA_{NO3} profiles was northwestern station 4. Southernmost station 1 was at odds with the other open ocean stations, as surface TA_{NO3} was higher than below the thermocline in spite of some evidence for calcification at the surface. Evidence of differential advection above and below the thermocline indicates that samples from the two depth layers may have originated from different water masses and thus had different calcification histories.

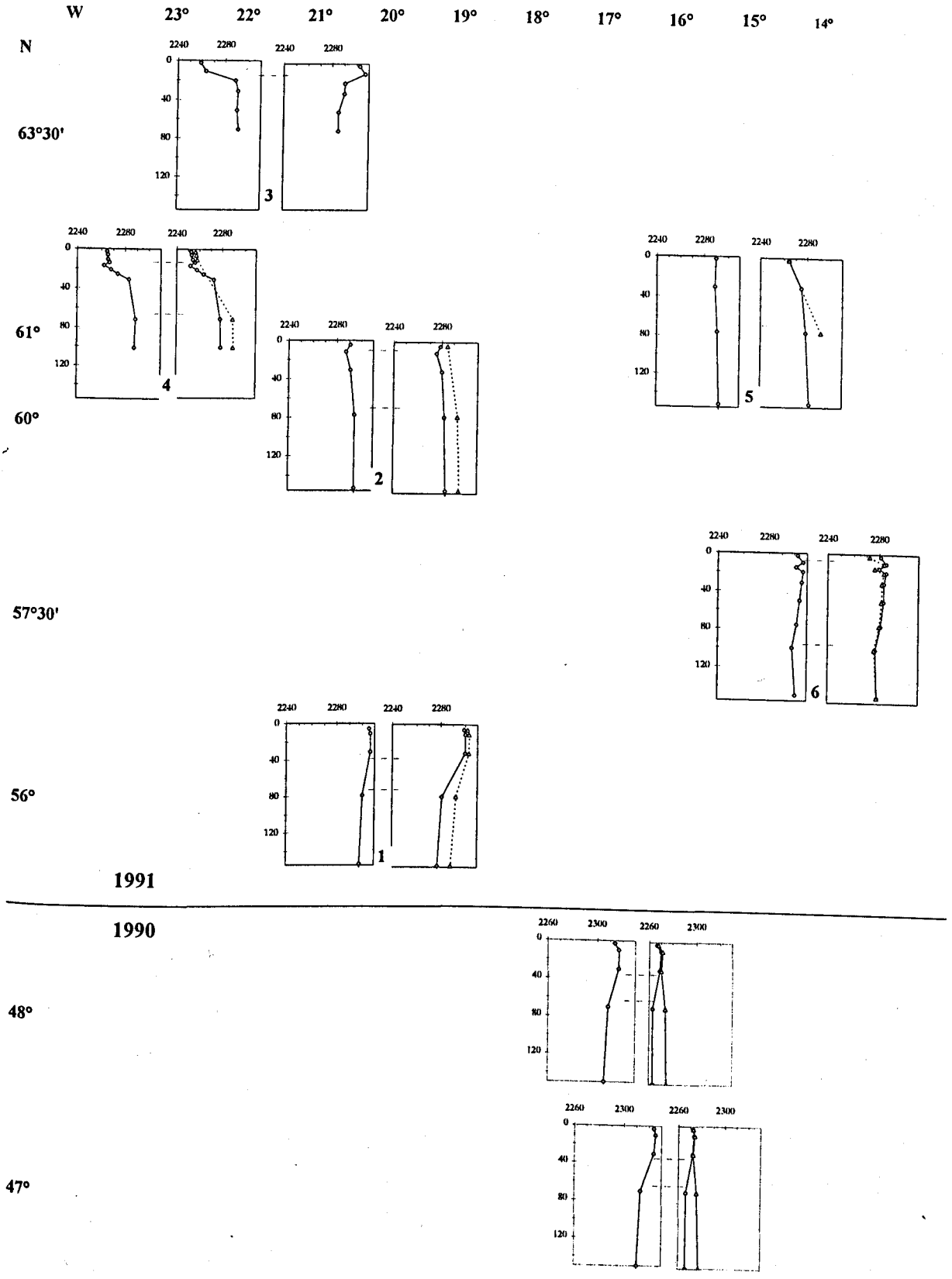

Figure 5.17: Comparison of vertical (m) profiles of TA and derived parameters (μeq $kgSW^{-1}$) in the upper 150 m from different regions of the Northeast Atlantic studied during the 1991 Coccolithophore Bloom Study and the 1990 Spring Bloom Experiment. Station numbers are included.
For each position the left graph shows the TA profile and the right graph depicts the profiles of specific (diamonds) and potential TA (triangles). The methods of deriving potential TA are described in the text. The results for 1990 represent mean values from the northern (N) and southern (S) transects studied that year. They are plotted on a slightly higher scale.
The broken lines between the graphs mark the depth boundaries used to make a distinction between samples from the SML and subthermocline depths. The depth range in between included the thermocline.

5.4.3.4. Correlations of TA and TA_{NO3} with other parameters

Relationships between photometric TA and hydrographic, optical, biological, and chemical parameters are presented in figure 5.18. There was a significant positive correlation between TA and salinity, but this trend was much less defined at lower salinities. No significant relationship was observed with temperature. The clearly negative correlations between TA and PIC, backscatter, and cell and lith counts resulted in a significantly negative correlation between TA and chlorophyll a, although there was considerable scatter in the data. From the PIC and backscatter plots it is apparent that a few data points occurred notably below the regression line. These results came from lower salinity NACW along the 15°W transect 6.

Comparison of the slopes involving counts of coccolithophorids and *Emiliania huxleyi* demonstrates that the latter species was associated with a greater reduction in TA than other coccolithophorid species. The considerable difference between 'total' and live *E. huxleyi* counts emphasizes the potential error that may arise in estimates of calcification quota per cell when dead *E. huxleyi* cells are not included in microscopic counts.

Results from regression analyses of TA_{NO3} against biological and optical parameters are provided in figure 5.19. Conclusive comparisons with regression results involving TA cannot be made since these were based on larger sample sizes. With the data available, it appears that corrections for salinity and nitrate uptake did not have an obvious impact on the relationship between TA and optical or biological parameters, although these corrections tended to reduce the slopes to varying extents. The relationship of TA_{NO3} with PIC of -1.6 (± 0.15) reveals three important points. First of all, it was far less negative than the relationship between TA and PIC. Assuming that TA_{NO3} correctly represented potential alkalinty, this implies that calcification estimates based on TA rather than TA_{NO3} would have on average been overestimated by a factor of 1.4. Secondly, it deviated from the theoretical relationship of -2 between potential alkalinity and PIC by a factor of 1.25. Although this relationship between TA_{NO3} and PIC was found not to be significantly different from the theoretical value when tested at the 95% confidence level, the error on the measured slope would not have included the theoretical value. Assuming no methodological errors, this would imply that the measured PIC concentrations were underestimates of the original amount of PIC that had brought about the TA_{NO3} changes.

The only process which could explain this phenomenon, would be vertical loss of PIC from the samples at 2-3 m. Thirdly, the outliers observed in the above relationship of TA versus PIC also tended to fall notably below the TA_{NO3} versus PIC regression line, i.e. they could not be explained by abnormal salinity or nitrate concentrations specific to these samples.

The difference between the measured and expected relationship of TA_{NO3} and PIC which was established above, may be used as an estimate of the average amount of PIC loss that had occurred, i.e. 20%. This information was applied to the relationship that had been established between TA_{NO3} and *Emiliania huxleyi* counts (figure 5.19), so that calcification quota per *E. huxleyi* cell could be derived which are corrected for sinking and removal by herbivory. The loss-adjusted relationship was:

$$TA_{NO3}\ (\mu eq\ kgSW^{-1}) = -1.8\ \ E.huxleyi\ (10^6\ dm^{-3}) - 2290.$$

This implies that 10^6 *E. huxleyi* cells dm^{-3} lowered TA by 1.8 μeq $kgSW^{-1}$, which translates to PIC production of about 0.9 μmol dm^{-3}.

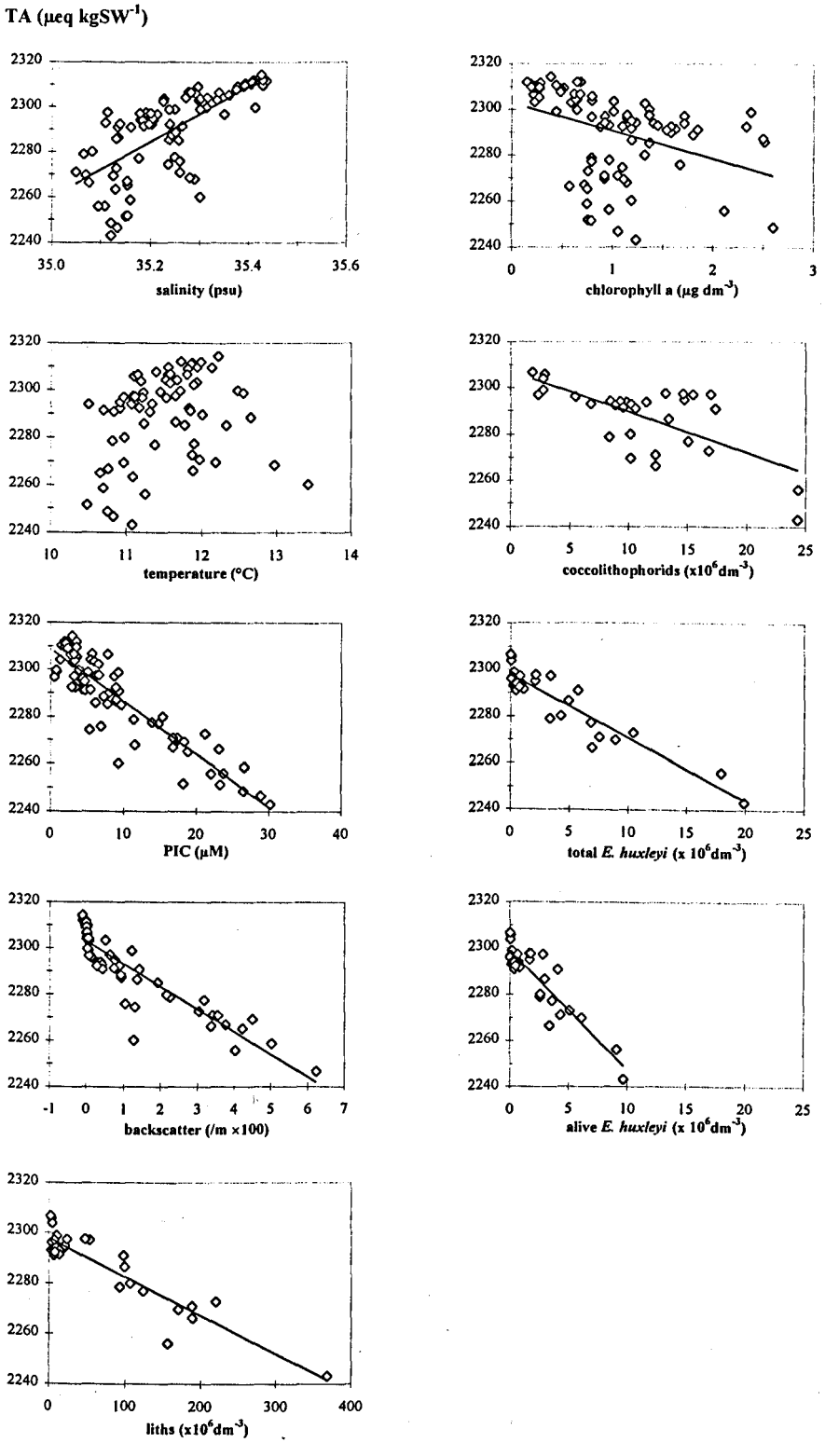

Figure 5.18: Relationships of photometric TA with hydrographic, optical, biological, and chemical parameters measured in surface samples during the 1991 Study in the North East Atlantic. Samples from sites where water depth was < 100m are exluded . Regression results and statistical information are:

TA = 124 (± 14) sal.-2092 (± 476); n = 87; R2 = 0.50; s.e.regr. = 13.2; P< 0.001
TA = -2.2 (± 0.12) PIC+2309 (± 1.3); n = 87; R2 = 0.81; s.e.regr. = 8.0; P< 0.001
TA = -9.8 (± 0.6) b'scatter+2303 (± 1.2); n = 59; R2 = 0.81; s.e.regr. = 7.4; P< 0.001
TA = -0.15 (± 0.012) liths +2298 (± 1.3); n = 32; R2 = 0.85; s.e.regr. = 5.7; P< 0.001
TA = -12.1 (± 3.2) chl.+2302 (± 3.7); n = 87; R2 = 0.15; s.e.regr. = 16.9; P< 0.001
TA = -1.7 (± 0.34) clphorids+2307 (± 4); n = 32; R2 = 0.46; s.e.regr. = 10.8; P< 0.001
TA = -2.7 (± 0.20) E. hux. +2297 (± 1.2); n = 32; R2 = 0.85; s.e.regr. = 5.6; P< 0.001
TA = -5.1 (± 0.44) aliveEhux+2299 (± 1.5); n = 32; R2 = 0.82; s.e.regr. = 6.3; P< 0.001

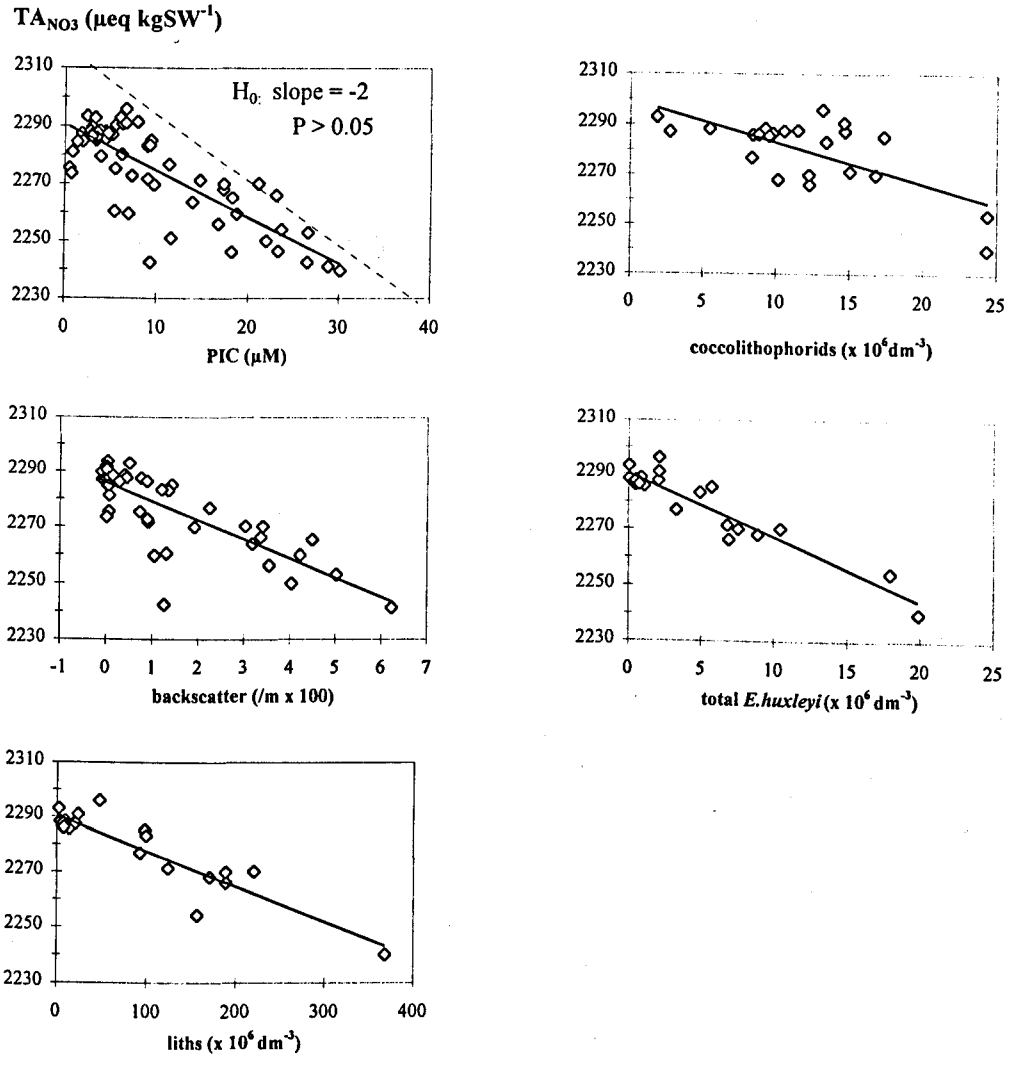

Figure 5.19: Relationships of photometric TA_{NO3} with optical and carbonate-related biological parameters measured in surface samples during the 1991 Study in the North East Atlantic. Samples from sites where water depth was < 100m are exluded.
In the case of PIC, the significance of the slope was tested against null hypothesis = -2.
The broken line in the PIC plot indicates the relationship of -2, which is be expected from the effect of PIC production on potential alkalinity.
Results from linear least squares regression analyses and additional statistics are:

TA_{NO3} = -1.6 (± 0.15) PIC+2291 (± 1.8); n = 64; R^2 = 0.65; s.e.regr. = 9.4; **$H_{0:\,slope}$=-2; P>0.05**
TA_{NO3} = -6.7 (± 0.8) b'scatter+2286 (± 1.7); n = 44; R^2 = 0.62; s.e.regr. = 8.7; P< 0.001
TA_{NO3} = -1.7 (± 0.38) clphorids+2300 (± 5); n = 23; R^2 = 0.47; s.e.regr. = 10.0; P< 0.001
TA_{NO3} = -2.3 (± 0.18) E. hux. +2290 (± 1.3); n = 23; R^2 = 0.88; s.e.regr. = 4.7; P< 0.001
TA_{NO3} = -0.12 (± 0.012) liths +2290 (± 1.5); n = 23; R^2 = 0.84; s.e.regr. = 5.6; P< 0.001

5.4.3.5. Estimation of regional differences in PIC loss from surface samples

While it was obvious that considerable calcification had occurred in areas with high PIC concentrations, it was desirable to identify areas where significant calcification and subsequent PIC loss from 2-3 m to any greater depth had taken place in days or weeks prior to sampling. The plot of 'PIC loss' (TA_{NO3} + 2 [PIC]) based on photometric TA measurements against latitude is presented in figure 5.20.a. Results from calculated TA in part (b) of that figure will be compared to the photometric results in section 5.4.3.8. It is important to bear in mind that this term did not necessarily imply that PIC would be lost from the SML altogether.

Apart from eastern transect 6, PIC loss varied within about 25 μeq $kgSW^{-1}$. The least amount of PIC loss was observed north of 61°N 20°W (transect 3). At transect 6, PIC loss was 10 to 50 μeq $kgSW^{-1}$ greater than along the other transects. The greatest loss out of that range was observed in lower salinity NACW which were already identified as abnormally low data points in the plots of TA_{NO3} against PIC. This suggests that PIC of up to 25 μmol dm^{-3} had been produced and subsequently lost to greater depths in this eastern region.

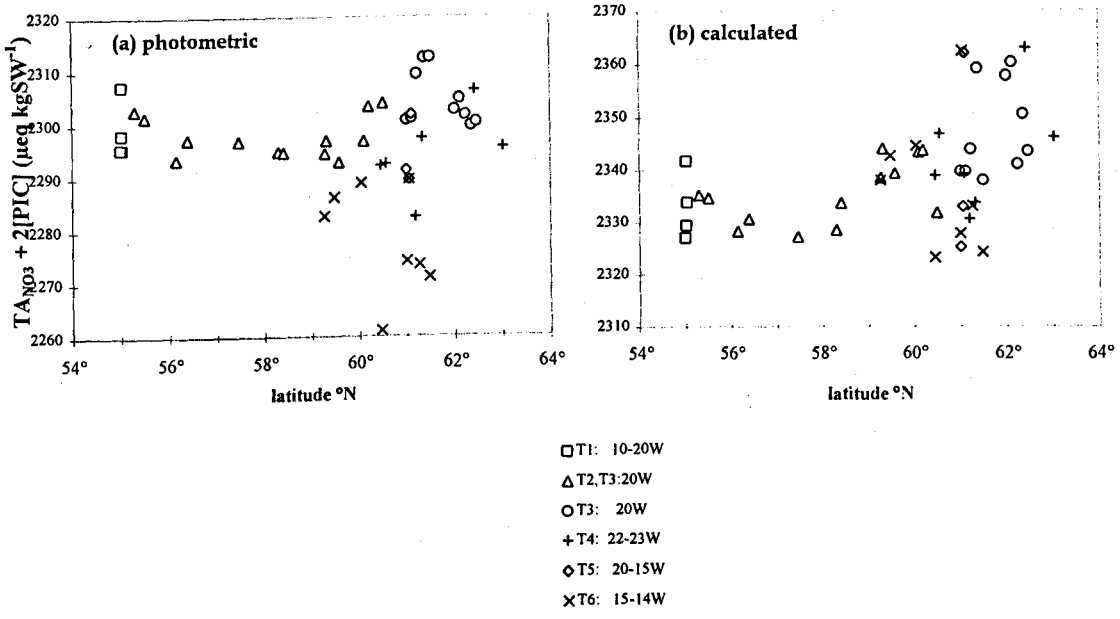

Figure 5.20: Regional distribution of the 'PIC loss' term, expressed as TA_{NO3} + 2 [PIC], from surface (2-3) samples collected during the 1991 Study in the Northeast Atlantic.
[PIC] is the concentration of PIC in µM.
Lower values of the PIC loss term imply that more PIC has been lost, and vice versa. In this form the term can only provide a relative quantification of PIC loss. It should be noted that this term does not necessarily imply that the lost PIC has left the SML altogether. A more detailed description of the PIC loss term is provided in section 5.4.2.2.
The loss term is based on (a) photometric TA and (b) TA calculated from pCO_2 and TCO_2. The two graphs show results from the same samples.
Regional identification was based on transects (T).

5.4.3.6. Difference in net production of PIC between biological regimes

Results from the comparison of PIC net production in surface samples between the *Emiliania huxleyi* bloom region north of 61°N 20°W and the non-bloom region south of that point at 20°W are presented in table 5.2. Photometric estimates in part (a) of the table suggest that within the bloom area PIC production was on average 9 μmol dm^{-3} higher than outside the bloom area. However, the range of PIC production spanned 28 μmol dm^{-3} north of 61°N, while it was only 3 μmol dm^{-3} outside of the bloom. Results from calculated TA in part (b) of the figure will be compared to the photometric results in section 5.4.3.8.

Table 5.2: Estimation of increased PIC production (μmol $kgSW^{-1}$) within the *Emiliania huxleyi* bloom area during the 1991 Study in the second half of June.
The difference of PIC production was derived from the comparison of surface TA_{NO3} values within the bloom area north of 61°N 20°W with those from the non-bloom regime south of this point. Information on variability of PIC production within each area is included. TA_{NO3} estimates were obtained by (a) photometry and (b) calculation from pCO_2 and TCO_2.

	(a) photometry		(b) calculation	
variability	range	s.d.(n-1)	range	s.d.(n-1)
non-bloom area (n = 13)	3	1	10.5	3.3
bloom area (n = 10)	21	7.6	24	8.2
relative increase in bloom area	9		6.5	

5.4.3.7. Net production ratios of POC:PIC

Results from the investigation of POC:PIC net production ratios during the preceding days or weeks, i.e. those based on photometric TA_{NO3} and TCO_2S, are presented in figure 5.21.a. Results from calculated TA in part (b) of that figure will be compared to the photometric results in section 5.4.3.8. An overall slope of photometric TA_{NO3} on TCO_2S of approximately 0.7 emerged when data from all six transects was used in the analysis. This suggests a POC:PIC net production ratio of 1.8 in the open ocean 1991 Study area. However, separate investigations of this ratio in two different hydrographic regimes, i.e. north and south of 61°N 20°W, revealed considerable regional variations. A slightly negative slope for data south of 61°N, which was not found to be significantly different from zero at the 95% c.l., implies that the given level of PIC net production had remained almost constant, while POC net production had varied by about 20 μmol dm^{-3}. North of 61°N, the slope of 1.4 implies that the POC:PIC net production ratio averaged at 0.4, i.e. net PIC production was more than twice as high as net POC production.

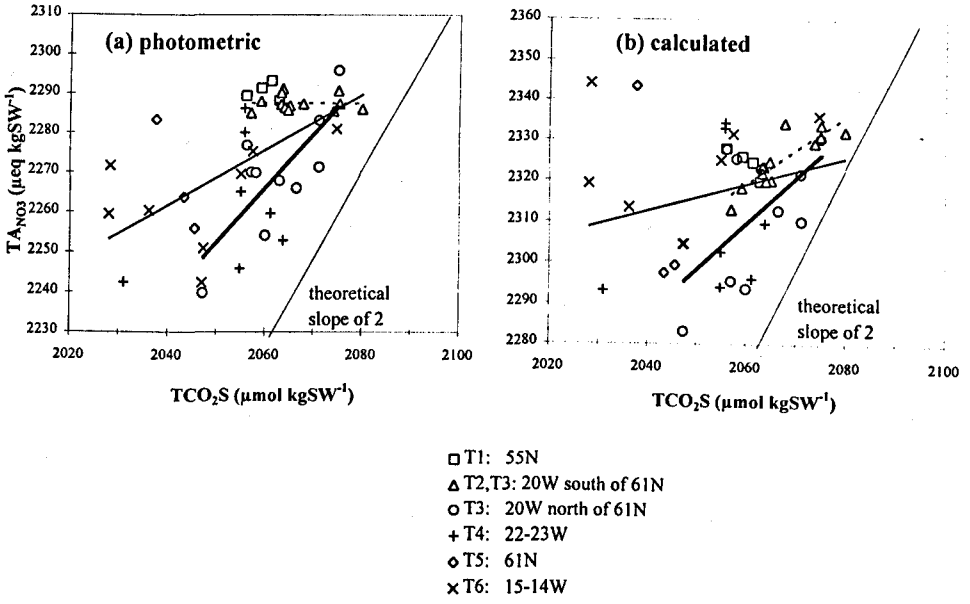

Figure 5.21: Estimates of the POC:PIC net production ratio based on the relationship of TA_{NO3} against salinity-normalized (35 psu) TCO_2 using (a) photometric TA and (b) TA calculated from pCO_2 and TCO_2. Samples were collected from the surface (2-3 m) during the 1991 Study in the Northeast Atlantic.

Data points are marked according to transects (T).
The main regression line is based on all data points (thin solid line). The relationship was also investigated separately for samples from 20°W north (T3: thick solid line) and south (T2, T3: brocken line) of 61°N. The regression equations and additional statistics are:

(a) all transects: photom. TA = **0.71** (± 0.16) TCO_2S+ 823 (± 330); n = 45; R^2 = 0.31; s.e.regr. = 13.3; P < 0.001
north of 61°N 20°W: photom. TA = **1.39** (± 0.41) TCO_2S - 554 (± 840); n = 10; R^2 = 0.56; s.e.regr. = 10.3; P < 0.01
south of 61°N20°W: photom. TA =**-0.007** (± 0.09) TCO_2S + 2303 (± 183); n = 13; R^2 = 0; s.e.regr. = 2.1; **n.s. at 0.05**

(b) all transects: calc. TA = **0.33** (± 0.17) TCO_2S + 1643 (± 357); n = 45; R^2 = 0.07; s.e.regr. = 14.4; **n.s. at 0.05**
north of 61°N20°W: calc. TA = **1.11** (± 0.56) TCO_2S + 12 (± 1158); n = 10; R^2 = 0.33; s.e.regr. = 14.3; **n.s. at 0.05**
south of 61°N20°W: calc. TA = **0.83** (± 0.15) TCO_2S - 598 (± 301); n = 13; R^2 = 0.75; s.e.regr. = 3.5; P < 0.001

A slope of zero implies that photosynthesis changed while calcification remained constant, and a slope of 2 means the reverse. A negative slope suggests that the amount of absolute net calcification was less in samples where net photosynthesis was higher.

Based on the above slope values, the resulting POC:PIC net production ratios are:

	(a) photometry	(b) calculation
all transects	**1.8**	**5.0**
north of 61°N 20°W	**0.4**	**0.8**
south of 61°N20°W	**-285**	**1.4**

The negative value of the ratio above implies that POC net production was not accompanied by PIC net production but by net dissolution instead. The large value of the negative ratio reflects the fact that this net dissolution was negligible compared to the net amount of POC that was being produced.

5.4.3.8. Comparison of photometric and calculated TA estimates

Considerable discrepancies between different TA methods have already emerged in the general intercomparison exercise (chapter 2) and the more detailed analysis of results from the 1990 Experiment (chapter 4). Results from surface samples collected during the 1991 Study revealed that photometric TA tended to be on average about 45 (± 10) μeq $kgSW^{-1}$ lower than calculated TA. The correlation of the two TA techniques showed that changes in photometric TA tended to be about 15 (± 10) % lower than calculated ones. This latter discrepancy was found not to be significant at the 95% confidence level. However, the error term of the slope did not include the expected relationship of 1. This relative discrepancy may lead to significant differences in the estimates of TA changes once these exceed about 40 μeq $kgSW^{-1}$. Furthermore, it may hide systematic differences that are related to different hydrographic/biological regimes. In this section, more detailed investigations of methodological differences focus on a few selected aspects of the Study.

In accordance with the above findings, the general agreement of both methods was also manifested in the similar slopes of TA_{NO3} with PIC and backscatter data (figure 5.22. a and b). However, the pattern of the residuals did reveal further differences between the two methods. These also became apparent when comparing latitudinal distributions of TA in figures 5.16.a and b. On one hand, calculated TA results confirmed a number of areal patterns established by photometry such as the

(i) generally higher TA along the 55°N transect 1 compared to transect 2;
(ii) generally higher TA south of 61°N 20°W (transect 2 and parts of transect 3) ;
(iii) considerable spread north of 61°N (transects 3, 4, 5, 6);
(iv) tendency for lower TA along transect 3 north of 61°N, and along western transect 4.

On the other hand, three major differences in the areal TA patterns emerged. Unlike photometric TA, calculated estimates did not reveal a significant decrease between 55° and 61°N 20°W. Secondly, the spread in calculated TA north of 61°N amounted to about 80 μeq $kgSW^{-1}$, and was therefore approximately 20 μeq $kgSW^{-1}$ larger than measured by photometry. Finally, and related to this point, was the finding that calculated TA from the 15°W transect 6 tended to be about 20 μeq $kgSW^{-1}$ higher than photometric TA on top of the overall discrepancy between the two methods. One consequence of this was that the

highest calculated TA during the 1991 Study was located in this eastern region, and it did not confirm the very low TA values in the 61°N 15°W region which stood out in the photometric analyses. This demonstrates that the discrepancy between the two methods was not constant within open ocean samples but varied between transects and thereby between different hydrographic/biological regimes.

The relative discrepancies were more or less carried over into the distribution patterns of TA_S and TA_{NO3} (figure 5.16.a and b). Most notably, the discrepancies in TA_{NO3} observed along the 15°W transect 6 would amount to a relative discrepancy of 10 μM between photometric and calculated estimates of PIC production. Further differences between methods became obvious in the comparison of the PIC loss term (figure 5.20). On top of the overall difference between the two methods, the PIC loss term from the calculation method would have been about 15 μeq $kgSW^{-1}$ lower along southern transects 1 and 2 and about 15 μeq $kgSW^{-1}$ higher along eastern transect 6. In other words, estimates from the calculation method suggest that some of the greater loss of PIC due to sinking or herbivory had occurred along the southern transects, while the photometric method had identified only the eastern transect 6 as an area of high PIC loss.

The relevance of the relative methodological discrepancies also became apparent in the comparison of PIC production between the bloom area north of 61°N 20°W and the non-bloom area south of this point (table 5.2. a and b). First of all, the calculation method recorded a greater spread in PIC production outside the bloom area, i.e. 10 μmol dm^{-3}, which was three times larger than in photometric estimates. Secondly, average PIC production was only about 6.5 μmol dm^{-3} greater in the bloom area, i.e. this estimate is smaller than the photometric one by 2.5 μmol dm^{-3}.

Further differences between the methods were observed in the estimates of POC:PIC net production ratios (figures 5.21 a and b). While both TA methods agreed on a POC:PIC ratio of less than 1 in the general bloom area north of 61°N 20°W, the estimate of 0.82 based on the calculation method was not found to be significant at the 95% confidence level. Furthermore, south of that point, the calculation method derived at a significant net production ratio of slightly more than unity, while photometric results clearly implied that POC production had occurred without any change in PIC production. When comparing the ratios from the entire comparable data set, the net production ratio amounted to about 5 by

the calculation method, which was based on a non-significant slope, while photometric results suggest a significant relationship of approximately 2.

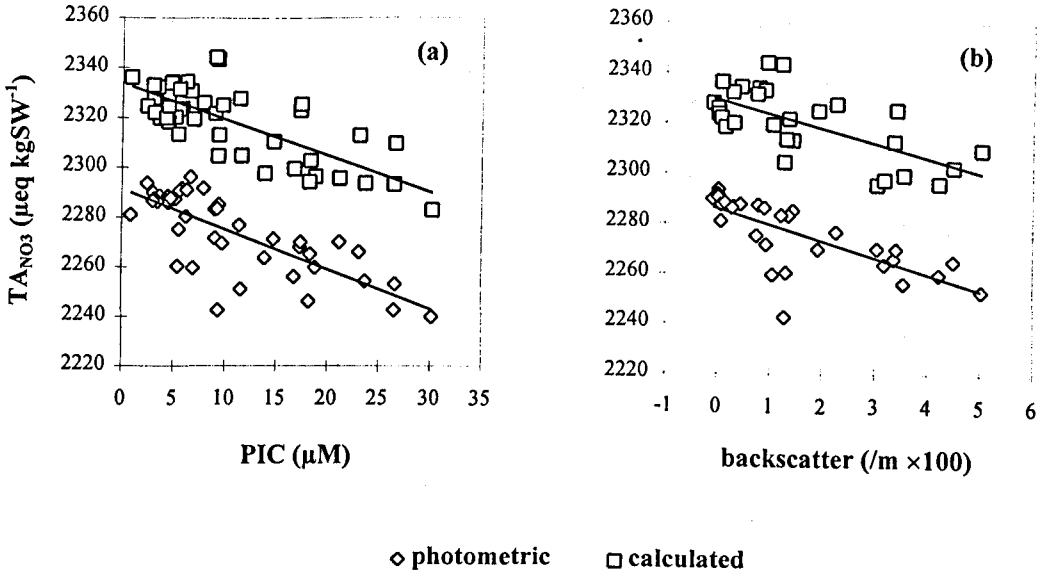

Figure 5.22: Comparison of photometric and calculated TA_{NO3} in the relationships with (a) PIC and (b) backscatter at 550 nm.
Samples were obtained from the 1991 Study in the Northeast Atlantic and were the same for both TA methods.
Regression equations and additional statistics are:

photom.TA_{NO3} = -1.60 (± 0.20) PIC +2291 (± 2.6); n = 45; R^2 = 0.59; s.e.regr.= 10.2
calc.TA_{NO3} = -1.45 (± 0.20) PIC +2334 (± 2.5); n = 45; R^2 = 0.56; s.e.regr.= 9.9

photom.TA_{NO3} = -6.45 (± 1.15) b.scatter +2286 (± 2.4); n = 31; R^2 = 0.52; s.e.regr.= 9.6
calc.TA_{NO3} = -5.75 (± 1.24) b.scatter +2329 (± 2.6); n = 31; R^2 = 0.42; s.e.regr.= 10.3

5.4.3.9. TA at 300 m and greater depths

An overview of TA and TA_S results at the four deep CTD stations is presented in figure 5.23. At 300 and 500 m, TA decreased from 2300 to 2290 μeq $kgSW^{-1}$ between 56°N and the more northern stations. The northwestern station 5 was the lowest. At the intermediate depth of 1000 m, TA generally ranged around 2285 μeq $kgSW^{-1}$, and around 2280 μeq $kgSW^{-1}$ at 1500 m or greater depths.

For depths at 300 m and below, a comparison of TA and TA_S profiles shows that the decrease in TA below 500 m was largely caused by the salinity decrease associated with a change from upper to intermediate water masses. Between intermediate and deep waters, salinity had little influence on the change in TA.

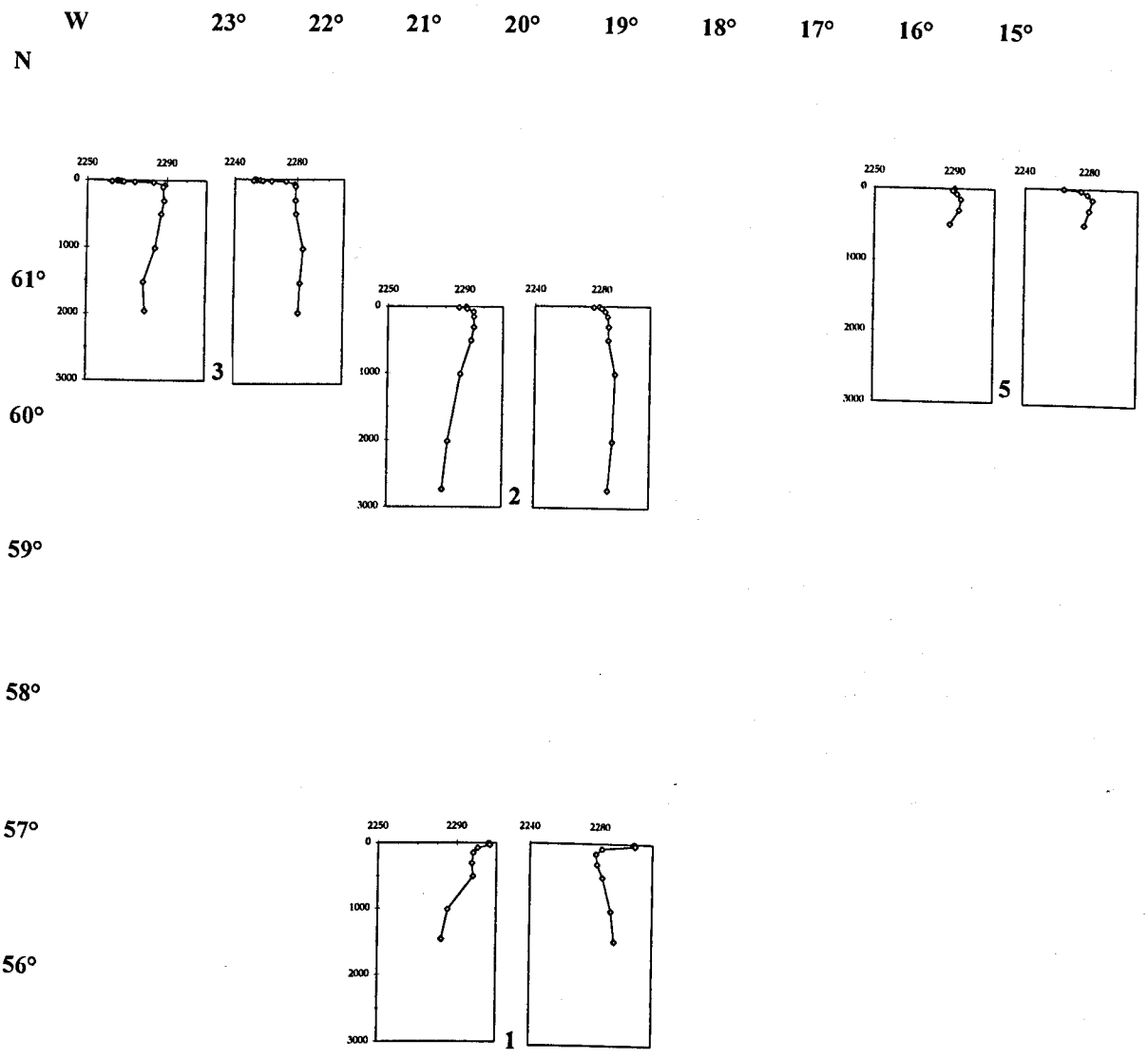

Figure 5.23: Comparison of vertical (m) profiles of TA and TAs (μeq $kgSW^{-1}$) at deep cast sites from different regions in the Northeast Atlantic studied during the 1991 Coccolithophore Bloom Study between 17 and 29 June.
For each position the left graph shows the TA profile and the right graph depicts the profile of specific TA. The numbers of the stations are included.

5.4.3.10. Comparisons between the 1990 and 1991 study areas

Before comparing the TA results from both years it has to be kept in mind that the samples from 1990 were not filtered prior to the analysis, and that ultimately, it is not possible to estimate the error on the 1990 samples since there was no concomitant PIC data available for those samples. On the basis of cell identification and counts from the preceding weeks, it was generally assumed that the concentration of PIC was negligible during the 1990 Experiment, and in the comparisons below the same assumption is made.

Figure 5.16.a shows that TA results from 1990 roughly matched the latitudinal trend of TA observed along the 20°W line south of 61°N in 1991. However, TA_S and TA_{NO3} from 1990 were lower than the above 1991 samples from transects 1 and 2 by about 10 to 20 µeq $kgSW^{-1}$. At first sight, this suggests that calcification in the 1990 study area was 5 - 10 µmol dm^{-3} greater than along the 55°N transect and the southern section of the 20°W transect in 1991. The omission of filtering the 1990 samples prior to their analyses provides no explanation for this interannual difference, since the presence of PIC in samples has been shown to increase TA results rather decrease them (see section 2.3.5). Instead, figure 5.17 revealed also differences in TA_{NO3} levels at sub-thermocline depths, i.e. they were about 15 µeq $kgSW^{-1}$ lower at 47°-48°N. Consequently, surface TA_{NO3} at the 1990 sites were lower because of lower preformed TA_{NO3} concentrations to start off. Once this was accounted for, the effect of calcification would have been more or less the same as for the areas along 55°N and along 20°W south of 61°N.

Photometric estimates of the POC:PIC net production ratio were very different between the study areas from 1990 and 1991 (figures 4.14 and 5.21). Results from 47°-48°N suggest that the total amount of PIC production in fact decreased as POC production increased. In 1991 this negative relationship was not observed. However, between 55° and 61°N 20°W there was no change in calcification while photosynthesis had increased. The relative importance of calcification in the 1991 study area, and in particular north of 61°N 20°W, was reflected in POC:PIC production ratios of less than 2 and 0.5, respectively. If these differences are interpreted on a regional basis, these results indicate clearly the increasing relative importance of PIC production towards the north of the Northeast Atlantic.

While the average differences between results from the two methods were similar in both years, it has become obvious that this discrepancy was related to the location of sampling. For example, figure 5.16 demonstrated that the difference in photometric TA between 47°-48°N (1990) and 55°-61°N (1991) was about 20 μeq $kgSW^{-1}$ larger in the calculated than in the photometric data set. Consequently, calculated TA_{NO3} at 47°-48°N (1990) was comparable to that at 55°-61°N 20°W (1991). Based on this comparison of surface TA_{NO3}, it may be concluded that the amount of calcification was similar at both sites. However, this conclusion cannot be confirmed without the concomitant comparison of sub-thermocline TA_{NO3} data from the calculation method, which was not available for the 1991 Study.

The difference between years in the net production ratios of POC:PIC was less marked in the data set based on calculated TA.

The results from the 1991 Study largely agreed with seasonal and regional observations made in 1989.

5.4.4. DISCUSSION OF FINDINGS FROM THE 1991 STUDY

5.4.4.1. Variations in hydrography

The 1991 Coccolithophore Bloom Study was conducted in an area which comprised a wide range of hydrographic regimes. In crude terms, these included NACW and MNAW as the upper water masses. On the basis of direction of flow and further distinctions in temperature and salinity, six different water types were identified in this study. The underlying criteria may have been a bit arbitrary, but the emerging longitudinal and latitudinal profiles in hydrography seemed to provide more useful reference points for the observed biological and chemical features than geographical position or major water mass. This was particularly relevant, since considerable small-scale changes in hydrography were observed, many of which were associated with meso-scale eddies. As an additional complication, there was clear evidence for differential advection above and below the thermocline at three of the six CTD stations visited. This phenomenon was already observed at 47°-48°N 16°-17°W in 1990.

5.4.4.2. Variations in biology

The first cruise of the 1991 Study had also covered a wide range of biological regimes. These included post-spring-bloom situations with variable amounts of phytoplankton biomass, mixed bloom assemblages with *Coccolithus pelagicus* as the dominant coccolithophorid species, and different stages of the *Emiliania huxleyi* bloom. The first regime was typically found in lower-salinity NACW south of 58°N 20°W and the second regime in eastward flowing MNAW. The *E. huxleyi* bloom regime was largely associated with the westward flowing MNAW, but localized increases in numbers were also observed in higher-temperature, lower-salinity NACW. Much of the hydrographic variability observed along the surface transects was reflected in the abundance of different phytoplankton species or their remains. The six depth profiles all represented quite diverse hydrographic and biological situations.

5.4.4.3. Variations in TA

On the basis of the above hydrographic and biological observations, it was not surprising to measure considerable large- and small-scale variations in surface TA during the Study. The overall TA range amounted to 70 μeq $kgSW^{-1}$ with the highest values in the high-salinity NACW along 55°N and the lowest ones in *Emiliania huxleyi* bloom waters. The sub-thermocline TA range of only about 10 μeq $kgSW^{-1}$ demonstrated that the considerable alterations observed in surface waters were largely caused by processes usually limited to the SML, i.e. they were too large to reflect variations in preformed TA.

5.4.4.4. Factors influencing TA

5.4.4.4.1. Hydrography

The general effect of salinity on TA in the 1991 Study area was reflected in the positive relationship between these two parameters, and was similar to that observed further south in 1990. About 20% of the variation in the SML could be attributed to differences in the water masses and their evaporation/precipitation history. This was the chief factor influencing the distribution of surface TA outside the *Emiliania huxleyi* bloom area. The steady salinity decrease towards the north in this part of the Atlantic therefore emerged as

the main cause for the linear latitudinal decrease in TA, which was estimated to be 2.3 μeq $kgSW^{-1}$ per 1° latitude between 55° and 61°N 20°W.

As would be expected, the salinity effect was larger in vertical profiles where the thermocline separated different water masses. Otherwise, the relatively small increases in salinity above the thermocline implied that evaporation tended to have an almost negligible impact on TA in the SML since stratification.

5.4.4.4.2. Nitrate uptake

Based on the observed range of nitrate concentrations and the concept of potential alkalinity, the shortcomings of which will be discussed in section 5.4.4.9, variations in nitrate uptake appeared to have a relatively minor effect on the overall distribution of surface TA, i.e. it seemed to account for no more than 7 μeq $kgSW^{-1}$. However, inferences from nitrate concentrations can lead to erroneous estimates of nitrate uptake and its effect on TA. This is the case when nitrate concentrations of winter mixed conditions, i.e. preformed nitrate concentrations, are not the same at different locations. In this case any significant phytoplankton growth in late winter or spring would start off at different nitrate concentrations. For example, according to Glover and Brewer (1988) the approximate preformed nitrate concentrations decreases from 14 μM at 55°N to 8 μM at 63°N 20°W, and for a given latitude concentrations tend to be slightly lower along the 15°W line. On this basis, estimates of regional variation in the nitrate effect on TA would have been inaccurate by up to 6 μeq $kgSW^{-1}$ in this study. This would have led to underestimates of the nitrate effect at 55°N and overestimates at 63°N 20°W. As a further complication, there is currently no consensus as to the absolute values and regional profile of preformed nitrate concentrations in the Northeast Atlantic, i.e. Garside and Garside (1993) derived at different preformed concentrations for the particular sites of interest in this study (see also section 3.3.1.2.2). Robertson et al. (1994) had also acknowledged this uncertainty. They assumed that preformed nitrate concentrations generally increased towards the north.

With the above mentioned uncertainty over preformed nitrate concentrations, it may be that corrections for nitrate uptake would have been more accurately conducted by applying corrections based on AOU and a given Redfield ratio. However, given the diversity of the biological regimes which were encountered in the 1991 Study, the usual assumptions of

equilibrated oxygen concentrations and a constant and accurate Redfield ratio may have introduced different types of errors.

5.4.4.4.3. Calcification

Since most of the lower TA_{NO3} values in the open ocean were measured in high calcite waters north and northwest of 61°N 20°W, it seemed justified to ascribe most of the spread in TA_{NO3}, i.e. about 55 μeq $kgSW^{-1}$, to variations in the abundance of coccolithophorids and their associated PIC production. In fact, this spread was almost equivalent to the maximum PIC concentration of 30 μM which had been observed in surface waters. Similarly, small-scale changes in TA and TA_{NO3} of up to 40 μeq $kgSW^{-1}$ over 40 km were accompanied by equivalent changes in the concentration of PIC and considerable changes in the numbers of *Emiliania huxleyi*. Furthermore, in a comparison of vertical profiles the largest vertical changes in TA_{NO3} were also matched by the largest vertical changes in PIC across the thermocline.

The general importance of biological calcification was also backed up by negative correlations between TA or TA_{NO3} and PIC or related biological parameters, which included chlorophyll a. However, a comparison of the relationships between TA with coccolithophorid and *Emiliania huxleyi* counts does not provide any information as to how much individual species within the coccolithophorid group contributed to PIC production. There is, however, sufficient circumstantial evidence in this and other studies that most of the calcification was due to *E. huxleyi*. First of all, there was usually little reduction in TA_{NO3} in waters where *E. huxleyi* numbers were small, even though other coccolithophorid species like *Coccolithus pelagicus* were abundant. Also, the greatest reductions in TA_{NO3} were observed where the proportion of *E. huxleyi* to other coccolithophorids was increased. In an empirical model of surface calcification, Fernandez et al. (1993) established that in terms of biomass the contribution of coccolithophorids other than *E. huxleyi* and *C. pelagicus* to calcification was negligible in the 1991 Study. Further, changes in biomass of *E. huxleyi* had a ten times greater effect on calcification than those of *C. pelagicus*. This was corroborated by observations in this study, i.e. TA_{NO3} was similar in the non-bloom and in the *C. pelagicus*-dominated regime along the 20°W transect 2.

5.4.4.5. Evidence of PIC loss

More quantitative investigations of the above evidence of the negative trends between TA_{NO3} and PIC revealed discrepancies between equivalent changes of these two parameters. This was most prominent in depth profiles and in the results from the regression analysis for TA_{NO3} and PIC, which had shown that average changes in TA_{NO3} were about 20% higher than the equivalent changes in PIC. So, either the TA_{NO3} or the PIC data set were misrepresenting the total amount of net calcification that had occurred in surface waters. Possible reasons for errors in the former data set are dealt with in another sections (5.4.4.9 and 5.4.4.10).

For the discussion here it is assumed that TA_{NO3} accurately represented the total production of PIC, as is frequently done in other studies. In this case, the standing stock of PIC measured in surface samples underestimated the total net production which had occurred in the surface waters by an average of 20%. Since there is no conceivable way of removing PIC other than by vertical sinking/scavenging or herbivore grazing, it was assumed that this discrepancy could be ascribed to such vertical loss from 2-3 m to any greater depths within or below the SML. There is no direct evidence from accompanying data which can back up this assumption, and evidence of sinking material at greater depths in July 1991 was not very conclusive (R. Harris, pers. comm.). Possibly supportive evidence for vertical loss comes from vertical profiles, where PIC concentrations of up to 5 μM were measured at sub-thermocline depths of around 70 m, i.e. below the light compensation depth. While this excludes significant amounts of coccolithophorid growth, it does not exclude the presence of other calcifying organisms such as foraminifera.

When considering this PIC loss, it also has to be born in mind that the PIC loss term merely refers to loss from the surface samples, i.e. displacement of a few meters can lead to a discrepant signal. Furthermore, this sinking loss will be greater as time progresses, so that it can be expected to increase in waters where the bloom has reached an advanced stage. Increased growth of heterotrophs typical for that stage may enhance PIC loss further. These theoretical considerations were confirmed by the fact that photometric estimates of PIC loss turned out to be highest in the northeastern region, which had been identified as a 'late bloom' region by Fernandez et al. (1993). This subject could be investigated further in a similar exercise for a POC loss using TCO_2S and POC. However, this may not necessarily be

conclusive, since the regeneration of POC and dissolution of PIC may be uncoupled spatially and temporally.

5.4.4.6. Estimates of seasonal PIC production based on TA measurements

The possible importance of absolute and relative amounts of POC and PIC export from the SML on geological time-scales has been described in section 1.3.2.2.3 and 1.3.2.2.4. The quantity and quality of this export and its fate at greater depths will first of all depend on the absolute and relative amounts produced in the SML (Boyd & Newton, 1995). This study has provided independent estimates of net PIC production for areas within and outside the *Emiliania huxleyi* bloom. In contrast to estimates based on PIC, cell counts, production rates, and the available knowledge on growth curves of *E. huxleyi*, the imprint of TA_{NO3} in the SML tends to provide a more long-term indication of net PIC production. Assuming that the SML is completely sealed off from sub-thermocline layers, potential alkalinity is still generally regarded as the most suitable parameter to estimate the amount of PIC which has been produced since the onset of stratification. Furthermore, it is in theory a more accurate parameter for net rather than gross production of PIC, which may be an important distinction considering some observations of PIC dissolution within the SML (J. Young, pers. comm.).

The TA_{NO3} depth profile at the 'early bloom' station in the west of the bloom area suggested that net PIC production within the SML may have reached at least 18 μmol dm^{-3} since the onset of stratification. The estimate at the 'late bloom' station 4 in the northeast confirmed this range. This compares well with estimates by Fernandez et al. (1993) based on PIC standing stock which indicated a maximum level of PIC production in the bloom of 17 μmol dm^{-3} when integrated over 35 m. At one CTD station outside the bloom area where there was no obvious evidence of differential advection, net PIC production seemed to have reached about 3 μmol dm^{-3}, which was similar to estimates from the 1990 Experiment during which the abundance of *Emiliania huxleyi* was found to be negligible in surface waters. These estimates are similar to the PIC standing stock measured outside the bloom area, which typically remained below 5 μM. Assuming an average PIC production of 4 μmol dm^{-3} in that area, typical net production of PIC within bloom waters would have exceeded the background level of PIC production by about 14 μmol dm^{-3}.

The above investigation had focused on specific points within the bloom area which were typical of an *Emiliania huxleyi* bloom situation. A more average estimate of the increase of PIC net production within the entire bloom area came from TA_{NO3} surface estimates along the 20°W transect. These indicated that the average elevation of PIC production within the bloom area only amounted to about 8 μmol dm^{-3}. This average came from a very heterogeneous group of samples, i.e. the relative elevation of PIC within the bloom area ranged from 0 to 24 μmol dm^{-3}. This spread reflected the considerable small-scale variations in hydrography and biology and possibly also vertical variations of PIC production within the euphotic zone. The latter had been demonstrated in productivity studies by Fernandez et al. (1993). Assuming the background level in PIC production of 4 μmol dm^{-3}, this implies that average production in the bloom areas was around 12 μmol dm^{-3}. Results from the western region of the bloom area (22°W transect 4), which were not presented here, would have been similar. This is lower than the estimate of 16.5 μmol dm^{-3} based on satellite reflectance data which had been calibrated against the beam attenuation coefficient and chlorophyll a (Holligan et al., 1993). An obvious reason for this disparity could be that the transects did not exactly represent the typical range of biological regimes encountered over the entire bloom area.

5.4.4.7. Estimates of seasonal POC:PIC production ratios based on TA measurements

Results from the estimates of POC:PIC net production ratios in the open ocean area of the 1991 Study suggested that production since the onset of stratification had occurred at an overall ratio of about 2. Comparison of ratios obtained north and south of 61°N 20°W showed that they varied between biological regimes, i.e. outside the bloom area, production of POC was not accompanied by any significant proportional change in PIC . This implies that any changes in net POC production occurred against an almost constant background level of PIC net production of about 4 μmol dm^{-3}. Within the bloom area, the average ratio had fallen to 0.4. Frankignoulle and Canon (1994) estimated a threshold ratio of 0.65 below which the combination of POC and PIC production would actually cause an increase in pCO_2. Accordingly, the photometric estimate of POC:PIC net production implies that biological production in the central part of the bloom area had led to an increase in pCO_2 relative to the background level of pCO_2. This does not necessarily mean that the pCO_2 would have to rise above atmospheric levels.

Whether the above conclusion based on the photometric TA results is accurate is not certain because estimates of this ratio varied with method, plus ratios from other methods have not always been obtained from the same samples and regions. The ratio based on calculated TA for the bloom region was less conclusive, because it did not come from a statistically significant slope of the TA_{NO3}/TCO_2S relationship. Nevertheless, it indicated a POC:PIC production ratio of 0.82, which was similar to the photometric one in as much as production of PIC exceeded that of POC, whereas it did not suggest any relative pCO_2 increase. In the study by Robertson et al. (1994), a ratio of 1.15 was obtained. It was derived from a far greater number of continuous samples, but included non-bloom areas between 58° and 61°N 20°W. Another ratio came from the study by Fernandez et al. (1993). It was reported to cover the 'bloom area', but it was not clear to what extent this included positions of low calcification within that area. Their POC production estimates were based on counts of total *Emiliania huxleyi* cells, and PIC was determined from actual PIC concentrations. Taking account of vertical loss by sinking and herbivory, they arrived at an estimate of 0.75, i.e. it was in between the photometric and calculated estimate and implied that biological production in the bloom area had an overall effect of slightly reducing the background level of pCO_2.

Discrepancies between the above estimates of the POC:PIC net production ratio may have arisen for various reasons. First of all, inclusion of regions dominated by non-calcifying algae tends to increase the ratio. Secondly, estimates based on concentrations or counts of particulates such as the one by Fernandez et al. (1993) limit their estimate to more recent growth and rely heavily on the accuracy of the assumptions needed to correct for vertical loss of POC and PIC. Furthermore, dissolution of PIC in the SML could not be estimated by the latter method, so that their results are presumably more reflective of net POC: gross PIC production. As already mentioned above, estimates based on concentrations of dissolved parameters tend to reflect longer-term production ratios, i.e. those that have occurred since the onset of stratification. In principle, they more accurately represent net productions of both, POC and PIC. However, the SML is never entirely sealed off from underlying layers of water, so that TCO_2 and TA in the SML are subjected to alterations by intruding water from the thermocline and sub-thermocline layer. Also, TCO_2 will suffer alterations from air-sea exchange of CO_2. Then, there is the re-occurring concern about the accuracy of the TA measurements and the potential error in the assumption that corrections for salinity and nitrate are sufficient to account for any processes that have altered TA other than

calcification. Possible short-comings of potential alkalinity and the way it has been used are discussed below (section 5.4.4.9).

5.4.4.8. Calibration of optical and biological data

5.4.4.8.1. Light backscatter

During the 1991 Study a good correlation was established between preliminary photometric TA estimates and light backscatter at 550 nm in surface samples (Holligan et al., 1993). In the study here, this correlation was re-investigated using corrected photometric TA data and excluding samples from shallow shelf sites (<100 m). The updated relationship had a lower intercept, a shallower slope, and was better correlated. Since the former relationship was based on TA, i.e. uncorrected for variations in salinity, the slope would have been too steep to accurately estimate the overall effect of *Emiliania huxleyi* growth on TA in surface waters. Instead TA_S should have been used for calibrations of any optical data. Together with information about salinity, the optical data may ultimately be used to determine TA in surface waters. The relationship between TA_S and backscatter has not been presented in this study, but due to the relatively minor changes in nitrate concentrations it could be assumed that it was similar to the one between TA_{NO3} and backscatter. The latter has been established in this study, and its considerably reduced slope demonstrates the importance of using TA_S rather than TA when intending to estimate the overall effect of *E. huxleyi* on TA by means of optical data from space.

For the above calibrations to be of any use, it is essential that the TA estimates used for the calibration are accurate in every sense. A comparison of calibrations using photometric and calculated TA showed that the calculation method inferred TA changes which were 10% smaller than those measured by photometry. In addition, absolute TA values differed greatly. The extent of these errors exceeds those acceptable for climate related studies and clearly demonstrates the need for a greater focus on accurate TA determinations.

5.4.4.8.2. Calcification quota for cells and liths of *Emiliania huxleyi*

For future estimates of TA reduction as a result of growth by a given number of *Emiliania huxleyi* cells, the relationship between these two parameters was presented in this study. It does, however, suffer the same shortcomings as discussed for the relationship with

backscatter data above, i.e. the use of salinity-corrected TA data is generally more appropriate. Equally, it could be assumed that the relationship between TA and *E. huxleyi* numbers, which suggests a change of -2.7 microequivalents per 10^6 cells, was overestimating the amount of TA change caused per cell. This error may have been further enhanced by vertical loss of PIC, which would have led to underestimates in the original numbers of *E. huxleyi* that were involved in the TA change. In the absence of a TA_S versus *E. huxleyi* relationship, a better approximation of how much TA was altered per cell was probably reflected in the change of TA_{NO3} which had also been corrected for PIC loss and which implied a change of 1.8 microequivalents per 10^6 *E. huxleyi* cells. In comparison, experiments with one particular strain of *E. huxleyi* suggest that the change in TA_{NO3} per 10^6 cells was much less, i.e. only about 0.2 to 0.3 microequivalents (chapter 6). Accompanying measurements of PIC confirmed, however, that this much smaller change in TA was largely due to generally less calcification of that strain under the given experimental conditions.

If one assumes that changes in TA_{NO3} accurately reflected changes in net PIC production by *Emiliania huxleyi* alone, the above relationship between TA_{NO3} and *E. huxleyi* counts suggests that 10^6 of these cells produced 0.9 micromoles of PIC. With an error of at least ± 0.1 µmol dm^{-3}, the quota for PIC production thus ranged from at least 0.8 to 1.0 micromoles of PIC production per 10^6 cells. This molar range translates to PIC production of 10 to 12 pg C or 80 to 100 pg $CaCO_3$ per one cell. The range of lith: cell ratios which was observed in the 'late bloom' regime of the 1991 Study was 50 to 110 (Fernandez et al., 1993) and largely agrees with observations in culture (J. Young, pers. comm.). However, these ratios may have been atypically high for much of the bloom, where the ratio ranged from 10 to 40, because low nitrate concentrations in the 'late bloom' area may have increased lith production above average levels or because of genotypical variations (Fernandez et al., 1993, and references therein). Using the average PIC per cell ratio from this study and an average lith: cell ratio of 20 from the general bloom area (Fernandez et al., 1993), PIC production per lith would have averaged around 0.56 pg C or 4.4 pg $CaCO_3$. This weight estimate per lith is about twice that recommended as a sensible value for normally calcified oceanic *E. huxleyi* cells, but it safely falls into the generally observed range of 0.6 to 4.6 pg $CaCO_3$ per lith (J. Young, pers. comm.). The average PIC per lith ratio for the whole bloom area from Fernandez et al. based on actual PIC concentrations and total lith estimates amounted to 3.9, which confirms

the relatively high amount of PIC per lith from this study. It is obvious, though, that this value chiefly depends on the chosen ratio of liths per cell.

One possible reason why the calcification estimate per *Emiliania huxleyi* cell which came from photometric TA may have been slightly greater than the one by Fernandez et al. (1993) is the fact that *Coccolithus pelagicus* would have contributed to the change measured in TA_{NO3}. If one uses the estimate of 10% for the contribution of *C. pelagicus* to calcification (Fernandez et al.) in order to correct photometrically established calcification quota, then average PIC production per cell would be 80 pg $CaCO_3$ per cell and 4.0 pg $CaCO_3$ per lith, which agrees even better with the estimate based on particulates by Fernandez et al..

5.4.4.9. Errors in calcification estimates based on potential alkalinity

Possible errors in TA and TA_{NO3} which may introduce significant errors in the estimation of calcification can arise from

(i) methodological errors in the estimates of TA;
(ii) omission of corrections for biological processes other than nitrate uptake;
(iii) variations in preformed levels of potential alkalinity and nitrate concentration between water masses;
(iv) other limitations of the experimental design.

Methodological problems are discussed in chapter 2 and below in section 5.4.4.10. Errors in the corrections for nitrate uptake due to variations in preformed nitrate concentrations have already been discussed in section 5.4.4.4.2.

5.4.4.9.1. Uncoupling of ammonia uptake/ regeneration

Uptake of ammonia by phytoplankton reduces the alkalinity on an equimolar basis. Regeneration of ammonia has the reverse effect. An underlying assumption in the potential alkalinity concept is that uptake and regeneration of ammonia are balanced in the SML, so that utilization by phytoplankton is assumed to have no net effect on TA. It has, however, been shown that it can be spatially uncoupled (e.g. Garside et al., 1990; Bury et al., 1990). As an example, Garside et al. observed an ammonia maximum at the base of the euphotic zone at 30 to 40 m, which they interpreted as possible evidence for increased heterotroph activity. Since the uncoupling may depend on light levels and the activity and behaviour of

heterotrophs, it does not appear straight forward to make a generalized statement about this effect on TA differences across the thermocline. However, concentrations in ammonia maxima usually do not exceed 2-3 μM, so that this effect will probably be negligible in most cases (Riebesell, pers. comm.).

5.4.4.9.2. Sulphate uptake

The potential effect of sulphur uptake has been described and discussed in section 1.4.2.9. It demonstrated that depending on the algal species and the biochemical end products, sulphate-uptake may increase TA by up to half the amount caused by nitrate uptake. The omission of a sulphate-correction presumably did not make a significant difference on the spatial distribution of potential alkalinity as observed in the 1991 Study area. However, it could have had a significant effect on the increase of TA within the SML compared to sub-thermocline layers, i.e. reaching up to 5 μeq $kgSW^{-1}$. In such a case, the potential alkalinity in form of TA_{NO3} would have been too high in the SML. Accordingly, the TA increase due to photosynthesis in the SML may have been more in the range of 15 μeq $kgSW^{-1}$ rather than 10 μeq $kgSW^{-1}$, which had been typically observed in open ocean casts during the 1990 and 1991 studies. This would imply that the amount of net calcification since the onset of stratification may have been underestimated in the SML by up to 2.5 μmol dm^{-3} in all open ocean waters of this study. In turn, this would mean that net calcification may have reached at least 6 μmol dm^{-3} at all the open ocean sites outside the *Emiliania huxleyi* bloom area, and that the average estimate of net calcification of this study from the bloom area (8 μmol dm^{-3}) would have been underestimated by about 30%. Within high-calcite samples (30 μM), this error would still amount to an underestimate of about 10%.

For a better understanding of the link between net calcification and the fate of PIC at greater depths, it is fundamental to accurately quantify the amount of calcite that actually leaves the SML. It seems that the possible error of net calcification estimates associated with sulphur-uptake is too large to be ignored, and that it should be investigated further, so that it can be quantified and routinely included in the potential alkalinity term.

5.4.4.9.3. Organic acid release

A. Dickson (pers. comm.) guessed that the presence of organic acids may raise TA by up to 10 μeq $kgSW^{-1}$ in open ocean waters where biological production occurs. The increase of

TA associated with its release is difficult to quantify because of the complications relating to the identification and quantification of the relevant organic acids as well as the uncertainties about their dissociation constants. It should, however, be born in mind that their release may cause underestimates of net PIC production by up to 5 μmol dm^{-3} in any regimes where significant amounts of phytoplankton production and heterotrophic activity lead to increased organic acid release.

5.4.4.9.4. N_2 fixation

Section 1.4.2.6 described and discussed the potential effect of N_2 fixation by some phytoplankton species and other organisms. Assuming that N_2 fixation does not alter TA, and that increased release of DON associated with such N_2 fixing species is negligible, N_2 fixation would not directly lead to an inaccurate estimate of TA_{NO3}. However, it could raise the amount of conversion from PON to ammonia within the SML, so that TA and TA_{NO3} would be raised after all. This possible increase in TA would not reflect the reduction of nitrate concentrations and would thus lead to an underestimate of the effect of new production on the increase of TA.

It is not known how important N_2-fixation was in the 1991 Study area. Based on the absence of known important N_2-fixing species and the absence of obvious microzones of oxygen depletion, it was probably negligible (I. Joint, pers. comm.).

In order to determine the overall effect of N_2-fixation on TA, it will first of all be necessary to establish the overall effect of different N_2-fixing species or strains. Secondly, growth rates of these organisms would have to be taken into account. The above theoretical considerations suggest that wherever the relevant organisms are present in the water column, potential alkalinity in form of TA_{NO3} would underestimate the amount of net calcification that has occurred.

5.4.4.9.5. Preformed potential alkalinity

Different water masses may have a different history of how their levels of TA_{NO3} are influenced. In principle, this first of all depends on the chemistry of the water that feeds these water masses and may be of greater importance in coastal regimes. These differences may not always be accurately accounted for by the salinity- and nitrate-normalization

procedures. More importantly in open ocean waters, though, is the amount of net PIC production/dissolution that has occurred in a parcel of water before it enters the study area. If it has differed significantly between two water masses which are being compared, this can lead to incorrect conclusions about the effect of biological processes in the study area of interest. In the case of the 1991 Study at least two major water masses, i.e. NACW and MNAW, were compared. The estimation of their preformed TA_{NO3} concentration does not seem to be a straight forward task. In order to obtain a rough idea of the potential error that is involved, one initial approach would be to compare winter-mixed levels of TA_{NO3} at sites within the study area which were typical for NACW and MNAW. Glover and Brewer (1988) have provided information for winter-mixed TA and nitrate but not for salinity.

5.4.4.9.6 Conceptual limitations in estimates of TA changes across the thermocline

Estimates of TA changes in the SML since the onset of stratification have been based on comparisons of measurements from the SML and those from sub-thermocline depths (70 - 150 m). The assumptions used to justify such exercise may be questioned on several grounds. Some of these are considered below.

Differential advection

Differential advection undermines the basic assumption that waters from above and below the thermocline have the same origin and thus the same preformed concentrations of TA and nitrate. This shortcoming was most obvious at station 1 (56°N 20°W), where TA_{NO3} was 10 μeq $kgSW^{-1}$ higher above the thermocline, although PIC concentrations indicated calcification of at least 5 μmol dm^{-3}. This would mean that the water in the SML originated from a water mass with a typically lower preformed TA_{NO3}. Similar shortcomings applied to coastal station 3, where interpretation was complicated further by terrestrial and possibly benthic influences on the chemistry of the seawater in addition to the more complex hydrography at such shallow sites. However, differential advection did not have any major apparent effect on the discrepancy between TA_{NO3} and PIC at eastern station 5 since depth profiles of these parameters were relatively compatible, especially if allowance was made for some PIC loss from the SML. This may have been a fortuitous coincidence, though.

Mixing across thermocline

Exchange of water between the SML and the sub-thermocline layer is limited but does occur to some extent, which largely depends on the strength of the thermocline. Consequently, the seasonal impact of processes which affect TA in the SML will be underestimated. This tendency may be counterbalanced to some degree by remineralization of PON and dissolution of PIC in the sub-thermocline layer. The overall error in the assumptions therefore depends partly on the amount of exchange that has occurred across the thermocline, and partly on the depth at which significant amounts of PON get remineralized and PIC dissolved. Quantification of the overall error involves detailed investigations in physical oceanography and the processes that took place at greater depths. These were outside the scope of this Study.

Phytoplankton growth within and below the thermocline

An additional shortcoming of the assumptions was the finding from productivity studies by Fernandez et al. (1993), that at some sites significant amounts of phytoplankton growth occurred within or below the thermocline. This would obviously have reduced any differences across the thermocline. The error was to some extent lessened by the fact that sub-thermocline estimates of TA were only analysed from samples at 70 m or greater depths, where primary production could be safely assumed to be negligible. While this problem does not really affect the accuracy of the estimates in the SML at that particular time of the season, it does underestimate the effect of phytoplankton when integrated to greater depths which cover the whole of the euphotic zone. Phytoplankton growth below the SML will not affect surface TA very much during stratified conditions, but would have an effect eventually when the thermocline is eroded in autumn.

Sampling depth below thermocline

If TA_{NO3} is not constant with depth below the thermocline, e.g. due to intruding water from greater depths, the sampling depth may also play a significant role.

5.4.4.9.7. Overview of errors and their effect on calcification estimates

Table 5.3 presents an overview of the above errors associated with calcification estimates if derived from a comparison of TA_{NO3} estimates above and below the thermocline. While

some effects remain unqualified or unquantified, the available information suggests that these errors may have led to underestimates of the total amount of net calcification within the SML. This error may amount to at least 7.5 μmol dm^{-3} by the time the spring bloom has reached its peak. In view of this, it may be worthwhile exploring or improving alternative ways of estimating calcification, such as the measurement of dissolved calcium.

Table 5.3: Overview of factors which may introduce errors into the estimate of potential alkalinity in form of TANO3 and the resulting estimates of calcification within the SML when compared to TANO3 at sub-thermocline depths.
Estimates are based on the discussion in section 5.4.4.9.

factor relating to:	errors in estimates of: potential alkalinity (μeq kgSW^{-1})	calcification in 1991 Study (μmol dm^{-3})
TA methodology, i.e. inaccurate estimation of variation in TA	variable: unquantified	variable: unquantified
omission of corrections for:		
uncoupled NH_4 uptake/regen.	probably insignificant	probably insignificant
sulphate uptake	overestimate by up to 5	underestimate by up to 2.5
organic acid release	overestimate by up to 10	underestimate by up to 5
N_2 - fixation	overestimate: negligible	underestimate: negligible
differential advection leading to possible difference in:		
preformed potential alkalinity	variable: unquantified	variable: unquantified
preformed nitrate concentration thus introducing error in correction for nitrate uptake	variable: unquantified	variable: unquantified
mixing across thermocline	overestimate: unquantified	underestimate: unquantified
algal growth below the SML	unaffected	underestimate: unquantified
sampling depth below thermocline	variable	variable

5.4.4.10. Comparison of photometric and calculated TA changes during the 1991 Study

When the entire photometric and calculated TA data sets were compared in chapter 2, it was established that photometric TA changed on average 15% less than calculated TA. The error on this relationship was greater than the precision of about 2 μeq $kgSW^{-1}$ specified for the photometric and calculated TA methods (chapter 2; Robertson et al., 1994). A more detailed investigation into the TA changes observed during the 1990 Experiment (chapter 4) revealed that correlations with hydrographic, chemical, and biological parameters more or less differed between methods. This had implications on the interpretation of spatial variations in TA and calcification estimates. In the 1991 Study, the diverse range of hydrographic and biological regimes lent itself to investigate the relative discrepancies even further by identifying the samples according to the regime they came from.

The calculation method generally showed a greater small-scale variability, or noise, in TA within and outside the bloom area. One consequence of this was that the latitudinal trend observed by the photometric method was absent or not as clear in the calculated results, and that the overall difference in calculated TA between these two biological areas was less distinct. Whether this meant, that the calculation method was less precise or that it was more sensitive to pick up small-scale and latitudinal variations could not be identified in this study. A possible reason for reduced precision in calculated TA may have arisen from the unsynchronized sampling associated with the different water supply systems for pCO_2 and TCO_2 during the 1991 cruise. Along the 15°W transect 6 the relative discrepancy between methods was even more pronounced, i.e. photometric TA was relatively lower by roughly 20 μeq $kgSW^{-1}$. In calculations of pCO_2 from TA and TCO_2, levels of pCO_2 derived from photometric TA would have been about 20 μatm greater than those based on calculated TA.

As a crude generalization the above findings suggest that the discrepancy between methods increased towards the north and east. In terms of water masses, they tended to be greater in MNAW and lower salinity NACW. With respect to biological regimes they tended to be higher in waters within the *Emiliania huxleyi* bloom, particularly at the eastern margin of the bloom. It is not clear whether latitudinal differences were caused by hydrographic or

biological factors. Further, it is uncertain why the discrepancy was notably larger in the eastern region. On one hand, there may be a biological explanation, i.e. it may have been related to the fact that some sites in this region had been identified as 'late bloom' regimes. On the other hand, the hydrography was also different to that of the central bloom area at 20°W. Relative discrepancies may thus have been particularly increased in such 'late bloom' waters, in low-salinity NACW, or in circumstances that have not been identified here.

The relative discrepancies also led to some differences in the interpretation of absolute and relative amounts of calcification, PIC loss from the upper 2-3 m, and the calibration of optical data. The comparison of calcification between the non-bloom and bloom areas along the 20°W line suggested that calcification was increased by 8 μmol dm^{-3} according to photometric TA_{NO3} estimates. This finding was about 30% greater than the one by the calculation method. This was also reflected in methodological differences with respect to POC:PIC net production ratios. The photometric method established a clear difference between the two biological areas, i.e. relatively insignificant PIC net production outside the bloom area and high relative production within the bloom. In contrast, the calculation method did not record marked differences between the two areas. In terms of possible absolute and relative amounts of PIC export from the SML, photometric results further assigned a notably greater importance to the bloom than the calculated results. Furthermore, photometric results of the POC:PIC production ratio implied that calcification in the bloom area had led to a relative increase in the CO_2 concentration and thus pCO_2 while the calculation method indicated that the pCO_2 reduction was merely lessened in that area.

The discrepancies were also reflected in the calibration curves of optical data for calcification, which indicated that the photometric TA_{NO3} change per given backscatter unit was larger by about 10% than the calculated TA_{NO3} change. This and the above results are at odds with the general observations in chapter 2, where the overall TA change generally tended to be larger in calculation method. This aspect has not been investigated further in this study but may be related to the smaller number of samples available for the optical data which may have led to systematic differences. It does however suggest that special care must be taken with respect to the choice of samples when such calibration curves are established for optical data. Furthermore, this discrepancy occurred on top of the absolute discrepancy of about 45 μeq $kgSW^{-1}$ between methods, which highlights the importance of

accurate TA measurements without which the optical data will be more or less useless in deriving at accurate estimates of calcification and pCO_2.

This study has revealed average discrepancies in TA estimates of about 2% between the photometric and the calculation method. Furthermore, the magnitude of this discrepancy has varied between regions. Therefore it is clear that at least one of the TA methods had provided inaccurate estimates of absolute TA and its relative changes. It will remain unresolved here as to which one it was. The principles of possible reasons for inaccurate TA measurements have already been covered in chapter 2. It may be, that these possible errors were exacerbated in the northern and eastern regions due to (a) the difference in the inorganic chemistry of sub-arctic water masses, and (b) possible changes in the dissolved organic matter associated with the different stages of phytoplankton blooms. Any type of inherent error in the conversion of raw titration data to TA, or in the calculation of TA from two other carbonate parameters, may have a different effect, the extent of which depends on the inorganic chemistry of that water. With respect to organic interferences, the presence of organic acids, which are unaccounted for in the calculation method, will tend to underestimate calculated TA. At the same time, the accuracy of photometric acid titration results may have been adversely affected, since the dissociation constant of the indicator used for the photometric titrations of this study was based on artificial seawater with a salinity of 35 psu. Consequently, the raw pH data from the titration and the derived modified Gran functions may have been inaccurate in waters with increased concentrations of dissolved or colloidal substances. While some attempt was made to keep the sample temperature close to 25°C during the titration, no adjustment was made for the effect of salinity variations on the pK of the indicator. Equally, no preliminary experiments were conducted to investigate the behaviour of the indicator in solutions which may contain increased amounts of dissolved or colloidal organic material, which may affect the pK values of acid-base indicators (Bishop, 1972).

5.4.5. METHODOLOGICAL CONCLUSION

The photometric method has provided estimates of TA variations within the Northeast Atlantic that largely fit into the general picture that has emerged from variations in hydrographic, biological, optical, and other chemical parameters. However, the more detailed investigation presented in this and the previous chapter has revealed considerable

discrepancies between methods with respect to absolute TA and its changes between different hydrographic and biological regimes. These discrepancies are too large to be complacent about in studies that ultimately intend to determine phytoplankton-induced changes in the seawater carbonate chemistry and in calcification as a result of climatic changes. It seems that much more effort should be put into the development of accurate TA methods. For this to be achieved, it will not be enough to calibrate a method against a TA standard based on artificial seawater or even natural deep-sea water. This study has demonstrated that there is an additional requirement for the better understanding of the factors that determine measured and calculated TA in surface waters. In order to increase the confidence in the results obtained by photometric acid titration methods, it seems essential to obtain a solid knowledge of the behaviour of the indicator, so that more accurate indicator pK values can be applied for the relevant ranges of salinity and organic loadings.

To account for the variability in the hydrography and inorganic chemistry in surface waters, it may be helpful to conduct intercomparisons at greater depths but still within the upper water mass so that conditions of hydrography and inorganic chemistry are more comparable to that of surface waters. With respect to biological variability in the upper water column, a first step would be to conduct intercomparisons of methods on different types of algal cultures or mesocosms, in which natural conditions should be simulated as far as possible.

6. ALKALINITY IN *EMILIANIA HUXLEYI* CULTURES

6.1. AIM

The aim of the experimental work presented in this chapter was to detect TA changes in batch cultures of *Emiliania huxleyi* over the course of approximately one week and compare the change in potential TA with that of concomitant PIC production estimates.

6.2. INTRODUCTION

Goldman and Brewer (1980) investigated the effect of nitrogen sources on phytoplankton-induced TA changes in continuous cultures of non-calcifying algae. They found that the TA changes could be explained by the stoichiometric equation which relates nitrate uptake to an equivalent increase in TA and ammonia uptake to an equivalent decrease in TA (equations 1.33 and 1.34). Their results suggest that the overall reaction for phosphate uptake leaves TA unaltered. However, little work has been carried out to test the additional stoichiometric equation which is generally used to predict TA changes due to $CaCO_3$ production by coccolithophorids (see equation 1.13).

This study intended to investigate whether the observed TA changes in batch cultures of *Emiliania huxleyi* can be accounted for by nitrate uptake and PIC production. Other biological factors which may have an effect on TA were not examined.

6.3. MATERIALS AND METHODS

Three replicates of 5 dm^{-3} batch cultures were grown for a week. One or two days after subculturing, 2 dm^{-3} were removed from each culture vessel for the analyses of

(i) TA (3 replicates);

(ii) PIC (5 replicates);

(iii) total particulate nitrogen (TPN) (5 replicates);

(iv) NO_3 (6 replicates);

(v) other measurements (cell counts, cell size, cell volume).

The same analyses were carried out five days later when the experiments were terminated.

The measured TA change within each culture was compared with the change in PIC and nitrate concentration according to:

expected change in TA $= 2 \times$ (change in [PIC]) - (change in [NO_3]) .

In order to investigate whether the effect of nitrate uptake on TA could also be quantified by the increase in TPN concentration, the expected TA change was also calculated using the change in TPN concentration instead of the change in nitrate concentration.

6.3.1. ALGAL CULTURES

The *Emiliania huxleyi* culture was obtained from J. Green, Plymouth Marine Laboratories, and had been isolated from a sample collected during one of the BOFS cruises to the North East Atlantic in 1990. No record exists of the exact strain identification and whether it was a low or high calcifying strain. It was grown in an artificial seawater medium described by Harrison et al. (1980). Alterations of the original composition included the omission of the silicate and ammonia components. The salinity of the medium was 30.5 psu. The composition of the medium is shown in table 6.1.

Although the nitrate and phosphate concentrations of the original and modified medium composition were unnaturally high, these concentrations were not altered for several reasons. At the time of planning the experiments, it appeared that not every medium would support the growth of calcifying strains of *Emiliania huxleyi* , and the experience with artificial culture media was limited. Due to logistic constraints, it was decided to settle for this particular medium and to keep the alterations to a minimum, since it had been used successfully by other algologists in connection with this species (B. Thake, pers. comm.). It was assumed that, although the high nutrient concentrations may alter the natural growth behaviour somewhat, this would not introduce any significant stress on the algae and thus would have no bearing on the comparison of measured and expected TA changes.

Table 6.1: Composition of the medium used for the growth of *Emiliania huxleyi* cultures based on the original composition by Harrison et al. (1980). Silicate and ammonia were excluded from this modified medium.

	final concentration
anhydrous salts	**(mM)**
NaCl	362.7
Na_2SO_4	24.99
KCl	8.038
$NaHCO_3$	2.066
KBr	0.7249
H_3BO_3	0.3715
NaF	0.06570
hydrated salts	**(mM)**
$MgCl_2\ 6H_2O$	47.18
$CaCl_2\ 2H_2O$	9.139
$SrCl_2\ 6H_2O$	0.0820
nutrients and trace metals	**(µM)**
$NaNO_3$	549.1
Na_2glyceroPO$_4$	21.79
Na_2EDTA	14.86
H_3BO_3	61.46
$FeCl_3\ 6H_2O$	6.56
$MnSO_4\ 4H_2O$	2.42
$ZnSO_4\ 7H_2O$	0.254
$CoSO_4\ 7H_2O$	0.569
vitamins	**(µM)**
thiamine HCl	0.297
vitamine B_{12}	1.47×10^{-3}
biotin	4.09×10^{-3}

Three batches of *Emiliania huxleyi* were grown in 5 dm^3 Erlenmeyer flasks at 15°C under light with a photon flux of 60 µmol m^{-2} s^{-1}. Instead of exposure to a more realistic light: dark cycle, the light turned out to be continuous. This was accidental, and as it was only discovered relatively late in the preparatory phase and the algae were growing and producing coccoliths, it was decided to keep the continuous light exposure. The algae were swirled around daily and subcultured every week. During the preparatory phase the cell numbers tended to increase from around 4×10^8 dm^{-3} at the start to around 10^9 dm^{-3} after 6 days when the cells entered the stationary phase.

6.3.2. CHEMICAL AND BIOLOGICAL ANALYSES

6.3.2.1. Total alkalinity

The determination of TA is described in chapter 2. The samples were filtered through Whatman cellulose nitrate filters with a pore size of 0.45 µm immediately after sampling and then stored in the dark at 4 °C for not more than two days until they were analysed for TA. Prior to the titration it was ensured that the sample had reached a temperature close to 25°C. Storage was necessary for logistic reasons, but could be assumed to have negligible bearing on the TA results. In contrast to the results described in the previous chapters, the culture TA results were expressed in µeq dm^{-3} at 25°C, because the density of the culture medium was not known, and because it allowed for a more accurate comparison with the other parameters which were also determined on a volume basis. While this distinction is of relevance when absolute TA values are compared, it has a negligible effect when the focus rests on TA changes.

6.3.2.2. PIC

For the PIC determinations the samples were collected on precombusted GF/F (0.8 µm) filters and analysed on a Europa Roboprep CN analyser. Glycine was used as the standard.

About 3 hours after removing the algal cultures from the culture room, 500.0 cm^3 of each culture were filtered through ten Whatman GF/F glassfibre filters (25 mm diameter), i.e. 50.00 cm^3 per filter. The vacuum pressure was about 0.2 bar. All filters had previously been precombusted for 4 hours at 500 °C. Five of the filters were dried in an oven overnight at 40 °C. The remaining 5 filters were placed in a dessicator and exposed to fumes of concentrated

hydrochloric acid for 24-48 hours. Afterwards they were also dried in the oven. All filters were kept in petri-dishes for up to 5 days. They then had to be wrapped into precombusted aluminium foil, which had to be compressed and shaped into a small pellet. In order to facilitate this, a cork borer was used to cut off the margin of the filter which was not obviously covered with particulates. While doing so, special care was taken not to remove any particulates from the filters. The pellets were then stored for up to 4 weeks in a dessicator until all the samples were analysed together.

The concentration of PIC was determined from the difference between the 5 replicates of acidified and unacidified samples.

The analysis of PIC from particulate calcium in connection with flame atomic absorption spectrometry, as was performed during the 1991 coccolithophore bloom study, was not an option for logistic reasons.

6.3.2.3. Nitrate

Approximately 4 hours after removing the algal cultures from the culture room, 200 cm^3 of each culture was filtered through 47mm Nuclepore polycarbonate filters of 0.2 µm pore size (100 cm^3 per filter). The delay in filtering the samples was unavoidable for logistic reasons. A vacuum pressure of about 0.2 bar was used. Each filter had been rinsed with about 50 cm^3 of sample beforehand. The filtrate was filled into three pre-rinsed polyethylene bottles of about 100 cm^3 volume and frozen at -20°C. The samples were stored for one to nine days and removed from the freezer the night before the analysis.

The nitrate analysis was carried out according to the method described by Parsons et al. (1984) for the determination in seawater, which involves the reduction to nitrite by running the sample through a column containing copper-coated cadmium filings. The nitrite produced is diazotized with suphanilamide hydrochloride and coupled with N-(1-napthyl-) ethylenediamine dihydrochloride to form an azo dye.

The calibration was carried out with KNO_3 using synthetic seawater as the background solution.

Since the nitrate concentrations in the algal cultures were expected to be much higher than in natural seawater for which the nitrate method is designed, a 40-fold dilution with synthetic seawater had to be carried out prior to the analysis.

6.3.2.4. TPN

Total particulate nitrogen values were obtained from the filters which held the TPC fraction.

6.3.2.5. Other analyses

Total dissolved phosphate was also measured but the data was not used as it was not assumed to affect TA.

Cell counts and estimates of cell diameter were carried out under the microscope with a haemocytometer as an initial check on the usual growth habit and conditions of the algal cultures. By doing this, it was ensured that the algae had grown according to the previously established range of cell numbers (see section 6.3.1), that they were covered with coccoliths, and that there was no obvious indication of similar numbers of contamination by other organisms. The cells were generally found to have a diameter of about 4 μm.

The standard errors on the results determined from differences between measurements were calculated according to Baird (1962).

6.4. RESULTS

An overview of the results from the cell counts and chemical determinations obtained in the three culture experiments are shown table 6.2. In all three experiments, cell counts increased over the course of 5 days from about 4 to 14 × 10^8 cells dm^{-3}. Changes in TA and PIC varied notably between experiments. Total alkalinity decreased by between 70 and 270 μeq dm^{-3}, while PIC increases of between 110 and 330 μM were observed. Nitrate decreased by 90 to 100 μM and the increase in TPN was about 10 μM less than the change in nitrate.

The results from the comparison between measured and expected TA changes are shown in table 6.3.a. The greatest measured and expected changes were observed in culture 1 and the least in culture 3. Expected TA changes were generally about two times larger than the

measured ones. This appeared to be independent of the nitrogen parameter used to calculate the expected changes.

Table 6.2.: Measurements of TA, PIC, NO_3, TPN, and cell counts at the start and end of 3 algal culture experiments using *Emiliania huxleyi* batch cultures. The duration of the experiments was 5 days.
Measurement of TPN shown here were taken from samples which had not been exposed to acid fume.
The standard error (s.e.) was determined according to Baird (1962).

	culture	cell counts	s.e.	TA	s.e.	PIC	s.e.	NO_3	s.e.	TPN	s.e.
		(10^8 dm^{-3})		(μeq dm^{-3})		(μM)		(μM)		(μM)	
start	1	3.0	0.2	2020	1.4	114	1.7	569	1.5	36	0.4
	2	3.9	0.1	1966	4.1	176	2.2	550	1.6	39	0.3
	3	3.6	0.3	2135	0.4	153	3.0	581	2.8	44	0.4
end	1	14.7	0.6	1750	0.5	439	15.9	475	2.3	119	1.7
	2	14.0	0.4	1763	2.6	395	13.7	456	1.7	126	1.6
	3	14.0	0.8	2063	2.1	268	25.1	482	1.5	130	2.8
change over 5 days	1	11.7	0.7	-270	1.5	325	16.0	-94	2.8	83	1.8
	2	10.0	0.5	-203	4.8	219	13.9	-93	2.3	87	1.6
	3	10.0	0.9	-71	2.1	115	25.3	-100	3.0	85	2.9

Tables 6.3: Summary of the comparison between measured and expected changes in TA (μeq dm^{-3}) in 3 batch cultures of *Emiliania huxleyi* over the course of five days. Expected changes were calculated from the increase in PIC and the

(a) decrease in NO_3 concentration
(b) increase in TPN concentration (using samples which were not acid fumed)

Negative changes in TA imply that TA decreased over the course of the experiment. A negative result for the difference between TA changes means that the expected decrease in TA was greater than the measured one.
The standard error (s.e.) was determined according to Baird (1962).

(a) using NO_3

culture	change in measured TA	s.e.	change in expected TA	s.e.	difference between measured and expected changes in TA (expected - measured)	s.e.	ratio of changes in TA (expected : measured)	s.e.
1	-270	1.5	-557	22.8	-287	22.8	2.1 : 1	0.09
2	-203	4.8	-344	19.8	-141	20.4	1.7 : 1	0.11
3	-71	2.1	-131	35.9	-59	36.0	1.8 : 1	0.51

(b) using TPN

culture	change in measured TA	s.e.	change in expected TA	s.e.	difference between measured and expected changes in TA (expected - measured)	s.e.	ratio of changes in TA (expected : measured)	s.e.
1	-270	1.5	-567	22.7	-298	22.7	2.1 : 1	0.09
2	-203	4.8	-350	19.7	-147	20.3	1.7 : 1	0.11
3	-71	2.1	-145	35.9	-74	36.0	2.0 : 1	0.51

6.5. DISCUSSION

The cell counts of *Emiliania huxleyi* were almost two orders of magnitude higher than those observed during the 1991 cruise. During the culture experiments large PIC increases and TA decreases were observed. In one culture a TA decrease of 270 μeq dm^{-3} and an increase in PIC concentration of 325 μM was measured. The observed TA and PIC changes varied considerably between cultures. This variation was not so notable for changes in nitrate and TPN. Nitrate decrease was about 90 μM and the TPN increase tended to be approximately 10 μM lower than for nitrate. Compared to results from the 1991 cruise, the high cell numbers in the cultures were not matched by the changes in TA and PIC. The TA change per *E. huxleyi* cell was about 6 to 9 times lower in the culture experiments, and the measured PIC change per cell was about 4 times lower. This was probably due to the particular strain used in these experiments or the unnatural growth conditions such as the continuous light regime or the high concentrations of nitrate and organophosphate in the artificial medium. Nevertheless, the relatively low amount of calcification that was associated with these algae should not have affected the TA change that occurs due to calcification. However, measured TA did not decrease as much as would have been expected from the change in PIC and nitrate or TPN. There are several possible explanations for this which are not mutually exclusive.

First of all, TA measurements may have underestimated the actual TA change. One reason may have been the exposure to continuous light which has been shown to cause stress to algae in some cases (Brand & Guillard, 1981). Any excessive DOM release may have affected the titration results in an adverse way, since the indicator pK value that was used in this study was not calibrated for culture media. In addition or alternatively, it may have increased the TA *per se*, i.e. by increasing the concentration of titratable organic acids.

Secondly, it is possible that the PIC results were overestimated due to underestimates of the POC measurements. Any error in the PIC concentrations is of particular concern since its error is doubled in equivalent terms. A likely cause for the underestimate may have been the acidification procedure used to remove the PIC fraction. It may have damaged the cells and thus caused a reduction in POC. Possible evidence for this was observed in form of the difference of up to 20 % between TPN in acidified and unacidified samples. Since the particulate nitrogen is thought to be almost solely in the organic form, this seems to indicate that particulate organic matter was lost during the acidification step. Different approaches to

separate the organic from the inorganic carbon fraction have been used by different authors (e.g. Sikes et al., 1980; Nimer & Merrett, 1992; Fernandez et al. (1993) or section 5.4.2.4), but unlike in the case of sediment samples, a thorough comparison has not been carried out for water samples.

A further partial reason for the discrepancy may have been a slight overestimate of the nitrate concentrations, resulting in an overestimate of the relative changes. Doubts over the accuracy of these measurements have arisen, since the measured nitrate values at the start of the experiments were found to be higher than would be expected from the modified recipe of the culture medium. Possible reasons include, first of all, the large dilution required to adjust the concentration of the sample to the operational range of the nitrate method, and secondly, the complexity of the algal culture medium, for which the method was not calibrated. In the latter case, the problem may have been solved by using the method of standard additions rather than following the fairly standard procedure for open ocean water of calibrating the nitrate method with synthetic medium.

The discrepancy observed between nitrate and TPN changes can easily be accounted for by the release of dissolved organic nitrogen in the algal cultures, by the possible overestimate of the nitrate results, and by loss of TPN during the filtration process. The latter point became apparent when the results from preliminary experiments were studied in more detail. They revealed, what in fact has been demonstrated by other authors, i.e. that the filtration can damage the cells which results in the reduction of particulate organic matter. In the preliminary experiment, two factors where investigated, i.e. the effect of sample volume filtered, and the effect of the vacuum pressure used. A comparison between pressures of 0.2 and 0.8 bar revealed a notable difference in the TPC results. The comparison between volumes filtered revealed that the TPC was higher in the smaller volumes. Although these findings were not statistically tested, they are consistent with the generally known fact that filtration can damage algal cells. This susceptibility may vary between species and physiological and environmental conditions, but should be paid far more attention to.

6.6. CONCLUSIONS

The discrepancy observed between the measured and expected TA reduction is indisputable in these experiments and has led to the reconsideration of much of the experimental design.

With respect to the analytical methods used, possible shortcomings were detected in all the major analyses that were used. The main focus should rest with the improvement of the PIC analysis, since any error in this parameter has the greatest impact on the discrepancies, i.e. an inaccurate PIC estimate may be interpreted as an error in TA of twice the equivalents. While a systematic intercomparison of the different methods to estimate PIC has not yet been conducted on water samples, it may be more appropriate to derive PIC data from the particulate calcium fraction on the filters as was done for the 1991 cruise. Like this, any possible problems associated with acidification procedures could be circumvented. Secondly, it is possible that the photometric TA method may not be suitable for determinations in experiments involving dense cultures, because the filtrate from the cultures cannot always be assumed to have a stable composition for which the pK of the pH indicator is known. In order to avoid these uncertainties associated with indicator pK values, it appears to be better to use a potentiometric TA method instead. Although the error associated with the nitrate analyses was comparatively minor in these experiments, it nevertheless should be reduced. This would be possible by using the method of standard additions for the calibration and by reducing the nitrate concentration of the medium to a level more typical for open ocean concentrations, so that the error associated with the dilution step prior to the nitrate analysis can be omitted or at least reduced.

Although the experimental conditions in this study were far from realistic, this should not lead to discrepancies between measured and expected TA *per se*. Nevertheless, in order to make the results more applicable to *in situ* situations, the growth conditions should generally be as natural as possible. Accordingly, continuous light should be avoided, and a more realistic light:dark light cycle should be used instead. Similarly, the concentrations of nitrate and phosphate should be reduced to far more natural levels, and it should be ensured that the *Emiliania huxleyi* strain used in the study is typical of a bloom-forming one such as was encountered in the 1991 study.

In addition to the above methodological considerations, it is possible that some of the discrepancies between measured and expected TA may have been the result of sulphate uptake and/or organic acid release by the algae. In the latter case, this may have happened during the actual growth phase and may have been enhanced by the continuous light, but it is also possible that some organic acids were released by the dense cultures during the

filtration of the TA samples. As demonstrated in table 5.3, these processes would have increased the measured TA in the final samples, which in turn could have contributed to the reduction in the measured change of TA over the course of the experiments.

7. SUMMARY AND GENERAL CONCLUSIONS

7.1. TA AND ITS ROLE IN CLIMATE CHANGE

This project was funded to contribute to the better understanding and more accurate predictions of climate change. The general aims of this study were to develop a suitably practical, precise, and accurate photometric TA method to measure changes in TA in the surface waters of the Northeast Atlantic and in coccolithophorid cultures. The likely causes of these changes were to be investigated with a particular focus on the effect of algal nitrate uptake and PIC production. The suitability of the method was to be examined in intercomparative exercises involving other TA methods used by other research teams. The findings were to be related to existing information on spatial and temporal variations of TA within the Northeast Atlantic and considered in the context of studies related to climate change.

In order to better understand the role of TA with respect to climate change, the general introduction intended to provide some information on past and current climate change, atmospheric CO_2 concentrations, the oceanic carbon cycle, and on processes involved in potentially affecting atmospheric CO_2. It then focused on TA, i.e. its definition, potentially influencing factors, global variation, and its relevance and applications in carbon cycle related studies. The IPCC (1996) concluded that the body of statistical evidence points towards human influence on our current global climate, the extent of which remains uncertain. By the year 2100 global mean temperature and sea level are expected to rise by 1 to 3.5 °C and 15 to 95 cm, respectively. If existing policies regarding fossil fuel emissions remain unaltered, atmospheric CO_2 concentrations are projected to surpass 700 ppmv before that year. Although other greenhouse gases may become increasingly important in the future, CO_2 is identified as currently the main anthropogenic cause for the observed global warming.

According to the carbon cycle models used for the IPCC (1996) climate predictions, a little less than half of the net emissions of CO_2 resulting from human activity remains in the atmosphere. One third of these emissions, i.e. 2.0 Gt C yr^{-1}, is absorbed by the global ocean, which constitutes by far the largest reservoir of carbon of all the components of the climate

system. The estimate of uptake by the ocean was derived from a combination of modelling and carbon isotope and other measurements, and it has an estimated error of ±0.8 Gt C yr^{-1}. This error term, which itself is not undisputed, arises partially from uncertainties due to discrepancies between the various models, short-term annual variations in atmosphere-ocean carbon fluxes, and possible biogeochemical feedback processes in response to climate change. Difficulties in estimating changes in some terrestrial carbon sinks make it necessary to derive these terrestrial estimates from the other known carbon flux components including the oceanic sink. This adds to the importance of accurately representing the various oceanic processes in carbon cycle models. However, some of our understanding of the mechanisms and information on the spatial and temporal variability of these processes is still insufficient.

While large-scale physical features such as the thermohaline circulation are modelled reasonably realistically, it is it is essential for more reliable representation of the carbon cycle to use eddy-resolving models. To represent more accurately the variability of biological and chemical processes associated with smaller-scale features, the resolution should ideally reach a scale down to 10 km. Modelling results suggest that the solubility pump is playing a major role in reducing atmospheric CO_2 at present, and that it was also important in the additional reduction during glacial times. The impact of this pump is expected to become less in the next hundred years due to the reduced buffering capacity of the oceans under rising CO_2 concentrations.

While models suggest that, similar to the solubility pump, the organic carbon pump has a reducing effect on atmospheric CO_2 concentrations, this pump may well have played a considerable part in further reduction of atmospheric CO_2 during glacial periods when combined with changes in ocean circulation. Proposed mechanisms for this include a change in the Redfield ratio of the export production in the deep ocean via changes in the aeolian input of limiting nutrients such as nitrate, phosphate and iron from exposed shelf regions. Other mechanisms involve changes in the ratio of dinitrogen fixation/ denitrification in different parts of the ocean. For changes in the organic carbon pump to have any significant effect in the near future, the Redfield ratio would have to change at least by 30%, which is unlikely to occur. With respect to dinitrogen fixation/denitrification,

it remains difficult to predict the extent and even the direction of any changes in the ocean. There is insufficient evidence to conclude that the strength of the biological pump has been significantly altered by recent climate change, and little change in atmospheric CO_2 is predicted for the near future due to the biological pump as a whole.

According to models, the effect of the biological $CaCO_3$ pump on present atmospheric CO_2 concentrations lessens the effect of the organic carbon pump only to a minor extent. Since the POC:PIC export production ratio may vary with the amount and type of phytoplankton species and the ecological structure of secondary producers, it has been considered that absolute and/or relative changes in the strength or the operational sites of the $CaCO_3$ pump may at least have contributed to the glacial-interglacial shifts in atmospheric CO_2. However, the proposed $CaCO_3$ compensating mechanism, which operates on a time-scale of at least about 2.5 kyr, is too slow to explain the relatively abrupt glacial-interglacial transitions in atmospheric CO_2 and is thus of no concern to the estimates for anticipated climate change. Similarly, the 'coral reef hypothesis', which relies on a relatively large fraction of PIC burial, does not account for the entire glacial-interglacial CO_2 signal. The effect of the relative importance of the two biological pumps was investigated in the 'rain ratio hypothesis' and the 'respiratory calcite dissolution hypothesis'. The former only provided a partial explanation for the glacial/interglacial changes in atmospheric CO_2. However, the latter could explain the entire change of 80 µatm between glacial and interglacial periods by taking account of changes in ocean circulation, POC:PIC export production ratios, and enhanced PIC dissolution in the sediments due to increased oxic POC degradation.

The relative importance of all the different oceanic carbon pumps in regulating the atmospheric CO_2 concentration in the modern ocean remains a matter of dispute. Estimates of the importance of the organic carbon pump range from one third to twice that of the solubility pump. In addition, the IPCC (1996) stresses that these and other results are preliminary because climate change may trigger biogeochemical imbalances which are not yet adequately understood let alone represented in these carbon cycle models. Such biogeochemical feedback mechanisms may involve, for example, potential changes in the

ecosystem structure of the SML, processes occurring in the interior of the oceans, and an enhancement of the 'alkalinity pump'.

A brief description of the global alkalinity cycle was provided before reviewing the TA-influencing factors such as temperature, pressure, salinity, $CaCO_3$, CO_2, nitrogen, phosphorus, silicate, sulphur, and organic acids. While most of the effects are relatively well established, special attention was drawn to processes which usually remain unconsidered or at least unaccounted for. In turn, this may lead to errors in derived parameters and conclusions. One of these processes is dinitrogen fixation, which may support up to half of the new production in the subtropical North Pacific Ocean. It is not expected to increase TA like in the case of algal nitrate uptake. Another process of concern is denitrification which is expected to increase TA by one equivalent for every mole of nitrate that is being converted to N_2. Since any climate induced changes in stratification may change the relative abundance of N_2 fixing/denitrifying species in the oceans, this may affect the vertical and horizontal TA profile of the oceans, which in turn may affect atmospheric CO_2 concentrations. With respect to sulphur, sulphate uptake and the resulting TA increase may vary with species and environmental conditions. Based on an average POC:POS ratio of 106: 1.6 the increase from sulphate uptake would be almost twice that due to phosphate uptake, but may even exceed the nitrate uptake effect in case of high DMSP producing species. Available field data suggests that DMSP production during an *Emiliania huxleyi* bloom was too low to have a detectable effect on TA. However, if the increased atmospheric sulphate concentrations during glacial times turned out to have been caused by increased DMSP production, it has been proposed here, that this would provide a further mechanism for increased TA in the surface waters during glacial periods. This mechanism has not yet been considered in glacial-interglacial carbon cycle models. Although frequently acknowledged as a potential factor influencing TA, the limited knowledge about the types and concentrations of titratable dissolved organic acids and their acid dissociation constants makes it almost impossible to accurately assess their impact on TA. It has been proposed in the past that their release may cause an increase in TA of up to about 10 $\mu eq\ kgSW^{-1}$ in the open ocean. The main processes affecting TA close to the seawater-sediment interface or in anoxic basins are generally very different to those prevailing in the SML and ocean interior.

An approximate indication of the global distribution of TA based on earlier TA data sets indicates that temperate Atlantic surface water tends to have the lowest TA and deep Pacific and Indian Ocean waters the highest TA.

The main role of TA in the global carbon cycle is its influence in determining the capacity of the seawater to absorb atmospheric CO_2. It is therefore a vital parameter in calculating CO_2 exchanges between atmosphere and ocean for past, present, and future when no direct CO_2 data is available. For some open ocean regions where biological effects have so far been found or assumed to be negligible, a constant TA has been assumed for the entire year. Constancy of TA has also been assumed in most carbon cycle models, including the models used for the IPCC (1996) climate predictions. However, the importance of realistic three-dimensional representation of the carbonate chemistry has been emphasized recently and has led to TA being used as one of the principle variables in a recent OGCM in order to calculate atmospheric pCO_2. The importance of data sets such as that collected as part of the JGOFS programme has been stressed for these purposes.

Further, TA measurements have been used to investigate the internal consistency of the seawater carbonate system, which can highlight potential problems with the analytical methods including the use of inaccurate dissociation constants, and it may indicate the presence of dissolved organic acids. In connection with TCO_2 measurements, TA has been used to determine the causes for disequilibria of pCO_2 between atmosphere and ocean. Similarly, in culture experiments TA was used in connection with pH measurements to identify the inorganic carbon source utilized by coccolithophorids grown in closed cultures.

An important application of TA data is in $CaCO_3$ precipitation/dissolution studies as an alternative to the direct measurement of dissolved calcium, which still poses significant analytical problems. For example, TA was used to back-calculate the original pCO_2 so that the penetration depth of anthropogenic CO_2 in different oceanic regions could be determined. This approach provides an alternative to modelled estimates of the penetration depth of excess CO_2, but this approach has its own shortcomings, which are also reviewed. The findings suggest that in the case of the western basin of the North

Atlantic the excess CO_2 may already have reached the ocean floor, i.e. a depth of about 4550 m. In these studies potential TA was generally derived from oxidative nitrate corrections, whereas in a back-calculation exercise conducted to determine pre-industrial carbon fluxes, the nitrate uptake effect was simply based on nitrate concentrations. Measurements of TA have also been used to improve our understanding of the factors which cause the difference between $CaCO_3$ compensation and lysocline depths. In this context, it is important to account for the appropriate TA-altering processes at the different depths in the oceans.

7.2. TA METHODOLOGY

Once the photometric TA method was fully set up, the entire analysis of a sample of about 120 cm^3 took approximately 50 minutes under optimal conditions. It consumed more attention than had originally been anticipated due to occasional instabilities of the spectrophotometric readings and the obstruction of bubbles in the optical path.

One-day experiments revealed a short-term precision of ± 0.1 %, which was comparable to that quoted for potentiometric and coulometric methods. While the precision was slightly poorer in blanks and samples originally or still containing *Emiliania huxleyi* cells, the precision was largely determined by the stability of the absorbance readings. However, during the 1991 cruise the calculation method generally showed a greater small-scale variability, or noise, in TA. Consequently, it did not discern the latitudinal trend and clear difference in TA between the bloom and non-bloom area as was done by the photometric method. A possible reason for this may have been the unsynchronized sampling associated with the different water supply systems for pCO_2 and TCO_2 during that cruise. Without stable TA reference material available during the study, it was not possible to obtain an accurate estimate of the longer-term precision of the method. Analyses of different Na_2CO_3 standards on the same acid did not reveal any obvious systematic change over a period of weeks or several months.

The discrepancy of less than 0.5% between photometric and coulometric TA for Na_2CO_3 standards was encouraging considering the coulometric method appears to be the most precise and accurate one on theoretical grounds. The discrepancy of 1% and 2% for natural seawater samples from various depths between photometric and other TA methods, i.e.

three potentiometric and a calculation method, respectively, led to doubts over the accuracy of the photometric method used in this study. This concern was enhanced when cruise results revealed that these discrepancies were not constant. First of all, they tended to be less at lower TA with the average change in photometric TA being 15% to 40% smaller than recorded by potentiometric and calculation methods. Superimposed on this general trend was an inverse relationship between photometric and one set of potentiometric TA data which was observed for samples limited to the SML in the 47°N 18°W area in 1990. In addition, the discrepancy between photometric and calculated TA tended to be greater in the northeastern part of the Northeast Atlantic in 1991, a regime characterized by low-salinity NACW and the late stage of a coccolithophorid bloom.

The above discrepancies would have led to significant differences in the interpretation of the field observations with respect to, for example,

(i) the horizontal distribution of TA at the surface as well as sub-thermocline depths;
(ii) quantitative relationships between TA and other parameters including an optical one ultimately intended for the calibration of optical satellite data; and
(iii) derived estimates of absolute and relative amounts of calcification and resulting estimates of the relative strength of the $CaCO_3$ pump.

In quantitative terms, the relative discrepancy between photometric and calculated TA of 20 $\mu eq\ kgSW^{-1}$ in the very northeastern part of the Atlantic would have led to a relative overestimate of about 20 μatm in that region, if pCO_2 had been calculated from photometric TA. The relationship between TA and salinity in 1990 would have been reversed in the case of potentiometry, and calcification estimates from optical data based on a calibration with TA_{NO3} would be 10% larger if derived from photometric rather than calculated TA. Further, this discrepancy would be superimposed on the absolute discrepancy between photometric and calculated TA of 45 $\mu eq\ kgSW^{-1}$, which would translate to a difference in calcification estimates of more than 20 $\mu mol\ dm^{-3}$. The estimate of calcification within the coccolithophorid bloom area was 30% greater when based on photometric rather than calculated TA estimates. These photometric estimates would imply that the overall effect of the $CaCO_3$ pump on pCO_2 was stronger than that of the organic carbon pump in the bloom

area by early summer of 1991, while this was not corroborated by the estimates based on calculated TA.

The main possible causes for inaccurate photometric TA results were identified to be inaccurate absorbance readings and/or inaccurate calculations of pH due to the use of an incorrect acid dissociation constant for the indicator at the given temperature, salinity, or composition of the background medium. The reasons for systematic variations in the discrepancies from 1991 appeared to be related to some horizontally varying parameter which was not identified.

While at least one of the TA methods had provided inaccurate estimates of absolute TA and its relative changes, it will remain unidentified here. Possible errors may have been exacerbated in the northeastern region due to some differences in the inorganic chemistry of sub-arctic water masses, and/or possible changes in the concentration and composition of DOM associated with different types and stages of phytoplankton blooms. Significant amounts of organic acids would have led to underestimates of calculated TA and possibly to inaccurate photometric TA data due to unaccounted for changes in the pK of the indicator. This latter source of error in photometric measurements also provided one of several possible explanations for the discrepant results obtained in the culture experiments.

An additional reason for possible variation in the discrepancies between photometric and the other methods in 1990 was the omission of filtering the samples for either of the three TA methods involved. On theoretical grounds, this error may have been reduced or negligible in the case of the potentiometric and the calculated TA. Any variation in PIC concentration may therefore account for at least some of the variable discrepancies between methods but does not explain why these photometric TA was generally lower. Unless proven unnecessary, this filtration step should be an integral part of all acid titrations of natural samples. It should involve inert filters with an effective pore size not exceeding 0.2 µm and a vacuum pressure not exceeding 0.2 bar. Further reduction of potential damage to any organisms retained on the filters can be achieved by keeping the particulate load per filter area relatively low.

If a photometric TA method is chosen, improvements to the method include the use of a multiple wavelength method with the main readings being taken at the wavelengths of maximum absorption of the unassociated and associated indicator forms. Complementary readings should be taken at wavelengths at which the absorbance remains stable throughout the titration, e.g. at the isosbestic wavelength, so that instrumental instabilities can be detected more easily. Absorbance readings at the main wavelengths should ideally be conducted in the range of 0.4 to 0.8 AU. To reduce errors due to the addition of the indicator, its concentration can be reduced by increasing the pathlength of the photocell and by choosing an indicator with a pK value more closely falling into the pH range of interest, in this case for example quinaldine red or p-nitrophenylhydrazine. Accurate pK values should be determined in every medium of interest covering the necessary range of salinities and temperatures. The titration should also be speeded up by conducting the titration in a photocell, which should be thermostatted and ideally completely sealed. Obstruction of the lightpath by bubbles in samples from greater depths can be reduced by immediately analysing the collected samples at their *in situ* temperature or by filtering the samples after collection. If the photometric set up proved successful, it should be considered to automate the method for routine analyses. If the pK of the indicator turns out to be highly variable in samples of cultures in which DOM concentrations and compositions are more likely to vary in an unpredictable way, it would appear safer to use a potentiometric TA method.

While there are several theoretical reasons to question the accuracy of the photometric TA method of this study, it was encouraging to find corroboration of some general latitudinal trends in photometric TA by the calculation method in both years. Further, vertical and thus seasonal estimates of TA changes were confirmed by the potentiometric and calculation method in 1990. Apart from this, it is important to bear in mind that the potentiometric and calculation methods may also have their weak points. The potentiometric method relies on the assumption that the pH meter returns stable readings. The calculation method depends heavily on the assumption that the dissociation constants used for carbonic acid are accurate and that the contribution from organic acids to TA is negligible. These assumptions cannot always be guaranteed to be correct, and major discrepancies in TA results from different methods and research teams have been observed. Furthermore, considerable discrepancies have been shown to arise from the choice of the

pH range in which the titration is carried out and the statistical method used in the conversion of the raw titration data to the final TA result. Discrepancies in the range of 1% were also observed between different data sets for TA during NABE which have largely remained unexplained. More recent intercomparisons and overdeterminations of the seawater carbonate system have provided evidence of internally far more consistent results derived from different carbonate parameters and methods. However, it needs to be borne in mind that these exercises were conducted in areas where the chemistry of the water was much less influenced by phytoplankton growth than was the case in the Northeast Atlantic during spring/early summer in 1990 and 1991. With respect to phytoplankton culture work, there seems to be no published record of any overdeterminations of the carbonate system. Consequently, the remaining theoretical shortcomings and reports of methodological discrepancies cast serious doubts over the justification of the general confidence with which some of the TA results are sometimes presented and interpreted in various exercises. Without appropriate certified TA standards, there was afterall no proven ground to discard the photometric TA data set as unsuitable for interpretation in the field and culture work of this study.

7.3. SPATIAL VARIATIONS OF TA IN THE NORTHEAST ATLANTIC

Spatial variations of about 10 μeq $kgSW^{-1}$ were observed by a potentiometric and a calculation method in the 47-48°N 20°W area in May 1989. At 60°N 20°W calculated TA was about 25 μeq $kgSW^{-1}$ lower than in the more southern study area.

In 1990, the general range of photometric TA observed within the SML around 47°N 17°W was between 2310 and 2330 μeq $kgSW^{-1}$, i.e. amounting to about 20 μeq $kgSW^{-1}$. The effect of hydrographic variations had contributed about one third to this, while variations due to nitrate uptake were found to be negligible. The range of TA_{NO3} suggested that two thirds of the variation in TA had been caused by variability in net calcification. On one hand, this net calcification estimate of 6.5 μmol dm^{-3} may have been an overestimate due to the imprecision of the photometric TA method and possible variations in the performed TA_{NO3} of the different water masses. On the other hand, the omission of filtering the samples prior to the analysis may have introduced an unquantified error, if PIC was present in any samples. The positive correlations of TA with salinity and temperature tie in with previous

observations made in the North Atlantic during the TTO program. A link with phytoplankton growth was not made, but this was not necessarily to be expected for several reasons. Photometric TA was 10 μeq $kgSW^{-1}$ lower along the northern transect due to lower salinity and possibly more net calcification there. Although not conclusive, these trends fit in with the latitudinal trends of the hydrography and phytoplankton ecology in the Northeast Atlantic.

The 1991 study area between 55 to 63.5°N and 5 to 24°W revealed a wide range and much variability of hydrographic and biological regimes, which gave rise to considerable large- and small-scale variations of surface TA. The overall photometric TA ranged from 2245 to 2315 μeq $kgSW^{-1}$, i.e. amounting to 70 μeq $kgSW^{-1}$, with the highest values in the high-salinity NACW and the lowest ones in *Emiliania huxleyi* bloom waters. The overall effect of salinity on variations in TA amounted to about 20%. Nevertheless, it was the chief factor influencing the distribution of surface TA outside the *E. huxleyi* bloom area causing a linear latitudinal TA decrease of 2.3 μeq $kgSW^{-1}$ per 1° latitude between 55° and 61°N 20°W. The positive relationship between salinity and TA in the 1991 study area was similar to that observed further south in 1990. Variations in nitrate uptake appeared to have a relatively minor effect on the overall areal distribution of surface TA at that time of the year, apparently accounting for no more than 7 μeq $kgSW^{-1}$. The potential errors associated with preformed NO_3 concentrations were considered. Most of the spread in TA_{NO3}, i.e. about 55 μeq $kgSW^{-1}$, was ascribed to variations in the abundance of coccolithophorids and their associated PIC production in the 1991 study area. Sufficient circumstantial evidence from this and other studies indicates that most of the calcification was due to *E. huxleyi*. The spread was almost equivalent to the maximum PIC concentration of 30 μM observed in surface waters. Similarly, small-scale changes in TA and TA_{NO3} of up to 40 μeq $kgSW^{-1}$ over 40 km were accompanied by equivalent changes in the concentration of PIC. Furthermore, in a comparison of vertical profiles the largest vertical changes in TA_{NO3} were also matched by the largest vertical changes in PIC across the thermocline.

The overall latitudinal profile of sub-thermocline TA from the 70 -150 m depth range based on photometric TA indicates that TA fell by about 20 μeq $kgSW^{-1}$ from 2310 μeq $kgSW^{-1}$ at 46°N 17°W to 2290 μeq $kgSW^{-1}$ at 63° 30'N 22°W. This suggests that the range of surface

TA of 90 μeq $kgSW^{-1}$ observed in the Northeast Atlantic in 1990 and 1991 was largely but not entirely caused by processes usually limited to the SML.

7.4. CALCIFICATION ESTIMATES IN THE NORTHEAST ATLANTIC

This study has provided independent estimates of net PIC production based on photometric TA measurements for areas within and outside the *Emiliania huxleyi* bloom. From depth profiles outside the bloom area it was deduced that net PIC production had reached about 3 μmol dm^{-3}. This estimate was similar to observations further south in 1990 when the abundance of *Emiliania huxleyi* was presumed to be negligible in surface waters. It also matched measurements of PIC standing stock in 1991, which typically remained below 5 μM.

Depth profiles of TA_{NO3} at 'early and late bloom' stations suggested that net PIC production within the SML may have reached at least 18 μmol dm^{-3} since the onset of stratification in 1991. This compared well with estimates based on PIC standing stock which indicated a maximum level of PIC production in the bloom of 17 μmol dm^{-3} when integrated over 35 m.

A more averaged estimate of the increase of PIC net production within the entire coccolithophorid bloom area in 1991 indicated an elevation of about 8 μmol dm^{-3} ranging from 0 to 24 μmol dm^{-3}. The spread reflected the considerable small-scale variations in hydrography and biology and possibly also vertical variations of PIC production within the euphotic zone. This implies that average net production of $CaCO_3$ in the bloom areas was around 12 μmol dm^{-3}, which is lower than the estimate of 16.5 μmol dm^{-3} based on satellite reflectance data.

The POC:PIC net production ratio at around 47°N changed from 9 in 1989 to a negative one in 1990. In the latter case, it was concluded that the negative result was caused by having sampled two different hydrographic/biological regimes. In either case, the relative importance of PIC production appeared to be small or insignificant. In contrast, estimates of POC:PIC net production ratios in the 1991 Study area north of 54°N indicated that net production since the onset of stratification had occurred at an overall ratio of about 2, and that the ratio varied notably with biological regime. Similar to the more southern study

area from 1990, production of POC was not accompanied by any significant proportional change in PIC outside the coccolithophorid bloom area. However, within the bloom area the average ratio was only 0.4. While this implies that the $CaCO_3$ pump was more effective than the organic carbon pump, it does not necessarily mean that the pCO_2 would have to rise above atmospheric levels. Another estimate from the 'bloom area' based on particulate parameters suggested a ratio of 0.75. Apart from analytical or conceptual shortcomings, this discrepancy between estimates may stem from unequal sampling and/or not quite the same processes being measured by the different methods.

Results from the quantitative relationship between TA_{NO3} and PIC showed that average changes in TA_{NO3} were about 20% higher than the equivalent changes in PIC. On one hand, possible errors in the TA_{NO3} analyses are acknowledged and discussed. On the other hand, if one assumes that TA_{NO3} accurately represented the total net production of PIC, as is frequently done in other studies, it could be concluded that the discrepancy was caused by vertical loss from 2-3 m to any greater depths within or below the SML. While there is no direct evidence for this, there was possible circumstantial evidence from vertical profiles and the finding that this loss was highest in a 'late bloom' region. Extended use of this approach of combining measurements of PIC standing stock and longer-term calcification estimates may thus provide an independent estimate of PIC export from the SML.

Following preliminary investigations, the correlation between photometric TA and light-backscatter was re-investigated using corrected data set of photometric TA and excluding samples from shallow shelf sites. This resulted in a lower intercept, a shallower slope, and a better correlation. However, it is stressed that TA_S or TA_{NO3} should be used instead of TA for calibrations of any optical data, so that together with salinity and/or nitrate data, this relationship may ultimately be used to estimate the effect of calcification on surface TA using optical satellite data.

Assuming particulate loss of 20%, TA was estimated to change by 1.8 microequivalents per 10^6 *Emiliania huxleyi* cells during the bloom in 1991. A difference in strain or the unnatural culturing conditions form likely explanations for this change to be considerably larger *in situ* than in the culture experiments of this study. Taking account of the estimate of 10% for

the contribution of *Coccolithus pelagicus* to calcification, the average PIC production would be 80 pg $CaCO_3$ per *E. huxleyi* cell and 4.0 pg $CaCO_3$ per lith. The latter estimate agreed well with an independent one derived from particulate parameters analysed during the 1991 Study.

7.5. SEASONAL CHANGES OF TA IN THE NORTHEAST ATLANTIC

During a Lagrangian study in 1989 the classic spring bloom sequence was observed, in which dissolved nutrients are reduced during formation of the SML, leading to depletion within one month. This sequence was accompanied by a change in the dominance of species within the phytoplankton assemblage from diatoms to coccolithophorids and later to flagellates and dinoflagellates. This pattern of species succession was observed at all latitudes between 47° and 60°N 20°W, with the start date of the bloom being delayed towards the north. One important finding of that study was the distinct increase in chlorophyll and associated decrease in nitrate concentration of about 6 µM from the preformed winter-mixing concentration before stratification and the development of the spring bloom had begun. In spite of methodological discrepancies, some general trends in TA emerged alongside these observations, and they were largely corroborated by TA results from this study in 1990 and 1991.

With respect to seasonal changes, it was proposed in this study to split the year into four periods based on hydrographic and biological changes, i.e.

(i) winter-mixing conditions with negligible phytoplankton growth;

(ii) increased phytoplankton growth some time before the onset of stratification;

(iii) the spring diatom bloom; and

(iv) subsequent phytoplankton growth involving non-calcifying or calcifying algae.

Baseline TA values for winter-mixing conditions had previously been modelled using TTO data. The northward decrease between 46° and 64°N of up to 20 µeq $kgSW^{-1}$ was corroborated by sub-thermocline TA data from 1990 and 1991. According to the reduced nitrate concentrations, phytoplankton growth may have already increased TA before the development of the thermocline by up to 6 µeq kg^{-1} in 1989 and 1990. It was not clear how important calcification becomes during that second phase, i.e. the overall effect of biological

activity on TA remains unquantified. According to phytoplankton and sediment trap data from the SML in 1989, significant coccolithophorid growth may occur at that time of year. However, there was no evidence for this in 1990. During the main diatom bloom phase which lasts approximately one month, TA was raised by a further 6 $\mu eq\ kg^{-1}$ due to nitrate uptake. The reduction in net calcification amounted to 12 and 5 $\mu eq\ kg^{-1}$ in 1989 and 1990, respectively. The overall effect of biology on TA at the end of the bloom would have been either insignificant or somewhat reduced, depending on the amount of calcification that occurs before and during the diatom bloom. The interannual difference in the size of the dominant spring bloom diatom species between 1989 and 1990 should not have affected the measured changes in TA in the SML, but may do so on the return to winter-mixing conditions, i.e. on an annual basis. During the post-bloom phase, increases due to nitrate can be assumed to become less important, since much of the continued growth is assumed to be sustained by regenerated nutrients. At the same time, coccolithophorids may continue to grow moderately at latitudes below about 55°N. In contrast, further north their increased importance after the main diatom bloom phase has been shown to be the principle cause for reductions of anything up to 40 $\mu eq\ kg^{-1}$. It was presumed that in winter TA depends upon the amount of export production of POC and PIC from the upper 200 m or whatever depth is reached by the mixed layer at that time.

Latitudinal changes can be assumed to depend first of all on the preformed TA values. In April and May, latitudinal differences will be further enhanced due to the time-lag in the onset of the spring bloom, i.e. it starts about 5 weeks later at 60°N than at 47°N. Once all the latitudes have experienced the main spring bloom, another latitudinal gradient can be expected when favourable conditions for coccolithophorid blooms north of 55°N lower TA by up to about 40 $\mu eq\ kgSW^{-1}$. Information about the effect of seasonal changes in the hydrological cycle is limited in this study. Measurements made at around late June in 1990 and 1991 suggest that since the start of stratification evaporation had led to an almost negligible TA increase of up to 5 $\mu eq\ kgSW^{-1}$ in the SML.

7.6. ERRORS IN POTENTIAL ALKALINITY AND DERIVED CALCIFICATION ESTIMATES

Possible factors introducing significant errors in TA and TA_{NO3} and thus in estimates of net calcification were reviewed and their impact was assessed with respect to the 1991 Study. Apart from methodological errors in the estimates of TA_{NO3} and errors arising from variations in preformed nitrate concentrations, inaccuracies may be introduced by omitting corrections for biological processes other than nitrate uptake, e.g. sulphate uptake, uncoupled ammonia uptake/ regeneration, organic acid release, and N_2 fixation. In addition, errors may emerge in the estimates of TA changes across the thermocline by other limitations of the experimental design, such as

(i) differential advection occurring in the SML and the 70-150 depth range;

(ii) mixing across the thermocline;

(iii) phytoplankton growth within and below the thermocline; and

(iv) sub-thermocline sampling depths not accounting for localized vertical displacement of isopycnals.

While it was concluded that the ammonia and N_2 factors probably had a negligible effect on net calcification estimates in the Northeast Atlantic, most factors remained unquantified. However, it was estimated that the sulphate and organic acid effects may have led to an overestimate in TA_{NO3} by up to 15 $\mu eq\ kgSW^{-1}$, which translates to an underestimate in net calcification of up to 7.5 $\mu mol\ dm^{-3}$ by the time the spring bloom has reached its peak. In view of this, it was concluded that it may be worthwhile putting more effort into improving the direct analysis of dissolved calcium to estimate $CaCO_3$ precipitation/dissolution.

7.7. FINDINGS FROM CULTURE EXPERIMENTS

A TA decrease of up to 270 $\mu eq\ dm^{-3}$ and an increase in PIC concentration of up to 325 μM was measured over the course of 5 days. Nitrate tended to decrease by about 90 μM, while the concomitant change in TPN tended to be approximately 10 μM less than that. While measured TA and PIC changes varied considerably between the three replicate cultures, the decrease in measured TA generally was about half that expected from changes in the concentration of PIC and NO_3 or TPN. Possible causes for this considerable discrepancy

include inaccurate measurements of the main parameters and/or an indication of significant TA-altering processes other than PIC production and nitrate uptake.

The error in TA due to an inaccurate indicator pK in the presence of elevated DOM concentrations has already been discussed. As the acidification procedure used to remove the PIC fraction may have damaged the phytoplankton cells, POC would have been underestimated and PIC overestimated. Possible evidence for this comes from TPN measurements which were reduced by 20% on those filters which had been exposed to acid fumes. A further partial reason for the discrepancy may have been a slight overestimate of nitrate concentrations. Inaccurate estimates of nitrate and its changes may have resulted from the large dilution step necessary in the analysis and the complexity of the algal culture medium for which the method was not calibrated. Further reasons for the discrepancy between nitrate and TPN changes include the release of dissolved organic nitrogen in the algal cultures and the loss of TPN during the filtration process. Preliminary experiments revealed that the filtration could damage the cells, thus leading to a reduction of particulate organic matter. It was shown in these experiments that the TPC fraction per sample volume was lower when filtered at a vacuum pressure of 0.8 rather than 0.2 bar and also when a larger sample volume was filtered. The susceptibility to potential stresses of vacuum filtration may vary between species and physiological and environmental conditions, but should be considered when planning the experiments.

The discrepant results obtained in the culture experiments led to the reconsideration of much of the experimental design. First of all, the focus should rest on the improvement of the PIC analysis, since any error in this parameter has the greatest impact on the discrepancies. While there is no published record of a systematic intercomparison of the different methods to estimate PIC in water samples, it may be more appropriate to derive PIC data from the particulate calcium fraction on the filters as was done for the 1991 cruise. Secondly, in order to avoid the uncertainties associated with indicator pK values, use of a potentiometric TA method should be considered. For greater confidence in the nitrate analyses the method should be calibrated using standard additions. Further, the nitrate concentration of the medium should be reduced to a level more typical of open ocean concentrations, so that the error associated with the dilution step prior to the nitrate

analysis can be omitted or at least reduced. This would make the results more applicable to *in situ* situations, even though this shortcoming should not have lead to the observed discrepancies between measured and expected TA *per se*. An additional vital adjustment would be the introduction of a more realistic light:dark light cycle when growing the cultures.

While the methodological shortcomings cast serious doubt over the quantitative validity of the results, it cannot be excluded that at least some of the discrepancies between measured and expected TA may have arisen from sulphate uptake and/or organic acid release by the algae. In the latter case, this may have occured over the 5 days of the experiment and may have been generally enhanced by the exposure to continuous light, but it is also possible that some organic acids were released by the dense cultures during the filtration of the TA samples.

7.8. GENERAL CONCLUSIONS

In a glacial/interglacial model of atmospheric CO_2, it was emphasized to take account of the variability of TA rather than assuming constant global TA values, which were used in the carbon cycle models for climate predictions. The JGOFS studies in the Northeast Atlantic between 1989 and 1991 have provided much evidence for small- and large-scale variability of TA during spring and summer which could be largely linked to hydrographic and phytoplankton-related features. In view of this, it seems that further detailed spatial and seasonal surveys are ultimately needed at the other times of the year and also in other oceanic regions where significant variability in hydrography and biology may occur.

The considerable absolute and relative discrepancies between TA data sets from different methods or similar methods used by different research teams highlight the continued need for a better understandingy of the seawater carbonate chemistry and the different TA methodologies. For this to be achieved, a starting point would be more systematic intercomparative studies of the different TA methods with the samples covering a realistic range of defined hydrographic and biological regimes, so that the causes for any discrepancies can be identified and subsequently accounted for. While methodological discrepancies persist, it seems advisable to use one relatively well-researched and generally

approved TA method when conducting surveys ultimately aimed at investigating climate change.

In order to minimise errors in estimates of CO_2 in some glacial-interglacial models and estimates of $CaCO_3$ precipitation/dissolution, there also seems to be a need to improve our understanding of some TA-influencing biological processes which usually remain unaccounted for, i.e. sulphur uptake, organic acid release, and N_2 fixation/denitrification.

The final conclusion from this study with respect to climate-related carbon cycle studies is that an increased emphasis should now be put on the development or identification of a generally accurate TA method. Before this is achieved, it may be argued that results from global TA surveys are only of limited use in the attempt to improve our understanding and to provide more accurate predictions of climate change.

REFERENCES

Adams, A.K. & Mackenzie, F.T. 1997. Deep inorganic carbon system of the Arabian Sea: evidence for calcite dissolution above the lysocline? Abstract. American Geophysical Union. Spring Meeting

Aebischer, N. J.; Coulson, J.C. & Colebrook, J.M. 1990. Parallel long-term trends across four marine trophic levels and weather. Nature 347: 753 - 755

Aiken, J. & Bellan, I. 1990. Optical oceanography: An assessment of a towed method. In 'Light and Life in the Sea' P.J. Herring; A.K. Campbell; M. Whitfield & L. Maddock (eds.) Cambridge Univ. Press. New York: 39 - 57

Almgren, T.; Dyrssen, D. & Fonselius, S. 1983. Determination of alkalinity and total carbonate. In 'Methods of Seawater Analysis' 2nd edn. K. Grasshoff; M. Ehrhardt & K. Kremling (eds.) Verlag Chemie. Weinheim: 99 - 124

Altabet, M.A.; Francois, R.; Murray, D.W. & Prell, W.L. 1995. Climate related variations in denitrification in the Arabian Sea from sediment 15N/14N ratios. Nature 373: 506 - 509

Anderson, D.H. & Robinson, R.J. 1946. Rapid electrometric determination of the alkalinity of seawater using a glass electrode. Ind. Eng. Chem. Analyt. Edit. 18: 767 - 769.

Anderson, L.A. & Sarmiento, J.L. 1994. Redfield ratios of remineralization determined by nutrient data analysis. Global Biogeochem. Cycles 8: 65 - 80

Anderson, L. G. & Dyrssen, D. 1994. Alkalinity and total carbonate in the Arabian Sea. Carbonate depletion in the Red Sea and Persian Gulf. Mar. Chem. 47: 195 - 202

Anderson, L.G. & Jones, E.P. 1985. Measurements of total alkalinity, calcium, and sulfate in natural sea ice. J. Geophys. Res. 90: 9194 - 9198

Anderson, L.G. & Wedborg, M. 1983. Determination of alkalinity and total carbonate in seawater by photometric titration. Oceanol. Acta 6 (4): 357 - 364.

Anderson, L.G. & Wedborg, M. 1985. Comparison of potentiometric and photometric titration methods for determination of alkalinity and total carbonate in seawater. Oceanol. Acta 8 (4): 479 - 483.

Andreae, M.O. 1986. The ocean as a source of atmospheric sulphur compounds. In 'The Role of Air-Sea exchange in Geochemical Cycling' P. Buat-Menard (ed.) Reidel. Dordrecht: 331 - 362

Andreae, M.O. & Jaeschke, W.A. 1992. Exchange of sulphur between biosphere and atmosphere over temperate and tropical regions. In 'Sulphur Cycling on the Continents'. R.W. Howarth, J.W. Stewart & M.V. Ivanov (eds.). John Wiley. Chichester: 27 - 61

Angel, M.V. 1989. Does mesopelagic biology affect the vertical flux. In 'Productivity of the Ocean: Present and Past. W.H.Berger; V.S. Smetacek & G. Wefer (eds.). John Wiley & Sons Ltd.. New York: 155 - 173

Angel, M. & Fasham, M. 1983. Eddies and biological processes. In 'Eddies in Marine Science' A. R. Robinson (ed.). Springer Verlag. New York: 492 - 524

Archer, D. 1991. Modeling the calcite lysocline. J. Geophys. Res. 96 (C9): 17037 - 17050

Archer, D. & Maier-Reimer, E. 1994. Effect of deep-sea sedimentary calcite preservation on atmospheric CO2 concentration. Nature 367: 260 - 263

Bacastow, R.B. 1976. Modulation of atmospheric carbon dioxide by the Southern Oscillation. Nature 261: 116 - 118

Bacastow, R.B. & Maier-Reimer, E. 1991. Dissolved organic carbon in modelling oceanic new production. Global Biogeochem. Cycles 5: 71 - 85

Baes, C.F. 1982. Ocean chemistry and biology. In 'Carbon Dioxide Review 1982' W.C. Clark (ed.). Clarendon Press. Oxford: 187 - 211

Baird,D.C. 1962. Experimentation. An introduction to measurement theory and experimental design. 2nd edn. Englewood Cliff N.J. Prentice-Hall.
Balch, W.M.; Holligan, P.M.; Ackleson, S.G. & Voss, K.J. 1991. Biological and optical properties of mesoscale coccolithophorid blooms in the Gulf of Maine. Limnol. Oceanogr. 36(4): 629 - 643.
Balch, W.M.; Holligan, P.M. & Kilpatrick, K.A. 1992. Calcification, photosynthesis, and the growth of the bloom-forming coccolithophore *Emiliania huxleyi*. Cont. Shelf Res. 12: 1353 - 1374
Barnola, J.M.; Raynaud, D.; Korotkevitch, Y.S. & Lorius, C. 1987. Vostok ice core: a 160,000 year record of atmospheric CO2. Nature 329: 408 - 414
Bates, N.R.; Michaels, A.F. & Knap, A.H. 1996a. Seasonal and interannual variability of oceanic carbon dioxide species at the U.S. JGOFS Bermude Atlantic Time - series Study (BATS) site. Deep-Sea Res. II 43 (2-3): 347 - 383
Bates, N.R.; Michaels, A.F. & Knap, A.H. 1996b. Alkalinity changes in the Sargasso Sea: geochemical evidence of calcification? Mar. Chem. 51: 347 - 358
Berger, A. 1980. The Milankovitch astronomical theory of palaeoclimates: a modern review. Vistas in Astronomy 24: 103 - 122
Berger, W.H. 1982. Increase of carbon dioxide in the atmosphere during deglaciation: the coral reef hypothesis. Naturwissenschaften 69: 87 - 88
Berger, W.H. & Keir, R.S. 1984. Glacial-Holocene changes in atmospheric CO_2 and the deep-sea record. AGU, Geophys. Monogr. Ser. 29: 337
Berger, W.H. & Labeyrie, L.D. (eds.) 1987. Abrupt climatic change: evidence and implications. Reidel. Dordrecht
Berner, R.A. & Lasaga, A.C. 1989. Modelling the geochemical carbon cycle. Scientific American 260(3): 54 - 61.
Billet, D.S.M.; Lampitt, R.S.; Rice, A.L. & Mantoura, R.F.C. 1983. Seasonal sedimentation of phytoplankton to the deep-sea benthos. Nature 302: 520 - 522
Bishop, E. 1972. Indicators. Pergamon Press. Oxford
Bishop, J.K.B.; Ketten, D.R. & Edmond, J.M. 1978. The chemistry, biology and vertical flux of particulate matter from the upper 400 m of the Cape Basin in the southeast Atlantic Ocean. Deep-Sea Res. 25: 1121 - 1161
Bleijswijk, J.D.L.; Kempers, R.S.; van der Wal, P.; Westbroek, P.; Egge, J.K. & Lukk, T. 1994. Standing stocks of POC, PON, and *Emiliania huxleyi* coccospheres and liths in seawater enclosures with different phosphate loadings. Sarsia 79: 307 - 317
Bolin, B. 1983. Changing global biogeochemistry. In 'Oceanography. The Present and Future.' P.G. Brewer (ed.). Springer Verlag. New York: 305 - 326
Bond, G.C. & Lotti, R. 1995. Iceberg discharges into the North Atlantic on millenial time scales during the last glaciation. Science 267: 1005 - 1010
Bond, G.C.; Broecker, W.S.; Johnson, S.J.; McManus, J.; Labeyrie, L.D.; Jouzel, J. & Bonani, G. 1993. Correlations between climate records from North Atlantic sediments and Greenland ice. Nature 365: 143 - 147
Boning, C.W.; Doscher, R.; Budich, R.G. 1991. Seasonal transport variations in the western subtropical North Atlantic: Experiments with an eddy-resolving model. J. Phys. Oceanogr. 21: 1271 - 1289
Bos, D. & Williams, R.T. 1982. History and development of the GEOSECS alkalinity titration system. In 'Workshop on Oceanic CO2 Standardization'. U.S. DOE Report CONF-7911173
Boulahdid, M. & Minster, J.-F. 1989. Oxygen-consumption and nutrient regeneration ratios along isopycnal horizons in the Pacific Ocean. Mar. Chem. 26: 133 - 153

Boyd, P. & Newton, P. 1995. Evidence of the potential influence of planktonic community structure on the interannual variability of particualte organic carbon flux. Deep-Sea Res. 42: 619 - 639
Boyd, P.; Harris, R.; Harbour, D.; Pomroy, A. & Bedo, A. 1990. Phytoplankton species composition and size spectra in the Northeast Atlantic, 47N, 20W - 59N 20W: Biogeochemical Ocean Flux Study 1989. (abstract). JGOFS Report No. 7, Abstracts. JGOFS North Atlantic Bloom Experiment International Scientific Symposium. SCOR/ICSU: 71- 72
Boyle, E.A. 1986. Paired carbon isotope and cadmium data for benthic foraminifera: Implications for changes in oceanic phosphorus, oceanic circulation and atmospheric carbon dioxide. Geochim. Cosmochim. Acta 50: 2655 - 2670
Boyle, E.A. 1988. The role of vertical chemical fractionation in controlling late Quarternary atmospheric carbon dioxide. J. Geophys. Res. 93: 15701 - 15714
Boyle, E.A. & Keigwin, L. 1987. North Atlantic thermohaline circulation during the past 20,000 years linked to high-latitude surface temperature. Nature 330: 35 - 40
Bradley, R.S. & Jones, P.D. 1993. Little ice age summer temperature variations: their nature and relevance to recent global warming trends. The Holocene 3: 367 - 376
Bradley, R.S. & Jones, P.D. 1995. Recent developments in studies of climate since AD 1500. In 'Climate Since AD 1500' (2nd edn.). R.S. Bradley & P.D. Jones (eds.). Routledge. London: 666 - 679
Bradshaw, A.L. & Brewer, P.G. 1988a. High precision measurements of alkalinity and total carbon dioxide in seawater by potentiometric titration - 1. Presence of unknown protolyte(s)? Mar. Chem. 23: 69 - 86
Bradshaw, A.L. & Brewer, P.G. 1988b. High precision measurements of alkalinity and total carbon dioxide in seawater by potentiometric titration - 2. Measurements on standard solutions. Mar. Chem. 23: 155 - 162
Bradshaw, A.L.; Brewer, P.G.; Shafer, D.K. & Williams, R.T. 1981. Measurements of total carbon dioxide and alkalinity by potentiometric titration in the GEOSECS program. Earth Planet. Sci. Lett. 55: 99 - 115
Brand, L.E. & Guillard, R.R.L. 1981. The effects of continuous light intensity on the reproduction rates of twenty-two species of marine phytoplankton. J. Exp. Mar. Biol. Ecol. 50: 119 - 132.
Brewer, P.G. 1978. Direct observation of the oceanic CO2 increase. Geophys. Res. Lett. 5 (12): 997 - 1000
Brewer,P.G. 1986. What controls the variability of carbon dioxide in the surface ocean? A plea for complete information. In: Dynamic Processes in the Chemistry of the Upper Ocean. J.D. Burton, P.G. Brewer & R. Chesselet (eds.). New York, Plenum Press: 215 - 231
Brewer, P.G. & Goldman, J.C. 1976. Alkalinity changes generated by phytoplankton growth. Limnol. Oceanogr. 21(1): 108 - 117.
Brewer, P.G.; Wong, G.T.F.; Bacon, M.P. & Spencer, D.W. 1975. An oceanic calcium problem? Earth Planet. Sci. Lett. 26: 81 - 87
Brewer, P.G.; Bradshaw, A.L. & Williams, R.T. 1986. Measurements of total carbon dioxide and alkalinity in the North Atlantic Ocean in 1981. In 'The Changing Carbon Cycle. A Global Analysis' J.R. Trabalka & R.E. Reichle (eds.). Springer Verlag. Berlin: 348 - 370
Brewer, P.G.; Goyet, C.& Friederich, G. 1997. Direct observation of the oceanic CO2 increase revisited. Proc. Natl. Acad. Sci. USA. 94: 8308 - 8313
Briffa,K.R.; Jones, P.D.; Schweigruber, F.H.; Shiyatov, S.G. & Cook, E.R. 1995. Unusual twentieth century summer warmth in a 1,000-year temperature record from Siberia. Nature 376: 156 - 159

Broccoli, A.J. & Manabe, S. 1987. The influence of continental ice, atmospheric CO2, and land albedo on the climate of the last glacial maximum. Clim. Dyn. 1: 87 - 99
Broecker, W.S. 1973. Factors controlling the CO2 content in the ocean and atmosphere. In 'Carbon and the Biosphere'. G.M Woodwell & E.V. Penn (eds.). United Atomic Energy Commission.: 32 - 50
Broecker, W.S. 1974. "NO", a conservative water mass tracer. Earth Planet. Sci. Lett. 23: 100 - 107
Broecker, W.S. 1982. Ocean chemistry during glacial time. Geochim. Cosmochim. Acta 46: 1689 - 1705
Broecker, W.S. 1987. Unpleasant surprises in the greenhouse. Nature 328: 123 - 126
Broecker, W.S. 1991. Keeping global change honest. Global Biogeochem. Cycles 5: 191 - 193
Broecker, W.S. & Peng, T.-H. 1989. The cause of the glacial to interglacial atmospheric CO2 change: a polar alkalinity hypothesis. Global Biogeochem. Cycles 3: 215 - 239.
Broecker, W.S. & Peng, T.-H. 1992. Interhemispheric transport of carbon dioxide by ocean circulation. Nature 356: 587 - 589
Broecker, W.S. & Peng, T.-H. 1994. Stratospheric contribution to the global bomb radiocarbon inventory: Model versus observation. Global Biogeochem. Cycles 8: 377 - 384
Broecker, W.S. & Takahashi, T. 1977. In 'The Fate of Fossil Fuel CO2 in the Oceans. N. Anderson & A. Malahoff (eds.) Plenum. New York: 213 - 241
Broecker, W.S.; Takahashi, T.; Simpson, H.J. & Peng, T.H. 1979. Fate of fossil fuel carbon dioxide and the global carbon budget. Science 206: 409 - 418
Broecker, W.S.; Peteet, D. & Rind, D. 1985a. Does the ocean-atmosphere system have more than one stable mode of operation? Nature 315: 21 - 26
Broecker, W.S.; Takahashi, T. & Peng, T.H. 1985b. Reconstruction of past atmospheric CO2 contents from the chemistry of the contemporary ocean: an evaluation. DOE Technical Report. DOE/OR-857
Broecker, W.S.; Andree, M.; Bonani, G.; Wolfli, W.; Oeschger, H.; Klas, M.; Mix, A. & Curry, W. 1988. Preliminary estimates for the radiocarbon age of deep water in the glacial ocean. Paleoceanogr. 3: 659 - 669
Broecker, W.S.; Peng, T.-H.; Trumbore, S.; Bonani, G. & Wolfli, W. 1990. The distribution of radiocarbon in the glacial ocean. Global Biogeochem. Cycles 4: 103 - 117
Broecker, W.S.; Sutherland, S.; Smethie, W.; Peng, T.-H. & Oestlund, G. 1995. Oceanic radiocarbon: Separation of the bomb and natural components. Global Biogeochem. Cycles 9: 263 - 288
Bryan, F. 1986. High latitude salinity effects and interhemispheric thermohaline circulations. Nature 305: 301 - 304
Bryan, F. & Holland, W.R. 1989. A high-resolution simulation of the wind- and thermohaline driven circulation in the North Atlantic Ocean. In 'Proceedings of the 'Aha Huliku', a Hawaiian Winter Workshop on Parameterization of Small Scale Processes'. P. Muller & D. Henderson (eds.). Hawaii Institute of Geophysics, Honolulu: 99 - 116
Budyko, M. & Israel, Y.A. (eds.) 1987. Anthropogenic climate changes. L. Gridrometeoizdat
Burkill, P.H.; Edwards, E.S.; John, A.W.J. & Sleigh, M.A. 1993. Microzooplankton and their herbivorous activity in the north eastern Atlantic Ocean. Deep-Sea Res. II 40: 479 - 493
Bury, S.J.; Boyd, P.; McArdle, P.; Owens, N.J.P. & Preston, T. 1990. Size-fractionated time-series measurements of new and regenerated productivity during a Northeast Atlantic bloom. (abstract). JGOFS Report No. 7, Abstracts. JGOFS North Atlantic Bloom Experiment International Scientific Symposium. SCOR/ICSU: 73

Butler, J.N. 1992. Alkalinity titration in seawater: how accurate can the data be fitted by an equilibrium model? Mar. Chem. 38: 251 - 282
Byrne, R.H. 1987. Standardization of standard buffers by visible spectrophotometry. Anal. Chem. 59: 1479 - 1481.
Byrne, R.H. & Breland, J.A. 1989. High precision multiwavelength pH determinations in seawater using cresol red. Deep-Sea Res. 36(5): 803 - 810.
Campos, J.D. & Bleck, R. 1992. A numerical study of the tropical Atlantic Ocean circulation with an isopycnic-coordinate circulation model - preliminary results. Trans. Amer. Geophys. Union 73 (suppl.): 292
Carter, P.W. 1978. Adsorption of amino acid-containing matter by calcite and quartz. Geochim. Cosmochim. Acta 42: 1239 - 1242.
Chappellaz, J.; Barnola, J.M.; Raynaud, D.; Korotkevich, Y.S. & Lorius, C. 1990. Ice-core record of atmospheric methane over the past 160,000 years. Nature 345: 127 - 131
Chave, K.E. & Suess, E. 1970. Calcium carbonate saturation in seawater: effects of dissolved organic matter. Limnol. Oceanogr. 15: 633 - 637.
Chen, C.-T. A. 1978. Decomposition of calcium carbonate and organic carbon in the deep oceans. Science 201: 735 - 736
Chen, C.-T. A. 1982a. Oceanic penetration of excess CO2 in a cross section between Alaska and Hawaii. Geophys. Res. Lett. 9 (2): 117 - 119
Chen, C.-T. A. 1982b. On the distribution of anthropogenic CO2 in the Atlantic and Southern oceans. Deep-Sea Res. 29 (5A): 563 - 580
Chen, C.-T. A. 1982c. Carbonate chemistry during WEPOLEX -81. Antarctic Journal of the U.S. 17: 5
Chen, C.-T.A. 1985. Preliminary observations of oxygen and carbon dioxide of the wintertime Bering Sea marginal ice zone. Continental Shelf Res. 4 (4): 465 - 483
Chen, C.-T. A. 1990. Rates of calcium carbonate dissolution and organic carbon decomposition in the North Pacific Ocean. J. Oceanogr. Soc. Japan 46: 201 - 210
Chen, C.-T.A. 1993. Carbonate chemistry of the wintertime Bering Sea marginal ice zone. Continental Shelf Res. 13 (1): 67 - 87
Chen, C.T. & Millero, F.J. 1979. Gradual increase of oceanic CO2. Nature 277: 205 - 206
Chen, C.-T. A. & Pytkowicz, R.M. 1979. On the total CO2-titration alkalinity-oxygen system in the Pacific Ocean. Nature 281: 362 - 365
Chen, C.T.; Millero, F.J. & Pytkowicz, R.M. 1982. Comment on calculating the oceanic CO2 increase: a need for caution by A.M. Shiller. J. Geophys. Res. 87 (C3): 2083 - 2085
Chen, C.-T. A.; Jones, E.P. & Lin, K. 1990. Wintertime total carbon dioxide measurements in the Norwegian and Greenland Seas. Deep-Sea Res. 37 (9): 1455 - 1473
Chen, C.-T.A.; Gong, G.-C.; Wang, S.-L. & Bychkov, A.S. 1996. Redfield ratios and regeneration rates of particulate matter in the Sea of Japan as a model of closed system. Geophys. Res. Lett. 23 (14): 1785 - 1788
Chipman, D.W.; Marra, J. & Takahashi, T. 1993. Primary production at 47N and 20W in the North Atlantic Ocean: a comparison between the 14C incubation method and the mixed layer carbon budget. Deep-Sea Res. II 40: 151 - 169
Ciais, P.; Tans, P.P.; White, J.W.C.; Trolier, M.; Francey, R.J.; Berry, J.A.; Randall, D.R.; Sellers, P.J.; Collatz, J.G. & Schimel, D.S. 1995a. Partitioning of ocean and land uptake CO2 as inferred by δ13C measurements from the NOAA Climate Monitoring and Diagnostics Laboratory Global Air Sampling Network. J. Geophys. Res. 100D: 5051 - 5070
Ciais, P.; Tans, P.P.; Trolier, M.; White, J.W.C.& Francey, R.J. 1995b. A large northern hemisphere terrestrial CO2 sink indicated by 13C/12C of atmospheric CO2. Science 269: 1098 - 1102

Clayton, T.D.; Byrne, R.H.; Breland, J.A.; Feely, R.A.; Millero, F.J.; Campbell, D.M.; Murphy, P.P. & Lamb, M.F. 1995. The role of pH measurements in modern oceanic CO2 system characterizations: Precision and thermodynamic consistency. Deep-Sea Res. 42: 411 - 429

Codispoti, L.A. 1995. Is the ocean losing nitrate? Nature 376: 724

Crawford, D.W. & Purdie, D.A. 1997. Increase of pCO2 during blooms of *Emiliania huxleyi* Theoretical considerations on the asymmetry between acquisition of HCO3- and respiration of free CO2. Limnol. Oceanogr. 42: 365 - 372

Crowley, T.J. 1994. Pleistocene temperature changes. Nature 371: 664

Dansgaard, W.; Johnson, S.J.; Clausen, H.B.; Dahl-Jensen, D.; Gunderstrup, N.S.; Hammer, C.U.; Hvidberg, C.S.; Steffensen, J.P.; Sveinbjornsdottir, A.; Jouzel, J. & Bond, G. 1993. Evidence for general instability of past climate from a 250-kyr ice-core record. Nature 364: 218 - 220

Deffeyes, K.S. 1965. Carbonate equilibria: a graphic and algebraic approach. Limnol. Oceanogr. 10: 412 - 426

Delworth, T.; Manabe, S. & Stouffer, R.J. 1993. Interdecadal variations of the thermohaline circulation in a coupled ocean-atmosphere model. J. Climate 6: 1993 - 2011

Deuser, W.G. 1970. Carbon-13 in Black Sea waters and implications for the origin of hydrogen sulfide. Science 168: 1575

Devol, A.H. 1991. Direct measurements of nitrogen gas fluxes from continental shelf sediments. Nature 349: 319 - 321

Dickinson, R.E.; Meleshko, V.; Randall, D.; Sarachik, E.; Silva-Dias, P. & Slingo, A. 1996. Climate processes. In 'Climate Change 1995. The Science of Climate Change. Contribution of Working Group I to the Second Assessment Report of the Intergovernmental Panel on Climate Change'. IPCC. J.T. Houghton, L.G. Meira Filho, B.A. Callandar, N. Harris, A. Kattenberg & K. Maskell (eds.). Cambridge University Press. Cambridge: 193 - 227

Dickson, A.G. 1981. An exact definition of total alkalinity and a procedure for the estimation of alkalinity and total inorganic carbon from titration data. Deep-Sea Res. 28A: 609 - 623.

Dickson, A.G. 1984. pH scales and proton transfer reactions in saline media such as sea water. Geochim. Cosmochim. Acta 48: 2299 - 2308.

Dickson, A.G. 1990. The oceanic carbon dioxide system: planning for quality data. U.S. JGOFS News 2(2): 2

Dickson, A.G. 1991a. Work in progress at the Scripps Institution of Oceanography, U.S.A. In 'Reference Materials for Oceanic Carbon Dioxide Measurements'. UNESCO Technical Papers in Marine Science 60: 34 - 38

Dickson, A.G. 1991b. The determination of total dissolved inorganic carbon in seawater using extraction/coulometry: the first stage of a collaborative study. Draft Document. Scripps Institute of Oceanography. La Jolla

Dickson, A.G. 1991c. Handbook of methods for the analysis of the various parameters of the carbon dioxide system in seawater. Draft Document for U.S. Dept. of Energy. Scripps Institute of Oceanography. La Jolla

Dickson, A.G. 1992. The development of the alkalinity concept in marine chemistry. Mar. Chem. 40: 49 - 63

Dickson, A.G. 1993. pH buffers for seawater media based on the total hydrogen ion concentration scale. Deep-Sea Res. 40(1): 107 - 118

Dickson, A.G. & Riley, J.P. 1979. The estimation of dissociation constantsin seawater media from potentiometric titrations with strong base. I. The ionic product of water KW. Mar. Chem. 7: 89 - 99

DOE 1994. Handbook of methods for the analysis of various parameters of the carbon dioxide system in seawater; version 2. A.G. Dickson & C. Goyet (eds.) ORNL/CDIAC-74
Doscher, R.; Boning, C.W. & Herrmann, P. 1994. Response of circulation and heat transport in the North Atlantic to changes in thermohaline forcing in northern latitudes: A model study. J. Phys. Oceanogr. 24: 2306 - 2320
Ducklow, H.W. 1989. Ships are home but bloom study continues. U.S. JGOFS News 1(3):1-9
Ducklow, H.W. & Harris, R.P. 1993. Introduction to JGOFS North Atlantic Bloom Experiment. Deep-Sea Res. II 40: 1 -8
Ducklow, H.W.; Kirchman, D.L.; Quinby, H.L.; Carlson, C.A. & Dam, H.G. 1993. Bacterioplankton carbon cycling during the spring bloom in the eastern North Atlantic Ocean. Deep-Sea Res. II 40: 245 - 263
Dugdale, R.C. & Goering, J.J. 1967. Uptake of new and regenerated forms of nitrogen in primary productivity. Limnol. Oceanogr. 12: 196 - 206
Duplessy, J.C.; Shackleton, N.J.; Fairbanks, R.G.; Labeyrie, L.; Oppo, D. & Kallel, N. 1988. Deepwater source variations during the last climatic cycle and their impact on the global deepwater circulation. Paleoceanogr. 3: 343 - 360
Duplessy, J.C.; Labeyrie, L.; Arnold, M.; Paterne, M.; Duprat, J. & Van Weering, T.C.E. 1992. North Atlantic sea surface salinity and abrupt climatic changes. Nature 358: 485 - 488
Dymond, J. & Lyle, M. 1985. Flux comparisons between sediments and sediment traps in the eastern tropical Pacific: Implications for CO2 variations during the Pleistocene. Limnol. Oceanogr. 30: 699 - 712
Dyrssen, D. 1965. A Gran titration of seawater on board 'Sagitta'. Acta Chem. Scand. 19: 1265
Edmond, J.M. 1970. High precision determination of titration alkalinity and total carbon dioxide content of seawater by potentiometric titration. Deep-Sea Res. 17: 737 - 750
Edmond, J.M. 1974. On the dissolution of carbonate and silicate in the deep ocean. Deep-Sea Res. 21: 455 - 480
Emerson, S.R. & Bender, M.L. 1981. Carbon fluxes at the sediment water interface of the deep-sea: calcium carbonate preservation. J. Mar. Res. 39: 139 - 162
Emery, W.J. & Meincke, J. 1986. Global water masses: summary and review. Oceanol. Acta 9 (4): 383 - 391
Esias, W.E.; Feldman, G.C.; McClain, C.R. & Elrod, J.A. 1986. Monthly satellite derived phytoplankton pigment distribution for the North Atlantic Ocean basin. EOS: 835 - 837
Fagerbakke, K.M.; Heldal, M.; Norland, S.; Heimdal, B.R. & Batvik, H. 1994. *Emiliania huxleyi*. Chemical composition and size of coccoliths from enclosure experiments and a Norwegian fjord. Sarsia 79: 349 - 355
Falkowski, P.G. 1997. Evolution of the nitrogen cycle and its influences on the biological sequestration of CO2 in the ocean. Nature 387: 272 - 275
Feely, R.A.; Wanninkhof, R.; Cosca, C.E.; McPhaden, M.J.; Byrne, R.H.; Millero, F.J.; Chavez, F.P.; Clayton, T.; Campbell, D.M. & Murphy, P.P. 1994. The effect of tropical instability waves on CO2 species distributions along the equator in the eastern equatorial Pacific during the 1992 ENSO event. Geophys. Res. Lett. 21 (4): 277 - 280
Feely, R.F.; Wanninkhof, R.; Cosca, C.E.; Murphy, P.P.; Lamb, M.F. & Steckley, M.D. 1995. CO2 distributions in the equatorial Pacific during the 1991-92 ENSO event. Deep-Sea Res. II 42: 365 - 386
Feely, R.A.; Wanninkhof, R.; Takahashi,T. & Tans, P. 1999. Influence of El Niño on the equatorial Pacific contribution to atmospheric CO2 accumulation. Nature 398: 597 - 601
Fernandez, E.; Boyd, P.; Holligan, P.M. & Harbour, D.S. 1993. Production of organic and inorganic carbon within a large scale coccolithophore bloom in the North-east Atlantic Ocean. Mar. Ecol. Prog. Ser. 97: 271 - 285

Fiadeiro, M. 1980. The alkalinity of the deep Pacific. Earth Planet Sci. Lett. 49: 499 - 505
Francey, R.J.; Tans, P.P.; Allison, C.E.; Enting, I.G.; White, J.W.C. & Trolier, M. 1995. Changes in terrestrial carbon uptake since 1982. Nature 373: 326 - 330
Frankignoulle, M. & Canon, C. 1994. Marine calcification as a source of carbon dioxide: Positive feedback of increasing atmospheric CO2. Limnol. Oceanogr. 39 (2): 458 - 462
Frankignoulle, M.; Bourge, I.; Canon, C. & Dauby, P. 1996. Distribution of surface seawater partial CO2 pressure in the English Channel and in the Southern Bight of the North Sea. Continental Shelf Res. 16 (3): 381 - 395
Frich, P. 1994. Precipitation trends in the North Atlantic European region. In 'Climate Variations in Europe'. R. Heino (ed.). Academy of Finland. Publication 3: 196 - 200
Ganeshram, R.S.; Pedersen, T.F.; Calvert, S.E. & Murray, J.W. 1995. Large changes in oceanic nutrient inventories from glacial to interglacial periods. Nature 376: 755 - 758
Garcon, V. & Minster, J.F. 1988. Heat, carbon and water fluxes in a 12-box model of the world ocean. Tellus 40(B): 161 - 177
Garside, G. & Garside, J.C. 1993. The "f-ratio" on 20W during the North Atlantic Bloom Experiment. Deep-Sea Res. II 40: 75 - 90
Garside, G.; McCarthy, J.J. & Nevins, J.L. 1990. Nitrogenous nutrient dynamics in the upper water column during NABE: May 22 - 31, 1989. (abstract). JGOFS Report No. 7, Abstracts. JGOFS North Atlantic Bloom Experiment International Scientific Symposium. SCOR/ICSU: 38-39
Gates, W.L.; Mitchell, J.F.B.; Boer, G.J.; Cubasch, U. & Meleshko, V.P. 1992. Climate modelling, climate prediction and model validation. In 'Climate Change. The Supplementary Report to the IPCC Scientific Assessment'. J.T. Houghton, B.A. Callandar & S.K. Varney (eds.). Cambridge University Press. Cambridge.: 97 - 134
Glibert, P.M. & Bronk, D.A. 1994. Release of dissolved organic nitrogen by marine diazotrophic cyanobacteria, *Trichodesmium* spp.. Appl. Environ. Microbiol. 60: 3996 - 4000
Glover, D.M.& Brewer, P.G. 1988. Estimates of wintertime mixed layer nutrient concentrations in the North Atlantic. Deep-Sea Res. 35: 1525 - 1546
Goldman, J.C. & Brewer, P.G. 1980. Effect of nitrogen source and growth rate on phytoplankton-mediated changes in alkalinity. Limnol. Oceanogr. 25 (2): 352 - 357
Goyet, C. & Brewer, P.G. 1993. Biochemical properties of the ocean carbon cycle. In 'Modeling Oceanic Climate Interactions'. J. Willebrand & D.L.T. Anderson (eds.). NATO Series I11. Springer. Berlin: 271 - 297
Goyet, C. & Poisson, A. 1989. New determination of carbonic acid dissociation constants in seawater as a function of temperature and salinity. Deep-Sea Res. 36: 1635 - 1654
Gran, G. 1952. Determination of the equivalence point in potentiometric titrations, II. Analyst 77: 661 - 671
Graneli, A. & Anfalt, T. 1977. A simple automatic photititrator for the determination of total carbonate and total alkalinity of seawater. Anal. Chim. Acta 91: 175 - 180
Green, J.C.; Perch-Nielsen, K. & Westbroek, P. 1990. Prymnesiophyta. In 'Handbook of Protoctista' L. Margulis, J. O. Corliss, M. Melkonian & D.J. Chapman (eds.) Jones and Bartlett. Boston: 293 - 317
Gripenberg, S. 1936. Communication 108. Vth Hydrological Conference of the Baltic States. Helsingfors
GRIP Members 1993. Climatic instability during the last interglacial period revealed in the Greenland Summit ice-core. Nature 364: 203 - 207
Hansen, I. 1973. A new set of pH-scales and standard buffers for seawater. Deep-Sea Res. 20: 479 - 491

Hansen, J.; Lacis, A.; Rind, D.; Russell, G.; Stone, P.; Fung, L; Ruedy, R. & Lerner, J. 1984. Climate sensitivity: analysis of feedback effects. In 'Climate processes and climate sensitivity'. AGU. Geophys. Monogr. Ser. 29: 130 - 163
Harris, R.P. 1994. Zooplankton grazing on the coccolithophore *Emiliania huxleyi* and its role in inorganic carbon flux. Mar. Biol. 119: 431 - 439
Harrison, P.J.; Waters, R.E. & Taylor, F.J.R. 1980. A broad spectrum artificial seawater medium for coastal and open ocean phytoplankton. J. Phycol. 16: 28 - 35
Harvey, J. 1982. θ - S relationships and water masses in the eastern North Atlantic. Deep-Sea Res. 29: 1021 - 1033
Hausman, E.D. & McElroy, M. B. 1996. Variations in the oceanic carbon cycle over glatial transitions: A time-dependent box model simulation. Abstract. American Geophysical Union. Fall Meeting
Headridge, J.B. 1961. Photometric titrations. Pergamon Press. Oxford
Heinze, C.E.; Maier-Reimer, E. & Winn, K. 1991. Glacial pCO2 reduction by the world ocean: experiments with the Hamburg carbon cycle model. Paleoceanogr. 6: 395 - 430
Hessheimer, V.; Heimann, M. & Levin, I. 1994. Radiocarbon evidence suggesting a smaller oceanic CO2 sink than hitherto assumed. Nature 370: 201 - 203
Holligan, P.M.; Fernandez, E.; Aiken, J.; Balch, W.M.; Boyd, P.; Burkill, P.H.; Finch, M.; Groom, S.B.; Malin, G.; Muller, K.; Purdie, D.A.; Robinson, C; Trees, C.C.; Turner, S.M.; van der Waal, P. 1993. A biogeochemical study of the coccolithophore *Emiliania huxleyi* in the North Atlantic. Global Biogeochem. Cycles 7(4): 879 - 900
Honjo, S. 1996. Export of carbon particles to the ocean interior sink. Abstract. American Geophysical Union. Fall Meeting
Hoppema, M.; Fahrbach, E.; Schroder, M.; Wisotzki, A. & deBaar, H.J.W. 1995. Winter-summer differences of carbon dioxide and oxygen in the Weddell Sea surface layer. Mar. Chem. 51 (3): 177 - 192
Howard, W.R. & Prell, W.L. 1992. Late Quarternary surface circulation of the Southern Indian Ocean and its relationship to orbital variations. Paleoceanogr. 7: 79 - 118
Howarth, R.W. & Stewart, J.W.B. 1992. The interactions of sulphur with other element cycles in ecosystems. In 'Sulphur Cycling on the Continents'. R.W. Howarth, J.W. Stewart & M.V. Ivanov (eds.).John Wiley. Chichester: 67 - 84
Hurrell, J.W. 1995. Decadal trends in the North Atlantic Oscillation and relationship to regional temperature and precipitation. Science 269: 676 -679
IPCC 1990. Climate Change. The IPCC Scientific Assessment. J.T. Houghton, G.J. Jenkins & J.J. Ephraums (eds.). Cambridge University Press. Cambridge
IPCC 1992. Climate Change 1992. The Supplementary Report to the IPCC Scientific Assessment. J.T. Houghton, B.A. Callander & S.K. Varney (eds.). Cambridge University Press. Cambridge
IPCC 1995. Climate Change 1994. Radiative Forcing of Climate Change and an Evaluation of the IPCC 1992 IS92 Emission Scenarios. J.T. Houghton, L.G. Meiro Filho, J. Bruce, H. Lee, B.A. Callandar, E.F. Haites, N. Harris & K. Maskell (eds.). Cambridge University Press. Cambridge
IPCC 1996. Climate Change 1995. The Science of Climate Change. Contribution of Working Group I to the Second Assessment Report of the Intergovernmental Panel on Climate Change. J.T. Houghton, L.G. Meira Filho, B.A. Callandar, N. Harris, A. Kattenberg & K. Maskell (eds.). Cambridge University Press. Cambridge
Jain, A.K.; Keshgi, H.S.; Hoffert, M.I. & Wuebbles, D.J. 1995. Distribution of radiocarbon as a test of global carbon cycle models. Global Biogeochem. Cycles 9: 153 - 166
JGOFS 1990a. The Joint Global Ocean Flux Study - JGOFS- Science Plan. JGOFS Report No. 5. Scientific Committee on Oceanic Research Secretariat. Dalhousie University. Halifax

JGOFS 1990b. North Atlantic Bloom Experiment. Report of the first data workshop. Kiel March 1990. JGOFS Report No. 4. JGOFS - Büro. Institut für Meereskunde. Kiel.
Johansson, O. & Wedborg, M. 1982. On the evaluation of potentiometric titrations of seawater with hydrochloric acid. Oceanol. Acta 5: 209 - 218
Johnson, S.J.; Clausen, H.; Dansgaard, W.; Fuhrer, K.; Gunderstrup, N.S.; Hammer, C.U.; Iverssen, P.; Jouzel, J.; Stauffer, B. & Steffensen, J.P. 1992. Irregular glacial interstadials recorded in a new Greenland ice core. Nature 359: 311 - 313
Joint, I.R.; Pomroy, A.; Savidge, G. & Boyd, P. 1993. Size fractionated primary productivity in the North East Atlantic in spring 1989. Deep-Sea Res. II 40: 423 - 440
Joos, F.; Sarmiento, J.L.; Siegenthaler, U. 1991. Estimates of the effect of Southern Ocean iron fertilization on atmospheric CO2 concentrations. Nature 349: 772 - 774
Joos, F.; Bruno, M.; Fink, R.; Siegenthaler, U.; Stocker, T.; Le Quere, C. & Sarmiento, J.L. 1996. An efficient and accurate representation of complex oceanic and biospheric models of anthropogenic carbon dioxide. Tellus 48 B: 397- 417
Jouzel, J.; Vaikmae, R.; Petit, J.R.; Martin, M.; Duclos, Y.; Stievenard, M.; Lorius, C.; Toots, M.; Melieres, M.A.; Burckle, M.H.; Barkov, N.I. & Kotyakov, V.M. 1995. The two-step shape and timing of the last deglaciation in Antarctica. Clim. Dyn. 11: 151 - 161
Kaduk, J. & Heimann, M. 1994. The climate sensitivity of the Osnabrueck Biosphere Model on the ENSO timescale. Ecological Modelling 75/76: 239 - 256
Karl, D.; Letelier, R.; Tupas, L.; Dore, J.; Chrisian, J. & Hebel, D. 1997. The role of nitrogen fixation in biogeochemical cycling in the subtropical North Pacific Ocean. Nature 388: 533 - 538
Keeling, C.D.; Piper, S.C. & Heimann, M. 1989a. A three-dimensional model of atmospheric CO2 transport based on observed winds: 4. Mean annual gradients and interannual variations. In 'Aspects of Climate Variability in the Pacific and the Western Americas'. D.H. Peterson (ed.). AGU. Geophys. Mono. 55: 305 - 363
Keeling, C.D.; Bacastow, R.B.; Carter, A.F.; Piper, S.C.; Wholf, T.P.; Heimann, M.; Mook, W.G. & Roeloffzen, H. 1989b. A three-dimensional model of atmospheric CO2 transport based on observed winds: 1. Analysis of observational data. In 'Aspects of Climate Variability in the Pacific and the Western Americas'. D.H. Peterson (ed.). AGU. Geophys. Mono. 55: 165 - 236
Keeling, C.D.; Whorf, TP.; Wahlen, M. & van der Plicht, J. 1995. Interannual extremes in the rate of rise of atmospheric carbon dioxide since 1980. Nature 375: 666 - 670
Keigwin, L.D.; Curry, W.B.; Lehman, S.J. & Johnson, S. 1994. The role of the deep ocean in North Atlantic climate change between 70 and 130 kyr ago. Nature 371: 323 - 326
Keir, R.S. 1994. Effects of ocean circulation changes and their effects on CO2. In 'The Carbon Cycle' T.M.L. Wigley & D. Schimel (eds.) Cambridge University Press. Stanford, C.A.: 229 - 237
Keller, M.D.; Bellows, W.K. & Guillard, R.R.L. 1989a. Dimethyl sulphide production in marine phytoplankton. In 'Biogenic Sulphur in the Environment' E.S. Salzman & W.J. Cooper (eds.). American Chemical Society Symposium Series, ACS. Washington. 393: 167 - 182
Keller, M.D.; Bellows, W.K.; Guillard, R.R.L. 1989b. Dimethylsulfide production and marine phytoplankton: an additional impact of unusual blooms. In 'Novel Phytoplankton Blooms. Causes and Impacts of Brown Tides and Other Unusual Blooms'. E.M. Cooper, V.M. Bricelj & E.J. Carpenter (eds.). Springer Verlag. Berlin: 101 - 115
Khoo, K.H.; Ramette, R.W.; Culberson, C.H. & Bates, R.G. 1977. Determination of hydrogen ion concentrations in seawater from 5 to 40C: Standard potentials at salinities from 20 to 45 ppt. Anal. Chem. 49: 29-34
Killworth, P.D. 1983. Deep convection in the world ocean. Rev. Geophys. 21: 1 - 26

King, D.W. & Kester, D.R. 1989. Determination of seawater pH from 1.5 to 8.5 using colorimetric indicators. Mar. Chem. 26 (1): 5 - 20
Kirst, G.O.; Thiel, C.; Wolff, H.; Nothnagel, J.; Wanzek, M. & Ulmke, R. 1991. Dimethylsulfoniopropionate (DMSP) in ice-algae and its possible biological role. Mar. Chem. 35: 381 - 388
Koeve, W.; Eppley, R.W.; Podewski, S. & Zeitschel, B. 1993. An unexpected nitrate distribution in the tropical North Atlantic at 18°N, 30°W - implication for new production. Deep-Sea Res. II 40: 521 - 536
Krauss, W. & Käse, R.H. 1984. Mean circulation and eddy kinetic energy in the Eastern North Atlantic. J. Geophys. Res. 89 (C3): 3407 - 3415
Lamb, P.J. & Peppler, R.A. 1991. West Africa. In 'Teleconnections linking worldwide climate anomalies'. M.H. Glantz, R.W. Katz & N. Nicholls (eds.). Cambridge University Press. Cambridge: 121 - 190
Lampitt, R.S.; Wishner, K.F.; Turley, C.M. & Angel, M.V. 1993. Marine snow studies in the Northeast Atlantic Ocean: distribution, composition and its role as a food source for migrating plankton. Mar. Biol. 116: 689 - 702
Lazier, J.R.N. 1995. The salinity decrease in the Labrador Sea over the past 30 years. In 'Natural climate variability on decade to century time scales'. D.G. Martinson, K. Bryan, M. Ghil, M.M. Hall, T.R. Karl, E.S. Sarachik, S. Sorooshian & L.D. Talley (eds.). National Academy Press. Washington, D.C.
Lee, K. & Millero, F.J. 1995. Thermodynamic studies of the carbonate system in seawater. Deep-Sea Res. I 42: 2035 - 2061
Lee, K.; Millero, F.J. & Campbell, D.M. 1996. The reliability of the thermodynamic constants for the dissociation of carbonic acid in seawater. Mar. Chem. 55: 233 - 245
Le Groupe Tourbillon 1983. The Tourbillon Experiment: a study of a mesoscale eddy in the eastern North Atlantic. Deep-Sea Res. 30: 475 - 511
Lehman, S.J. & Keigwin, L.D. 1992. Sudden changes in North Atlantic circulation during the last deglaciation. Nature 356: 757 - 762
Lewis, E.R. & Wallace, D.W.R. 1995. Basic programs for the CO2 system in seawater. Brookhaven National Laboratory. Upton, N.Y.. Informal Publication
Lisitzin, A.P. 1971. Distribution of carbonate microfossils in suspension and in bottom sediments. In 'The Micropaleontology of Oceans' B.M. Funnell & W.R. Riedel (eds.) Cambridge University Press. London: 173 - 195
Lochte, K., Ducklow, H.W., Fasham, M.J.R. & Stienen, C. 1993. Plankton succession and carbon cycling at 47°N, 20°W during the JGOFS North Atlantic bloom experiment. Deep-Sea Res. II 40: 91 - 114.
Longhurst, A.R. & Harrison, W.G. 1988. Vertical nitrogen flux from the oceanic photic zone by diel migrant zooplankton and nekton. Deep-Sea Res. 35: 881 - 889
Maier-Reimer, E. 1993. Geochemical cycles in an ocean general circulation model. Pre-industrial tracer distributions. Global Biogeochem. Cycles 7: 645 - 677
Malin, G.; Turner, S.M. & Liss, P.S. 1992. Sulphur: the plankton/climate connection. J. Phycol. 28: 590 - 597
Manabe, S. & Stouffer, R.J. 1988. Two stable equilibria of a coupled atmosphere-ocean model. J. Climate 1: 841 - 866
Manabe, S. & Stouffer, R.J. 1993. Century-scale effects of increased atmospheric CO2 on the ocean-atmosphere system. Nature 364: 215 - 218
Manabe, S. & Stouffer, R.J. 1994. Multiple century response of a coupled ocean-atmosphere model to an increase of atmospheric carbon dioxide. J. Climate 7: 5 - 23

Marotzke, J. 1988. Instabilities and multiple steady states of the thermohaline circulation. In 'Oceanic Circulation Models: Combining Data and Dynamics'. D.L.T. Anderson & J. Willebrand (eds.). NATO ASI Series. Kluwer: 501 - 511

Marotzke, J. & Wunsch, C. 1993. Finding the steady state of a general circulation model through data assimilation: Application to the North Atlantic ocean. J. Geophys. Res. 98 (C11): 20149 - 20167

Martin, J.H. & Fitzwater, S.E. 1988. Iron deficiency limits phytoplankton growth in the subarctic north-east Pacific. Nature 331: 341 - 343

Martin, J.H.; Knauer, G.A.; Karl, D.M. & Broenkow, W.W. 1987. VERTEX. Carbon cycling in the northeast Pacific. Deep-Sea Res. 34: 267 - 285

Martin, J.H.; Fitzwater, S.E.; Gordon, R.M.; Hunter, C.N. & Tanner, S.J. 1993. Iron, primary production and flux studies during the JGOFS North Atlantic Bloom Experiment. Deep-Sea Res. II 40: 115 - 134

Matrai, P.A. & Keller, M.D. 1993. Dimethylsufide production in a large-scale coccolithophorid bloom in the Gulf of Maine. Cont. Shelf Res. 13: 831 - 843

Mayewski, P.A.; Meeker, L.D.; Whitlow, S.; Twicker, M.S.; Morrison, M.C.; Grootes, P.M.; Bond, G.C.; Alley, R.B.; Meese, D.A.; Gow, A.J.; Taylor, K.C.; Ram, M. & Wunkes, M. 1994. Changes in atmospheric circulation and ocean ice cover over the North Atlantic during the last 41,000 years. Science 263: 1747 - 1751

McManus, J.F.; Bond, G.C.; Broecker, W. S.; Johnson, S.J.; Labeyrie, L. & Higgins, S. 1994. High-resolution climate records from the North Atlantic during the last interglacial. Nature 371: 326 - 329

Millero, F.J. 1995. Thermodynamics of the carbon dioxide system in the oceans. Geochim. Cosmochim. Acta 59: 661 - 677

Millero, F.J. & Poisson, A. 1982. International one-atmosphere equation of seawater. Deep-Sea Res. 28: 625 - 639

Millero, F.J.; Byrne, R.H.; Wanninkhof, R.; Feely, R.; Clayton, T.; Murphy, P. & Lamb, M.F. 1993. The internal consistency of CO2 measurements in the equatorial Pacific. Mar. Chem. 44: 269 - 280

Milliman, J.D.; Troy, P.J.; Balch, W.M.; Adams, A.K.; Li, Y.H. & Mackenzie, F.T. 1999. Biologically mediated dissolution of calcium carbonate above the chemical lysocline? Deep-Sea Res. 46: 1653 - 1669

Mittelstaedt, E. 1987. Cyclonic cold-core eddy in the eastern North Atlantic- I. Physical description. Mar. Ecol. Prog. Ser. 39: 145 - 152

Najjar, R.G.; Sarmiento, J.L.; Toggweiler, J.R. 1992. Downward transport and fate of organic matter in the ocean: simulations with a general circulation model. Global Biogeochem. Cycles 6: 45 - 76

Newman, L.; Krouse, H.R. & Grinenko, V.A. 1991. Sulphur isotope variations in the atmosphere. In 'Stable Isotopes in the Assessment of Natural and Anthropogenic Sulphur in the Environment. H.R. Krouse & V.A. Grinenko (eds.). John Wiley. Chichester: 133 - 176

Newton, P.P.; Lampitt, R.S.; Jickells, T.D.; King, P. & Boutle, C. 1994. Temporal and spatial variability of biogenic particle fluxes during the JGOFS northeast Atlantic process studies at 47N 20W. Deep-Sea Res. 41: 1617 - 1642

Nicholls, N.; Gruza, G.V.; Jouzel, J.; Karl, T.R.; Ogallo, L.A. & Parker, D.E. 1996. Observed climate variability and change. In 'Climate Change 1995. The Science of Climate Change. Contribution of Working Group I to the Second Assessment Report of the Intergovernmental Panel on Climate Change'. IPCC. J.T. Houghton, L.G. Meira Filho, B.A. Callandar, N. Harris, A. Kattenberg & K. Maskell (eds.). Cambridge University Press. Cambridge: 133 - 192

Nimer, N.A. & Merrett, N.J. 1992. Calcification and utilization of inorganic carbon by the coccolithophorid *Emiliania huxleyi* Lohman. New Phytol. 121: 173 - 177
Opdyke, B.N. & Walker, J.C.G. 1992. Return of the coral reef hypothesis: Basin to shelf partitioning of CaCO3 and its effect on atmospheric CO2. Geology 20: 733 - 736
Oppo, D. & Fairbanks, R.G. 1987. Variability in the deep and intermediate water circulation of the Atlantic Ocean during the past 25,000 years: Northern hemisphere modulation of the Southern Ocean. Earth Planet Sci. Lett. 86: 1 - 15
Orr, J.C. 1993. Accord between ocean models predicting uptake of ocean CO2. Water, Air and Soil Pollution 70: 465 - 481
OU 1991. Ocean circulation. Pergamon Press. Oxford
Paasche, E. 1962. Coccolith formation. Nature 193: 1094 - 1095
Paasche, E. & Bruback, S. 1994. Enhanced calcification in the coccolithophorid *Emiliania huxleyi* (Haptophyceae) under phosphorus limitation. Phycologia 33: 324 - 330
Paerl, H.W. & Carlton, R.G. 1988. Control of nitrogen fixation by oxygen depletion in surface-associated microzones. Nature 332: 260 - 262
Park, P.K. 1969. Oceanic CO2 system: an evaluation of ten methods of investigation. Limnol. Oceanogr. 14: 179 - 186
Parsons, T.S.; Maita, Y. & Lalli, C.M. 1984. A manual of chemical and biological methods for seawater analysis. Pergamon. Oxford
Pegler, K. 1997. Das CO2-System in Nordostatlantik. Saisonaler Einfluss auf die regionale Verteilung des gelösten anorganischen Kohlenstoffs. PhD Thesis. Berichte aus dem Zentrum für Meeres- und Klimaforschung. D 2. Institut für Biochemie und Meereschemie. Hamburg
Peierls, B.J. & Paerl, H.W. 1997. Bioavailability of atmospheric organic nitrogen deposition to coastal phytoplankton. Limnol. Oceanogr. 42: 1819 - 1823
Peinert, R.; von Bodungen, B. & Smetacek, V.S. 1989. Food web structure and loss rate. In 'Productivity of the Ocean: Present and Past. W.H.Berger; V.S. Smetacek & G. Wefer (eds.). John Wiley & Sons Ltd.. New York: 35 - 48
Peng, T.-H.; Takahashi, T.; Broecker, W.S. & Olafsson, J. 1987. Seasonal variability of carbon dioxide, nutrients and oxygen in the northern North Atlantic surface waters: observations and a model. Tellus 39B: 439 - 458
Perez, F.F. & Fraga, F. 1987. The pH measurements in seawater on the NBS scale. Mar. Chem. 21: 315 - 327
Pfannkuche, O. 1993. Benthic response to the sedimentation of particulate organic matter at the BIOTRANS station 47N, 20W. Deep-Sea Res. II 40: 135 - 149
Pingree, R.D. 1993. Flow of surface waters to the west of the British Isles and in the Bay of Biscay. Deep-Sea Res. II 40: 369 - 388
Poisson, A. & Chen, C.-T. A. 1987. Why is there little anthropogenic CO2 in the Antarctic Bottom Water? Deep-Sea Res. 34 (7): 1255 - 1275
Purdie, D. A. & Finch, M.S. 1994. Impact of a coccolithophorid bloom on dissolved carbon dioxide in seawater enclosures in a Norwegian fjord. Sarsia 79: 379 - 387
Ramette, R.W.; Culberson, C.H. & Bates, R.G. 1977. Acid-base properties of tris (hydroxy methyl) aminomethane (TRIS) buffers in seawater from 5 to 40C. Anal. Chem. 49: 867 - 870
Raven, J.A. 1980. Nutrient transport in microalgae. Adv. Microb. Physiol. 21: 47 - 226
Raven, J.A. 1986. Biochemical disposal of excess H+ in growing plants. New Phytol. 104: 175 - 206
Raven, J.A. 1993. Carbon: a phycocentric view. In 'Towards a Model of Ocean Biogeochemical Processes' G.T. Evans & M.J.R. Fasham (eds.) Springer Verlag. Berlin. NATO ASI Series 10: 123 - 152

Read, J.F. & Gould, W.J. 1992. Cooling and freshening of the subpolar North Atlantic Ocean since the 1960s. Nature 360: 55 -57
Redfield, A.C.; Ketchum, B.H. & Richards, F.A. 1963. The influence of organisms on the composition of seawater. In 'The Sea' vol. 2. M.N. Hill (ed.) Interscience. New York: 26 - 77
Riding, R. (ed.) 1991. Calcareous algae and strombolites. Springer Berlin
Riebesell, U.; Wolf-Gladrow, D.A. & Smetacek, V. 1993. Carbon dioxide limitation of marine phytoplankton growth rates. Nature 361: 249 - 251
Robert-Baldo, G.L.; Morris, M.J. & Byrne, R.H. 1985. Spectrophotometric determinations of seawater pH using phenol red. Anal. Chem. 57: 2564 - 2567
Robertson, J.E. & Watson, A.J. 1992. Thermal skin effect of the surface ocean and its implications for CO2 uptake. Nature 358: 738 - 740
Robertson, J.E.; Watson, A.J.; Turner, D.R.; Taylor, A.H.; Knox, S.; Robinson, C.; Fasham, M.J. & Williams, P.J.leB. 1990. Drawdown of atmospheric CO2 during the spring bloom in the NE Atlantic. Abstract. JGOFS Report No. 7. Abstracts. JGOFS North Atlantic Bloom Experiment International Scientific Symposium. SCOR/ICSU: 62
Robertson, J.E.; Watson, A.J.; Langdon, C.; Ling, R.D. & Wood, J. 1993. Diurnal variations in surface pCO2 and oxygen at 60N 20W in the N.E. Atlantic. Deep-Sea Res. 40: 409 - 422
Robertson, J.E.; Robinson, C.; Turner, D.R.; Holligan, P.M.; Watson,A.J.; Boyd,P.; Fernandez, E. & Finch, M. 1994. The impact of a coccolithophore bloom on oceanic carbon uptake in the N.E. Atlantic during summer 1991. Deep-Sea Res. 41: 297 - 314
Robinson, A.R.; McGillicuddy, D.J.; Colman, J.; Ducklow, H.W.; Fasham, M.J.R.; Hoge, F.E.; Leslie, W.G.; McCarthy, J.J.; Podewski, S.; Porter, D.L.; Saure, G. & Yoder, J.A. 1993. Mesoscale and upper ocean variabilities during the 1989 JGOFS bloom study. Deep-Sea Res. II 40 (1/2): 9 -35
Robinson, C. & Williams, P.J. leB. 1991. Development and assessment of an analytical system for the accurate and continual measurement of total dissolved inorganic carbon. Mar. Chem. 34: 157 - 175
Rommets, J.W. 1988. The carbon dioxide system; its behaviour in decomposition processes in East Indonesian Basins. Netherlands J. of Sea Research 22: 383 - 393
Roy, R.N.; Roy, L.N.; Vogel, K.M.; Moore, C.P.; Pearson, T.; Good, C.P.; Millero, F.J. & Cambell, D.J. 1993. The dissociation constants of carbonic acid in seawater at salinities 5 to 45 and temperatures 0 to 45 C. Mar. Chem. 44: 249 - 267
Sambrotto, R.N.; Martin, J.H.; Broenkow, W.W.; Carlson, C.A. & Fitzwater, S.E. 1993a. Nitrate utilization in surface waters of the Iceland Basin during spring and summer 1989. Deep-Sea Res. II 40: 441 - 457
Sambrotto, R.N.; Savidge, G.; Robinson, C.; Boyd, P.; Takahashi, T.; Karl, D.; Langdon, D.; Chipman, D.; Marra, J. & Codispoti, L. 1993b. Elevated consumption of carbon relative to nitrogen in the surface ocean. Nature 363: 248 - 250
Santer, B.D.; Wigley, T.M.L.; Barnett, T.P. & Anyamba, E. 1996. Detection of climate change and attribution of causes. In IPCC (1996) see above: 407 - 443
Sarmiento, J.L. & Orr, J.C. 1991. Three-dimensional simulation of the impact of Southern Ocean nutrient depletion on atmospheric CO2 and ocean chemistry. Limnol. Oceanogr. 36: 1928 - 1950
Sarmiento, J.L. & Siegenthaler, U. 1992. New production and the global carbon cycle. In 'Primary Productivity and Biogeochemical Cycles in the Sea' P.G. Falkowski & A.D. Woodhead (eds.) Plenum. New York: 317 - 332
Sarmiento, J.L. & Toggweiler, J.R. 1984. A new model for the role of the oceans in determining atmospheric PCO2. Nature 308: 621 - 624
Sarmiento, J.L.; Toggweiler, J.R. & Najjar, R. 1988. Ocean carbon cycle dynamics and atmospheric pCO2. Philos. Trans. Roy. Soc. A 325: 3 - 21

Sarmiento, J.L.; Orr, J.C. & Siegenthaler, U. 1992. A perturbation simulation of CO2 uptake in an ocean general circulation model. J. Geophys. 97: 3621 - 3646
Sarmiento, J.L.; Le Quere, C. & Pacala, S.W. 1995. Limiting future atmospheric carbon dioxide. Global Biogeochem. Cycles 9: 121 - 137
Savidge, G; Turner, D.R.; Burkill, P.H.; Watson, A.J.; Angel, M.V.; Pingree, R.D.; Leach, H. & Richards, K.J. 1992. The BOFS 1990 Spring Bloom Experiment: Temporal evolution and spatial variability of the hydrographic field. Prog. Oceanog. 29: 235 - 281
Savidge, G.; Boyd, P.; Pomroy, A.; Harbour, D. & Joint, I. 1995. Phytoplankton production and biomass estimates in the northeast Atlantic Ocean, May-June 1990. Deep-Sea Res. 42 (5): 599 - 617
Schauer, U. 1989. A deep saline cyclonic eddy in the West European Basin. Deep-Sea Res. 36: 1549 - 1565
Schimel, D. S.; Enting, I.; Heimann, M.; Wigley, T.M.L.; Raynaud, D.; Alves, D. & Siegenthaler, U. 1995. CO2 and the carbon cycle. In 'Climate Change 1994'. J.T. Houghton, L.G. Meira Filho, J. Bruce, H. Lee, B.H. Callander, E. Haites, N. Harris & K. Maskell (eds.) Cambridge University Press, Cambridge: 35 - 71
Schimel, D. S.; Alves, D.; Enting, M.; Heimann, M.; Joos, F. et al. 1996. Radiative forcing of climate change. In 'Climate Change 1995. The Science of Climate Change. Contribution of Working Group I to the Second Assessment Report of the Intergovernmental Panel on Climate Change' IPCC. J.T. Houghton, L.G. Meira Filho, B.A. Callandar, N. Harris, A. Kattenberg & K. Maskell (eds.). Cambridge University Press. Cambridge: 65 - 131
Schmitz, W.J. & McCartney, M.S. 1993. On the North Atlantic circulation. Rev. Geophys. 31: 29 - 49
Schneider, B.; Kremling, K. & Duinker, J.C. 1992. CO2 partial pressure in the Northeast Atlantic and adjacent shelf waters: processes and seasonal variability. J. Mar. Systems 3: 453 - 463
SCOR 1987. The Joint Global Ocean Flux Study - background, goals, organization, and next steps. report of the International Scientific Planning and Coordination Meeting for Global Ocean Flux Studies sponsored by the Scientific Committee on Oceanic Research helod at ICSU headquarters, Paris, 17-19 February, 1987.
Shackleton, N.J.; Duplessy, J.-C.; Arnold, M.; Maurice, P.; Hall, M.A. & Cartlidge, J. 1988. Radiocarbon age of last glacial Pacific deep water. Nature 355: 708 - 711
Shaffer, G. 1993. Effects of the marine biota on global carbon cycling. In 'The Global Carbon Cycle' M. Heimann (ed.). Springer Verlag. Berlin: 431 - 455
Shiller, A.M. 1981. Calculating the oceanic CO2 increase: a need for caution. J. Geophys. Res. 86 (C11): 11083 - 11088
Shiller, A.M. 1982. Reply. J. Geophys. Res. 87 (C3): 2086
Shiller, A.M. & Gieskes, J.M. 1980. Processes affecting the oceanic distributions of dissolved calcium and alkalinity. J. Geophys. Res. 85: 2719 - 2727
Siegenthaler, U. & Joos, F. 1992. Use of a simple model for studying oceanic tracer distributions and the global carbon cycle. Tellus 39B: 140 - 154
Siegenthaler, U. & Sarmiento, J.L. 1993. Atmospheric carbon dioxide and the ocean. Nature 365: 119 - 125
Siegenthaler, U. & Wenk, T. 1984. Rapid atmospheric CO2 variations and ocean circulation. Nature 308: 624 - 625
Sikes, C.S.; Roer, R.D. & Wilbur, K.M. 1980. Photosynthesis and coccolith formation. Inorganic carbon sources and net inorganic reaction of deposition. Limnol. Oceanogr. 25: 248 - 261
Skirrow, G. 1975. The dissolved gases - carbon dioxide. In 'Chemical Oceanography' vol. 3. J.P. Riley & G. Skirrow (eds.). Academic Press. London: 1 - 192

Sokal, R.R. & Rohlf, F.J. 1981. Biometry. W.H. Freeman & Co.. New York
Stoll, M.H.C. 1994. Inorganic carbon behaviour in the North East Atlantic ocean. PhD thesis. University Groningen
Stoll, M.H.C.; Rommets, J.W. & de Baar, H.J.W. 1990. Determination of total carbon dioxide in seawater by two independent methods. (abstract). JGOFS Report No. 7, Abstracts. JGOFS North Atlantic Bloom Experiment International Scientific Symposium. SCOR/ICSU: 60
Stoll, M.H.C.; Rommets, J.W. & de Baar, H.J.W. 1993. Effect of selected calculation routines and dissociation constants on the determination of total carbon dioxide in seawater. Deep-Sea Res. 40: 1307 - 1322
Stommel, H. 1961. Thermohaline convection with two stable regimes of flow. Tellus 13: 224 - 230
Street-Perrott, F.A. & Perrot, R.A. 1990. Abrupt climate fluctiations in the tropics: The influence of the Atlantic circulation. Nature 343: 607 - 612
Strickland, J.D.H. & Parsons, T.R. 1972. A practical handbook of seawater analysis. Bull. Fish. Res. Bd. Can. 167
Stuiver, M.; Quay, P.D. & Ostlund, H.G. 1983. Abyssal water carbon-14 distribution and the age of the world oceans. Science 219: 849 - 851
Stumm, W. & Morgan, J.J. 1981. Aquatic chemistry. 2nd edn. Wiley-Interscience. New York
Suess, H.E. 1955. Radiocarbon concentration in modern wood. Science 122: 415 - 417
Sverdrup, H.U.; Johnson, M.W. & Fleming, R.H. 1942. The oceans: their physics, chemistry and general biology. Englewood Cliffs/NJ. Prentice- Hall, Inc.
Takahashi, T.; Broecker, W.S. & Langer, S. 1985. Redfield ratio based on chemical data from isopycnal surfaces. J. Geophys. Res. 90: 6907 - 6924
Takahashi, T.; Goyet, C.; Chipman, D.; Peltzer, E.; Goddard, J.; Brewer, P.G. 1990. Ratio of organic carbon and calcium carbonate productions observed at the JGOFS 47°N 20°W site. (abstract). JGOFS Report No. 7, Abstracts. JGOFS North Atlantic Bloom Experiment International Scientific Symposium. SCOR/ICSU: 76 - 77
Tans, P.P.; Fung, I.Y. & Takahashi, T. 1990. Observational constraints on the global atmospheric CO2 budget. Science 247: 1431 - 1438
Taylor, A.H. & Stephens, J.A. 1993. Diurnal variations of convective mixing and the spring bloom of phytoplankton. Deep-Sea Res. II 40: 389 - 408
Taylor, A.H. & Stephens, J.A. 1998. The North Atlantic Oscillation and the latitude of the Gulf Stream. Tellus 50A: 134 - 142
Taylor, A.H.; Watson, A.J. & Robertson, J.E. 1992. The influence of the spring phytoplankton bloom on carbon dioxide and oxygen concentrations in the surface waters of the northeast Atlantic during 1989. Deep-Sea Res. 39: 137 - 152
Taylor, A.H.; Jordan, M.B. & Stephens, J.A. 1998. Gulf Stream shifts following ENSO events. Nature 393: 638
Thompson, L.G.; Mosley-Thompson, E.; Davis, M.E.; Lin, P.-N.; Henderson, K.A.; Cole-Dai, J.; Bolzan, J.F. & Liu, K.-B. 1995. Late glacial stage and Holocene tropical ice core records from Huascarcn, Peru. Science 269: 46 - 50
Thompson, T.G. & Nelson, K.H. 1956. Concentration of brines and deposition of salts from water under frigid conditions. Am. J. Sci. 254: 227 - 238
Trenburth, K.E. & Hurrell, J.W. 1994. Decadal atmosphere-ocean variations in the Pacific. Clim. Dyn. 9: 303 - 319

Tsunogai, S. & Noriki, S. 1991. Particulate fluxes of carbonate and inorganic carbon in the ocean. Is the marine biological activity working as a sink of the atmospheric carbon? Tellus 43 (B): 256 - 266

Turley, C. M. 1986. Urea uptake by phytoplankton at different fronts and associated stratified and mixed waters on the European Shelf. Br. Phycol. J. 21: 225 - 238

Turner, D.R. 1990. Cruise Report: Discovery 192 (BOFS leg A3) 9 - 27 June 1990. Plymouth Marine Laboratories/ NERC

Turner, S.M.; Malin, G. & Liss, P.S. 1989. Dimethylsulphide and (dimethylsulphonio) propionate in European coastal and shelf waters. In 'Biogenic Sulphur in the Environment' E.S. Saltzman & W.J. Cooper (eds.). American Chemical Society Symposium Series. ACS. Washington 393: 183 - 200

Tyrrel, T. & Taylor, A.H. 1995. Latitudinal and seasonal variations in carbon dioxide and oxygen in the northeast Atlantic and the effects on *Emiliania huxleyi* and other phytoplankton. Global Biogeochem. Cycles: 585 - 604

Tyrrel, T. & Taylor, A.H. 1996. A modelling study of *Emiliania huxleyi* in the NE Atlantic. J. Mar. Sys. 9: 83 - 112

Unesco 1983. Thermodynamics of the CO2 system in seawater. Unesco technical papers in marine science 42

Unesco 1990. Intercomparison of total alkalinity and total inorganic carbon determinations in seawater. Unesco technical papers in marine science 59

U.S. JGOFS 1989. U.S. GOFS Bloom Study Cruises: First Impressions. GOFS News 1 (2): 1-5

Vairavamurthy, A.; Andreae, M.O. & Iverson, R.L. 1985. Biosynthesis of dimethylsulfide and dimethylpropiothetin by *Hymenomonas carterae* in relation to sulfur source and salinity variations. Limnol. Oceanogr. 30: 59 - 70

Varushchenko, S.I.; Varushchenko, A.N. & Klige, R.K. 1980. Changes in the Caspian Sea regime and closed water bodies in palaeotimes. M. Nauka

Veldhuis, M.J.W.; Kraay, G.W. & Gieskes, W.C. 1993. Growth and fluorescence characteristics of ultraplankton on a north-south transect in the eastern North Atlantic. Deep-Sea Res. II 40: 609 - 626

Verity, P.G.; Stoecker, D.K.; Sieracki, M.E.; Burkill, P.H.; Edwards, E.S. & Tronzo, C.R. 1993. Abundance, biomass and distribution of heterotrophic dinoflagellates during the North Atlantic Spring Bloom. Deep-Sea Res. II 40: 227 - 244

Vogel, A.I.; Bassett, J.; Denney, R.C.; Jeffrey,G.H. & Mendham,J. 1978. A textbook of quantitative inorganic analysis, including elementary instrumental analysis. Longman. New York

Volk, T. & Hoffert, M.I. 1985. Ocean carbon pumps: analysis of relative strengths and efficiencies in ocean driven atmospheric CO2 changes. Geophys. Monogr. Ser. 32: 99 - 110

Wallace, J.M. 1995. Natural and forced variability in the climate record. In 'The Natural Variability of the Climate System on Decade-to-Century Time Scales'. D.G. Martinson, K. Bryan, M. Ghil, M.M. Hall, T.R. Karl, E.S. Sarachik, S. Sorooshian & L.D. Talley (eds.). National Academy Press. Washington, D.C.

Watson, A.J. & Whitfield, M. 1985. Composition of particles in the global ocean. Deep-Sea Res. 32: 1023 - 1039

Watson, A.J.; Robinson, C.; Robertson, J.E.; leB Williams, P.J. & Fasham, M.J.R. 1991. Spatial variability in the sink for atmospheric carbon dioxide in the North Atlantic. Nature 350: 50 - 53

Weaver, A.J.& Sarachik, E.S. 1991. Evidence for decadal variability in an ocean general circulation model: An advective mechanism. Atmosphere-Ocean 29: 197 - 231

Weaver, A.J.; Sarachik, E.S. & Marotzke, J. 1991. Freshwater flux forcing of decadal/interdecadal oceanic variability. Nature 353: 836 - 838
Weaver, A.J.; Marotzke, P.F.; Cummins, P.F. & Sarachik, E.S. 1993. Stability and variability of the thermohaline circulation. J. Phys. Oceanogr. 23: 39 - 60
Weeks, A.; Aiken, J.; Bellan, I.; Harbour, D. & Fasham, M. 1990. The seasonal development of the spring bloom in the North Atlantic in 1989. (abstract). JGOFS Report No. 7, Abstracts. JGOFS North Atlantic Bloom Experiment International Scientific Symposium. SCOR/ICSU: 55
Weeks, A.; Conte, M.H.; Harris, R.P.; Bedo, A.; Bellan, I.; Burkill, P.H.; Edwards, E.S.; Harbour, D.S.; Kennedy, H.; Llewellyn, C.; Mantoura, R.F.C.; Morales, C.E.; Pomroy, A.J. & Turley, C.M. 1993. The physical and chemical environment and changes in community structure associated with bloom evolution: the JGOFS North Atlantic Bloom Experiment. Deep-Sea Res. II 40: 347 - 368
Weiss, R.F. 1970. The solubility of nitrogen, oxygen, and argon in water and seawater. Deep-Sea Res. 17: 721 - 735
Weiss, R.F. 1974. Carbon dioxide in water and seawater- the solubility of a non-ideal gas. Mar. Chem. 2: 203 - 215
Weiss, R.F.; Ostlund, H.G. & Craig, H. 1979. Geochemical studies of the Weddell Sea. Deep-Sea Res. 26: 1093 - 1120
Weiss, R.F.; Jahnke, R.A. & Keeling, C.D. 1982. Seasonal effects of temperature and salinity on the partial pressure of CO2 in seawater. Nature 300: 511 - 513
Wigley, T.M.L. 1993. Balancing the global carbon budget. Implications for projections of future carbon dioxide concentration changes. Tellus 45B: 409 - 425
Wigley, T.M.L. & Kelly, P.M. 1990. Holocene climatic change, 14C wiggles and variations in solar irradiance. Phil. Trans. R. Soc. Lond. A 330: 547 - 560
Williams, P.J. leB. & Jenkinson, N.W. 1982. A transportable microprocessor-controlled precise Winkler titration suitable for field station and shipboard use. Limnol. Oceanogr. 27: 576 - 584
Williams, R. 1974. Biological sampling at ocean weather station India (59N 19W) in 1972. Ann. Biol. Copenhagen 29: 41 - 44
Williams, R. & Hopkins, C.C. 1975. Biological sampling at ocean weather station India (59N 19W) in 1973. Ann. Biol. Copenhagen 30: 60 - 62
Williamson, P. 1991. Adrift in the North Atlantic: BOFS 1990 cruises follow up NABE findings. U.S JGOFS News 2(3): 7 - 8
Winguth, A.M.E.; Heimann, M.; Kurz, K.D.; Maier-Reimer, E.; Mikolajewicz, U. & Segeschneider, J. 1994. El Nino Southern Oscillation related fluctuations of the marine carbon cycle. Global Biogeochem. Cycles 8: 39 - 63
Winter, A. & Siesser, W.G. (eds.) 1994. Coccolithophores. Cambridge Univ. Press. Cambridge
Winton, M. 1993. Deep decoupling oscillations of the oceanic thermohaline circulation. In 'Ice in the Climate System' W.R. Peltier (ed.). NATO ASI Series, I 12. Springer Verlag. Berlin: 417 - 432
Winton, M. & Sarachik, E.S. 1993. Thermohaline oscillations of an oceanic general circulation model induced by strong steady salinity forcing. J. Phys. Oceanogr. 23: 1389 - 1410
Wolf, K.U. & Woods, J.D. 1988. Lagrangian simulation of primary production in the physical environment- the deep chlorophyll maximum and nutricline. In 'Toward a Theory on Biological-Physical Interactions in the World Ocean' B. J. Rothschild (ed.) Kluwer Academic Publishers. Dordrecht: 51 - 70

Wolfe, G.V.; Steinke, M. & Kirst, G.O. 1997. Grazing-activated chemical defence in a unicellular marine alga. Nature 387: 894 - 897
Yamanaka, Y. & Tajika, E. 1996. The role of the vertical fluxes of particulate organic matter and calcite in the oceanic carbon cycle: studies using an ocean biogeochemical general circulation model. Global Biogeochem. Cycles 10 (2): 361 - 382
Yoder, J.A.; Aiken, J.; Swift, R.N.; Hoge, F.E. & Stegemann, P.M. 1993. Spatial variability in near-surface chlorophyll a fluorescence measured by the airborne oceanographic LIDAR (AOL). Deep-Sea Res. II 40: 37 - 53
Young, J. 1994. Variations in *Emiliania huxleyi* coccolith morphology in samples from the Norwegian EHUX mesocosm experiment, 1992. Sarsia 79: 417 - 425

APPENDIX 1: LIST OF STEPS AND EQUATIONS USED TO CALCULATE TOTAL ALKALINITY AND ACID STRENGTH

APPENDIX 1

LIST OF STEPS AND EQUATIONS USED TO CALCULATE TA AND ACID STRENGTH

1. Exclude superfluous data from HP8452 raw data file
2. Read absorbance data (A1/A2) of two wavelengths
3. Calculate ratios of absorbance data during actual titration:

$$A1/A2 = \frac{abs.\ at\ 590nm}{abs.\ at\ 496nm}$$

4. Calculate mean value of 12 absorbance maximum ratios
5. Calculate mean value of 12 absorbance minimum ratios
6. Calculate $E(A^-)$, E(HA), and E2 terms including dilution correction for E2:

$$E(A^-) = \frac{abs.\ max.\ at\ 590nm}{abs.\ max.\ at\ 496nm}$$

$$E(HA) = \frac{abs.\ min.\ at\ 590nm}{abs.\ min.\ at\ 496nm}$$

$$E2 = \frac{abs.\ max.\ at\ 496nm}{abs.\ min.\ at\ 496nm} * \frac{(vb+vi+1)}{(vb+vi)} * \frac{(vb+vi+1-4+4)}{(vb+vi+1-4)}$$

N.B. The first correction term accounts for the addition of 1 cm^3 of acid, the second correction term accounts for the removal of 4 cm^3 of sample and subsequent addition of 4 cm^3 of 50% HCl, which prevents the sample from overspilling

7. Calculate pH on free H^+-pH scale according to King and Kester (1989):

$$pH_{free} = pK_{Ind} + \log\frac{A1/A2 - E(HA)}{E(A^-) - A1/A2} - \log(E2)$$

8. Correct $[H+]_{free}$ for the presence of Ind^-, HSO_4^-, and HF in the sample according to Dickson (1981) and Anderson and Wedborg (1983):

$$[H^+]_{S,F,I\ corrected} = [H^+]_{free} + [HSO_4^-] + [HF] - [Ind^-]$$

$$= [H^+]_{free} * (1 + (\frac{S_T * dil * K_{HSO_4^-}}{1 + K_{HSO_4^-} * [H^+]_{free}}) + (\frac{F_T * dil * K_{HF_4^-}}{1 + K_{HF_4^-} * [H^+]_{free}})$$

$$-Ind_T * dil + (\frac{Ind_T * K_{Ind}}{1 + K_{Ind} * [H^+]_{free}}))$$

where

$$dil = \frac{vb}{vb + vi + va}$$

9. Correct $[H^+]_{S,F,I\ corrected}$ for the presence of HCO_3^- and CO_3^{2-}, i.e. CA, according to Dickson (1981):

$$[H^+]_{S,F,I,C\ corrected} = [H^+]_{S,F,I\ corrected} - [HCO_3^-] - 2[CO_3^{2-}]$$

10. Define upper and lower boundaries of pH values to be included in regression analysis
11. Calculate mean values of duplicate titration points
12. Calculate the equivalents in the acid and sample (x and y values) for the linear least squares regression:
    x = $[H^+]$ added from acid (value from RT) expressed as added to one litre of sample plus indicator (25°C)
    y = equivalents in sample expressed per litre of sample plus indicator (25°C)

$$x = \frac{va * [acid]_{RT}}{vb + vi}$$

$$y = [H^+]_{S,F,I,C\ corrected} * \frac{vb + vi + va}{vb + vi}$$

13. Linear least squares regression analysis:

$$a = \overline{Y} - b * \overline{X}$$

$$b=\frac{\Sigma X_i * Y_i - \frac{1}{n}\Sigma X_i * \Sigma Y_i}{\Sigma X_i^2 - \frac{1}{n} * (\Sigma X_i)^2}$$

$$\hat{Y}=a+bX=| \text{ of best fit}$$

where ΣX_i = sum of values of volume of acid added

ΣY_i = sum of values of modified Gran functions

$\Sigma X_i Y_i$ = sum of values of volume of acid added * modified Gran functions

ΣX_i^2 = sum of values of (volume of acid squared)

X(BAR) = mean of values of volume of acid added

Y(BAR) = mean of values of modified Gran functions

14. Calculate TA per litre (25°C):

$$TA_{25^{oc}}=X_c=\frac{\hat{Y}-a}{b} * \frac{vb+vi}{vb} \quad with\ \hat{Y}=zero$$

N.B. X_c represents the intercept with the x-axis here and thus the equivalence point. The dilution term corrects for the fact that the titration is carried out in a sample plus indicator solution and not just in the sample itself.

15. Calculate 95% confidence limits on the equivalence point (Estimaton of x from y and its 95% confidence limits according to Sokal and Rohlf (1981):

$$\hat{X}=\frac{Y-a}{b}$$

$$D=b^2 - t^2_{0.5[n-2]} * s^2_b$$

$$s^2_b=\frac{ResMS}{\Sigma (X_i-\bar{X})^2}$$

$$ResMS=\frac{1}{n-2} * \Sigma^n_{i=1} (Y_i-\hat{Y}_i)^2$$

$$H = \frac{t_{0.5[n-2]}}{D} * \sqrt{s^2 b * (D * (1 + \frac{1}{n}) + \frac{(Y_i - \overline{Y})^2}{\Sigma X^2}}$$

$$L_{1(\mu eq)} = \overline{X} + \frac{b(Y_i - \overline{Y})}{D} - H$$

$$L_{2(\mu eq)} = \overline{X} + \frac{b(Y_i - \overline{Y})}{D} + H$$

where $t_{0.5}$ = value from t-distribution (two-tailed 95% confidence limit)

$L_{1,2(\mu eq)}$ = 95 % confidence limit on the equivalence point in μeq/litre (25°C)

$$L_{1,2(\%)} = \frac{L_{1,2(\%)} * 100}{\overline{X}}$$

where $L_{1,2(\mu eq)}$ = 95 % confidence limit on the equivalence point in %

16. Calculate TA per kgSW:

$$TA_{kgSW} = \frac{TA_{25°C}}{density\ of\ sample\ at\ 25°C}$$

17. Option of making correction for blank
    If yes: subtract equivalents of blank from that of Na_2CO_3 standard

18. Calculate acid concentration per litre (RT):

$$[acid]_{RT} = \frac{[standard\ TA]_{25°C} * input\ [acid]_{RT}}{TA_{25°C}}$$

19. Calculate acid concentration per litre (20°C)

$$[acid]_{20°C} = [acid]_{RT} * \frac{density\ of\ acid\ at\ 20°C}{density\ of\ acid\ at\ RT}$$

N.B.For the density of acid a salinity of 35 psu has been

assumed. The calculation for this density term is given in point 30 below.

20. Calculate pK of indicator in molarity units on free-H^+-pH scale:
pK_{Ind} = 3.695 (in kgH_2O units at 25°C and 35 psu) according to King and Kester (1989);
Conversion of pK_{Ind} to molarity units (25°C) according to D. Turner (pers. comm.):

$$akhi_{moles/kgH_2O} = \frac{1}{10^{-3.695}}$$

$$akhi_{moles/litre_{25°C}} = \frac{akhi_{moles/kgH_2O}}{density\ of\ sample_{(25°C)} * (1-0.035179*sal/35)}$$

$$dkhi_{moles/litre} = \frac{1}{akhi_{moles/litre_{25°C}}}$$

$$pK_{Ind_{moles/litre_{25°C}}} = log10(dkhi_{moles/litre_{25°C}}) * (-1)$$

N.B. The density term here, which describes the density of the sample during the titration, is given in point 30 below.
The term (1-0.035179*sal/35) is omitted when a conversion is carried out from moles/kgSW to molarity units. The value 0.035179 represents the concentration of dissolved solids at a salinity of 35 psu.

21. Calculate association constant of HSO_4^- (moles/kgH_2O) on free H^+-pH scale according to Khoo et al. (1977):

$$\log\beta_{HSO_4^-} = \frac{647.59}{T_K} - 6.3451 + 0.019085\,T_K - 0.5208\,I^{1/2}$$

N.B. For the 'real ionic strength term' (I) see point 24 below.

22. Calculate association constant of HF (moles/kgH_2O) on free

H^+-pH scale according to Dickson and Riley (1979):

$$\ln\beta_{HF} = \frac{-1590.2}{T_K} + 12.641 - 1.525\, I^{1/2}$$

23. Convert association constants of HSO_4^- and HF to molarity units (25°C):

$$\beta_{HSO_4^- HF_{moles/litre_{25°C}}} = \frac{\beta_{HSO_4^- HF_{moles/kgH_2O}}}{density\,of\,sample_{25°C} * (1 - 0.039179 * sal/35)}$$

24. Calculate real ionic strength (moles/kgH_2O) of sample according to Ramette et al. (1977):

$$I = 0.00287 + 0.0185751 * sal + 1.639 * 10^{-5} * sal^2$$

25. Calculate total sulphate and total fluoride concentrations (moles/kgSW) of sample according to Wilson (1975):

	weight of compound in 1kg of seawater (35 ρsu) (g)	molecular weight (g)	concentration (moles/kgSW)
total sulphate	2.712	96.059	0.02823
total fluoride	0.0013	18.998	6.8428*10(-5)

Thus:

$$S_{T_{moles/kgSW}} = \frac{sal * 0.02823}{35}$$

$$F_{T_{moles/kgSW}} = \frac{sal * 6.8428 * 10^{-5}}{35}$$

26. Convert total sulphate and total fluoride concentrations to

molarity units:

$$S_{T_{moles/litre}} = S_{T_{moles/kgSW}} * density\ of\ sample$$

$$F_{T_{moles/litre}} = F_{T_{moles/kgSW}} * density\ of\ sample$$

N.B. The density term here, which describes the density of the sample when it is filled into the titration vessel, is given in point 30.

27. Calculate CA (moles/litre at 25°C) according to Skirrow (1975) including dilution corrections:

$$[HCO_3^-] + 2[CO_3^{2-}] = TCO_2 * dil * \frac{K_{1C} * [H^+] + 2 * K_{1C} * K_{2C}}{[H^+]^2 + K_{1C} * [H^+] + K_{1C} * K_{2C}}$$

N.B. In case of the acid standardization the input [TCO_2] equals half the TA of the Na_2CO_3 standard.

28. Calculate pK_{1C} and pK_{2C} for H_2CO_3 (moles/kg solution) on SW pH-scale (i.e. including S and F) according to Goyet and Poisson (1989):

$$pK_{1C_{moles/kgsolution}} = 812.27/T_C + 3.356 - 0.00171 * sal * \ln(T_C) + 0.000091 * sal^2$$

$$pK_{2C} = 1450.87/T_C + 4.604 - 0.00385 * sal * \ln(T_C) + 0.000182 * sal^2$$

29. Calculating K_{1C} and K_{2C} for H_2CO_3 in molarity units (25°C):

$$K_{1,2C_{moles/litre}} = 10^{(-pK_{1,2C})} * density\ of\ sample_{25°C}$$

30. Calculate density of seawater (here also used for acids and Na_2CO_3 standards to which NaCl has been added) according to Millero and Poisson (1982):

$$density\ of\ seawater = \rho_o + AS + BS^{3/2} + CS^2$$

$$B = -5.72466 * 10^{-3} + 1.0227 * 10^{-4} T_K - 1.6546 * 10^{-6} T_K^2$$

$$A = 8.24493 * 10^{-1} - 4.0899 * 10^{-3} T_K + 7.6438 * 10^{-5} T_K^2 - 8.2467 * 10^{-7} T_K^3 + 5.3875 * 10^{-9} T_K^4$$

$$C = 4.8314 * 10^{-4}$$

$$\rho_o = 999.842594 + 6.793952 * 10^{-2} T_K - 9.095290 * 10^{-3} T_K^2 + 1.001685 * 10^{-4} T_K^3 - 1.120083 * 10^{-6} T_K^4 + 6.536336 * 10^{-9} T_K^5$$

31. Calculate sample volume at 25°C:

$$volume_{25°C} = volume\ at\ input\ temp. * \frac{density\ at\ input\ temp.}{density\ at\ 25°C}$$

N.B. The input temperature is the temperature of the sample when filled into the titration vessel.

32. Calculate acid concentration at temperature of acid (usually RT):

$$[acid]_{RT} = [acid]_{25°C} * \frac{density\ of\ acid\ at\ input\ temp.}{density\ of\ acid\ at\ 25°C}$$

N.B. The input temperature is the temperature of the acid when it is added to the sample from the volumetric burette.

33. Calculate TA of the standard at 25°C:

$$[standard]_{25°C} = [standard]_{20°C} * \frac{density\ of\ standard\ at\ 25°C}{density\ of\ standard\ at\ input\ temp.}$$

N.B. The input temperature is the temperature of the standard when it is made up.

34. Read absorbance data (A1) of one wavelength
35. Calculate mean value of 12 absorbance maximum readings (A1(A^-))
36. Calculate mean value of 12 absorbance minimum readings (A1(HA))
37. Calculate the pH on the free H^+-pH scale according to Anderson and Wedborg (1983) including dilution corrections:

$$pH_{free} = pK_{Ind} + \log\left(\frac{A1(HA)_c - A1_c}{A1_c - A1(A^-)}\right)$$

where

$$A1(HA)_c = A1(HA) * \frac{vb+vi+va}{vb+vi} * \frac{vb+vi+va-4+4}{vb+vi+va-4}$$

$$A1_c = A1 * \frac{vb+vi+va}{vb+vi}$$

N.B.The correction terms are explained in point 6 above.

APPENDIX 2: TURBO BASIC COMPUTER PROGRAM TO CALCULATE TOTAL ALKALINITY WITH THE SINGLE WAVELENGTH METHOD

APPENDIX 2

TURBO BASIC COMPUTER PROGRAM FOR CALCULATING TA WITH THE SINGLE WAVELENGTH METHOD

(N.B. The numbers in the brackets after the 'rem' statements refer to the respective parts in the list of equations in appendix

```
print "TA1LPC.BAS;18-Feb-1993"
dim a1(100),a2(100),a$[16],b$[3],c$[2],d$[3],a3(100),a3#(100),
   x(50),y(50),h#(100),ca(100),dil(100),va(100)
dim x#(100),y#(100),m1#(100),v4#(100),L10#(100),L11#(100),
   v6#(100),L12#(100),v7#(100),Res#(100)
a$="a:\intcal\ic"
print "exp.no"
   input b$
print "file= .?, a.?, b.?, c.?"
   input c$
d$="wav"
file1$=a$+b$+c$+d$
print "exp=";file1$
rem: q=number of steps
   q=35
print "init acid vol in burette units?"
   input va
va=va/5000
print "init. acid vol.=" using "#.####cm3";
print "volume:indicator addition in cm3"
   vi=4.000
print "final indicator concentration in uM/litre?"
   input ind
print "final indicator concentration=" using "##.#
   uM/litre";ind
print "Bottle Volume in cm3="
   input vb0
print "bottle volume in cm3=" using "###.###";vb0
print "salinity of sample="
   input sal2
print "salinity of sample=" using "##.###%";sal2
print "stand. acid-conc(mM)?"
   input acid0
print "standardized acid conc. at 25C=" using
   "###.###mM*litre-1";acid0
rem:(1)exclude superfluous data from HP8452 raw data file
   open file1$ for input as #1
   for n=1 to 22
      input #1,x
   next n
rem:(34)read absorbance data of one wavelength (A1)
   for n=23 to (q*2)+24+22
      input #1,a2(n-22),a1(n-22)
   next n
   close #1
   for n=13 to 12+(q*2)
      a3(n-12)=a1(n)
   next n
rem:(35)calculate mean value of 12 absorbance maximum readings
```

```
   for n=1 to 12
      a1max=a1(n)+a1max
   next n
   a1max=a1max/12
   for n=13 to 12+(q*2)
   next n
rem:(36)calculate mean value of 12 absorbance minimum readings
   for n=13+(q*2) to 13+(q*2)+11
      a1min=a1(n)+a1min
   next n
   a1min=a1min/12
rem:(24)calculate real ionic strength of sample according to
   Ramette et al. 1977 (mol/kg-H2O)
   ionst2#=0.00287+0.0185751*sal2+1.639*10^(-5)*(sal2*sal2)
   print "ionic strength=" using "#.######";ionst2#
rem:(30)calculate density of seawater when filled into titration
   vessel (dsw2#) according to Millero & Poisson 1982
   print "temp of sample into O2-bottle?"
      input temp2
   print "sample temp. into O2-bottle=" using "##.##C";temp2
   tk2=temp2+273.15
   dzero2#=999.842594+6.793952*10^(-2)*temp2-9.095290*10^(-3)
      *(temp2^2)+1.001685*10^(-4)*(temp2^3)-1.120083*10^(-6)
      *(temp2^4)+6.536336*10^(-9)*(temp2^5)
   a2#=8.24493*10^(-1)-4.0899*10^(-3)*temp2+7.6438*10^(-5)
      *(temp2^2)-8.2467*10^(-7)*(temp2^3)+5.3875*10^(-9)
      *(temp2^4)
   b2#=-5.72466*10^(-3)+1.0227*10^(-4)*temp2-1.6546*10^(-6)
      *(temp2^2)
   c2#=4.8314*10^(-4)
   dsw2#=(dzero2#+a2#*sal2+b2#*sal2^(3/2)+c2#*sal2*sal2)/1000
   print "density of sample when into O2-bottle=" using
      "#.#####";dsw2#
rem:(31)calculate sample volume at 25C
rem:(30)calculate density of sample volume at 25C and input
   salinity (sal2) according to Millero & Poisson, 1982
   dzero3#=999.842594+6.793952*10^(-2)*25-9.095290*10^(-3)
      *(25^2)+1.001685*10^(-4)*(25^3)-1.120083*10^(-6)*(25^4)
      +6.536336*10^(-9)*(25^5)
   a3#=8.24493*10^(-1)-4.0899*10^(-3)*25+7.6438*10^(-5)
      *(25^2)-8.2467*10^(-7)*(25^3)+5.3875*10^(-9)*(25^4)
   b3#=-5.72466*10^(-3)+1.0227*10^(-4)*25-1.6546*10^(-6)*(25^2)
   c3#=4.8314*10^(-4)
   dsw3#=(dzero3#+a3#*sal2+b3#*sal2^(3/2)+c3#*sal2*sal2)/1000
   print "density of sample at 25C=" using "##.########";dsw3#
   vb1=vb0*dsw2#/dsw3#
   print "temp.corrected sample volume=" using "###.###cm3";vb1
rem:(30)calculate density of seawater during titration at 25C
   (dsw0#) according to Millero & Poisson, 1982
   tk0=25+273.15
   dzero0#=999.842594+6.793952*10^(-2)*25-9.095290*10^(-3)
      *(25^2)+1.001685*10^(-4)*(25^3)-1.120083*10^(-6)
      *(25^4)+6.536336*10^(-9)*(25^5)
   a0#=8.24493*10^(-1)-4.0899*10^(-3)*25+7.6438*10^(-5)
      *(25^2)-8.2467*10^(-7)*(25^3)+5.3875*10^(-9)*(25^4)
   b0#=-5.72466*10^(-3)+1.0227*10^(-4)*25-1.6546*10^(-6)*(25^2)
```

```
    c0#=4.8314*10^(-4)
    dsw0#=(dzero0#+a0#*sal2+b0#*sal2^(3/2)+c0#*sal2*sal2)/1000
    print "density of sample during titration=" using
       "#.######";dsw0#
rem:(30)calculate density of acid in the burette at room
    temperature assuming salinity of 35% (dsw1#) according to
    Millero & Poisson, 1981
    print "temp of acid in burette?"
       input temp1
    print "temp. of acid in burette=" using "##.##C";temp1
    tk1=temp1+273.15
    dzero1#=999.842594+6.793952*10^(-2)*temp1-9.095290*10^(-3)
       *(temp1^2)+1.001685*10^(-4)*(temp1^3)-1.120083
       *10^(-6)*(temp1^4)+6.536336*10^(-9)*(temp1^5)
    a1#=8.24493*10^(-1)-4.0899*10^(-3)*temp1+7.6438*10^(-5)
       *(temp1^2)-8.2467*10^(-7)*(temp1^3)+5.3875*10^(-9)
       *(temp1^4)
    b1#=-5.72466*10^(-3)+1.0227*10^(-4)*temp1-1.6546*10^(-6)
       *(temp1^2)
    c1#=4.8314*10^(-4)
    dsw1#=(dzero1#+a1#*35+b1#*35^(3/2)+c1#*35*35)/1000
    print "density of acid in burette=" using "#.######";dsw1#
rem:(32)calculate acid concentration at temperature of acid
    (assumed to be RT)
    acid1=acid0*dsw1#/1.0233431
    print "temp.corrected [acid]=" using "###.######mM/litre at
       temperature of acid";acid1
rem:(20)calculate pK of indicator in molarity units on
    "free"-H+-pH-scale using pK value in moles/kg-H2O from King
    & Kester, 1989
    akhi#=1/(10^(-3.695))
    akhi#=akhi#/(dsw0#*(1-0.035179*sal2/35))
    dkhi#=1/akhi#
    pkhi#=log10(dkhi#)*(-1)
    print akhi#,dkhi#,pkhi#
    print "adjusted pkind=";pkhi#
rem:(37)calculate pH on "free"-H+-pH-scale according to Anderson
    & Wedborg, 1983, including dilution corrections
    for n=1 to (q*2)
       va(n)=va-(12.5/5000/2)+(n-1)*(12.5/5000)
          a3#(n)=pkhi#+log10(((a1min*(vb0+vi+va(n))/(vb0+vi)
             *(vb0+vi+va(n)-4+4)/(vb0+vi+va(n)-4))-(a3(n)
             *(vb0+vi+va(n))/(vb0+vi)))/((a3(n)*(vb0+vi+va(n))
             /(vb0+vi))-a1max))
       print a3#(n)
       next n
rem:(21)calculate association constant of HSO4- (moles/kg-H2O)
    on "free"-H+-pH-scale according to Khoo et al., 1977
rem:(23)convert association constant of HSO4- to molarity units
    akhs#=10^(647.59/tk0-6.3451+0.019085*tk0-0.5208*ionst2#^(1/2))
    akhs#=akhs#/(dsw0#*(1-0.035179*sal2/35))
    print "associationK(HSO4)=";akhs#
    pkhs#=log10(1/akhs#)*(-1)
    print "adjusted pKHSO4=";pkhs#
rem:(22)calculate association constant of HF (moles/kg-H2O) on
    "free"-H+-pH-scale according to Dickson & Riley, 1979
```

```
rem:(23)convert association constant of HF to molarity units
   akhf#=exp(-1590.2/tk0+12.641-1.525*ionst2#^(1/2))
   akhf#=akhf#/(dsw0#*(1-0.035179*sal2/35))
   print "associationK(HF)=";akhf#
   pkhf#=log10(1/akhf#)*(-1)
   print "adjusted pkHF=";pkhf#
rem:(25)calculate total sulphate concentration of sample
   (moles/kg-SW) according to Wilson, 1975
rem:(26)convert total sulphate concentration to molarity units;
   correct for dilution of sample with indicator and acid
   ts#=(sal2*0.02823/35)*dsw2#
   print "total sulphate=";ts#
rem:(25)calculate total fluoride concentration of sample
   (moles/kg-SW) according to Wilson, 1975
rem:(26)convert total fluoride concentration to molarity units;
   correct for dilution of sample with indicator and acid
   tf#=(sal2*(6.8428*10^(-5))/35)*dsw2#
   print "total fluoride=";tf#
rem:(8)correct free[H+] for the presence of In-, HSO4-, HF in the
   sample according to Dickson, 1981, and Anderson & Wedborg,
   1983
   print "old [H+]                          old pH"
   print "[HSO4]                            [HF]
    [HInd]"
   print "new[H+]                           new pH"
   for n=1 to (q*2)
      dil(n)=(vb1)/(vb1+vi+va(n))
      print 10^(-a3#(n)),a3#(n)
      print (10^(-a3#(n))*(ts#*dil(n)*akhs#/(1+akhs#
         *10^(-a3#(n)))))),(10^(-a3#(n))*(tf#*dil(n)*akhf#
         /(1+akhf#*10^(-a3#(n))))),(10^(-a3#(n))*(ind*10^(-6)
         *dil(n)*akhi#/(1+akhi#*10^(-a3#(n)))))
      h#(n)=10^(-a3#(n))*(1+(ts#*dil(n)*akhs#/(1+akhs#
         *10^(-a3#(n))))+(tf#*dil(n)*akhf#/(1+akhf#
         *10^(-a3#(n)))))-ind*10^(-6)*dil(n)+(10^(-a3#(n))
         *(ind*10^(-6)*dil(n)*akhi#/(1+akhi#*10^(-a3#(n))))))
      a3#(n)=log10(h#(n))*(-1)
      print h#(n),a3#(n)
94 next n
rem:(28)calculate pK1 and pK2 for H2CO3 (moles/kg-solution) on
   the SW-pH-scale i.e. including HSO4- and HF) acc. to Goyet &
   Poisson, 1989
   pkc1#=812.27/tk0+3.356-0.00171*sal2*log(tk0)+0.000091
      *sal2*sal2
   pkc2#=1450.87/tk0+4.604-0.00385*sal2*log(tk0)+0.000182
      *sal2*sal2
   print "pK(HCO3) values=";pkc1#,pkc2#
rem:(29)calculate K1 and K2 of H2CO3 in molarity units
   dkhc1#=(10^(-pkc1#))*dsw2#
   dkhc2#=(10^(-pkc2#))*dsw2#
   pkc1#=log10(dkhc1#)*(-1)
   pkc2#=log10(dkhc2#)*(-1)
   print "adjusted pK(HCO3) values=";pkc1#,pkc2#
rem:(27)calulate carbonate alkalinity (moles/litre at 25C)
   according to Riley & Skirrow, 1975; correct for dilution of
   sample with indicator and acid
```

```
   print "old [H+]                              old pH"
   print "[CA]                                 new [H+]
  new pH"
   print "TCO2 concentration in M/litre?"
      input tco2
   print "[TCO2]=" using "#.######M/litre";tco2
   for n=1 to (q*2)
      print h#(n),a3#(n)
      ca(n)=(tco2*dil(n)*(h#(n)*dkhc1#+2*dkhc1#*dkhc2#))/(h#(n)
         *h#(n)+dkhc1#*h#(n)+dkhc1#*dkhc2#)
rem:(9)correct [H+]corr. for presence of HCO3- and CO3--
   according to Dickson, 1981
      h#(n)=h#(n)-ca(n)
      a3#(n)=log10(h#(n))*(-1)
      print ca(n),h#(n),a3#(n)
   next n
 95 s=1
rem:(10)define upper and lower boundaries of pH values in
   regression analysis
   print "constrain value:Y or N"
   r$="N"
   if r$="N" or  r$="n" then 120
   H=3.2
   L=2.0
   print "reset values of high and low pH:Y or N"
      input r$
   if r$="N" or  r$="n" then 103
   print "high pH limit"
   input H
   print "low pH limit"
      input L
   print "pH range=" using "#.### #.###";H,L
 103 f=q*2
   for i=1 to q*2
      if a3#(i)>H then s=s+1
      if a3#(i)<L then f=f-1
   next i
   f=2*(int(f/2))
   s=(2*(int((s)/2)))+1
   q=((f-s+1)/2)
   n=0
   for i=s to f
      n=n+1
      a3#(n)=a3#(i)
 118 next i
 120 rem:
   for i=0 to q-1
      for j=1 to 2
         n=(i*2)+j
 126 rem:
      next j
   next i
 129 rem:(12)calculate mean values in duplicate titration points
   m=1
   n=1
   for i=1 to q*2 step 2
```

```
      h1#(m)=h#(n)
      h2#(m)=h#(n+1)
      h#(m)=(h#(n)+h#(n+1))/2
      a3#(m)=log10(h#(m))*(-1)
print a3#(m),h#(m)
143   m=m+1
      n=n+2
   next i
rem:plotting pH vs. no. acid additions
   screen 2
   window (0,2)-(35,4)
   rem:drawing grid lines
      line (0,2)-(35,2): line (0,2)-(0,4)
      line (35,2)-(35,4): line (0,4)-(35,4)
   rem:drawing plots
      for i=1 to q
         pset (i,a3#(i)),2
         line (i,a3#(i))-((i+1), a3#(i+1))
      next i
rem:(12)calculate the equivalents in the acid and the sample (x
   and y values) for the linear least squares regression analysis
   dim e$[3],f$[15]
   e$="res"
   f$="c:\user\clp"
   file2$=f$+b$+c$+e$
   print "file with residuals=";file2$
   open file2$ for output as #2
   for i=1 to q
      h#(i)=h#(i)*(vb1+vi+(va+(((i-1)+((s-1)/2))*(25/5000))))
         /(vb1+vi)
      print (va+(((i-1)+((s-1)/2))*(25/5000)))*acid1*1000
         /(vb1+vi), h#(i)
      write #2,(va+(((i-1)+((s-1)/2))*(25/5000)))*acid1*1000
         /(vb1+vi)-(va+(((i-2)+((s-1)/2))*(25/5000)))*acid1*1000
         /(vb1+vi),(h#(i)-h#(i-1))*10^(6)
      print (va+(((i-1)+((s-1)/2))*(25/5000)))*acid1*1000
         /(vb1+vi)-(va+(((i-2)+((s-1)/2))*(25/5000)))*acid1*1000
         /(vb1+vi),(h#(i)-h#(i-1))*10^(6)
152next i
   close #2
rem:plotting Gran functions vs. no. acid additions
   screen 2
   window (0,0)-(35,10^(-3))
   rem:drawing grid lines
      line (0,0)-(35,0): line (0,0)-(0,10^(-3))
      line (35,0)-(35,10^(-3)): line (0,10^(-3))-(35,10^(-3))
   rem:drawing plots
      for i=1 to q
         pset (i,h#(i)),2
         line (i,h#(i))-((i+1), h#(i+1))
      next i
160 rem:(13)linear least squares regression analysis
   i=1
   y#=h#(i)
   x#=(va+(((i-1)+((s-1)/2))*(25/5000)))*acid1*1000/(vb1+vi)
   m1#=h#(i)*(va+(((i-1)+((s-1)/2))*(25/5000)))*acid1*1000
```

```
    /(vb1+vi)
  v4#=((va+(((i-1)+((s-1)/2))*(25/5000)))*acid1*1000/(vb1+vi))^2
  for i=1 to q-1
    y#=y#+h#(i+1)
    x#=x#+(va+(((i)+((s-1)/2))*(25/5000)))*acid1*1000/(vb1+vi)
    m1#=m1#+(h#(i+1)*(va+(((i)+((s-1)/2))*(25/5000)))*acid1
      *1000/(vb1+vi))
    v4#=v4#+((va+(((i)+((s-1)/2))*(25/5000)))*acid1*1000
      /(vb1+vi))^2
  next i
  v5#=x#/q
  L9#=y#/q
  d#=(m1#-(1/q)*x#*y#)/(v4#-(1/q)*x#*x#)
  c#=L9#-d#*v5#
rem:(14)calculate total alkalinity per litre at 25C
  TA0#=((0-c#)/d#*(vb1+vi)/vb1)
  TA1#=TA0#
  print "TA=" using "####.###uM per litre at 25C";TA1#
rem:(16)calculate total alkalinity per kg-SW
  TA2#=TA1#/dsw3#
  print "TA=" using "####.###uM per kg of SW";TA2#
rem:(15)calculating 95% confidence limits (m2#,m3#) on the
  equivalence point according to Sokal & Rohlf, 1981
  if q=4 then
  t=4.303:elseif q=5 then
  t=3.182:elseif q=6 then
  t=2.776:elseif q=7 then
  t=2.571: elseif q=8 then
  t=2.447:elseif q=9 then
  t=2.365:elseif q=10 then
  t=2.306:elseif q=11 then
  t=2.262:elseif q=12 then
  t=2.228:elseif q=13 then
  t=2.201:elseif q=14 then
  t=2.179:elseif q=15 then
  t=2.16:elseif q=16 then
  t=2.145:elseif q=17 then
  t=2.131:elseif q=18 then
  t=2.12:elseif q=19 then
  t=2.11:elseif q=20 then
  t=2.101:elseif q=21 then
  t=2.093:elseif q=22 then
  t=2.086:elseif q=23 then
  t=2.08:elseif q=24 then
  t=2.074:elseif q=25 then
  t=2.069:elseif q=26 then
  t=2.064:elseif q=27 then
  t=2.06:elseif q=28 then
  t=2.056:elseif q=29 then
  t=2.052:elseif q=30 then
  t=2.048:elseif q=31 then
  t=2.045:elseif q=32 then
  t=2.042:elseif q=33 then
  t=2.039:elseif q=34 then
  t=2.036:elseif q=35 then
  t=2.033:elseif q=36 then
```

```
   t=2.030:elseif q=37 then
   t=2.028:elseif q=38 then
   t=2.026:elseif q=39 then
   t=2.024:elseif q=40 then
   t=2.023:elseif q=41 then
   t=2.022:elseif q=42 then
   t=2.021
   end if
   for i=1 to q
      L10#(i)=c#+d#*((va+(((i-1)+((s-1)/2))*(25/5000)))*acid1
         *1000/(vb1+vi))
      Res#(i)=h#(i)-L10#(i)
      print Res#(i)
268   L11#(i)=(h#(i)-L10#(i))^2
      v6#(i)=(((va+(((i-1)+((s-1)/2))*(25/5000)))*acid1
      *1000/(vb1+vi))-v5#)^2
   next i
   i=1
   L12#=(h#(i)-L10#(i))^2
   v7#=(((va+(((i-1)+((s-1)/2))*(25/5000)))*acid1*1000
      /(vb1+vi))-v5#)^2
   for i=1 to q-1
      L12#=L12#+((h#(i+1)-L10#(i+1))^2)
      v7#=v7#+(((va+(((i)+((s-1)/2))*(25/5000)))*acid1*1000
         /(vb1+vi))-v5#)^2
   next i
   s1#=1/(q-2)*L12#
   s2#=s1#/v7#
   E#=d#^2-t^2*s2#
   H1#=(t/E#)*(s1#*(E#*(1+(1/q))+(((0-L9#)^2)/v4#)))^0.5
   m5#=h1#*100/TA0#
   taeverror=(m5#*TA0#/100)
   print "no. points incl. in regression=" using "##";q
   print "m5#=%eq.vol.error=" using "#.######%";m5#
   print "approx. TA-eq-vol-error=" using "+-##.###uM per litre
      25C";h1#
goto 377
365rem:plotting Gran residuals vs. no. acid additions
   dim e$[3],f$[15]
   e$="res"
   f$="c:\user\clp"
   file2$=f$+b$+c$+e$
   print "file with residuals=";file2$
   open file2$ for output as #2
377   screen 2
   window (0,5*10^(-6))-(q,-5*10^(-6))
   print "pH/Gran functions/Gran residuals vs. no. acid
      additions"
   rem:drawing grid lines
      line (0,0)-(q,0)
   rem:drawing plots
      for i=1 to q
         pset (i,Res#(i)),2
         line (i,Res#(i))-((i+1), Res#(i+1))
388      next i
end
```